

SOLUTION POLYMERIZATION OF
ACRYLAMIDE TO HIGH CONVERSION

BY

TOSHIYUKI ISHIGE, B.Sc., M.Sc.

A Thesis

Submitted to the School of Graduate Studies

In Partial Fulfilment of the Requirements

For the Degree

Doctor of Philosophy

McMaster University

June 1972

DOCTOR OF PHILOSOPHY (1972)
(Chemical Engineering)

MCMASTER UNIVERSITY
Hamilton, Ontario

TITLE : Solution Polymerization of Acrylamide to
High Conversion

AUTHOR : Toshiyuki Ishige
B.Sc. Tokyo Institute of Technology, Japan
M.Sc. University of Alberta

SUPERVISOR : Professor A.E. Hamielec

NUMBER OF PAGES : (X), I-137, II-92

SCOPE AND CONTENT :

This thesis reports an experimental investigation of the free radical polymerization of acrylamide in water (Part I) and the development of gel permeation chromatography (GPC) technology for the measurement of molecular weight distribution and conversion (Part II).

The aim of Part I was to develop a kinetic model for the polymerization capable of predicting conversion and molecular weight distribution up to high conversion with the production of polymer of number-average molecular weight over one million. The aim of Part II was to develop numerical techniques required for instrumental spreading correction in GPC data interpretation. A further aim was to experimentally investigate the feasibility of molecular weight distribution and conversion analysis of polyacrylamide in aqueous carrier solvent.

ACKNOWLEDGEMENTS

The author would like to express his sincere thanks to his research director, Dr. A.E. Hamielec for his guidance, encouragement and assistance throughout the course of this study.

Appreciation is also extended to:

The members of the Ph.D. Supervisory Committee, Dr. J. Vlachopoulos and Dr. J.D. Embury for their advice in this study and in the final writing of this thesis.

Dr. S.-I. Lee for his helpful suggestions and constructive criticism.

Dr. K. Sato and Mr. P. Kumar for their experimental assistance in light scattering and electron microscopy respectively.

Mr. G. Walther for providing a computer program in machine language.

Miss C. Traplin for her typing of this thesis.

Nalco Chemical Company (Chicago, Illinois, U.S.A.) for providing financial support for this study.

Finally to my wife, Sachiko, for her moral and financial support and for her patience in performing the art work.

TABLE OF CONTENTS

PART I

Page

KINETIC STUDY OF THE SOLUTION POLYMERIZATION OF ACRYLAMIDE TO HIGH CONVERSION

I-1	INTRODUCTION	I-1
I-2	THEORETICAL BACKGROUND AND LITERATURE REVIEW	I-5
I-2-1	Some Properties of Acrylamide, Polyacrylamide and Details of the Aqueous Polymerization	I-5
I-2-2	Kinetic Features of Acrylamide Polymerization in Water	I-7
I-2-3	Analytical Techniques for Conversion and Molecular Weight	I-19
I-3	EXPERIMENTAL	I-22
I-3-1	Reagents	I-22
I-3-2	Analytical Techniques	I-24
I-3-3	Apparatus and Procedures	I-25
I-3-4	Experimental Conditions and Results	I-31
I-4	DATA INTERPRETATION AND RESULTS	I-44
I-4-1	Initial Rate of Polymerization	I-44
I-4-2	Kinetic Mechanism and Rate Constants	I-45
I-4-3	Comparison of Measured and Predicted Quantities	I-58
I-5	DISCUSSION	I-79
I-5-1	Mechanism and Rate Constants	I-79
I-5-2	Conversion and Molecular Weight Comparison	I-80
I-6	CONCLUSION	I-83
I-7	NOMENCLATURES	I-86
I-8	REFERENCES	I-90

	<u>Page</u>	
Appendix I-1	Viscosity Measurements	I-93
Appendix I-2	Light Scattering Measurements	I-110
Appendix I-3	Electron Microscope Measurements of Molecular Weight Distribution	I-116
Appendix I-4	Decomposition Rate of ACV at 80°C	I-124
Appendix I-5	Calculation of Molecular Weight Distributions from the Kinetic Model	I-127

PART II

DEVELOPMENT OF GPC TECHNOLOGY

II-1	INTRODUCTION	II-1
II-2	THEORETICAL BACKGROUND AND LITERATURE REVIEW	II-3
II-2-1	Separation Mechanism and Calibration Curve	II-3
II-2-2	Criteria for Effectiveness of Separation	II-7
II-2-3	Instrumental Spreading Function	II-10
II-2-4	Instrumental Spreading Correction	II-15
II-3	DEVELOPMENT AND EVALUATION OF NUMERICAL METHODS FOR INSTRUMENTAL SPREADING CORRECTION	II-26
II-3-1	Theory	II-26
II-3-2	Evaluation of Method-1, Method-2 and a Comparison with the Method of Chang and Huang	II-30
II-3-3	Application of Method-1 and Method-2 to Experimental Chromatograms	II-50
II-4	EXPERIMENTS RELATED TO KINETIC STUDY OF ACRYLAMIDE POLYMERIZATION	II-60
II-4-1	Experimental Set-up of the Instrument	II-60
II-4-2	Conversion Analysis by GPC	II-62
II-4-3	Molecular Weight Analysis of Polyacrylamide	II-72

	<u>Page</u>
II-5 DISCUSSION	II-81
II-6 CONCLUSION	II-85
II-7 NOMENCLATURE	II-87
II-8 REFERENCES	II-90

TABLE INDEX

	<u>Page</u>
I-2-1 List of Kinetic Studies of Acrylamide Polymerization in Water	I-8
I-2-2 Comparison of Rate Constants at 50°C	I-12
I-3-1 Summary of Experimental Conditions	I-33
I-3-2 Summary of Initial Rate Runs	I-34
I-3-3 Summary of Continuous Runs	I-36
I-3-4 Summary of Measured Intrinsic Viscosities	I-42
AI-1-1 Viscometer Constants and Recommended Ranges	I-94
AI-1-2 Comparison of Viscosities Measured by Two Viscometers 75-L181 and 50-A620	I-98
AI-1-3 Summary of Reproducibility Test	I-99
AI-1-4 Effect of Stirring on Viscosity	I-103
AI-1-5 Summary of Viscosity Measurement	I-105
AI-2-1 Refractive Index Difference Measurements	I-111
AI-2-2 Angular and Concentration Dependence of Scattered Light Intensity	I-113
AI-3-1 Shadow Length and Diameter of Standard Polystyrene Particle	I-118
AI-3-2 Number of Molecule vs. Shadow Length	I-120
II-3-1 Comparisons of Average Molecular Weights	II-34
II-3-2 Numerical Values of $F(v)$ used in Case 1A and Case 2A	II-36
II-3-3 Comparisons of Computation Time and Number of Iterations	II-49
II-3-4 Reported Average Molecular Weight of Standards	II-53
II-3-5 List of PRV, $\bar{M}_n(\infty)$, $\bar{M}_w(\infty)$ and $p(\infty)$	II-53
II-3-6 Two Parameters for Instrumental Spreading	II-55

	<u>Page</u>
II-3-7 Effective Calibration Curve Constants in $M = D_1 \exp(-D_2 v)$	II-55
II-3-8 Comparison of Average Molecular Weights	II-59
II-4-1 Polymer-Monomer Mixture Prepared and Their Peak Area Fraction	II-65
II-4-2 Observed Peak Area vs. Concentration	II-69

FIGURE INDEX

I-3-1 GPC Responses of Purified Acrylamide	I-23
I-3-2 Dimensions of Pyrex Ampoules Used	I-27
I-3-3 Schematic Diagram of Deaeration Apparatus	I-28
I-3-4 Ampoule Connection to the Deaeration Apparatus	I-30
I-4-1 Dependence of R_{p_0} on C_0	I-46
I-4-2 Dependence of R_{p_0} on M_0	I-47
I-4-3 A Plot of $1/\bar{r}_n$ vs. R_{p_0}/M_0^2	I-53
I-4-4 Comparison of k_d ($f \cdot k_d$)	I-57
I-4-5 Dependence of f on M	I-59
I-4-6 Comparison of Conversion and \bar{M}_n Runs: I5011, C5011(A)-(D)	I-60
I-4-7 Comparison of Conversion and \bar{M}_n Runs: I5014, C5014(A), (B)	I-61
I-4-8 Comparison of Conversion and \bar{M}_n Runs: C5021(A), (B)	I-62
I-4-9 Comparison of Conversion and \bar{M}_n Runs: I5024, C5024(A), (B)	I-63
I-4-10 Comparison of Conversion and \bar{M}_n Runs: I5044, C5044	I-64
I-4-11 Comparison of Conversion and \bar{M}_n Runs: C50S(A), (B)	I-65
I-4-12 Comparison of Conversion Runs: C4011, C4024(A), (B)	I-66
I-4-13 Comparison of Conversion and \bar{M}_n Runs: I4014, C4014	I-67
I-4-14 Comparison of Conversion and \bar{M}_n Run: C4044	I-68

	<u>Page</u>
I-4-15 Comparison of \bar{M}_w Runs: C5011(A),(B)	I-69
I-4-16 Comparison of \bar{M}_w Runs: I5014, C5014	I-70
I-4-17 Comparison of Molecular Weight Distribution	I-71
I-4-18 Comparison of Molecular Weight Distribution	I-72
I-4-19 Comparison of Molecular Weight Distribution	I-73
I-4-20 \bar{M}_n Dependence on M_o	I-75
I-4-21 \bar{M}_n Dependence on C_o	I-76
I-4-22 Variation of $(k_t/k_p^2)/(k_t/k_p^2)_o$ with Conversion	I-78
AI-1-1 Viscometer Set-up	I-94
AI-1-2 Density and Viscosity of Monomer Solution	I-96
AI-1-3 Difference in Two Viscometers	I-100
AI-1-4 Reproducibility Test	I-101
AI-1-5 Effect of Stirring on Viscosity	I-104
AI-2-1 Refractive Index Difference vs. Polymer Concentration (546 m μ)	I-112
AI-2-2 Zimm Plot for Sample C5011(C)-8	I-115
AI-3-1 Example of Micrographs (Original \sim x 20,000, enlarged to 1.5 times)	I-117
AI-3-2 Shadow Length and Particle Dimension	I-118
AI-3-3 Shadow Length Histogram Sample C5011(C)-8	I-121
AI-4-1 Change of C/C_o with Time	I-126

	<u>Page</u>
II-2-1 GPC Separation Process	II-4
II-2-2 GPC Chromatogram	II-4
II-2-3 General Shape of Calibration Curve	II-8
II-2-4 Effectiveness of Separation	II-8
II-2-5 Processes Involved in Chromatogram Interpretation	II-18
II-3-1 $\Delta F_1 = F - G\{F\}$	II-28
II-3-2 $\Delta F_2 = F_1 - G\{\Delta F_1\}$	II-28
II-3-3 Direction of Correction by Method-2	II-31
II-3-4 Evaluation Routine	II-32
II-3-5 Recovery of $W(y)$ - Case 1A ($h = 0.5$)	II-39
II-3-6 Recovery of $W(y)$ - Case 2A ($h = 0.5$)	II-41
II-3-7 Recovery of $W(y)$ - Case 1B ($h = 0.2$)	II-43
II-3-8 Recovery of $W(y)$ - Case 1C (variable h)	II-45
II-3-9 Recovery of $W(y)$ - Case 1D ($h = .5, \mu_3 = 1.0$)	II-47
II-3-10 Molecular Weight Calibration Curve	II-52
II-3-11 Comparisons of Corrected Chromatograms	II-57
II-4-1 Syphon Dump Flow Counter	II-63
II-4-2 Comparison of Weight Fraction vs. Peak Area Fraction	II-66
II-4-3 An Example of Polymer and Monomer Response and Area Fraction Calculation	II-67
II-4-4 Concentration Dependence of Area Under Peak	II-70
II-4-5 GPC Response for ACV	II-71
II-4-6 Linearity Test	II-73
II-4-7 Chromatograms and Effective Calibration Curves	II-75
II-4-8 Finding an Effective Calibration Curve in Low Molecular Weight End	II-77
II-4-9 Effective Calibration Curves in Lower Molecular Weight Range	II-80

PART I

KINETIC STUDY OF THE SOLUTION POLYMERIZATION OF ACRYLAMIDE TO HIGH CONVERSION

I-1 INTRODUCTION

Polyacrylamide is a product of the polymerization of the vinyl monomer, acrylamide. It is unique among other addition polymers in that it is virtually insoluble in common organic solvents. It is however, appreciably soluble in water. Therefore, its uses are found in applications involving water. Most important are those associated with flocculation and settling of aqueous suspensions, paper treatment and gelling or stabilizing agents for solids and muds. Current interest in waste water treatment with water soluble polymers has stimulated increasing interest in this polymer and its properties.

In the presence of free-radicals, acrylamide readily polymerizes to high molecular weight polyacrylamide. Free-radical polymerization of acrylamide in water has been studied with a number of initiator systems. However, kinetic studies reported in the literature are limited to the low conversion range, generally less than 10% conversion. Although a few kinetic studies were made up to 80% conversion or over, they did not involve extensive polymer characterization and usually employed low monomer concentration and relatively fast initiation rates producing relatively small molecular weight polymers of little interest in waste water treatment.

The following are the main objectives of the present experimental investigation;

1. to obtain data on the variation of both conversion and molecular weight averages with reaction time at relatively high monomer concentration (up to 2.2 (mol/l)) to yield polyacrylamide of number-average molecular weight greater than one million and
2. to develop a kinetic model suitable for the design simulation and optimization of polyacrylamide reactors. This would involve the ability to predict conversion and molecular weight distribution of the polymer up to essentially complete conversion.

Reaction conditions involving high monomer concentration and conversions are of special importance in industrial processes. Kinetic data for these reaction conditions are not available in the literature despite their importance in the design, simulation, optimization and operation of commercial polyacrylamide reactors.

The polymerization reaction was followed by measuring the change of conversion and number-average molecular weight with time. Conversion measurements were done using gravimetric techniques and by the use of gel permeation chromatography. Number-average molecular weights were measured using viscometry. Knowledge of more than one molecular weight average or of the molecular weight distribution itself, though not essential for the evaluation of model parameters, gives a consistency test of a proposed kinetic model. Gel permeation chromatography, light scattering, and electron microscopy were used for this purpose.

The development of a kinetic model involved first finding an

acceptable kinetic mechanism for the initial stage of the polymerization using initial rate data obtained in this investigation. This model includes all the elementary reactions involved and permits the prediction of conversion and molecular weight distribution at higher conversions of monomer. Measured values were then compared with those predicted.

The kinetic mechanisms of free radical polymerization have often been studied. It is well established that free radical polymerizations generally involve the following elementary steps:

1. Initiation; generation of free radicals of chain length unity.
2. Propagation; chain growth of radicals by addition of monomer molecules.
3. Transfer; transfer of radical from a growing chain to another molecule forming an inactive polymer chain.
4. Termination; reaction of two radicals to form one or two polymer chains.

In order to make an analysis of the above reactions tractable, the following assumptions which are usually justified are generally made:

1. The intrinsic reactivity of a radical is independent of its molecular weight and conversion. This permits the use of a single rate constant which depends upon temperature alone.
2. The average chain length is large. This permits one to neglect consumption of monomer in all reactions other than propagation.
3. Volume change during the reaction is negligible. One can therefore neglect volume contraction with conversion.
5. The stationary state applied to free radical is valid. This permits the reduction of a set of ordinary differential equations for radical concentrations to algebraic equations.

In fact, almost all of the reported rate constants in the above mentioned reaction steps have been evaluated using these assumptions. Good agreement with experimental data has shown their validity at low conversion. The reaction behaviour at high conversion however often invalidates some of the above assumptions. This is mostly due to the increase in polymer concentration of the reaction mixture, under which translational and segmental diffusion of radical chains can be significantly reduced. In other words, reactions involving long radical chains can become diffusion controlled. The often observed phenomena associated with this are called "gel effect" and it has been reported in many vinyl polymerizations. Although aqueous homogeneous polymerization represented by acrylamide polymerization has been known to follow classical kinetics, their validity at high conversions and molecular weights has not been substantiated in any experimental investigation in the literature. Under the reaction conditions chosen for the present investigation, it was expected that termination reactions would be diffusion controlled resulting in a significant "gel effect". The "gel effect" is usually responsible for an acceleration in the rate of polymerization and significant increases in molecular weight with conversion. When transfer reactions control the molecular weight of the polymer, increases in molecular weight are not observed even though the rate of polymerization may accelerate. Transfer reactions involve small molecules and do not become diffusion control until the glass transition point of the reaction mixture is approached.

I-2 THEORETICAL BACKGROUND AND LITERATURE REVIEW

I-2-1 Some Properties of Acrylamide, Polyacrylamide and Details of the Aqueous Polymerization

Acrylamide is a vinyl monomer of form $\text{CH}_2 = \text{CHCONH}_2$. The monomer is a white crystalline water-soluble solid melting at 84.5°C .⁽¹⁾ It possesses good thermal stability and there is no evidence of polymer formation at 50°C . It undergoes the usual reactions of the amide group and of the double bond.⁽²⁾

In the presence of free radicals, acrylamide in aqueous solution polymerizes to water-soluble polyacrylamide. The heat evolved in converting monomer to polymer is about 19.5 (Kcal/mol)⁽³⁾. The solid state polymerization initiated by radiation has also been reported^(4,5). Organic liquids that are solvents for the monomer may be used as a reaction medium, but the molecular weights produced using these solvents are usually too low to be of commercial interest. Aqueous polymerization is generally preferred and water-soluble alcohols are used as transfer agents to moderate molecular weight⁽⁶⁾.

The polymer is insoluble in most organic solvents and is usually a linear polymer with head to tail structure⁽⁶⁾. Polymers with significant amount of chain branching are obtained under special reaction conditions⁽⁷⁾. Since the main application of the polymer is in aqueous solutions little is known about the solid polymer. Solutions of polyacrylamide in water are very viscous. Equations relating intrinsic viscosity to average molecular weights of the polymer have been found to be;

$$[\eta] = 6.31 \times 10^{-5} (\bar{M}_w)^{0.80} \quad 25^\circ\text{C in H}_2\text{O}^{(8)} \quad (\text{I-2-1})$$

$$[\eta] = 3.73 \times 10^{-4} (\bar{M}_w)^{0.66} \quad 30^\circ\text{C in 1 N NaOH}^{(9)} \quad (\text{I-2-2})$$

$$[\eta] = 6.80 \times 10^{-4} (\bar{M}_n)^{0.66} \quad 25^\circ\text{C in H}_2\text{O}^{(10)} \quad (\text{I-2-3})$$

Aqueous polymerization is considered a free radical process as opposed to an ionic process. This is due to the fact that an ionic polymerization involving a vinyl monomer is not sustainable in water because of rapid chain transfer to produce H^+ or OH^- ions that are incapable of initiating vinyl polymerization⁽⁶⁾. Of all the solvents, water is unique in having a chain transfer constant of practically zero in free radical processes⁽¹¹⁾. This partly accounts for the high molecular weight polymers obtainable in aqueous polymerization. The polymerization falls into two categories, homogeneous polymerization in which the polymer formed is soluble in aqueous solution and heterogeneous polymerization in which the polymer precipitates from the aqueous solution as formed. Acrylamide polymerization is an example of the first kind while polymerization of methylmethacrylate and vinyl acetate in water are examples of the second kind.

I-2-2 Kinetic Features of Acrylamide Polymerization in Water

Kinetic studies have been reported for a number of initiator systems. These include radiation initiation with x-rays, γ -rays, and UV light, and chemical initiation with redox systems, peroxide and azo compounds. Chemical initiation is the most common method used in industrial processes,

Table I-2-1 summarizes published works of interest. Among those, Dainton and his co-workers made a series of comprehensive studies^(10,12-15) to elucidate the reaction mechanism and to evaluate the individual rate constants. It was shown that the polymerization follows typical stationary state kinetics at low conversion (less than 10%). The rate constants and activation energies are listed in Table I-2-2 and compared with those for other vinyl monomers.

The rate constants k_p and k_t have been unanimously employed by the following workers and no further studies have been made to obtain these individual rate constants. As compared with other typical vinyl monomers, it can be seen that k_p is exceptionally large and k_t rather low. In fact, the ratio k_p/k_t exceeds that reported for any other monomer⁽¹⁹⁾ indicating a formation of very high molecular weight polymer.

Various aspects of the polymerization rate expression and reaction mechanism will now be described.

Table I-2-1 List of Kinetic Studies of Acrylamide Polymerization in Water

Workers	Temp. T (°C) Monomer M ₀ (mol/l) Initiator	Conversion (Method and range)	Molecular Wt. (Method and range)	Rate Expression	Remarks
Schulz et.al (20)	T = 50-90 M ₀ = 0.2-0.8 γ-ray, (NH ₄) ₂ S ₂ O ₄ H ₂ O ₂ , H ₂ O ₂ -Fe II Ultrasonic Waves		Viscometry [η] _{20°C} = 0.04-2.0	R _p ∝ M _I ^{1.35} I _{abs} ^{0.22}	Different methods of initiation were tested. Relation between R _p vs. [η] was sought for dif- ferent initia- tions.
Collinson, Dainton and McNaughton (12)	T = 25-40 M ₀ = 0.1-2.0 x-ray, γ-ray	Dilatometry < 10%	Viscometry M _n = 0.7-6.0 x 10 ⁶	R _{po} ∝ M _I ^{1.0} I _{abs} ^{0.5}	To obtain R _p dependence on M and I _{abs} k _p ² /k _t was evaluated at 25°C.
Collinson, Dainton and McNaughton (10)	T = 25 M ₀ = 0.01 - 0.5 x-ray, γ-ray in presence of Fe ^{III}	Dilatometry < 10%	Viscometry M _n = 0.1 - 3.5 x 10 ⁵	R _{po} ∝ M _I ^{1.0} I _{abs} ^{1.0} at Fe ^{III} > 10 ⁻³ (mol/l)	Linear termina- tion by Fe ^{III} was concluded. The relation between [η] vs. M _n was obtained.
Dainton and Tordoff (13)	T = 25 M ₀ = 0.1 - 0.6 H ₂ O ₂ + hv	Dilatometry < 10%	Viscometry M _w = 3.5-7.0 x 10 ⁶	R _{po} ∝ M _I ^{1.0} C ^{0.5}	Rotating sector method was used to obtain k _p /k _t . Transfer rate constants k _{fm} , k _{fc} were evalu- ated.

Table I-2-1 List of Kinetic Studies of Acrylamide Polymerization in Water

Workers	Temp. T (°C) Monomer M ₀ (mol/l) Initiator	Conversion (Method and range)	Molecular Wt. (Method and range)	Rate Expression	Remarks
Suen, Jen and Lockwood (37)	T = 50 M ₀ = 0.3 - 1.1 C10 ₃ - S0 ₃ (C ₁) (C ₂)	Bromine titration, up to 50%	Viscometry M _n = 0.4-1.2 x 10 ⁶ (at conversion >50%)	$R_p \propto \frac{M^{2.5}}{M_o^{1.5}} \times (C_1 \cdot C_2)^{0.5}$	To obtain kinetics by C10 ₃ - S0 ₃ initiation. Conversion followed the rate expression to 50%.
Rodriguez and Givey (38)	T = 30 M ₀ = 0.4-2.0 S20 ₈ - S20 ₅ (C ₁) (C ₂)	Bromine titration, up to 50%	Viscometry M _n = 0.2-3.0 x 10 ⁵ (at ~ 100% conversion)	$R_p \propto \frac{M^{2.5}}{M_o^{1.5}} \times (C_1 \cdot C_2)^{0.5}$	To obtain kinetics of S20 ₈ - S20 ₅ initiation. Conversion followed the rate expression to 50%.
Cavell (21)	T = 25 M ₀ = 0.3 - 0.6 ACV	Dilatometry < 10%	Viscometry M _w = 5.0 - 7.0 x 10 ⁶	$R_{p0} \propto M^{1.0} C^{0.5}$	To obtain kinetics of ACV initiation. k _{fm} /k _p was evaluated.
Cavell, Gilson and Meek (22)	T = 15-25 M ₀ = 1.0 ACV in presence of F _e (C10 ₄) ₃	Dilatometry, gravimetry < 10%	Not done	$k_f C_i = \frac{k_f F_{III}}{k_p M_p} \cdot R_{p0} + k_t \cdot \left(\frac{R_{p0}}{k_p}\right)^2$	Effect of the presence of F _e (C10 ₄) ₃ in ACV initiated polymerization was studied.

continued.....

Table I-2-1 List of Kinetic Studies of Acrylamide Polymerization in Water

Workers	Temp. T (°C) Monomer M ₀ (mol/l) Initiator	Conversion (Method and range)	Molecular Wt. (Method and range)	Rate Expression	Remarks
Cavell and Gilson (23)	T = 25 M ₀ = 1.0 ACV in presence of FeCl ₃	Dilatometry, gravimetry < 10%	Viscometry M _w = 1.0 - 3.0 x 10 ⁵	$R_{po} = \left\{ \frac{k_p M_0}{k_4 \cdot F_{Cl_3}} \right\}^x$ (k ₁ · F _{Cl₃} + f k _i C)	Effect of the presence of FeCl ₃ in ACV initiated polymerization was studied.
Riggs and Rodriguez (34)	T = 30-50 M ₀ = 0.05 - 0.4 K ₂ S ₂ O ₈	Dilatometry up to 80%	Viscometry M _n = 0.5 - 10 x 10 ⁵	R _p ∝ M ^{1.25} C ^{0.5}	To obtain kine- tics by K ₂ S ₂ O ₈ initiation. Conversion fol- lowed the rate expression to 80%
Riggs and Rodriguez (42)	T = 30-50 M ₀ = 0.05 - 1.0 S ₂ O ₈ ²⁻ - S ₂ O ₃ ²⁻ (C ₁) (C ₂)	Dilatometry up to >80%	Viscometry M _n = 0.5 - 4.0 x 10 ⁵	R _p ∝ C ₁ ^{0.5} , no constant exponent on M	To obtain kine- tics of S ₂ O ₈ ²⁻ - S ₂ O ₃ ²⁻ initiation
Venkatarao and Santappa (36)	T = 35 M ₀ = 0.3 UOII + hv	Bromine titration, range not reported	Viscometry Values not reported	R _p ∝ M ^{1.5} I _{abs} ^{0.5}	To obtain kine- tics of UOII + hv
Friend and Alexander (35)	T = 50 M ₀ = 0.1 - 0.5 K ₂ S ₂ O ₈	Dilatometry up to >90%	Viscometry M _n = 0.6 - 2.3 x 10 ⁵ (at 80% con- version)	R _p ∝ M ^{1.25} C ^{0.5}	Influence of surfactants added in the system was studied. Con- version followed the rate expres- sion to 90%.

continued.....

Table I-2-1 List of Kinetic Studies of Acrylamide Polymerization in Water

Workers	Temp. T (°C) Monomer M ₀ (mol/l) Initiator	Conversion (Method and range)	Molecular Wt. (Method and range)	Rate Expression	Remarks
Venkatarao and Santappa (40)	T = 35 M ₀ = 0.5 O ₂ + hv	Bromine titration, allowed to 90% conversion	Fractionation and viscometry. Largest M _n in the fraction ~5 x 10 ⁵	Not obtained, employed the previous (34) result.	Comparison was made between MWD and predicted MWD at 90% conversion.

Note: C catalyst concentration

I_{abs} initiation intensity

+ hv photo-sensitized initiation

Table I-2-2 Comparison of Rate Constants at 50°C

	k_p	k_t	E_p	E_t
Acrylamide ^{(13), (15)}	21,400	1.45×10^7	1.38	0
Styrene ⁽¹⁶⁾	123	6.5×10^7	7.8	2.4
Methylmethacrylate ⁽¹⁷⁾	580	6.9×10^7	4.4	1.0
Vinylacetate ⁽¹⁸⁾	2,640	11.7×10^7	7.3	5.2

(k_p and k_t (l/mol.sec), E_p and E_t in (Kcal/mol)).

Polymerization Rate Expression

Observed dependence of the rate of polymerization R_p on monomer concentration M and initiator concentration C (or in case of radiation initiation, the radiation intensity I_{abs}) are listed in Table I-2-1. Although the square root dependence of R_p on C was always observed in the absence of a linear terminator, the dependence of M differed significantly (exponent of 1.0 to 2.5) depending upon the particular mode of initiation used. Dainton et.al.^(10,12,13) obtained the simplest form $R_p \propto M^{1.0} I_{abs}^{0.5}$ for their x-ray, γ -ray and photoinitiated polymerization attributing the quite different relation previously obtained⁽²⁰⁾ to a presence of impurities and diffusion control at high conversion. The rate dependence of monomer to the first power and square root of initiator is what classical kinetic theory predicts. However with initiators, except for the works of Cavell and his co-workers⁽²¹⁻²³⁾ the rate expressions differed significantly from the above monomer dependence and can not solely be attributed to impurities. In fact, monomer dependence of order between 1.0 and 1.5 has been reported with other vinyl monomers using initiators.⁽²⁴⁻²⁸⁾ These have been explained in terms of monomer

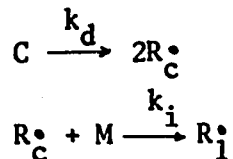
interaction in the initiation step or by a change in the termination step rather than assuming an abnormality in the propagation step.⁽²⁹⁾ Cavell's confirmation of Dainton's rate expression using 4, 4' azobis-4-cyanovaleric acid (ACV) is very interesting as this initiator was the one chosen for the present study. Nalco Chemical Company (Chicago, Illinois) recommended this initiator as one of potential commercial importance. The same initiator when used for styrene polymerization in dimethylformamide⁽²⁷⁾ did not exhibit the first order dependence of R_p on M , but again the order varied from 1.0 to 1.5 depending upon the monomer concentration. The decomposition rate constant k_d of ACV was reported to be 8.97×10^{-5} (1/sec.) at 80°C with an activation energy of 34 (Kcal/mol).⁽³⁰⁾ Cavell and Gilson's data at 25°C for $f \cdot k_d$ where f is the efficiency factor of the initiation was about six times larger than k_d calculated using this activation energy and a reason for the discrepancy was not given.

Reaction Mechanism

A general reaction scheme developed for free radical polymerization has been applied to acrylamide polymerization. The general scheme has been described in detail in texts by Bamford et.al.⁽³¹⁾, Bevington⁽²⁹⁾ and North⁽³²⁾. Among many possible elementary reactions proposed in the general reaction scheme, the following set of reactions are believed to be significant for acrylamide polymerization in water.

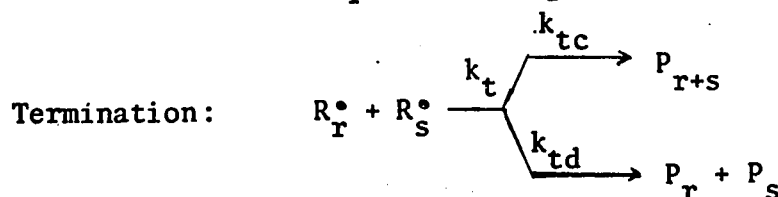
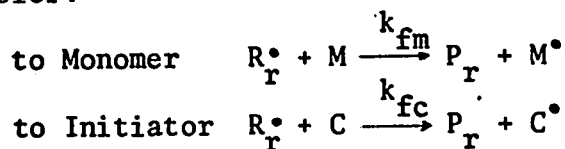
Initiation: By radiation or with an initiator $\rightarrow R_1^\bullet$

For example by ACV,



Propagation: $R_r^\bullet + M \xrightarrow{k_p} R_{r+1}^\bullet$

Transfer:



$$(k_{tc} + k_{td} = k_t)$$

The total radical concentration in this scheme with stationary state assumption leads to an expression

$$R^\bullet = (2f k_d C / k_t)^{0.5}$$

where f denotes the initiation efficiency of the initiator radical R_c^\bullet .

Therefore the rate of polymerization is given by

$$R_p = k_p M R^\bullet = \left(\frac{k_p^2}{k_t} \right)^{0.5} (2f k_d C)^{0.5} M$$

agreeing with the experimental relation obtained by Cavell⁽²¹⁾ and by Dainton et.al^(10,12,13).

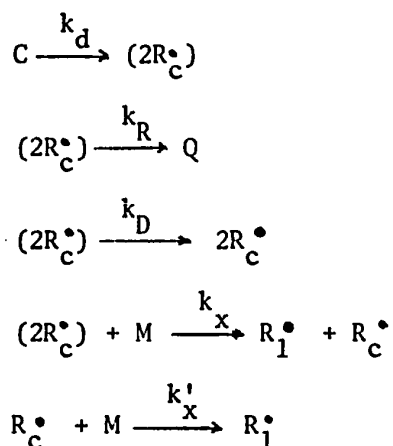
Monomer dependence of the rate of order between 1.0 and 1.5 has generally been explained using a more complicated initiation mechanism leading to a monomer dependent initiation rate. A reduction in the rate constant for termination with conversion, a phenomenon associated with high polymer concentrations and limitations of translational and segmental diffusion, could explain the monomer dependence. Primary radical termination might also be involved. However, the latter would lead to a deviation from a square root dependence of the initiator concentration, $R_p \propto C^{0.5}$. The often observed square root dependence in acrylamide polymerization eliminates this possibility. Primary radical termination would also lead to reduction in molecular weight.

In general, the initiation mechanisms leading to a monomer dependent initiation rate fall into two categories. The first is called "complex theory", the other "cage effect". Schulz and Husemann⁽²⁴⁾ have shown that the polymerization rate of styrene and methylmethacrylate initiated by benzoyl peroxide can be expressed by

$$R_p \propto C^{0.5} \cdot M \cdot \left(\frac{K \cdot M}{1 + K \cdot M} \right)^{0.5}$$

To obtain this, it was assumed that the initiator and monomer exist in equilibrium with a complex (equilibrium constant K in the above) which rearranges to give the first radical unit in the growing chain (complex theory). Later, Matheson⁽³³⁾ gave an explanation to the above using a diffusion process of primary radicals competing with the reaction with

monomer. The initiator molecules in solution are imagined as existing at a site surrounded by a barrier of neighbouring solvent molecules, this is termed solvent cage. The decomposition of the initiator gives rise to two radicals in the same solvent cage. They may then react with each other, react with other molecules or diffuse out of the cage (cage effect). The kinetic consequence can be described as follows⁽³²⁾ by denoting radicals trapped in a solvent cage by symbols in parenthesis and letting Q represent either a waste product or the original initiator molecule.



With the assumption that $k_D \ll k_x M$, this leads to an expression

$$R_p \propto C^{0.5} \cdot M \cdot \left(\frac{M}{k_R/k_x + M} \right)^{0.5}$$

which is identical to the form derived from the complex theory if k_R/k_x is replaced by $1/K$. The reason why an explanation using the cage effect was proposed is that there is no experimental evidence of a complex and that the value K showed the complex to be more stable at higher temperature which is unrealistic.

Riggs and Rodriguez⁽³⁴⁾ applied both theories with the rate expression $R_p \propto C^{0.5} M^{1.25}$ obtained in acrylamide polymerization initiated by potassium persulfate. Though no conclusive evidence was found, they favoured the latter explanation from the point of view of the activation energy expected for complex formation. Their rate dependence itself was later confirmed by Friend and Alexander⁽³⁵⁾. On the other hand, the complex theory was applied apparently successfully in uranyl ion photo-sensitized acrylamide polymerization.⁽³⁶⁾

Suen et al.⁽³⁷⁾ proposed a quite different explanation from the above two. They postulated the existence of "free monomer" and assumed that part of the monomer is adsorbed by polymer thus becoming inactive for propagation. However, this was rejected by Rodriguez and Givey⁽³⁸⁾ who added dead polymers to their initial reaction systems and observed that the rate decrease due to the dead polymer was greater than that predicted by the free monomer theory.

The significance of transfer reactions to monomer and to initiator have been evaluated using molecular weight measurements. Although the transfer reactions do not alter the overall rate expression, their presence lowers the molecular weight in the following manner:

$$\frac{1}{\bar{r}_n} = \frac{(2k_{td} + k_{tc})(2fk_d C)^{0.5}}{2(k_{tc} + k_{td})^{0.5} \cdot k_p} \cdot \frac{1}{M} + \frac{k_{fm}}{k_p} + \frac{k_{fc} C}{k_p M}$$

In the hydrogen peroxide photo-sensitized polymerization, Dainton and Tordoff⁽¹³⁾ found that the ratio $k_{fm}/k_p = 1.2 \times 10^{-5}$ and k_{fc}/k_p (to H_2O_2) = 5×10^{-4} at 25°C from the observed dependence of \bar{r}_n on C at fixed monomer concentration. Later, the magnitude of the transfer to monomer was found

similar, 1.6×10^{-5} (21) or 2.0×10^{-5} (23) in ACV initiated polymerization. Transfer to ACV was of negligible importance since \bar{r}_n was independent of the initiator concentration (23). Transfer to dead polymer was studied (7) by radio tracer technique and it was concluded that it is negligible at the reaction temperature of 50°C, while at 78°C, a significant amount of branching was observed indicating the importance of transfer to dead polymer.

As far as the termination step is concerned, there is evidence that it is mostly via disproportionation. In the effort to prepare monomer-free polyacrylamide, it was found impossible to eliminate the last trace of unsaturation (39). With a repetition of precipitation and solution in acetone and in water respectively, the residual unsaturation remained practically constant after one or two precipitations. Then assuming that the termination is by disproportionation, number-average molecular weight was estimated from the value of the unsaturation. This was close to the number-average molecular weight measured by viscometry. Later, Venkatarao and Santappa (40) analyzed molecular weight distribution by fractionation and it was shown that the disproportionation gave better agreement between measured and predicted molecular weight distributions than did termination by recombination.

The validity of the kinetic scheme to conversions as high as 80-90% has been shown (34,35,40) from the fact that the measured conversions agreed well with predicted values up to these high conversions. However, no measurements of molecular weight change with reaction time were made; they were measured only at the final conversions. Also these observations were made with monomer concentrations less than 0.5 (mol/l)

where the molecular weights of the product polymers were in the order of 10^5 .

It should be mentioned here that all of the so far described studies were made in small batch reactors. Suen, Shiller and Russel⁽⁴¹⁾ made a laboratory scale continuous process for acrylamide polymerization. Although no detailed kinetic study was made with this process, it was reported that the reaction conditions can be held constant within narrow limits, a unique character that the batch process can not give, thus enabling the assessment of the effect of individual variables such as temperature, initiator concentration and chain transfer agent concentration at higher conversions.

I-2-3 Analytical Techniques for Conversion and Molecular Weight

Conversion measurements reported for acrylamide polymerization include gravimetry, dilatometry and bromine or iodine double bond titration for residual monomer, among which dilatometry is most often employed.

Dilatometry makes use of volume contraction as monomer is converted to polymer. Therefore, it requires a priori knowledge of the volume contraction factor at specified reaction conditions. This technique is very powerful in measuring initial rate of polymerization. Also the existence of an induction period if any could easily be detected. It's application to high conversion (80%) has been shown^(34,42) but it is not applicable for the reaction system that involves the formation of gas bubbles (often N_2 or CO_2 from the decomposition of initiator) in the reaction mixture. The accuracy of this method in conversion measurements is not reported, but the initial rate of

polymerization obtained by this technique has been claimed to be within 10% error.⁽⁴³⁾

Gravimetry on the other hand is applicable to the entire range of conversion and is well suited when the isolation of product polymer is required for later use. However, it requires a considerable amount of reaction mixture to precipitate out a measurable quantity of polymer. Care must be taken so that smaller molecular weight polymer is not lost during polymer precipitation. The accuracy of this technique as applied to bulk polymerization of styrene has been reported as $\pm 1.0\%$ in conversion.⁽⁴⁴⁾

Bromine or iodine double bond analysis for the residual monomer is also applicable in the entire range of conversion and may be well suited for conversion measurements with small samples. However, this technique may be too tedious to carry out a large number of measurements.

Average molecular weight analysis in the kinetic studies previously described has mostly been carried out using viscometry. The range covered by this method extends to an intrinsic viscosity of 20 ($\bar{M}_n \sim 7 \times 10^6$). Most of the recent studies make use of the intrinsic viscosity vs. average molecular weight relationships, Eq. I-2-2 or Eq. I-2-3. Eq. I-2-3 was derived for polydisperse samples from kinetic measurements in which the exclusive linear termination was assured.⁽¹⁰⁾ Simultaneous use of these equations have been made^(37,38) to evaluate both \bar{M}_n and \bar{M}_w from a single $[\eta]$ value though this would prefix the polydispersity of the sample polymer. In this case a question arises as to which of the equations yields the correct average molecular weight.

Application of light scattering measurements is reported for polyacrylamide of \bar{M}_w $2-7 \times 10^5$ (38) and of $\bar{M}_w \sim 10^6$ (5). However, the number of samples analyzed by this method is limited and detailed information is not available.

Molecular weight distribution has been obtained by fractionation⁽⁴⁰⁾ and by electron microscopy.^(45,46) No application of gel permeation chromatography has been reported.

Measurement of molecular weight averages or distribution is very difficult for the molecular weight range of a few million or greater. However, a recent report⁽⁴⁶⁾ has shown that electron microscopy works well for this difficult, extremely high molecular weight range.

I-3 EXPERIMENTAL

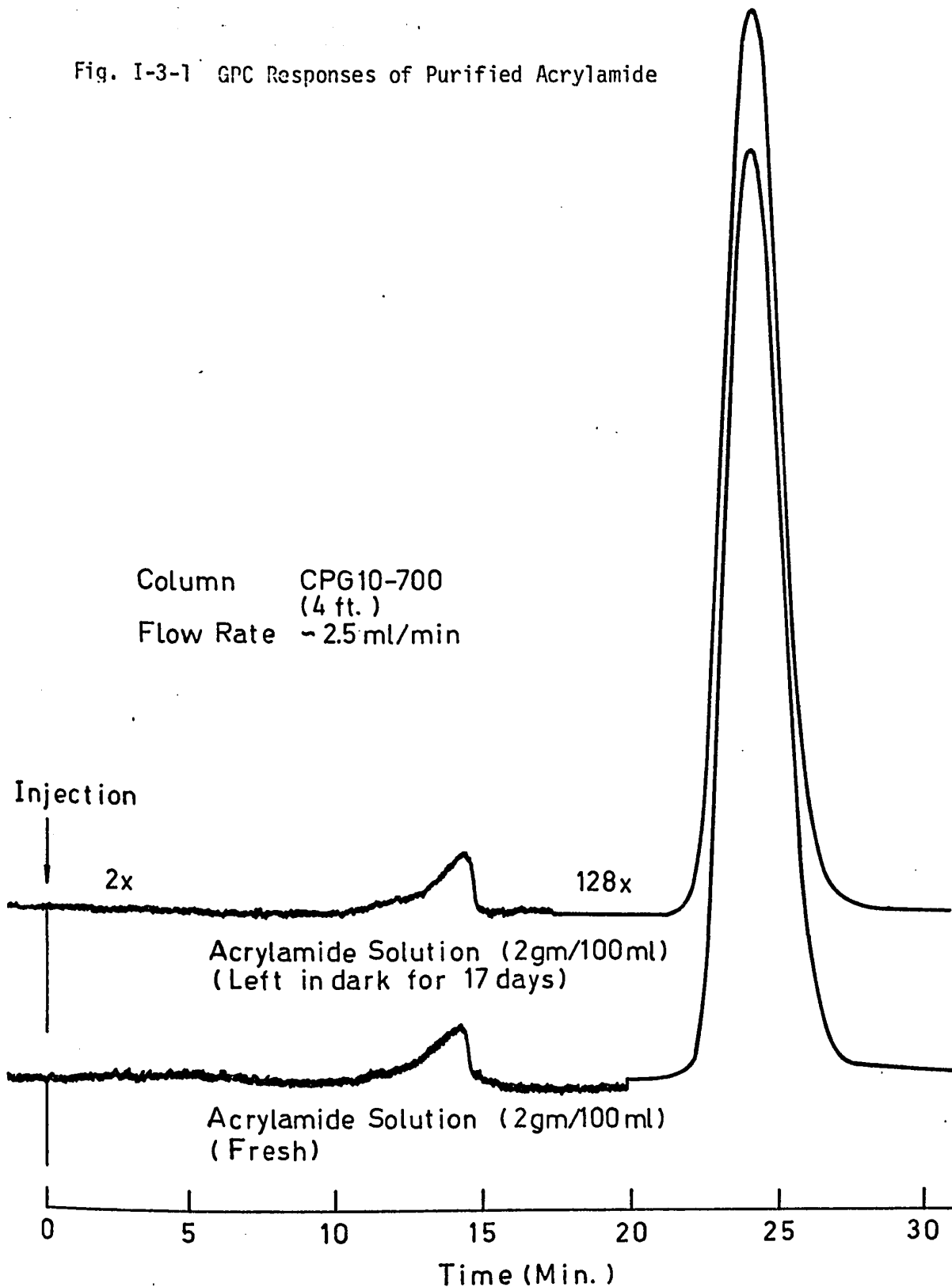
I-3-1 Reagents

Acrylamide was supplied by Nalco Chemical Company Limited, Chicago, Illinois. This technical grade monomer contains an appreciable amount of impurities which do not dissolve in chloroform as well as some visible dust particles. It was therefore twice recrystallized from chloroform⁽¹³⁾, first dissolving the acrylamide at 50°C and removing undissolved impurities by filtration. The filtrate was then cooled in an ice-bath with precipitated solids washed with benzene and dried under vacuum at room temperature. Large flakes of crystalline acrylamide thus obtained were crushed into powder in a porcelain mortar and again dried under vacuum for 24 hours to further remove the remaining solvents. The acrylamide purified in this manner had a melting point of 84.3 ± 0.5°C. It was stored in a dessicator over CaSO₄.

An aqueous solution of the acrylamide was injected into a GPC (Waters ALC Model 201) to check for the presence of polymeric impurities. This was done for the freshly prepared solution and for the same solution kept in dark at room temperature over the period of 17 days. The results are shown in Fig. I-3-1. It was found that the purified monomer contains some polymeric impurities of less than 0.1% and that no polymerization takes place in the aqueous solution of the monomer at room temperature when kept in the dark.

The initiator, 4, 4' azobis-4-cyanovaleric acid,

Fig. I-3-1 GPC Responses of Purified Acrylamide



$\text{HOOC} - \text{CH}_2 - \text{CH}_2 - \text{C}(\text{CH}_3)(\text{CN}) - \text{N} = \text{N} - \text{C}(\text{CH}_3)(\text{CN}) - \text{CH}_2 - \text{CH}_2 - \text{COOH}$, (ACV) was purchased from Aldrich Chemical Company Inc., Montreal, Quebec. It was purified as follows^(43,47) The ACV was suspended in water at room temperature and sodium bicarbonate was added until the solid just dissolved. The solution was then acidified with 1N HCl until it was slightly acid causing precipitation of the ACV. The solid was recovered by filtration on a sintered glass filter and was washed with ice-cold water. It was dried under vacuum at room temperature for 24 hours. The yield of the purified ACV was nearly 30% agreeing with the reported procedure.⁽⁴³⁾ This ACV decomposed rapidly at $129 \pm 0.5^\circ\text{C}$ rather than melting. It was stored in a fridge in an air tight bottle before use.

Water used for preparing aqueous solutions of reagents and for final rinsing of ampoules was triply distilled water with the final distillation made using potassium permanganate. The conductivity of this water was less than 1.2×10^{-6} mho.

The following reagents were used as received; chloroform (Malinckroft, Analytical Reagent), benzene, methanol, potassium permanganate (Fisher, certified) and hydroquinone (Eastern Chemical)

I-3-2 Analytical Techniques

Conversion of monomer to polymer was measured gravimetrically. The total reaction mixture in an ampoule was first diluted 10 to 100 times depending upon conversion by adding water together with a few drops of aqueous solution of hydroquinone⁽³⁸⁾ (~ 0.1 gm/l). Then the solution was slowly poured into methanol of at least a ten-fold excess while stirring. The precipitated polymer was filtered on a sintered glass

filter (~10 μ) and dried under vacuum at 50°C for 24 hours. Conversion was calculated as the weight fraction of the recovered polymer to the weight of monomer initially present. Later, the conversion was measured by injecting the diluted reaction mixture into a GPC and measuring the area fraction of the polymer peak. This permitted the rapid measurement of conversion with a much smaller sample size, permitting the use of smaller ampoules. This is advantageous with regard to temperature control. The detailed explanation of this is reported in Part II-4-2.

The number average molecular weight of precipitated polymers were calculated from measured intrinsic viscosities using an empirical relation $[\eta] = 6.80 \times 10^{-4} \bar{M}_n^{0.66}$ (10). Weight-average molecular weight was also calculated from the intrinsic viscosity using Eq. I-2-1 and Eq. I-2-2. Viscosity measurements are reported in Appendix I-1.

Light scattering measurements were carried out for one sample to obtain \bar{M}_w independently. This is reported in Appendix I-2.

Molecular weight distributions were analyzed by electron microscopy, the details of which are given in Appendix I-3, and by gel permeation chromatography (See Part II-4-3).

I-3-3 Apparatus and Procedures

Polymerization reactions were carried out in Pyrex glass ampoules of three different sizes. For gravimetric determination of conversions, the larger two sizes (O.D. 12 mm and O.D. 15 mm) equipped with a tapered glass joint on one end were used. The largest one was used for a run made with a monomer concentration of 0.28 (mol/l). This run was done to obtain small molecular weight polymer samples. The neck of the

ampoules was made of thick walled glass which enabled easy sealing with a torch. The smallest ampoules (O.D. 6 mm) were used when conversion measurements were carried out by GPC. In this case the open end of the ampoule was connected to a 3/16" tygon tube and sealed by a pinch cock. The actual dimensions of the three ampoules are shown in Fig. I-3-2. The use of O.D. 9 mm ampoules has been reported to be satisfactory in obtaining isothermal polymerization of styrene⁽⁴⁴⁾. This should also be true for the present experiments considering the rate of polymerization, heat of reaction and monomer concentrations used. In fact, the measured conversions in the larger two ampoules did not show any significant difference from that obtained in the smallest ampoules. This will be elaborated upon later.

The apparatus built for deaeration of monomer and catalyst solutions is shown in Fig. I-3-3. Freeze and thaw technique commonly used for deaeration of an ampoule with a reaction mixture was found unsuitable for acrylamide-ACV since a considerable polymerization took place during the thaw period. The apparatus consists of a vacuum line, two tanks (25 ml burettes with ice-jacket) holding monomer and initiator solutions, and a nitrogen purification line. The vacuum pump used was a single stage reciprocal type giving absolute pressure down to 10^{-2} mm Hg. Nitrogen was introduced over heated (-300°C) copper wire in order to remove impurity oxygen, then it was passed through CaSO_4 drier. This was used as an inert gas to deaerate the monomer and initiator solutions, and to fill the ampoule. The deaeration procedure is as follows.

- (1) Charge monomer and initiator solutions of known concentration into ice-cold tanks A and B.

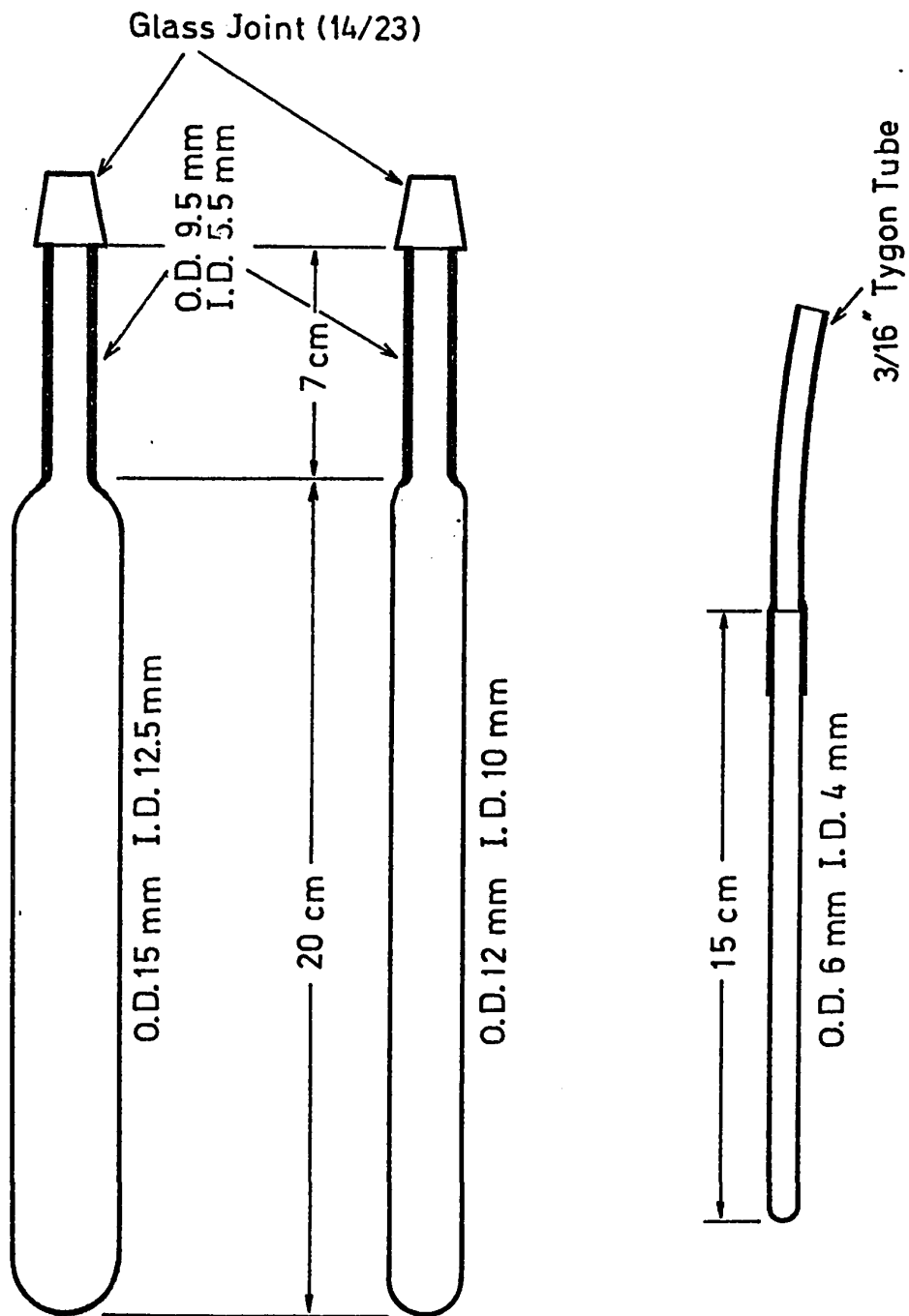


Fig. I-3-2 Dimensions of Pyrex Ampoules Used

A Monomer Tank
B Initiator Tank
C₁-C₁₁ Stop Cock

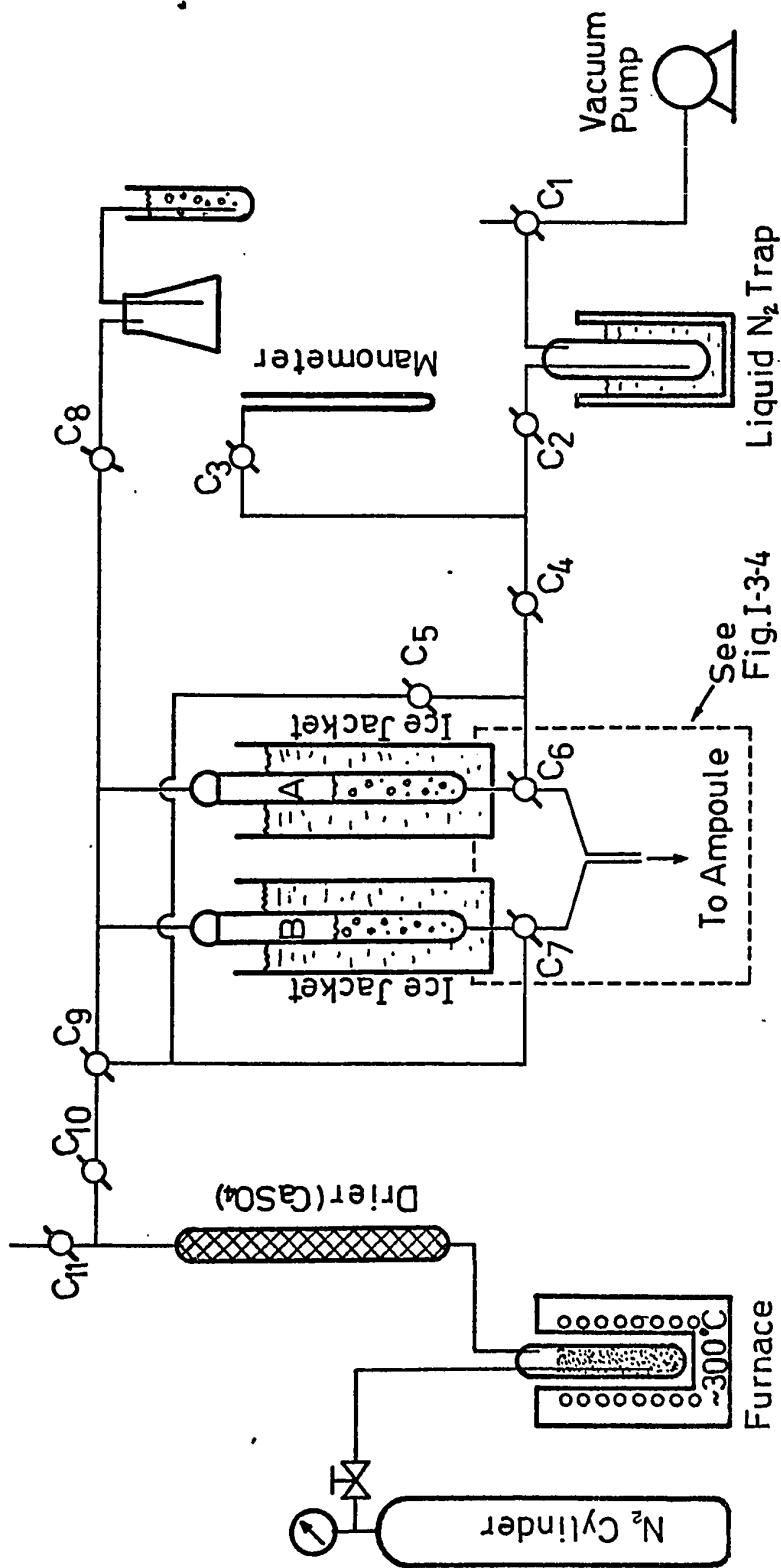


Fig. I-3-3 Schematic Diagram of Deaeration Apparatus

See Fig. I-3-4

- (2) Replace the gas in the system with the purified nitrogen by applying vacuum first and refilling with nitrogen. Repeat this five times.
- (3) Bubble nitrogen through monomer and initiator solutions for 1 hours.

Deaeration period of 75 min. by nitrogen⁽³⁶⁾ or 15 min. by carbon dioxide⁽³⁷⁾ has been reported successful in eliminating an induction period.

Fig. I-3-4 shows the ampoule connection part in the deaeration apparatus. The above deaerated solutions were introduced into an ampoule as follows.

- (1) Connect the ampoule to the system and hold it in an ice-bath.
- (2) Displace the air in the ampoule with the purified nitrogen five times.
- (3) Introduce the desired amount (3 ~ 7 ml) of the monomer and initiator solutions.
- (4) Seal off the neck of the ampoule.

The ampoule is now shaken a few times and transferred into a thermostatted reaction bath. With the smallest ampoules, the two deaerated solutions were first taken into an ice-cold premixer and then introduced into the ampoule and sealed with a pinch cock under nitrogen atmosphere.

A test was made to check for prepolymerization before transferring the ampoules into the reaction bath by breaking the seal and analyzing for polymer formation. Prepolymerization was found negligible.

The reaction was quenched at a desired time by thrusting the ampoule into liquid nitrogen.

- C₆, C₇, C₁₂ Stop Cock (1 mm Bore)
- L₁, L₂ Teflon Tube (O.D. 2 mm, I.D. 1 mm)
- L₃, L₄ Polyethylene Tube (O.D. .082", I.D. .062")

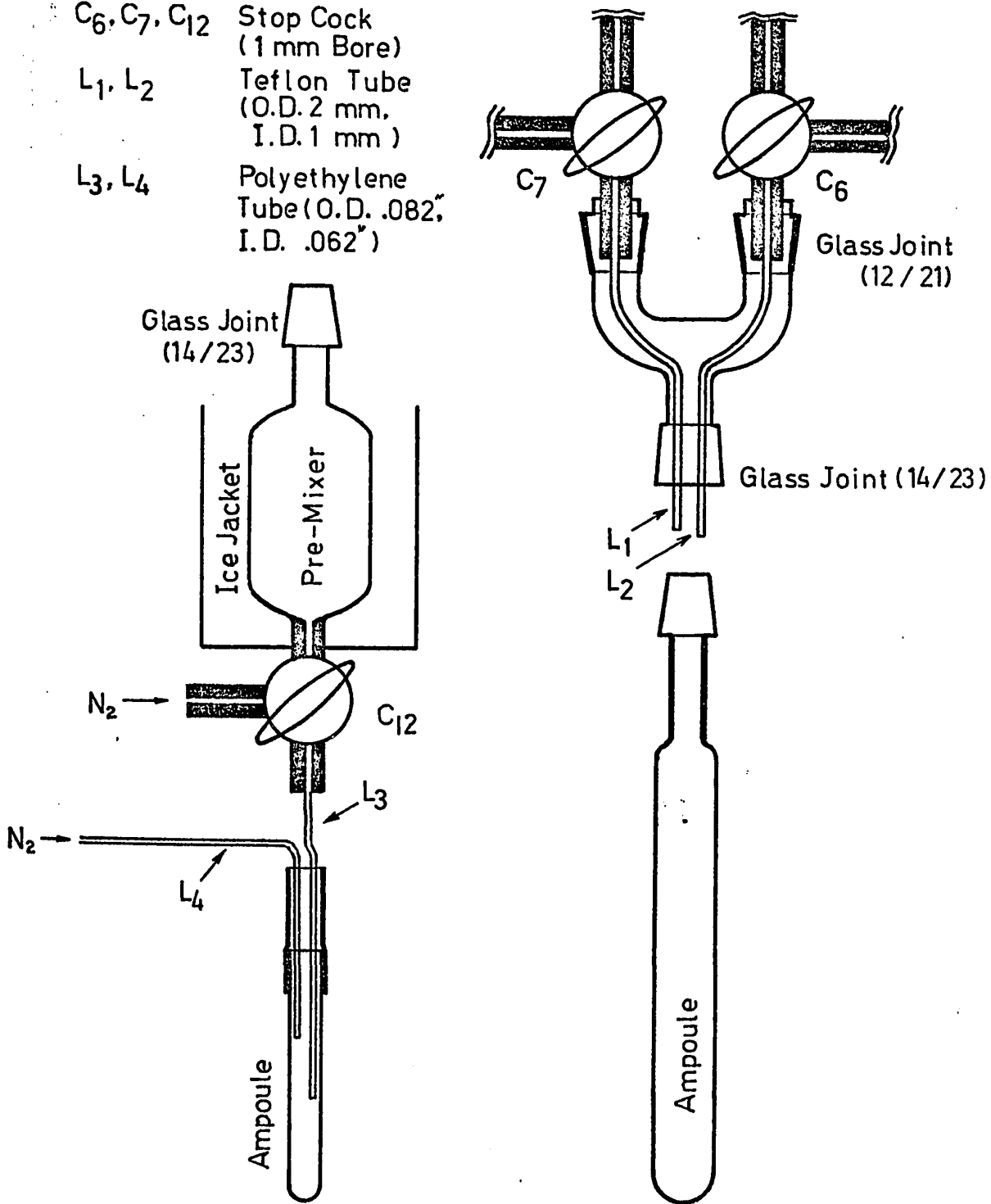


Fig. I-3-4 Ampoule Connection to the Deaeration Apparatus

I-3-4 Experimental Conditions and Results

Polymerizations were carried out at temperatures of 25-50°C, monomer concentrations, 0.281-2.252 (mol/l) and initiator concentrations, $1.78 - 7.14 \times 10^{-4}$ (mol/l). Most experiments were done at 50°C where the reaction proceeds at a rate of commercial interest. The experimental conditions of the runs made are summarized in Table I-3-1. The runs made were of two kinds; initial rate runs and continuous high conversion runs. The initial rate runs were made to obtain reliable initial rate of polymerization, starting several ampoules at once and quenching all of them at one time near conversion of 10%. These runs were designated by the first letter I. The continuous runs, designated by the first letter C, were made to follow the change of conversion with respect to time by quenching the ampoule one after another. The reactions were followed generally to over 90% conversion.

Table I-3-2 and I-3-3 list measured conversions in the initial rate runs and the continuous, respectively. The intrinsic viscosity of the polymer samples analyzed are summarized in Table I-3-4 together with calculated average molecular weights. Predicted values of conversions and number- and weight-average molecular weights in the Tables were obtained from the kinetic scheme described in Section I-4-2.

For conversion measurements or for polymer separation from a reaction mixture, it was necessary to dilute the mixture with water first. However, a difficulty was encountered for the continuous runs carried out with initial monomer concentrations of 1.126 or 2.252 (mol/l), especially at conversions over 30%. The mixture swells when left in

water overnight at room temperature, but it did not dissolve with successive hand-shaking. The reaction mixture obtained at 40°C (Run C4044, 4 hours of reaction time) remained as a swollen mass even after three months. Therefore, the reaction mixtures that did not dissolve with residence overnight in water and hand-shaking were stirred by a magnet to obtain diluted solutions. Heating of the mixture at 90°C caused dissolution of mass within several hours but this was not employed because of the possibility of further reaction⁽³⁹⁾ and possible polymer degradation.

The continuous runs C5011(A), (B), (C) and (D) show reproducibility of conversion obtained by gravimetry. Four replicates at fixed reaction time (1 hour) gave a standard deviation of 2.5% in conversion from the average value, 30.7%. The five replicates of conversion in the initial rate run I2512 measured by GPC gave a standard deviation of 0.97% from the average value of 11.2%. No significant difference between conversions measured by gravimetry and by GPC was observed (Run C5014(A) and (B)).

Number-average molecular weight was found reproducible to $\pm 4\%$ for a particular polymer sample obtained. However, the process involved in polymer recovery, particularly stirring of the reaction mixture for dilution, appeared to introduce a large error. This error was of the order 10 - 15%.

Table I-3-1 Summary of Experimental Conditions

Run No.	Temperature (°C)	Monomer Conc. (mol/l)	Initiator Conc. $\times 10^4$ (mol/l)
I5011, C5011(A), C5011(B) C5011(C), C5011(D)	50	0.563	1.78
I5012	50	0.563	3.56
I5014, C5014(A), C5014(B)	50	0.563	7.14
C5021(A), C5021(B)	50	1.126	1.78
I5024, C5024(A), C5024(B)	50	1.126	7.14
I5044, C5044	50	2.252	7.14
C50S(A), C50S(B)	50	0.281	7.14
I4014, C4014	40	0.563	7.14
C4024	40	1.126	7.14
C4044	40	2.252	7.14
I3014	30	0.563	7.14
I2511	25	0.563	1.78
I2512	25	0.563	3.56
I2514	25	0.563	7.14

Table I-3-2

Summary of Initial Rate Runs

Run No.	I5011	I5012	I5014	I5024	I5044
Reaction time (min.)	15	12	8	8	6
Conversion (by GPC)	.101	.101	.107	.131	.114
	.096	.112	.109	.137	.105
	.092	.106	.109	.121	.111
	.090	.116	.112	.119	.115
		.125	.096	.143	.106
Average Conversion	.095	.112	.107	.134	.110
$R_{p_0}^{(a)}$	5.97×10^{-5}	8.76×10^{-5}	1.25×10^{-4}	3.05×10^{-4}	6.89×10^{-4}
$f \cdot k_d^{(b)}$	9.9×10^{-7}	1.07×10^{-6}	1.08×10^{-6}	1.57×10^{-6}	2.08×10^{-6}

Table I-3-2 continued.....

Run No.	I4014	I3014	I2511	I2512	I2514
Reaction Time (min.)	17	60	180	140	90
Conversion (by GPC)	.079	.117	.100	.099	.101
	.088	.097	.089	.116	.089
	.093	.101	.092	.101	.085
	.082	.115	.092	.120	.094
				.122	.103
Average Conversion	.086	.108	.093	.112	.094
R_{p_o}	4.73×10^{-5}	1.69×10^{-5}	4.85×10^{-7}	7.49×10^{-7}	9.85×10^{-6}
$f \cdot k_d$	1.8×10^{-7}	2.6×10^{-7}	9.32×10^{-9}	1.11×10^{-8}	9.6×10^{-9}

(a) R_{p_o} was calculated by $M_o \times (\Delta x / \Delta t)$ where Δx is the average conversion and Δt is the reaction time.

(b) $f \cdot k_d$ was calculated by $R_{p_o}^2 / 2(k_p^2/k_t) \cdot C_o \cdot M_o^2$

Table I-3-3

Summary of Continuous Runs

Runs: C5011(A), C5011(B), C5011(C) and C5011(D)

<u>Reaction Time (hr.)</u>	<u>Measured Conversion</u>				<u>Predicted Conversion</u>
	(A)	(B) (All by Gravimetry)	(C)	(D)	
0.50	.176	.147	.154	.187 (1)	.177
1.00	.320 (2)	.276	.292	.341 (2)	.314
2.00		.475 (3)	.483 (3)	.503	.507
3.00	.634 (3)	.620	.621	.650 (4)	.632
4.00	.731	.691	.712		.716
5.00	.790 (5)		.787	.763	.775
6.00	.810 (6)		.827		.817
			.854 (8)	.860 (7)	.849

Note: Numbers in parenthesis after conversion values designate polymer samples analyzed for molecular weight. For example, C5011(A)-2 represents the polymer obtained in the run C5011(A) at reaction time of 1 hour.

Table I-3-3 continued.....

Runs: C5014(A) and C5014(B)

Reaction Time (hr.)	<u>Measured Conversion</u>		<u>Predicted Conversion</u>
	(A) (By Gravimetry)	(B) (by GPC)	
0.25	.158 (1)	.173	.177
0.50	.283 (2)	.308	.315
1.00	.487	.506	.509
1.50	.616	.617	.634
2.50	.756	.771	.777
3.50	.856 (6)	.821	.850
5.00	.922 (7)	.897	.908

Runs: C5021(A) and C5021(B)

Reaction Time (hr.)	<u>Measured Conversion</u>		<u>Predicted Conversion</u>
	(A) (both by Gravimetry)	(B)	
0.5	.192 (1)	.190	.211
1.0	.390	.358	.368
2.0	.619 (3)	.620	.578
3.0	.744	.780	.703
4.0	.824 (5)	.850	.782
5.0	.871	.909	.835
6.0	.906 (7)	.927	.870

Table I-3-3 continued.....

Runs: C5024(A) and C5024(B)

<u>Reaction Time (hr.)</u>	<u>Measured Conversion</u>		<u>Predicted Conversion</u>
	(A) (by Gravimetry)	(B) (by GPC)	
0.25	.171	.181	.211
0.50	.369 (2)	.363	.369
1.0	.599 (3)	.627	.579
1.5	.760 (4)		.704
2.0		.838	.784
3.5		.917	.298
5.0		.984	.942

Run: C5044

<u>Reaction Time (hr.)</u>	<u>Measured Conversion</u> (by GPC)	<u>Predicted Conversion</u>
0.25	.220	.238
0.50	.423 (2)	.412
1.0	.694	.634
2.0	.903	.834
3.0	.953 (5)	.911

Table I-3-3 continued

Runs: C50S(A) and C50S(B)

<u>Reaction Time (hr.)</u>	<u>Measured Conversion</u>		<u>Predicted Conversion</u>
	(A) (by Gravimetry)	(B) (by GPC)	
0.25		.135	.142
0.50		.250	.257
1.00	.435 (1)	.447	.429
1.50		.550	.550
2.50	.697 (2)	.708	.700
5.00	.850 (3)	.873	.861

Run: C4011

<u>Reaction Time (hr.)</u>	<u>Measured Conversion</u> (by GPC)	<u>Predicted Conversion</u>
1.0	.172	.153
2.0	.292	.276
4.0	.451	.457
6.5	.612	.604
10.0	.718	.731

Table I-3-3 continued.....

Run: C4014

<u>Reaction Time (hr.)</u>	<u>Measured Conversion (by GPC)</u>	<u>Predicted Conversion</u>
0.5	.163	.154
1.0	.274	.277
2.0	.483 (3)	.458
3.0	.600	.581
5.0	.735	.731
7.0	.810	.809
10.0	.881 (7)	.883

Runs: C4024(A) and C4024(B)

<u>Reaction Time (hr.)</u>	<u>Measured Conversion</u>		<u>Predicted Conversion</u>
	<u>(A)</u>	<u>(B)</u>	
	<u>(both by GPC)</u>		
0.5	.172	.160	.185
1.0	.298	.325	.329
2.0	.524	.562	.529
3.0	.725	.720	.657
5.0	.877	.863	.799
7.0	.914	.909	.870
10.0	.955		.923

Table I-3-3 continued.....

Run: C4044

Reaction Time (hr.)	<u>Measured Conversion</u> (by GPC)	<u>Predicted Conversion</u>
0.5	.198	.213
1.0	.379 (2)	.374
2.0	.657 (3)	.589
3.0	.852	.718
4.0	Not measured (E-1)	.798
5.0	.926	.850
7.0	.962 (6)	.910

Table I-3-4 Summary of Measured Intrinsic ViscositiesPolymer Samples of Initial Rate Runs

Sample (or Run No.)	[η]	Measured Values			Predicted Values	
		$\bar{M}_n \times 10^{-6}$	$\bar{M}_w \times 10^{-6}$		$\bar{M}_n \times 10^{-6}$	$\bar{M}_w \times 10^{-6}$
		(Eq. I-2-3)	(Eq. I-2-1)	(Eq. I-2-2)		
I5011	13.0	3.07	4.39	7.61	3.21	6.41
I5012	12.9	3.03	4.35	7.54	2.86	5.71
I5014	10.8	2.32	3.48	5.76	2.48	4.96
I5024	14.1	3.47	4.86	8.62	3.01	6.01
I5044	15.5	4.01	5.47	9.95	3.51	7.03
I4014	15.0	3.81	5.25	9.47	3.48	6.96
I2511	18.2	5.11	6.68	12.7	5.50	11.1
I2512	18.2	5.11	6.68	12.7	5.38	10.8
I2514	17.3	4.73	6.27	11.8	5.22	10.4

Polymer Samples of Continuous Runs

Sample Code	[η]	Measured Values			Predicted Values	
		$\bar{M}_n \times 10^{-6}$	$\bar{M}_w \times 10^{-6}$		$\bar{M}_n \times 10^{-6}$	$\bar{M}_w \times 10^{-6}$
		(Eq. I-2-3)	(Eq. I-2-1)	(Eq. I-2-2)		
C5011(A)-2	15.3	3.93	5.38	9.76	3.13	6.26
C5011(A)-3	13.6	3.29	4.64	8.16	2.96	5.94
C5011(A)-5	11.9	2.68	3.93	6.67	2.86	5.76
C5011(A)-6	10.9	2.35	3.52	5.84	2.81	5.69

Table I-3-4 Summary of Measured Intrinsic Viscosities continued.....

Sample Code	[η]	Measured Values			Predicted Values	
		$\bar{M}_n \times 10^{-6}$ (Eq. I-2-3)	$\bar{M}_w \times 10^{-6}$ (Eq. I-2-1)	$\bar{M}_w \times 10^{-6}$ (Eq. I-2-2)	$\bar{M}_n \times 10^{-6}$	$\bar{M}_w \times 10^{-6}$
C5011(B)-3	13.4±.3	3.21±0.11	4.56±.13	7.98±.27	3.04	6.08
C5011(C)-3	13.2±.2	3.14±0.07	4.48±.08	7.80±.36	3.04	6.08
C5011(C)-8	12.4	2.86	6.3 (Light Scattering)		2.78	5.63
C5011(D)-1	14.6	3.66	5.07	9.09	3.18	6.36
C5011(D)-2	15.1	3.85	5.29	9.57	3.13	6.26
C5011(D)-4	12.6	2.93	4.22	7.27	2.96	5.94
C5011(D)-7	12.4	2.86	4.14	7.10	2.78	5.63
C5014(A)-1	11.3	2.48	3.68	6.17	2.45	4.90
C5014(A)-2	10.6	2.25	3.40	5.60	2.39	4.78
C5014(A)-6	9.9	2.03	3.12	5.05	2.00	4.12
C5014(A)-7	9.0	1.76	2.77	4.37	1.92	4.01
C5021(A)-1	15.5	4.01	5.47	9.95	3.59	7.17
C5021(A)-3	13.8	3.36	4.73	8.35	3.43	6.87
C5021(A)-5	12.8	3.00	4.31	7.45	3.29	6.62
C5021(A)-7	11.9	2.68	3.93	6.67	3.19	6.46
C5024(A)-2	12.2	2.79	4.05	6.92	2.89	5.79
C5024(A)-3	12.5	2.89	4.18	7.18	2.76	5.54
C5024(A)-4	12.3	2.82	4.10	7.01	2.65	5.36
C5044 -2	12.9	3.03	4.35	7.54	3.38	6.77
C5044 -5	13.2	3.14	4.47	7.80	2.92	6.00
C50S (A)-1	8.9	1.73	2.73	4.29	1.85	3.70
C50S (A)-2	8.5	1.61	2.58	4.00	1.69	3.43
C50S (A)-3	8.3	1.56	2.51	3.86	1.56	3.22
C4014-3	13.1	3.11	4.43	7.71	3.31	6.64
C4014-7	12.0	2.72	3.97	6.75	2.95	6.01
C4044-2	13.9	3.40	4.77	8.44	4.25	8.50
C4044-3	10.5	2.22	3.36	5.52	4.15	8.31
C4044-E1	13.5	3.25	4.60	8.07	4.00	8.03
C4044-6	11.8	2.65	3.89	6.58	3.87	7.83

I-4 DATA INTERPRETATION AND RESULTS

Initial rate runs were first analyzed to obtain a relationship between the initial rate of polymerization R_{p_0} and the monomer and initiator concentrations M_0 and C_0 . Then using this information together with some conclusions obtained by previous workers, the kinetic scheme was elucidated for the initial stage of the reaction. The rate constants required for the calculation of the rate of polymerization and average molecular weights were evaluated also using the initial rate data. Applicability of the kinetic scheme to high conversions was then tested by comparing conversions and number-average molecular weights predicted with those experimentally obtained in continuous runs. Comparisons of molecular weight distributions obtained by GPC or by electron microscopy and those predicted were also made to provide a further consistency test on the proposed kinetic scheme.

In the following treatment of the data, volume contraction was neglected. The volume contraction factor reported is 0.221 ml/gm polymer at 50°C⁽³⁵⁾, which causes maximum 3.5% volume change with 100% conversion in the highest monomer concentration runs.

I-4-1 Initial Rate of Polymerization

Initial rate of polymerization R_{p_0} was calculated as follows from the average values of conversion obtained in the initial rate runs.

$$R_{p_0} = - \frac{dM}{dt} = M_0 \frac{dx}{dt} \approx M_0 \frac{\Delta x}{\Delta t} \quad (\text{I-4-1})$$

where Δx is the average conversion in the reaction time of Δt . Errors introduced by the last approximation is negligible compared to those due to conversion measurements. The R_{p_0} thus calculated had a reproducibility of $\pm 10\%$, and are given in Table I-3-2. Plots of R_{p_0} vs. C_0 and R_{p_0} vs. M_0 are shown in Figs. I-4-1 and I-4-2. It can be seen that the square root dependence of R_{p_0} on C_0 is well followed while a deviation from the first order dependence of R_{p_0} on M_0 is statistically significant. The least-square fit for the latter gave $R_{p_0} \propto M_0^{1.24}$. The observed dependence on M_0 gives faster conversion increase at higher monomer concentration. The deviation from the first order dependence was further clarified when the conversions of continuous runs were compared for the two runs with same C_0 but different M_0 . If $R_{p_0} \propto M_0^{1.0}$, the conversion curves should follow the same course regardless of M_0 .

I-4-2 Kinetic Mechanism and Rate Constants

The experimentally observed deviation from the first order dependence of R_{p_0} on M_0 has often been found with other initiation systems and with other vinyl monomers as was described in Section I-2-2. Again in the present experiments, the observed square root dependence of R_{p_0} on C_0 implies that termination is a bimolecular reaction and that the deviation could be attributed to the initiation rate dependence on monomer concentration.

The dependence of initiation on monomer concentration can be rationalized on the basis of cage effect or of the complex theory.

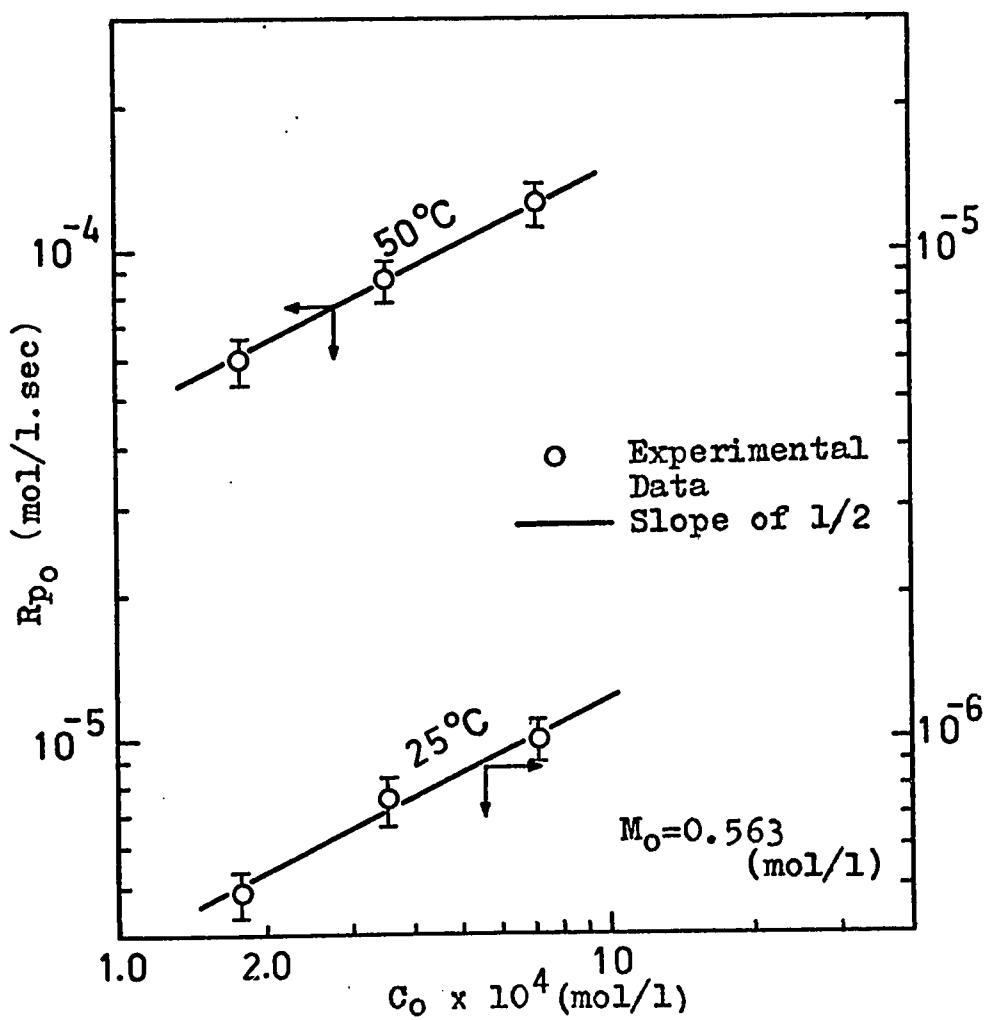
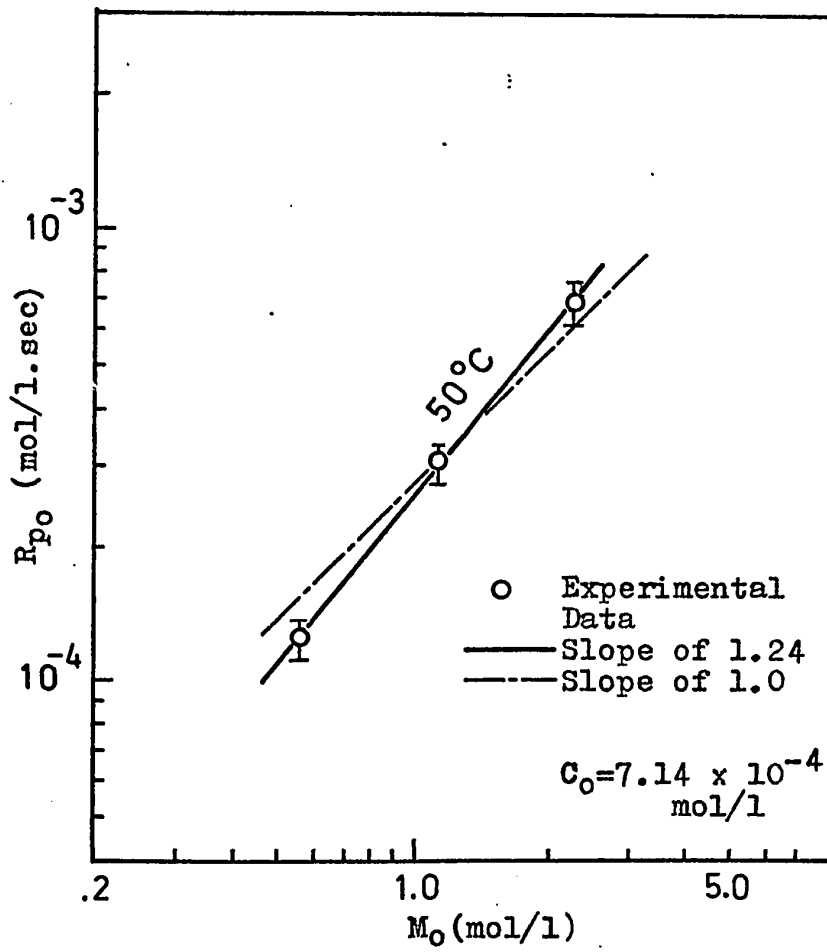
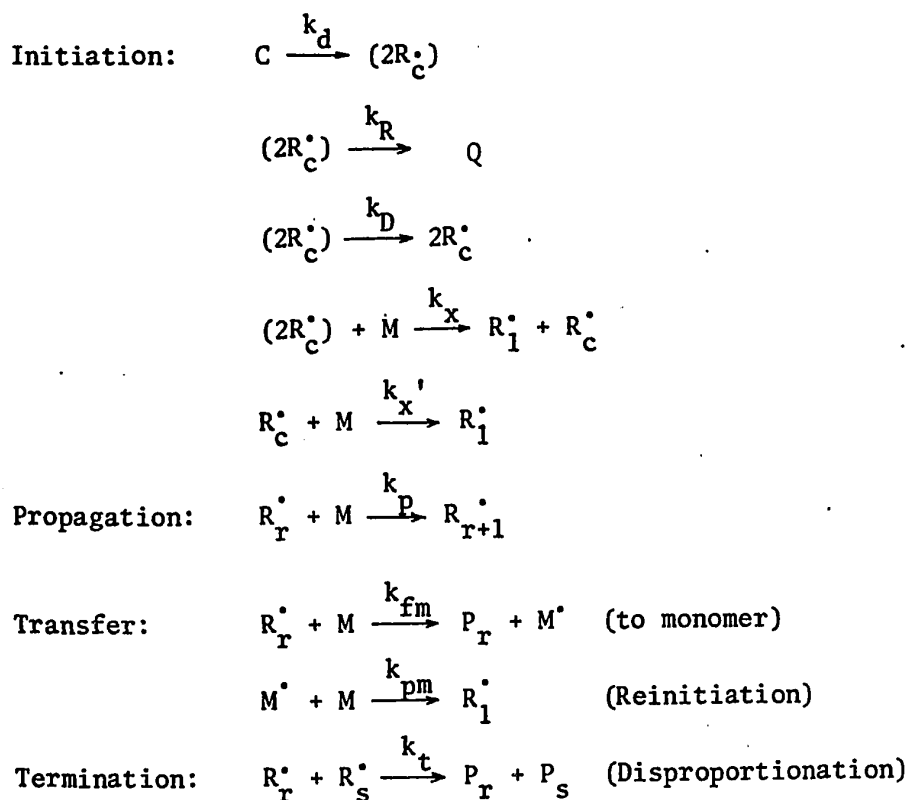
Fig. I-4-1 Dependence of R_{p_0} on C_0 

Fig. I-4-2 Dependence of R_{p_0} on M_0 

Although the concepts differ, an interesting feature is that both explanations lead to the identical rate expression. Our concern here is to predict conversion and molecular weights for which it will soon be shown that only the rate expression for initiation and not the initiation mechanism itself, is required. Using molecular weight data, no preference can be made for either. In the present study, however, the former explanation was employed simply as a vehicle to derive a quantitative expression for initiation rate. The reaction scheme thus considered is described below.



The notations in the above scheme are the same as were used in describing reaction mechanism in Section I-2-2.

Applying the kinetic stationary state assumption and assuming that rate constants are independent of chain length, we may write,

$$\frac{d(2R_c^{\bullet})}{dt} = k_d C - k_R(2R_c^{\bullet}) - k_x(2R_c^{\bullet})M - k_D(2R_c^{\bullet}) = 0 \quad (\text{I-4-2a})$$

$$\frac{dR_c^{\bullet}}{dt} = 2k_D(2R_c^{\bullet}) + k_x(2R_c^{\bullet})M - k_x' R_c^{\bullet} M = 0 \quad (\text{I-4-2b})$$

$$\frac{dR^{\bullet}}{dt} = k_x(2R_c^{\bullet})M + k_x' R_c^{\bullet} M + k_{pm} M^{\bullet} M - k_{fm} R^{\bullet} M - k_t R^{\bullet 2} = 0 \quad (\text{I-4-2c})$$

$$\frac{dM^{\bullet}}{dt} = k_{fm} R^{\bullet} M - k_{pm} M^{\bullet} M = 0 \quad (\text{I-4-2d})$$

A criterion for the validity of the kinetic stationary state assumption has been derived by Bamford et.al.⁽³¹⁾ and is expressed by

$$(I k_t)^{\frac{1}{2}} t \gg 1 \quad (\text{I-4-3})$$

where I is the initiation rate. In the present reaction system, the magnitude of I is $\sim 10^{-10}$ (mol/l·sec.) since $k_d \sim 10^{-6}$ (1/sec) and $C \sim 10^{-4}$ (mol/l), and k_t is $\sim 10^7$ (l/mol·sec). Therefore the assumption can be well justified after a reaction time of a few minutes.

Combination of Eqs. (I-4-2a - d) yields the total radical concentration R^{\bullet} as follows:

$$R^{\bullet} = \left(\frac{2k_d C}{k_t} \right)^{0.5} \left(\frac{k_D + k_x M}{k_R + k_D + k_x M} \right)^{0.5} \quad (\text{I-4-4a})$$

Also the initiation rate can be written

$$I = 2k_d C \left(\frac{k_D + k_x M}{k_R + k_D + k_x M} \right) \quad (\text{I-4-5a})$$

Assuming $k_D \ll k_x M$ which is one extreme case of the two alternative routes that the initiator radical may escape from the cage,

$$R^* = \left(\frac{2k_d C}{k_t} \right)^{0.5} \left(\frac{M}{k_R/k_x + M} \right)^{0.5} \quad (\text{I-4-4b})$$

$$I = 2k_d C \left(\frac{M}{k_R/k_x + M} \right) \quad (\text{I-4-5b})$$

Other extreme cases, i.e., $k_D \gg k_x M$, leads to the independence of I or R^* on M hence $R_p \propto M^{1.0}$, which conflicts with the experimental observation.

It should be worth mentioning here that the expression of Eq. (I-4-5b) is compatible with the conventional expression with the initiator efficiency factor f ,

$$I = 2 f k_d C \quad (\text{I-4-6})$$

by defining

$$f = \frac{M}{k_R/k_x + M} \quad (\text{I-4-6})$$

Now the rate of polymerization can be written

$$R_p = k_p R^* M = \left(\frac{k_p}{k_t} \right)^{0.5} \left(\frac{2k_d C M}{k_R/k_x + M} \right)^{0.5} M \quad (\text{I-4-7})$$

or in terms of conversion,

$$\frac{dx}{dt} = \left(\frac{k_p^2}{k_t} \right)^{0.5} \left(\frac{2k_d C M_o (1-x)}{k_R/k_x + M_o (1-x)} \right)^{0.5} (1-x) \quad (\text{I-4-8})$$

The Eq. (I-4-7) gives $R_p \propto M^{1.0 - 1.5} C^{0.5}$ depending upon the level of M , which is a form which can explain the experimental results.

The instantaneous molecular weight distribution of dead polymer being produced at any time t can be written as follows in terms of chain length r .

$$w(r) = \frac{r}{\bar{r}_n} \exp \left(-\frac{r}{\bar{r}_n} \right) \quad (\text{I-4-9})$$

where \bar{r}_n is the instantaneous number-average chain length and is given by

$$\bar{r}_n = \frac{1}{\left(\frac{k_t}{k_p^2} \right) \frac{R_p}{M^2} + \frac{k_{fm}}{k_p}} \quad (\text{I-4-10})$$

The instantaneous weight-average chain length \bar{r}_w is related to \bar{r}_n .

$$\bar{r}_w = 2\bar{r}_n \quad (\text{I-4-11})$$

The derivation of Eqs. (I-4-9)-(I-4-11) is given in Appendix I-5.

The above forms are particularly convenient since they are given in terms of an easily measurable group R_p/M^2 . However, these do not represent the molecular weight of cumulative dead polymer produced in a reaction time interval of $0 \sim t$, as were measured in continuous runs.

The cumulative dead polymer is composed of some of the dead polymer produced at time instant t for which the above forms are valid and can be obtained from

$$W(r) = \frac{1}{x} \int_0^x \frac{r}{\bar{r}_n} \exp\left(-\frac{r}{\bar{r}_n}\right) dx$$

It is now clear that the conversion and molecular weight distribution is governed by the two groups of rate constants, i.e., (k_p^2/k_t) and (k_{fm}/k_p) , not their individual values when the initiation rate is given. Conversion or rate of polymerization data and number-average molecular weight data are sufficient to evaluate the two groups of the rate constants. Weight-average molecular weight or molecular weight distribution itself, however, would be of great advantage if obtained to make a further test on the validity of the reaction scheme employed.

A plot of $1/\bar{r}_n$ vs. R_{p0}/M_o^2 was made using the data of initial rate runs (both R_{p0} and \bar{M}_n) together with the first point number-average molecular weight data in continuous runs. Fig. I-4-3 shows the plot. From the slope and intercept of the least-square fitted line, (k_p^2/k_t) and (k_{fm}/k_p) were obtained as follows.

	<u>Present Experiment</u>	<u>Literature Value</u> (13,15)
k_p^2/k_t	27.70 (50°C)	31.85 (50°C)
k_{fm}/k_p	1.45×10^{-5} (50°C)	1.22×10^{-5} (25°C)

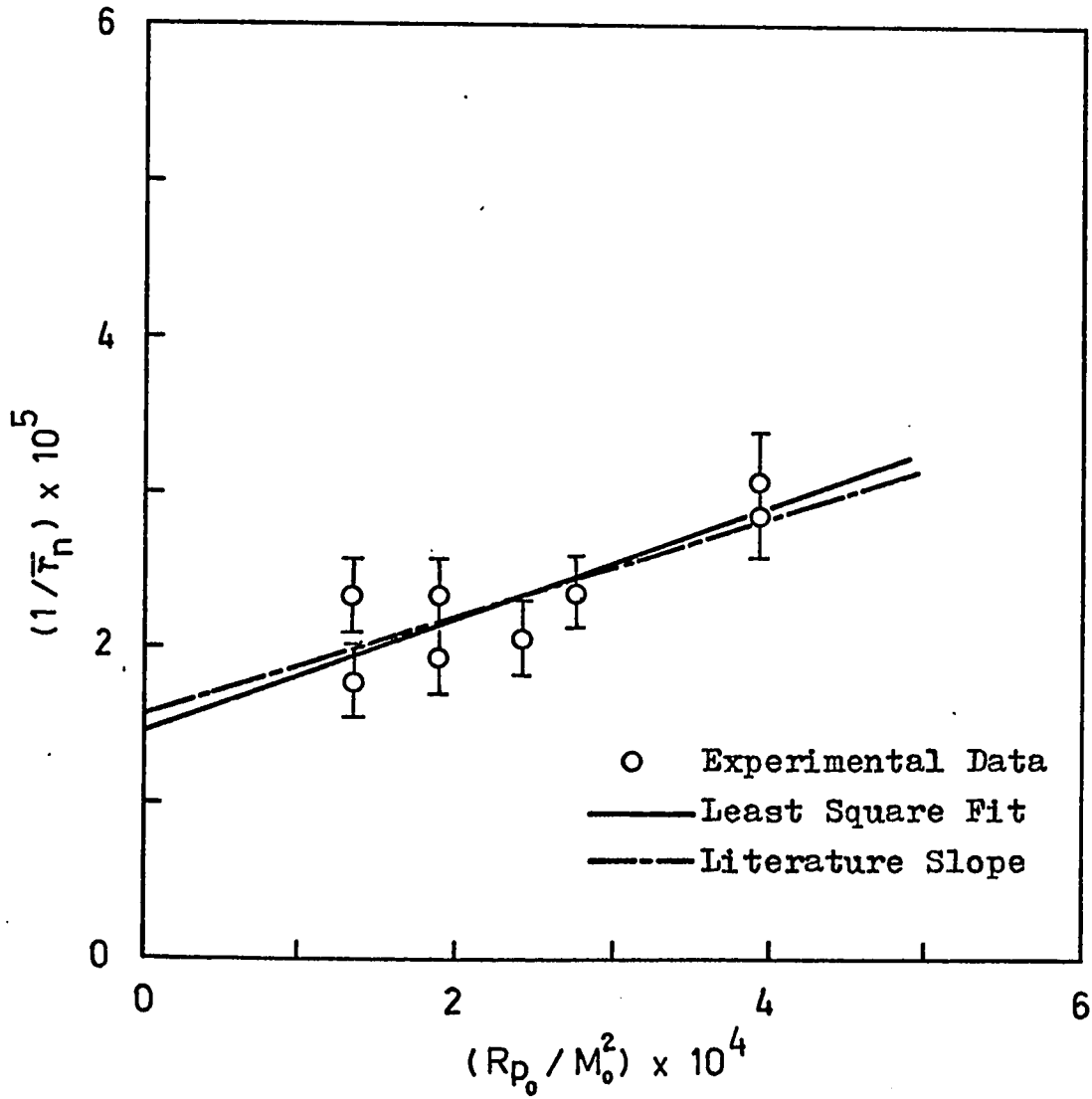


Fig. I-4-3 A Plot of $1/\bar{r}_n$ vs. R_{p_0}/M_0^2

Considering the errors involved in R_{p_0} and \bar{r}_n , the agreement is reasonable. A scatter of data points from the least-square fitted line gives a total variance of 3.85×10^{-11} while the total variance from the best fitting line using the slope given by the literature value^(13,15) is 4.02×10^{-11} (with $k_{fm}/k_p = 1.57 \times 10^{-5}$ in this case). This difference of the variances is not significant at the 1% level. Since (k_p^2/k_t) is important in evaluating the decomposition rate constant k_d , it was decided to use the literature value which has often been used to evaluate the initiation rate constant for various initiators. This will permit the comparison of k_d value on the same basis. Further, this does not alter the predicted conversion at all since R_p or $M_0(dx/dt) \propto (k_p^2/k_t)^{0.5} \cdot (k_d)^{0.5}$.

Now, the evaluation of k_d and k_R/k_x follows. Firstly, k_R/k_x may be obtained from two sets of initial polymerization rates $(R_{p_0})_1$ and $(R_{p_0})_2$ measured at two different initial monomer concentrations $(M_0)_1$ and $(M_0)_2$ keeping temperature and the initiator concentration constant. Using Eq. (I-4-7),

$$(R_{p_0})_1 = \left(\frac{k_p^2}{k_t} \right) \left(\frac{2k_d C_o (M_0)_1}{k_R/k_x + (M_0)_1} \right)^{0.5} (M_0)_1$$

$$(R_{p_0})_2 = \left(\frac{k_p^2}{k_t} \right) \left(\frac{2k_d C_o (M_0)_2}{k_R/k_x + (M_0)_2} \right)^{0.5} (M_0)_2$$

$$\therefore \frac{(R_{p_0})_1}{(R_{p_0})_2} = \left(\frac{k_R/k_x + (M_0)_2}{k_R/k_x + (M_0)_1} \right)^{0.5} \left(\frac{(M_0)_1}{(M_0)_2} \right)^{1.5} \therefore \frac{k_R}{k_x} = \frac{(M_0)_2^{-\delta} \cdot (M_0)_1}{\delta - 1} \quad (\text{I-4-12a})$$

$$\text{where } \delta = \left(\frac{(R_{p_0})_1}{(R_{p_0})_2} \right)^2 \left/ \left(\frac{(M_0)_1}{(M_0)_2} \right)^3 \right. \quad (\text{I-4-12b})$$

Once k_R/k_x is obtained, k_d may be calculated using

$$k_d = R_{p_0}^2 \left(\frac{k_t}{k_p^2} \right) / \left\{ 2C_0 \left(\frac{M_0}{k_R/k_x + M_0} \right) \cdot M_0^2 \right\} \quad (\text{I-4-13})$$

The two sets of initial rate data at 50°C gave the following k_R/k_x and k_d .

Set	k_R/k_x	$k_d \times 10^6$ (1/sec.)
I5014 and I5024	1.08	3.18
I5024 and I5044	.86	2.87
I5044 and I5014	.96	2.97

The average values of the above are

$$k_R/k_x = 0.97 \quad (50^\circ\text{C})$$

$$k_d = 3.00 \times 10^{-6} \text{ (1/sec.) } (50^\circ\text{C})$$

Applying the same procedure for 40°C data (I4014 and C4044 in which the first conversion data was used to assess R_{p_0}), the following values were obtained.

$$k_R/k_x = 1.20 \quad (40^\circ\text{C})$$

$$k_d = 7.20 \times 10^{-7} \quad (40^\circ\text{C})$$

For 25°C and 30°C data, the term $f \cdot k_d = \left(\frac{M_0}{k_R/k_x + M_0} \right) \cdot k_d$ was evaluated and values are tabulated in Table I-3-2.

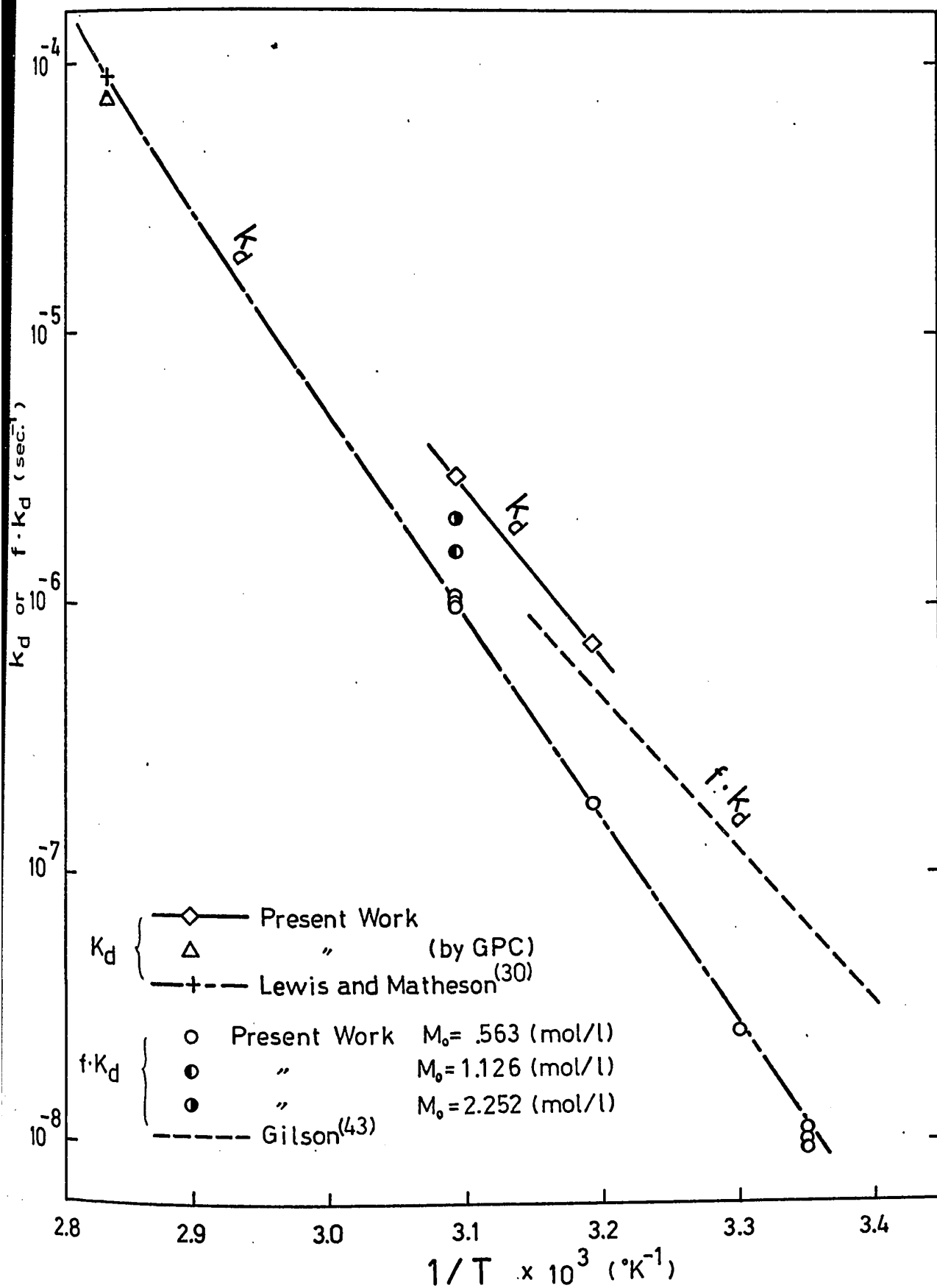
Comparison of k_d or $f \cdot k_d$ values are made in Fig. I-4-4 with those reported in the literature.^(30,43) The solid line represents k_d based on the present data at 40°C and 50°C,

$$k_d = 7.70 \times 10^{13} \exp(-28.7 \times 10^3/RT)$$

Lewis and Matheson⁽³⁰⁾ have reported $k_d = 8.97 \times 10^{-5}$ (1/sec.) at 80°C together with the activation energy of 34.0 (kcal/mol). These were obtained using a measurement of nitrogen evolution, however their temperature range of the measurement is not reported. The - - - - line represents their k_d values calculated using the activation energy, while the dotted line represents reported $f \cdot k_d$ values obtained by measuring the rate of acrylamide polymerization.⁽⁴³⁾ Present $f \cdot k_d$ values at $M_0 = 0.563$ (mol/l) agree well with Lewis and Matheson's k_d data. However, at higher monomer concentrations, the values of $f \cdot k_d$ exceeded their k_d values showing an apparent contradiction with $f > 1.0$. The same contradiction occurred when Gilson⁽⁴³⁾ compared his $f \cdot k_d$ values with Lewis and Matheson's k_d . The present k_d data are reasonable in that initiator efficiencies are less than unity for both Gilson's $f \cdot k_d$ values as well as for the present values.

The decomposition of the initiator ACV was therefore followed using GPC to obtain and compare k_d values at 80°C. The measured k_d value is in reasonable agreement with Lewis and Matheson's value and with the value expected based on the present polymerization data at 40°C and 50°C. The measurement of k_d using GPC is described in Appendix I-4.

The present kinetic model permits the estimation of the

Fig. I-4-4 Comparison of k_d ($f \cdot k_d$)

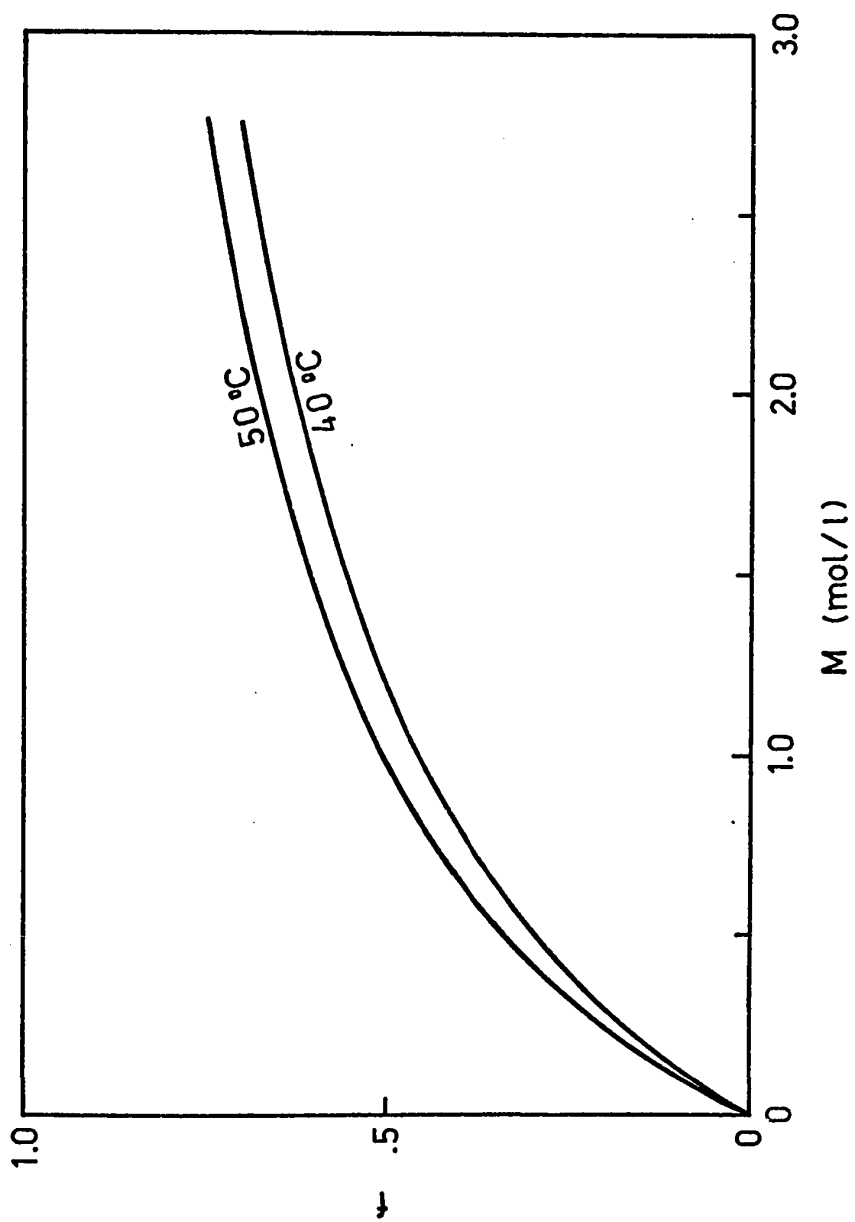
initiator efficiency f using Eq. I-4-6. The monomer dependence of the values of f is shown in Fig. I-4-5. The efficiency increases rapidly as monomer concentration increases from 0 to 1.0 (mol/l), and very slowly approaches unity with further increase of monomer concentration. In the experimental region $M \leq 2.252$ (mol/l), the efficiency factor is less than 0.7. The general trend and magnitude of f is in agreement with the measured efficiency factor for the most well-studied azo-initiator, azobis isobutyronitrile (AIBN).⁽³¹⁾

I-4-3 Comparison of Measured and Predicted Quantities

The initiator decomposition rate constant k_d and the groups of rate constants k_R/k_x , k_p^2/k_t and k_{fm}/k_p obtained in the previous section were used to calculate the variation of conversion and molecular weight distribution.

In Fig. I-4-6 to Fig. I-4-14, the present experimental values of conversion and number-average molecular weight are compared with those predicted. Weight-average molecular weights calculated from two different equations^(8,9) (Eqs. (I-2-1) and (I-2-2)) are compared in Figs. I-4-15 and I-4-16. Molecular weight distributions obtained by GPC and by electron microscopy are compared with the predicted ones in Fig. I-4-17 to Fig. I-4-19.

It was found that the theoretical kinetic rate expressions predict well the change of conversion and \bar{M}_n with time for the runs starting from $M_0 = 0.563$ (mol/l) or less. However in the runs starting from higher monomer concentrations, the experimental conversion data was always greater than the predicted ones at conversions over 40%. The

Fig. I-4-5 Dependence of f on M

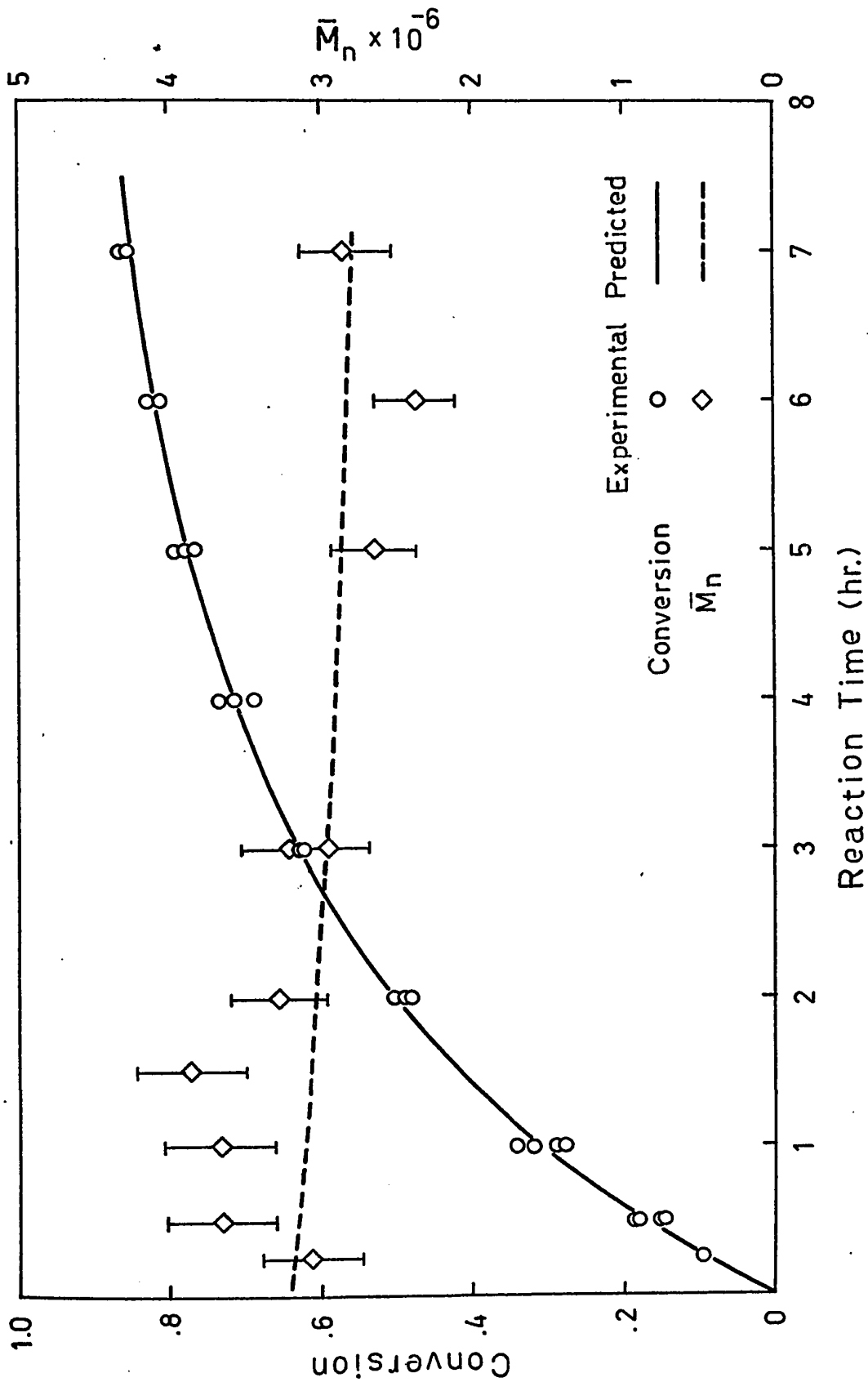


Fig. I-4-6 Comparison of Conversion and \bar{M}_n Runs: I5011, C5011(A)-(D)

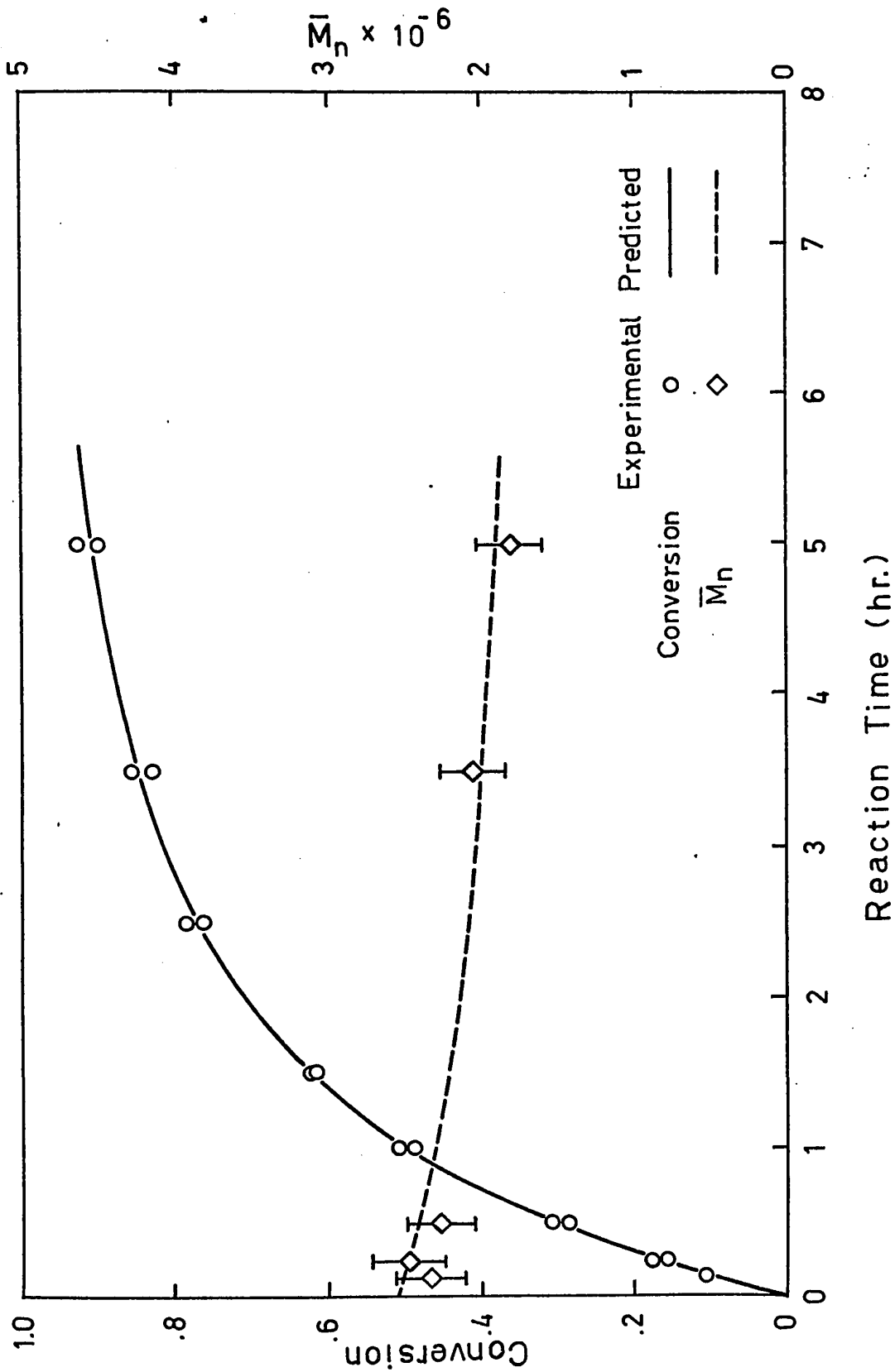


Fig. I-4-7 Comparison of Conversion and \bar{M}_n Runs: I5014, C5014(A),(B)

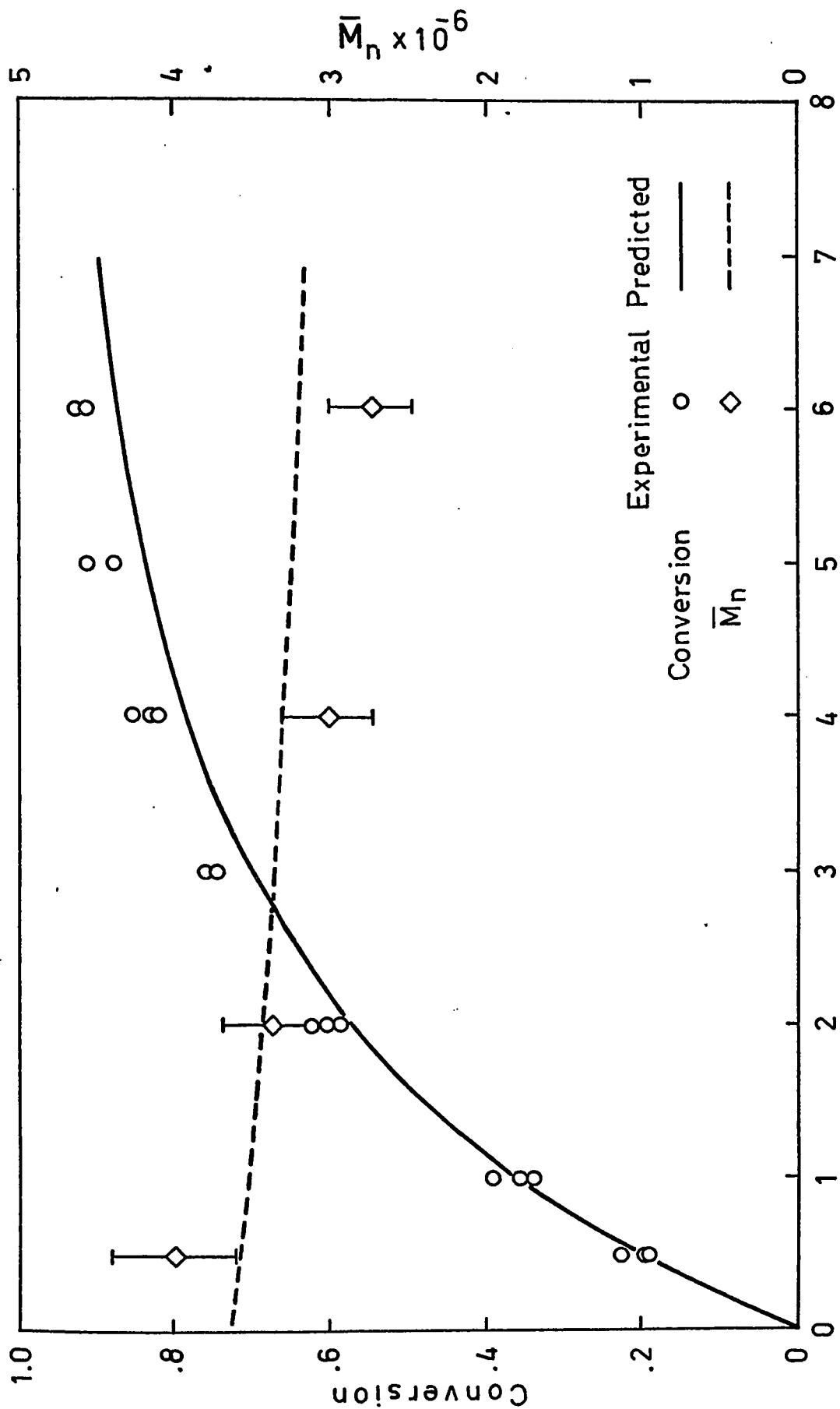
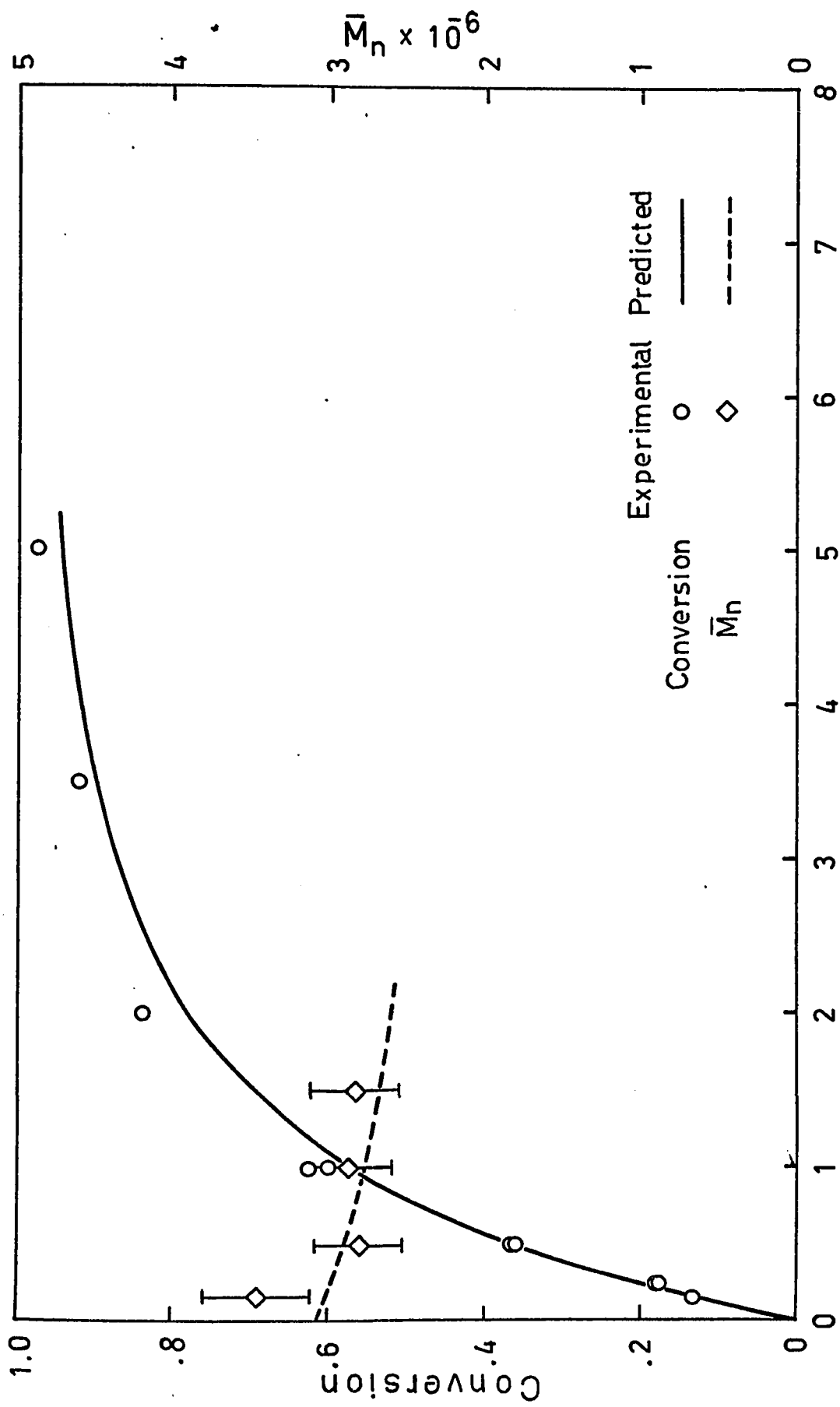


Fig. I-4-8 Comparison of Conversion and \bar{M}_n Runs: C5021(A), (B)



Reaction Time (hr.)

Fig. I-4-9 Comparison of Conversion and \bar{M}_n Runs: I5024, C5024(A), (B)

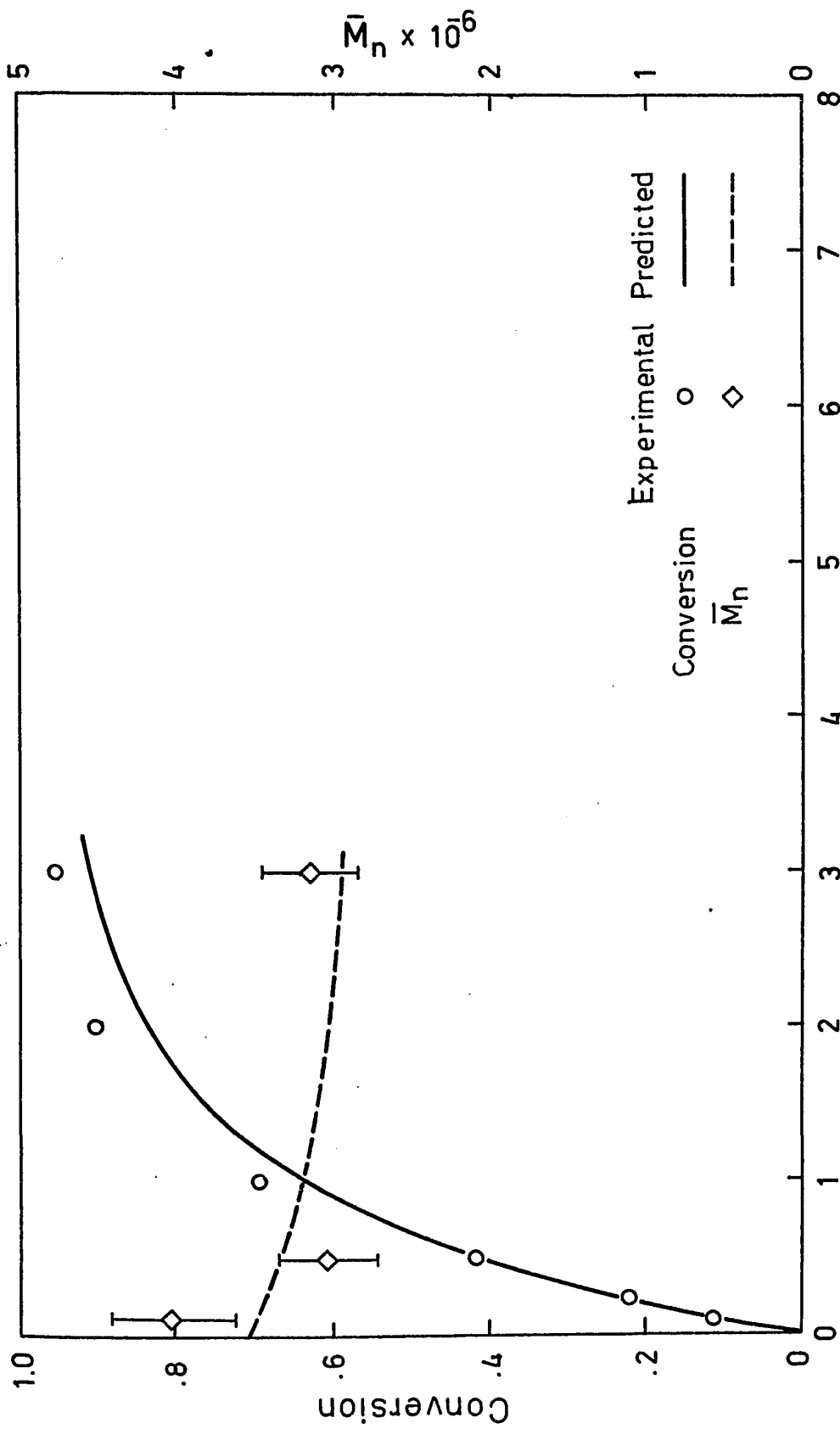


Fig. I-4-10 Comparison of Conversion and \bar{M}_n

Runs: I5044, C5044

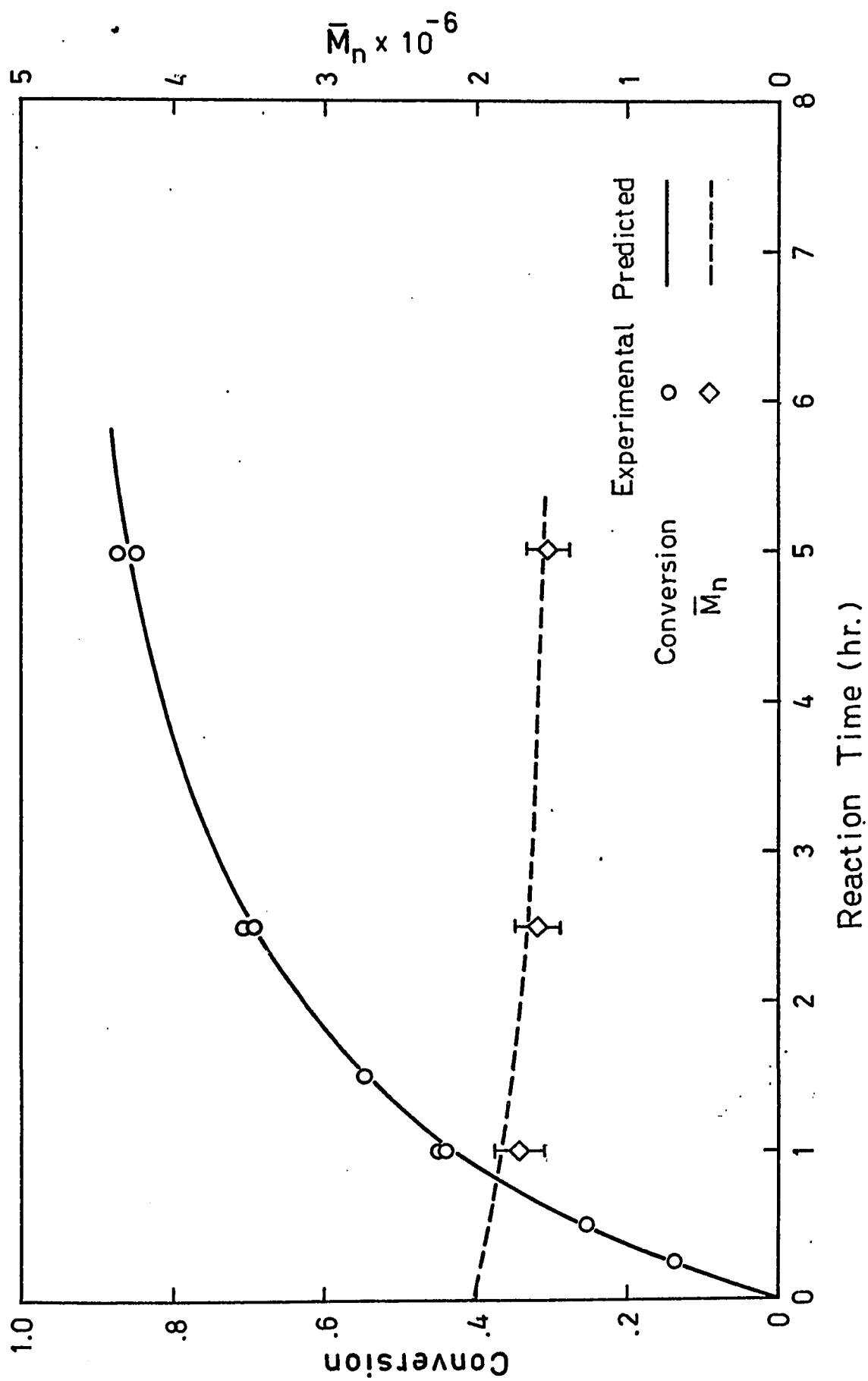
Fig. I-4-11 Comparison of Conversion and \bar{M}_n Runs: C50S(A), (B)

Fig. I-4-12 Comparison of Conversion Runs: C4011, C4024(A),(B)

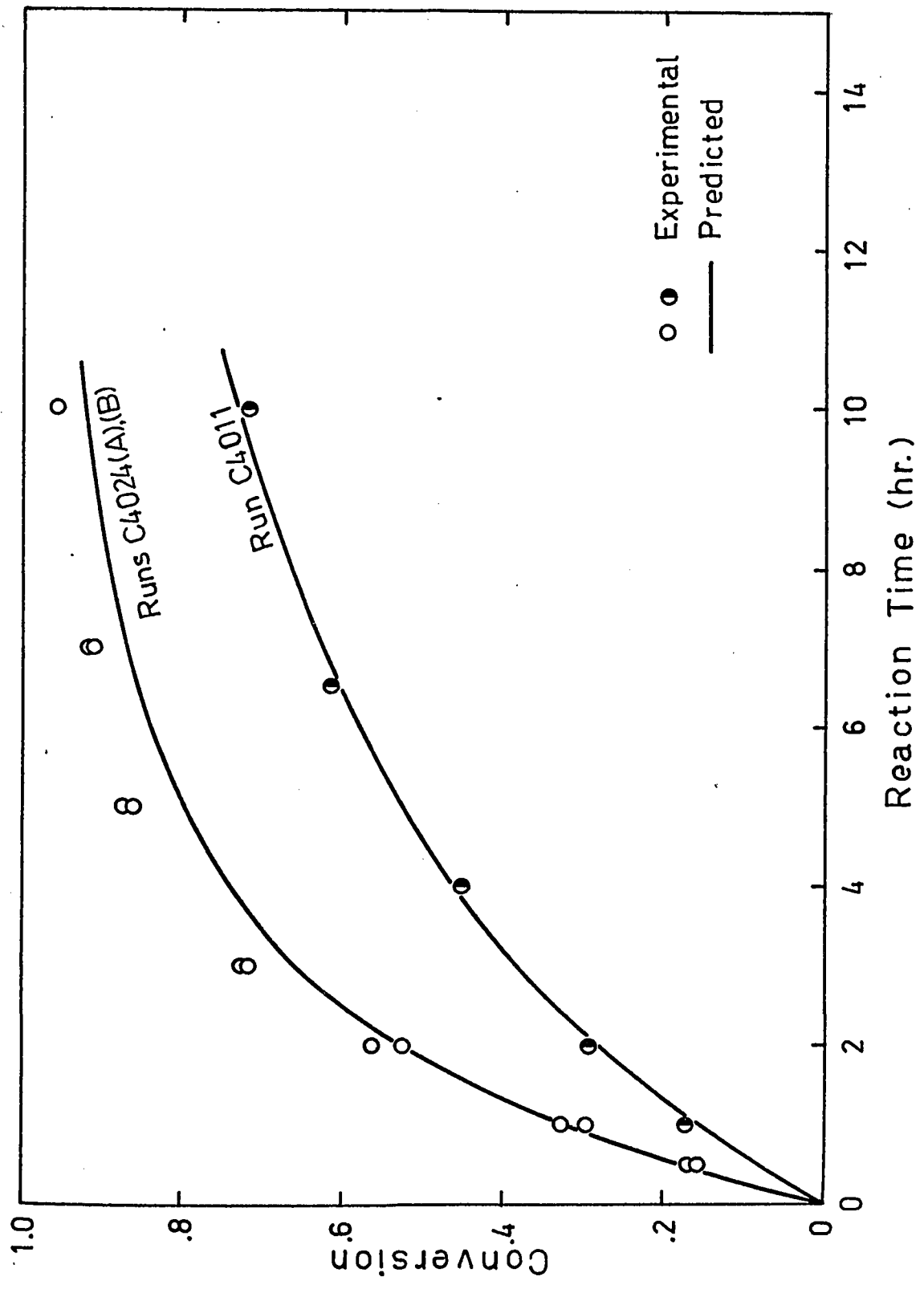


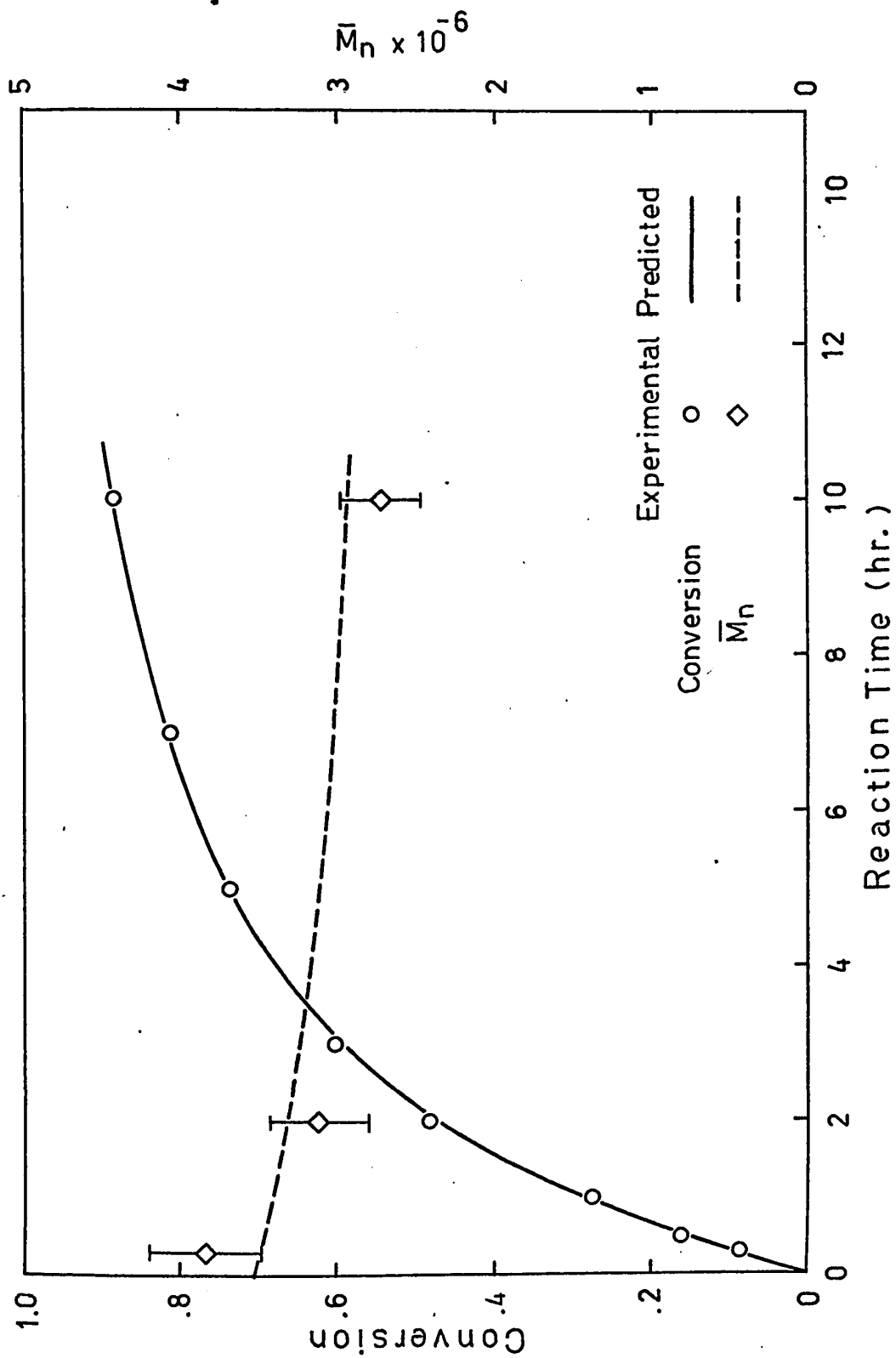
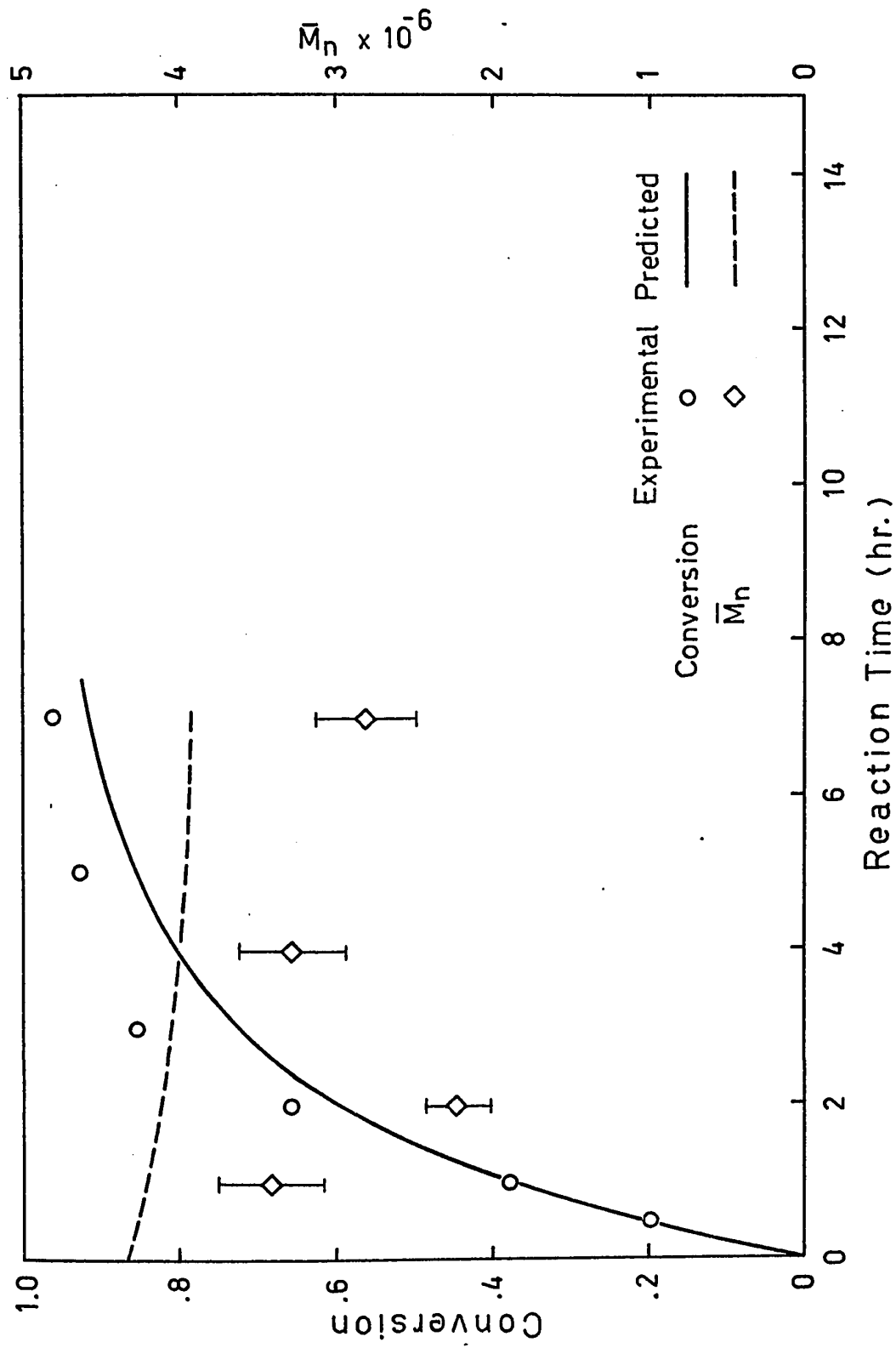
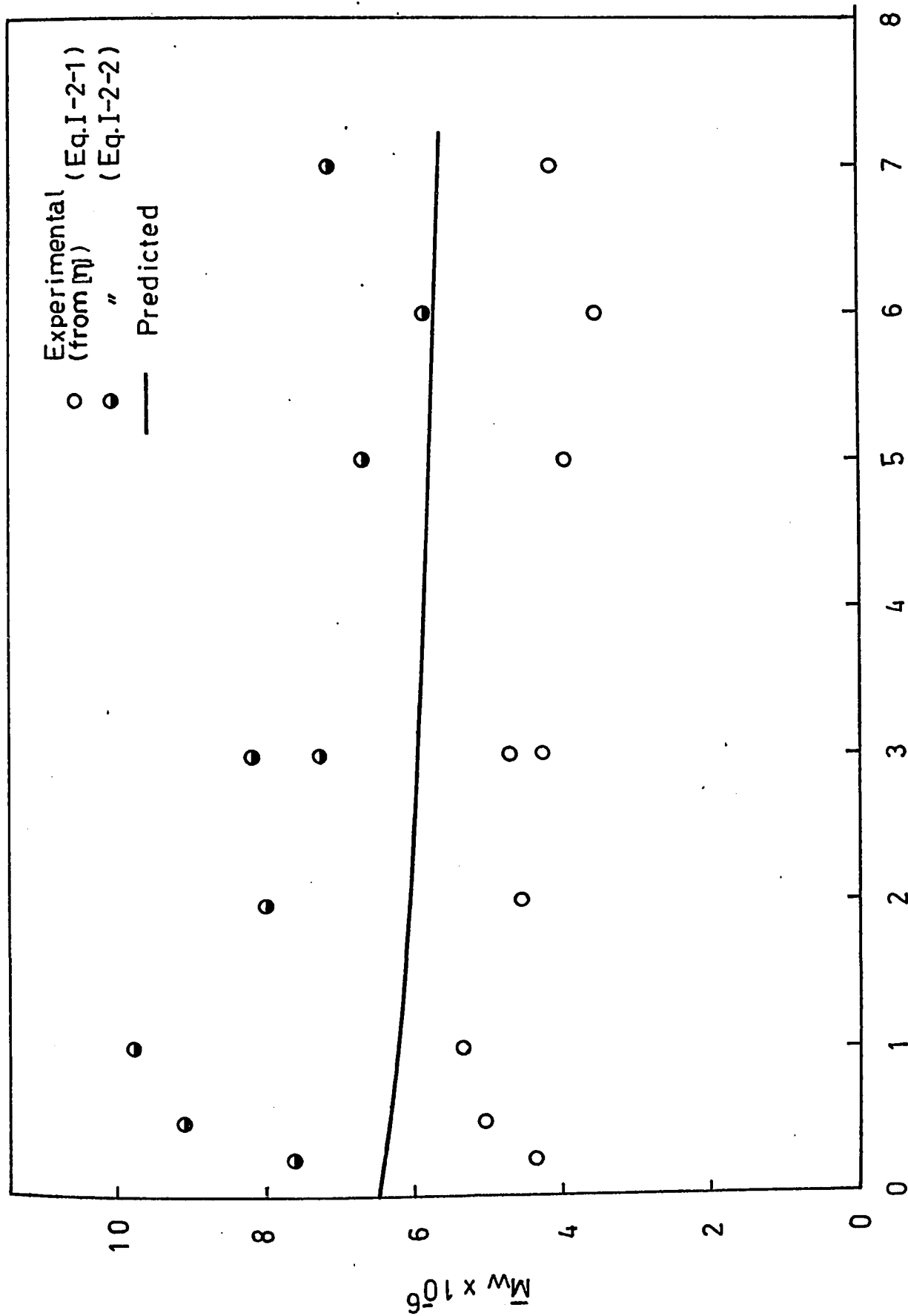
Fig. I-4-13 Comparison of Conversion and \bar{M}_n Runs: I4014, C4014

Fig. I-4-14 Comparison of Conversion and \bar{M}_n : Run: C4044





Reaction Time (hr.)
Fig. I-4-15 Comparison of \bar{M}_w Runs: C5011(A), (B)

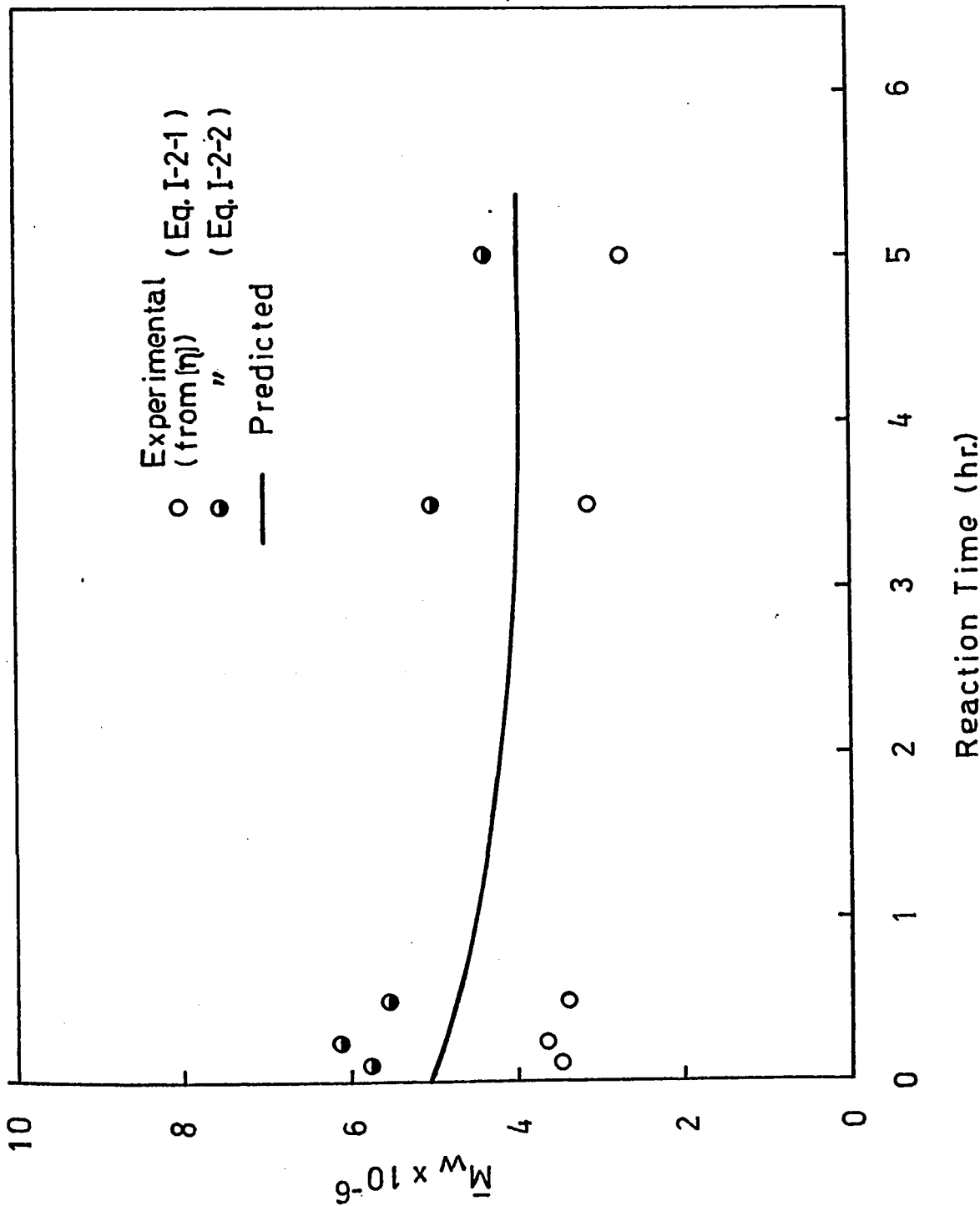


Fig. I-4-16 Comparison of \bar{M}_w Runs: I5014, C5014

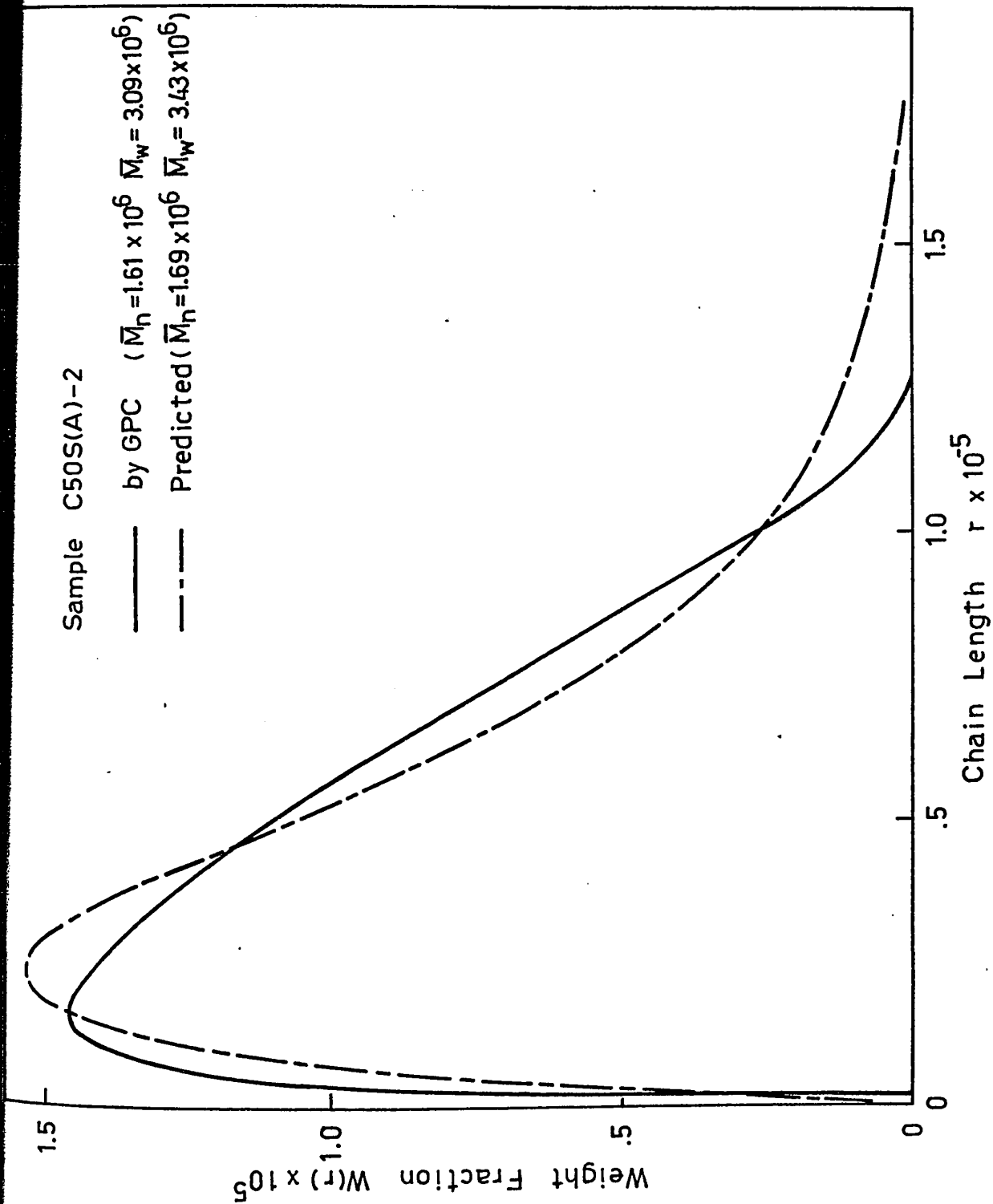


Fig. I-4-17 Comparison of Molecular Weight Distribution

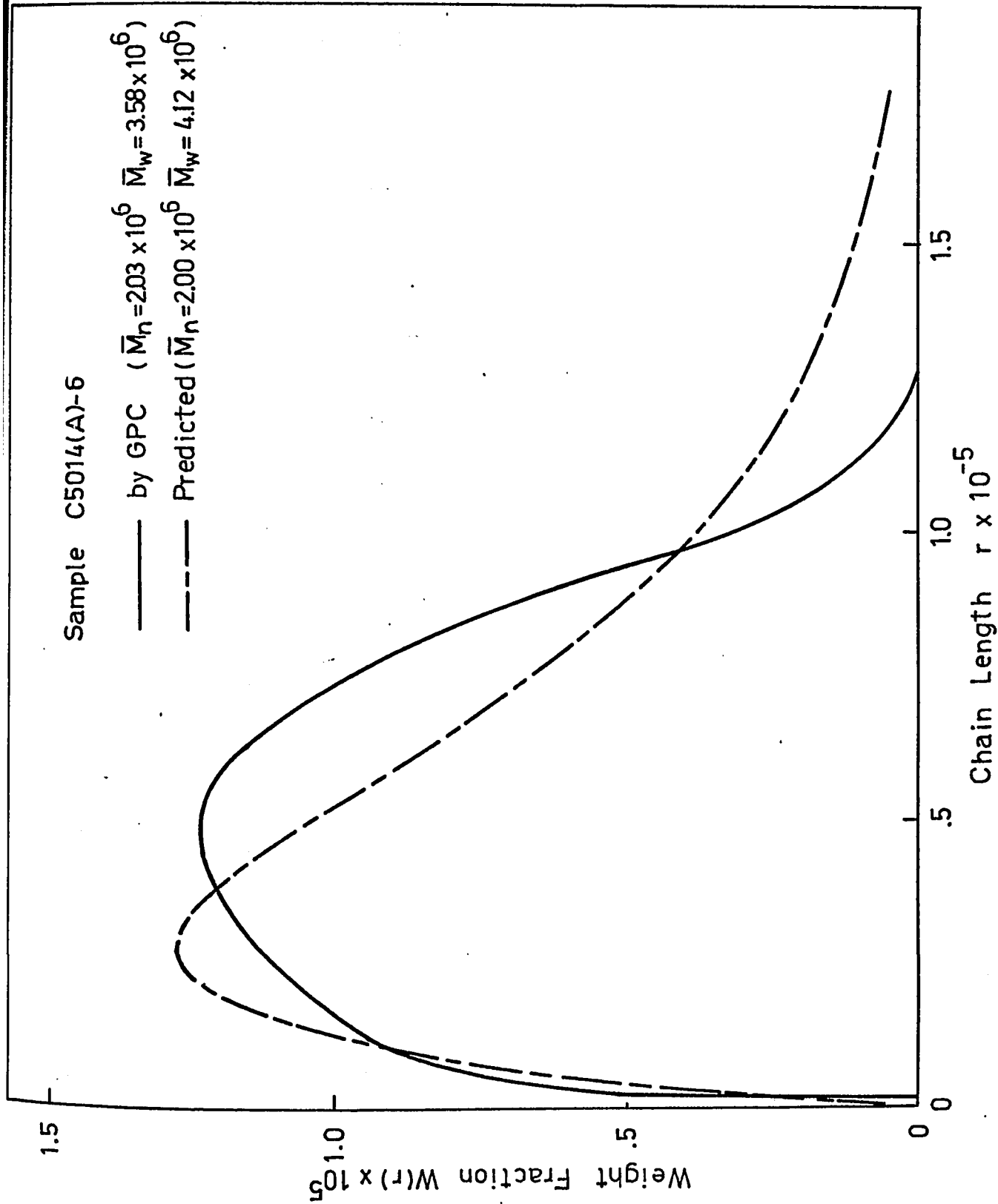


Fig. I-4-18 Comparison of Molecular Weight Distribution

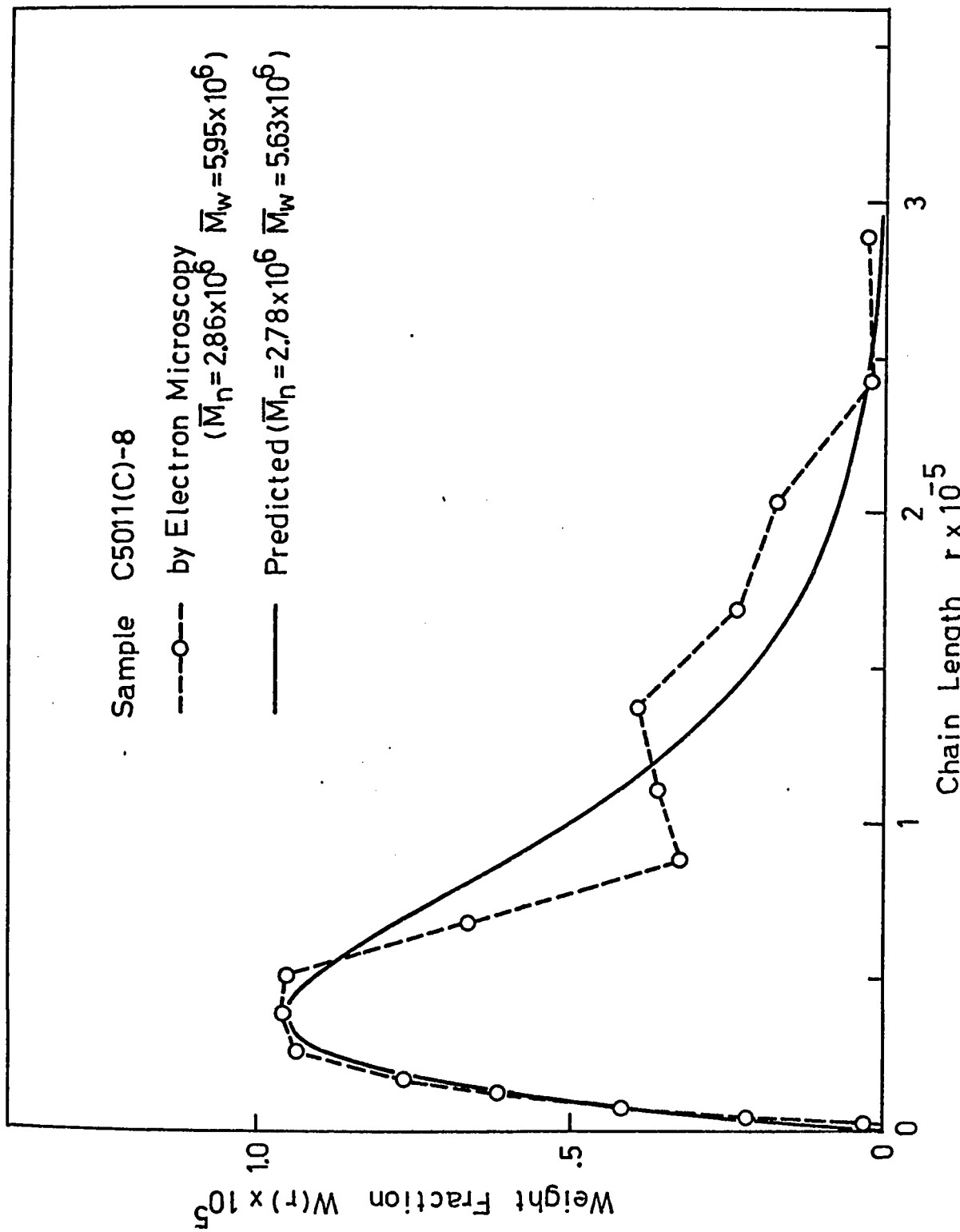
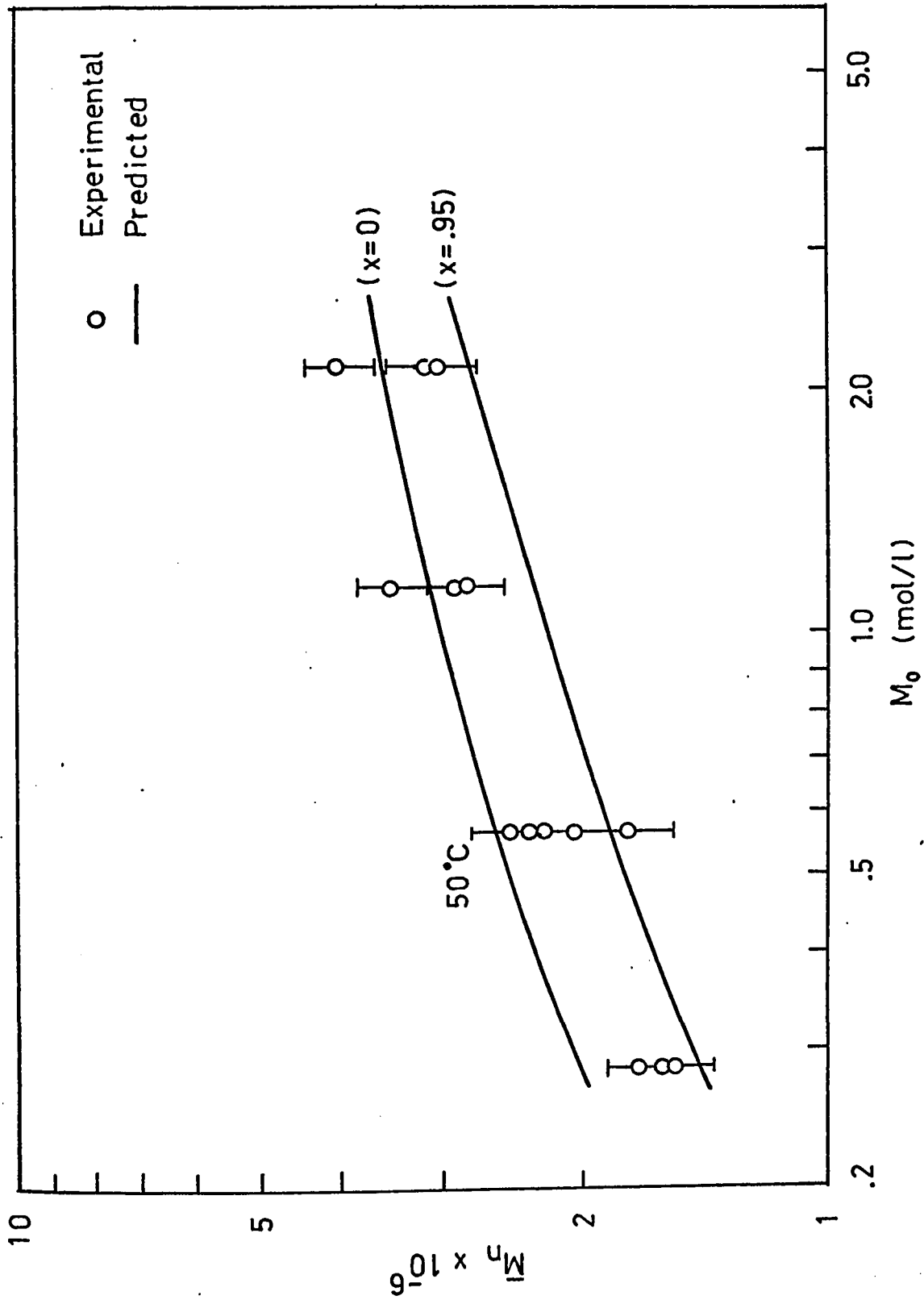


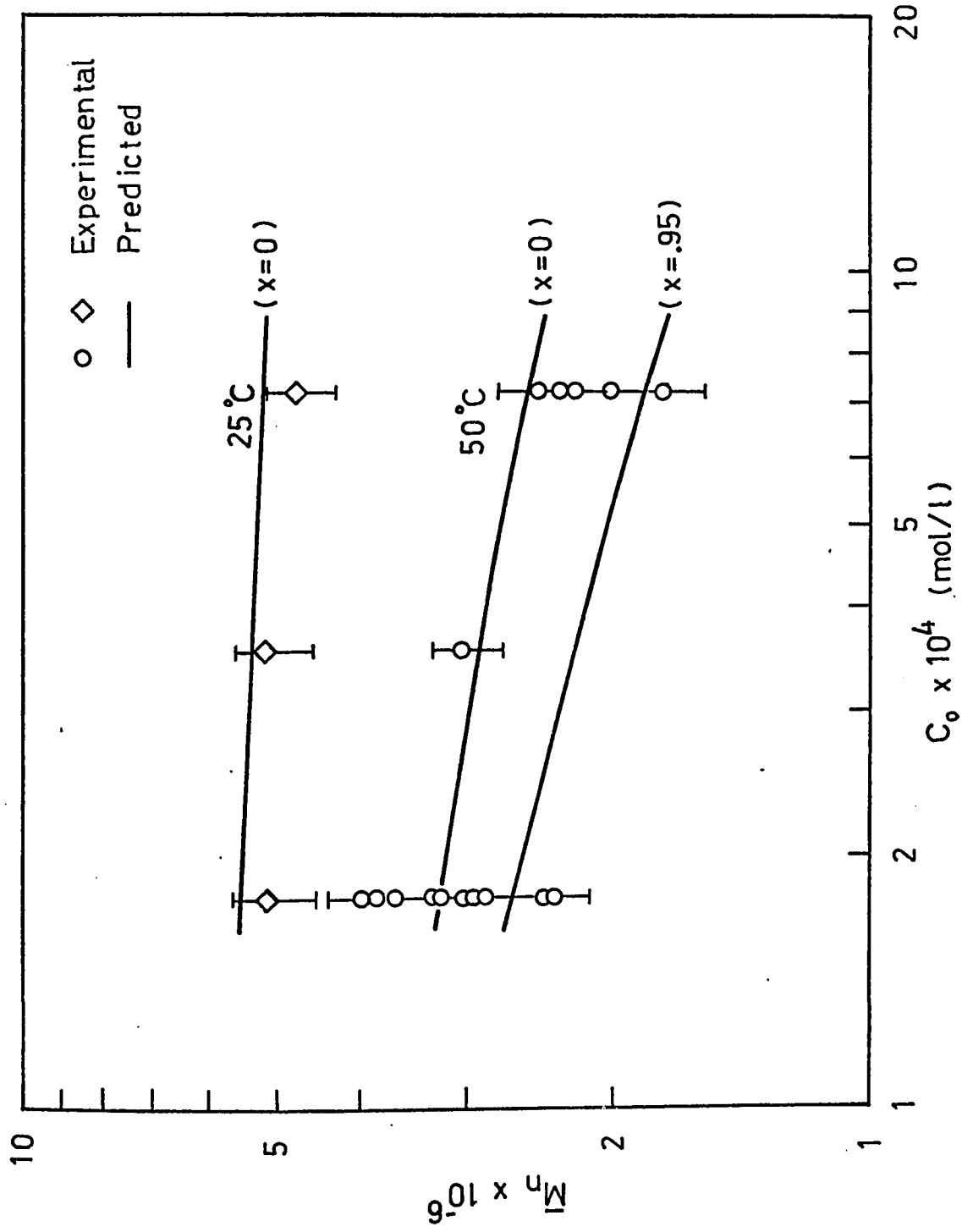
Fig. I-4-19 Comparison of Molecular Weight Distribution

maximum difference was ~10% in conversion at 50°C runs, while it was ~15% at 40°C runs. As for number-average molecular weight is concerned, the agreement was satisfactory at all conversions. Large difference observed in Run C4044 was a result of excessive stirring applied to the reaction mixture in this run.

Weight-average molecular weights predicted were found to lie in between values calculated using two different equations. However, the two equations yielded \bar{M}_w values nearly 50% apart in value. Light scattering data showed $\bar{M}_w = 6.3 \times 10^6$ for the polymer sample C5011(C)-8 giving a polydispersity of the sample of 2.2. This is in reasonable agreement with theoretical kinetics which gives the polydispersity of 2.0.

The molecular weight distribution obtained by GPC for sample C50S(A)-2 gave $\bar{M}_w/\bar{M}_n = 1.9$. Although comparisons of the distribution curves showed remarkable difference for the sample C5014(A)-6, this is due to the limit of column resolution of the GPC and not any limitation of the theory. All the molecules above certain molecular weight were eluted alike at certain retention volume, thus the tailing portion of the distribution was not detected. However, electron microscopy clearly shows the existence of a large molecular weight tail. As opposed to GPC, the electron microscopy has a certain lower molecular weight limit for the detection of an individual molecule. However, in the molecular weight range of a few million, it does not suffer from this limitation. The polydispersity of the sample analyzed was 2.1. As it was found that the decrease of number-average molecular weight was relatively small during the course of reaction, these data were pooled and plotted against monomer concentration and initiator concentration in Figs. I-4-20 and I-4-21. The range of

Fig. I-4-20 \bar{M}_n Dependence on M_0

Fig. I-4-21 \bar{M}_n Dependence on C_0

variation expected from the model was also included in these figures. The number-average molecular weight was found relatively insensitive to these variables.

On the basis that the higher measured conversions in the runs $M_0 > 1.0$ (mol/l) are due to diffusion control of the termination reaction ("gel effect"), the change of (k_p^2/k_t) with respect to conversion was estimated from experimental conversion curves.

$$\begin{aligned} \frac{k_p^2}{k_t} &= R_p^2 / \{2k_d C \left(\frac{M}{k_R/k_x + M} \right) \cdot M^2\} \\ &= \left(\frac{dx}{dt} \right)^2 / \{2k_d C \left(\frac{M_0(1-x)}{k_R/k_x + M_0(1-x)} \right) \cdot (1-x)^2\} \end{aligned}$$

The estimation assumes that the kinetic mechanism is still valid and particularly that the termination constant is independent of chain length. If we assume that rate constant other than k_t are independent of conversion, the estimated change of k_p^2/k_t represents the change in k_t . Fig. I-4-22 shows the change of k_p^2/k_t with conversion in acrylamide polymerization compared with that obtained in styrene polymerization in toluene. (48)

It can be seen that the acrylamide polymerization is subject to a much smaller gel effect.

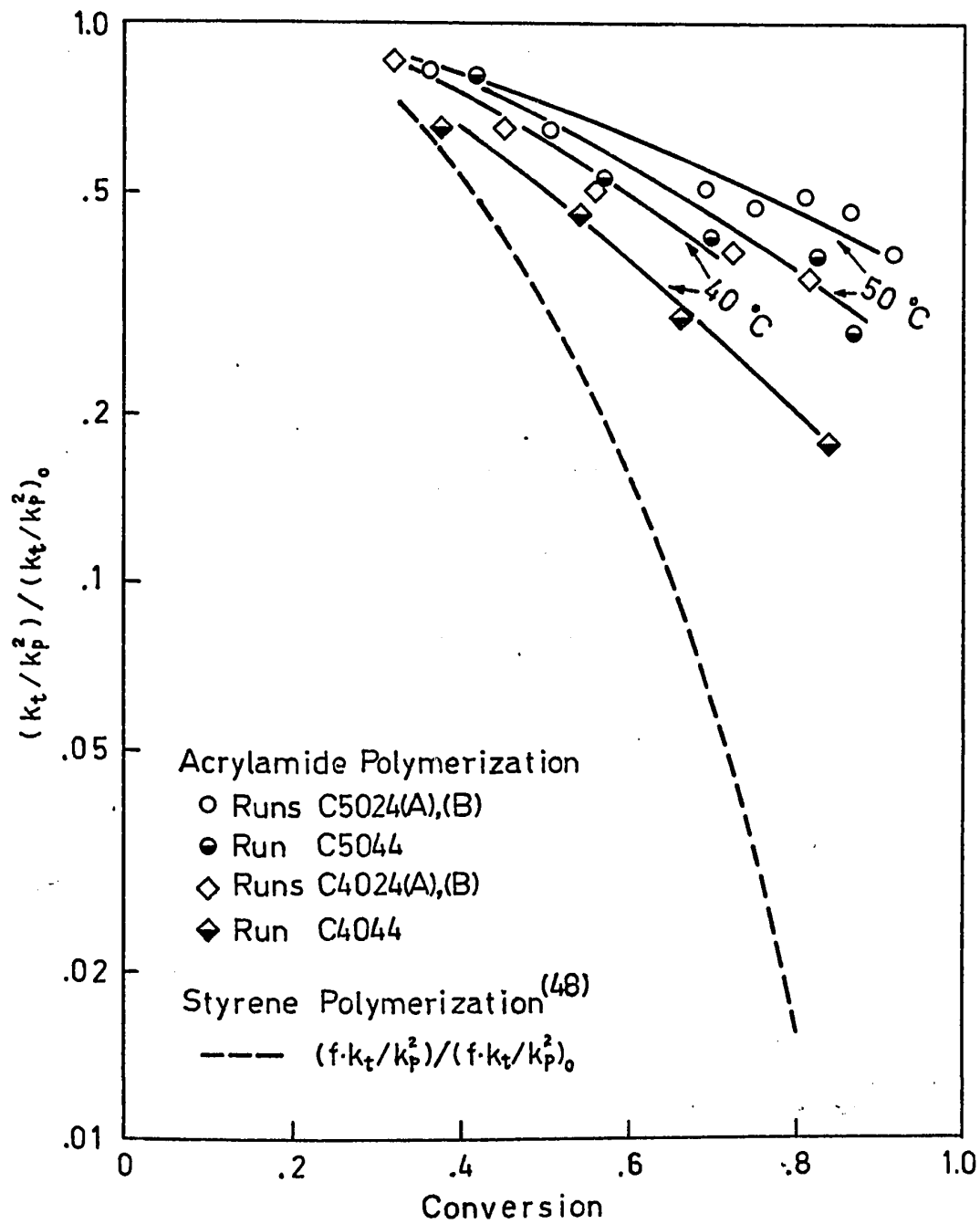


Fig. I-4-22 Variation of $(k_t/k_p^2)/(k_t/k_p^2)_0$ with Conversion

I-5 DISCUSSION

I-5-1 Mechanism and Rate Constants

Observed rate dependence of $R_{p_0} \propto C^{0.5} M^{1.24}$ in ACV initiated polymerization agrees with the previously reported work^(21,43) in regard to the exponent of the initiator concentration but differs in the exponent of the monomer concentration. The present data agree better with polymerizations initiated by potassium persulfate^(34,35) and other initiators where the monomer dependence of R_{p_0} was always greater than unity. Also the ACV initiator when employed in styrene polymerization showed a monomer dependence greater than unity.⁽²⁷⁾ From this view, the present results are not unexpected but the disagreement with Cavell⁽²¹⁾ and Gilson's⁽⁴³⁾ work is difficult to explain. In terms of ACV decomposition rate constant k_d , the present results give no contradiction with their results. The decomposition rate constant of ACV was significantly higher than the one based on measurements of nitrogen evolution at 80°C⁽³⁰⁾. Since reasonable agreement in k_d at 80°C is obtained in all the three experiments, the activation energy quoted for ACV decomposition may be a little too large. The present k_d data can be used to explain the observed $f \cdot k_d$ in Cavell and Gilson's work.

The kinetic scheme describing monomer dependent initiation could well explain the observed rate dependence. The choice of the cage effect to explain the results may be more reasonable than complex theory.

If one uses the complex theory, the evaluated equilibrium constant K

($\propto 1/(k_R/k_x)$) for the complex shows a larger value at 50°C than at 40°C, and this is the reason why the cage effect theory is generally preferred over the complex theory. The groups of rate constants k_p^2/k_t and k_{fm}/k_p evaluated from the initial rate and number-average molecular weight data by the least square fit also could be said to agree well with reported data data,^(13,15) generally this kind of comparison gives a large scatter⁽³⁷⁾ due to the errors involved in molecular weight measurements.

I-5-2 Conversion and Molecular Weight Comparison

Agreement in both conversion and number-average molecular weight between measured and predicted were very satisfactory for monomer concentrations less than 0.563 (mol/l). Previously it was indicated that a single kinetic scheme was valid to 80 - 90% conversion when the product polymer is in the order of 10^5 in molecular weight.^(34,35,40) The present results extended this to 10^6 when the monomer concentration is relatively low. Even at a monomer concentration of 2.252 (mol/l), the conversions did not deviate more than 10% at 50°C from those predicted. Analysis of the variation of k_p^2/k_t with conversion showed that its change is fairly small indicating that the "gel effect" is not as important as with other vinyl polymerizations. Although k_t is rather small in the acrylamide polymerization as compared to the others, its magnitude cannot solely explain the situation since in the diffusion controlled regime, a decrease of k_t has been shown to 1/10 - 1/100 or even more.^(49,50) The fact that k_p is relatively large must be coupled with small k_t . The effect of diffusion control may be influencing both k_p and k_t , leaving the ratio k_p^2/k_t relatively constant. While in polymerizations such as for polystyrene,

the diffusion control is believed to have a strong effect on the k_t first, k_p relatively unchanged except at high conversion. (51)

Use of literature value of k_p^2/k_t can be justified since the difference of variance between the two different slopes, one least square fitted and the other obtained from the literature was not statistically significant. The difference is largely due to the inaccuracy involved in determining number-average molecular weight. Further, the use of the literature value permits a comparison of other rate constants with different worker's values on a common basis.

Relative constancy of number-average molecular weight can be explained in terms of the magnitude of k_{fm}/k_p . Although this term was very small in absolute value, $(k_t/k_p^2)(R_p/M^2)$ was found even smaller but of the same order of magnitude as k_{fm}/k_p . This explains why \bar{M}_n is not greatly affected by the variation of R_p/M^2 due to a change in C, M or conversion. At a temperature 25°C, k_{fm}/k_p exceeds the value of $(k_t/k_p^2)(R_p/M^2)$ by nearly 10 times, leaving \bar{M}_n virtually constant as was observed. This could also explain the results of Cavell, (21) who obtained almost constant values for the average molecular weights over an initiator concentration changed by 10 fold. This must be considered an important feature of the reaction. When molecular weights of order 10^6 are desired, R_p/M^2 has to be kept small making k_{fm}/k_p dominant in controlling the obtainable molecular weights. The maximum is expected to be $\bar{M}_n \sim 5 \times 10^6$ at 50°C. On the other hand, when the polymer of molecular weight $\sim 10^5$ is produced, this indicates that R_p/M^2 is much larger than

k_{fm}/k_p . Therefore \bar{M}_n would strongly depend on M and C, provided that no other transfer reaction is important.

The predicted weight-average molecular weights fell in between those calculated from the intrinsic viscosity values. However, the difference in values based on the two empirical correlations^(8,9) is too large to be useful in testing the validity of the kinetic model. However, average molecular weight data obtained here by GPC, light scattering and electron microscopy indicated that the polydispersity of the product polyacrylamide is nearly 2.0 in agreement with theory. All this adds further support for the kinetic model.

I-6 CONCLUSION

Experimental investigation was made on polymerization of acrylamide in water with 4,4' azobis-4-cyanovaleric acid (ACV) in such conditions that the product polymer had a number average molecular weight over one million. Two types of polymerization experiments were made; initial rate runs in which the reaction behavior at low conversion was investigated in terms of the monomer and the initiator dependence of the rate of polymerization, and continuous runs in which the variations of both conversion and number-average molecular weight with respect to reaction time were investigated. Conversions were determined either by gravimetry or by the use of gel permeation chromatography. Number-average molecular weights were obtained by viscometry. Additional molecular weight analysis were carried out by light scattering, by gel permeation chromatography and by electron microscopy. The present data may be of industrial interest since the polymerization was followed to high conversion and the molecular weight of product polymer is very large. No kinetic studies have been previously reported for the combination of the above two.

The initial rate runs resulted in the polymerization rate expression $R_{p_0} \propto C_o^{0.5} M_o^{1.24}$. Dependence on the initiator concentration was in agreement with previous studies by Cavel⁽²¹⁾ and Gilson⁽⁴³⁾ while the dependence on the monomer agreed better with polymerization initiated by potassium persulfate and other initiators where the monomer dependence was always greater than unity. Although the initiator ACV was shown to give the polymerization rate dependence of the order 1.0 to 1.5 with decreasing monomer concentration when used for styrene polymerization,⁽²⁷⁾

the disagreement with Cavell and Gilson's result remains unresolved. Based on the present observation, the classical kinetic theory was modified according to "cage effect" theory. Evaluation of the rate constants involved in the kinetic scheme was made by using initial rate and number-average molecular weight data. The evaluated k_p^2/k_t and k_{fm}/k_p showed a reasonable agreement with those reported. (13,15) The decomposition rate constant k_d however was larger than that calculated using the reported k_d at 80°C and the activation energy. (33) The quoted activation may be a little too large.

Predictions of conversion and molecular weight variations with respect to reaction time were made using the proposed kinetic scheme. These were compared with the data obtained in continuous runs. It was found that the predicted values agreed well with those measured indicating the validity of the kinetic model to high conversion when initial monomer concentration is less than 0.56 mol/l. At the initial monomer concentration of 1.12 and 2.25 (mol/l), the predicted conversions were always lower than the measured ones at high conversions. The maximum deviation was ~15% at 40°C. These differences were explained as a consequence of the gel effect and it was shown that the magnitude of the gel effect is very much smaller than that observed in styrene polymerization. Number-average molecular weight both measured and predicted showed that it is relatively insensitive to such variables as reaction time, monomer and initiator concentrations. This is due to the fact that transfer to monomer is dominant in controlling the molecular weight when the molecular weight is as high as a few million. For this reason, the gel effect does not affect the molecular weight of the polymer.

Weight-average molecular weight obtained by light scattering and molecular weight distribution obtained by gel permeation chromatography and electron microscopy give further support for the validity of the kinetic scheme.

I-7 NOMENCLATURE

a	a constant ($= k_{tc}/k_t$)
ACV	4,4' azobis-4-cyanovaleric acid
AIBN	azobis-isobutyronitrile
c, Δc	concentration
C, C_1 , C_2	initiators and their concentration (mol/l)
C_0	initial initiator concentration (mol/l)
C^\cdot	initiator radical
Δd	difference in scale reading of differential refractometer
D'_s	diameter of polystyrene molecule in micrograph (cm)
D.W.	distilled water
E_p , E_t	activation energy for propagation and termination reaction (Kcal/mol)
f	initiator efficiency
F	filter or filters combination
$f_n(r)$, $f_w(r)$	number- and weight-based molecular weight distribution of dead polymer (with respect to chain length, instantaneous)
$f_N(r_p)$	number-based molecular weight distribution (with respect to molecular radius)
$\dot{f}_n(r)$, $\dot{f}_w(r)$, $\dot{f}_z(r)$	number-, weight- and z-based molecular weight distribution of polymer radical (with respect to chain length)
$F_n(r)$, $F_w(r)$	number- and weight-based molecular weight distribution of polymer (with respect to chain length, cumulative)
$F_N(M)$, $F_W(M)$	number- and weight-based molecular weight distribution of polymer (with respect to molecular weight)

GPC	gel permeation chromatography
G'_θ, G_θ	scattered light intensity at θ° with and without filter
G_w	light intensity at $\theta = 0^\circ$
HQ	hydroquinone
I	initiation rate (mol/l.sec)
I_0	initial initiation rate (mol/l.sec)
I_{abs}	absorbed light intensity
k	kinetic rate constant (see page I-89 for subscripts)
K	equilibrium constant, or angular constant (in Appendix I-2)
L', L'_s	shadow length of polyacrylamide and polystyrene molecule in micrograph (cm.)
M	monomer and its concentration, or molecular weight (in Appendix I-3)
M_0	initial monomer concentration (mol/l)
M^\cdot	monomer radical
\bar{M}_n, \bar{M}_w	number- and weight-average molecular weight
MWD	molecular weight distribution
N	Avogadro's Number
[P]	total polymer concentration (mol/l)
\bar{P}_n, \bar{P}_w	number- and weight-average chain length (cumulative)
P_r	polymer with chain length r and its concentration (mol/l)
Q	waste product or initiator
r	chain length
\bar{r}_n, \bar{r}_w	number- and weight-average chain length (instantaneous)
r_p	molecular radius of polyacrylamide molecule

r_p', r_s'	molecular radius of polyacrylamide and polystyrene molecule in micrograph (cm.)
R	gas constant (cal/deg.mol)
R_p, R_t, R_f	rate of propagation (or polymerization), termination and transfer
R_{p_0}	initial rate of polymerization
R_θ	Rayleigh ratio
R^\bullet	total radical concentration (mol/l)
R_c^\bullet	decomposed initiator radical and its concentration (mol/l)
R_r^\bullet	radical with chain length r and its concentration (mol/l)
S	solvent (or initiator) and its concentration (mol/l)
S^\bullet	solvent (or initiator) radical and its concentration (mol/l)
t, Δt	reaction time (sec.)
T	temperature ($^\circ K$) or a parameter (in Appendix I-5)
x, Δx	conversion of monomer to polymer
w(r)	molecular weight distribution, same as $f_w(r)$
W(r)	molecular weight distribution, same as $F_w(r)$

Greek Symbols

α	a parameter
β	a parameter
γ	a parameter
δ	a constant, (Eq. I-4-12b)
η	viscosity (c.p.)
η_r	relative viscosity

η_{sp}	specific viscosity
$[\eta]$	intrinsic viscosity
θ	observation angle or shadow angle
λ	propagation probability
λ_0	wave length
ν	average chain length of polymer radical
ρ	density (gm/cm^3)
τ	a parameter
ϕ	a parameter

Subscripts for rate constant k

d	decomposition of initiator
D	caged radical to escape from the cage
fc	transfer to initiator
fm	transfer to monomer
fs	transfer to S (solvent or initiator)
i	reaction between monomer and decomposed initiator radical
p	propagation
pm	reinitiation by M'
ps	reinitiation by S'
R	reaction of caged radical to form Q
t	termination (total)
tc	termination by recombination
td	termination by disproportionation
x	reaction between monomer and caged radical
x'	reaction between monomer and decomposed initiator radical (same as i)
l	initiation by ferric chloride
4	termination involving ferric salt

I-8 REFERENCES

1. E.L. Carpenter and H.S. Davis, *J. Appl. Chem.*, 7, 671 (1957).
2. Technical Bulletin, "Acrylamide", American Cyanamide Co., New York (1959).
3. R.M. Joshi, *J. Poly. Sci.*, 60, S56 (1962).
4. H. Morawetz and T.A. Fadner, *Makromol. Chem.*, 34, 162 (1959).
5. T.A. Fadner and H. Morawetz, *J. Poly. Sci.*, 45, 475 (1960).
6. *Encyclopedia of Polymer Science and Technology*, Vol. 1, p. 177, Vol. 2, p. 229, John Wiley and Sons Inc., New York (1964).
7. E.H. Gleason, M.L. Miller and G.F. Sheats, *J. Poly. Sci.*, 38, 133 (1959).
8. W. Scholtan, *Makromol. Chem.* 14, 169 (1954).
9. Technical Bulletin, "Cyanamer Polyacrylamide", American Cyanamide Co. Wayne, N.J. (1967).
10. E. Collinson, F.S. Dainton and G.S. McNaughton, *Trans. Faraday Soc.*, 53, 489 (1957).
11. F.S. Dainton, *J. Chem. Soc.*, 1533 (1952).
12. E. Collinson, F.S. Dainton and G.S. McNaughton, *Trans. Faraday Soc.*, 53, 476 (1957).
13. F.S. Dainton and M. Tordoff, *ibid*, 53, 499 (1957).
14. F.S. Dainton and M. Tordoff, *ibid*, 53, 666 (1957).
15. E. Collinson, F.S. Dainton, D.R. Smith, G.J. Trudel and S. Tazuke, *Discussion Faraday Soc.*, 29, 188 (1960).
16. M.S. Matheson, E.E. Auer, E.B. Bevilacqua and E.J. Hart, *J. American Chem. Soc.*, 73, 1700 (1951).
17. M.H. Mackay and H.W. Melville, *Trans. Faraday Soc.*, 45, 323 (1949).
18. M.S. Matheson, E.E. Auer, E.B. Bevilacqua and E.J. Hart, *J. Amer. Chem. Soc.*, 71, 2610 (1949).
19. *Polymer Handbook*, p. I-57, Interscience Publishers (1966).
20. R. Schulz, G. Renner, A. Henglein and W. Kern, *Makromol. Chem.*, 12 20 (1954).

21. E.A.S. Cavell, Makromol. Chem., 54, 70 (1962).
22. E.A.S. Cavell, I.T. Gilson and A.C. Meeks, Makromol. Chem., 73, 145 (1964).
23. E.A.S. Cavell and I.T. Gilson, J. Poly. Sci., Part A-1, 4, 541 (1966).
24. G.V. Schulz and E. Husemann, Z. Phys. Chem., 39, 246 (1938).
25. J. Abere, G. Goldfinger, H. Naidus and H. Mark, J. Phys. Chem., 49 211 (1945).
26. C.G. Oberberger, P. Fram and T. Alfrey, Jr., J. Poly. Sci., 6, 539 (1951).
27. G.S. Misra, R.C. Rastogi and V.P. Gupta, Makromol. Chem., 50, 72 (1961).
28. M.M. Horikx and J.J. Hermans, J. Polymer Sci., 11, 325 (1953).
29. J.C. Bevington, Radical Polymerization, Academic Press Inc., (1961).
30. F.M. Lewis and M.S. Matheson, J. American Chem. Soc., 71, 747 (1949).
31. C.H. Bamford, W.G. Barb, A.D. Jenkins and P.F. Onyon, "The Kinetics of Vinyl Polymerization by Radical Mechanism", Butterworth Scientific Publication, London (1958).
32. A.M. North, "The Kinetics of Free Radical Polymerization", The International Encyclopedia of Physical Chemistry and Chemical Physics, Topic 17, Vol. 1, Pergamon Press (1966).
33. M.S. Matheson, J. Chem. Phys., 13, 585 (1945).
34. J.P. Riggs and F. Rodriguez, J. Poly. Sci., Part A-1, 5, 3151 (1967).
35. J.P. Friend and A.E. Alexander, J. Poly. Sci., Part A-1, 6, 1833 (1968).
36. K. Venkatarao and M. Santappa, J. Poly. Sci., Part A-1, 5, 637 (1967).
37. T.J. Suen, Y. Jen and J.V. Lockwood, J. Poly. Sci., 31, 481 (1958).
38. F. Rodriguez and R.D. Givey, J. Poly. Sci., 55, 713 (1961).
39. T.J. Suen and D.F. Rossler, J. Appl. Poly. Sci., 3, No. 7, 126 (1960).
40. K. Venkatarao and M. Santappa, J. Poly. Sci., Part A-1, 8, 1785 (1970).
41. T.J. Suen, A.M. Shiller and W.N. Russel, Advance in Chemistry Series, No. 34, p. 217. American Chemical Society, Washington, D.C. (1962).
42. J.P. Riggs and F. Rodriguez, J. Poly. Sci., Part A-1, 5, 3167 (1967).

43. I.T. Gilson, Ph.D. Thesis, University of Southampton (1963).
44. A. Hui, Ph.D. Thesis, McMaster University (1970).
45. D.V. Quayle, *Polymer*, 8, 217 (1967).
46. J.H.T. Wade and P. Kumar, *J. Hydronautics*, 6, 40 (1972).
47. C.H. Bamford, A.D. Jenkins and R.P. Wayne, *Trans. Faraday Soc.*, 56, 932 (1960).
48. M. Harada, T. Yamada, K. Tanaka, W. Eguchi and S. Nagata, *Kagaku Kōgaku*, 29, 301 (1965).
49. S.W. Benson and A.M. North, *J. Amer. Chem. Soc.* 81, 1339 (1959).
50. A.M. North and G.A. Reed, *Trans. Faraday Soc.*, 57, 859 (1961).
51. W.I. Bengough and H.W. Melville, *Proc. Roy. Soc. (London)*, A230, 429 (1955).
52. J.H. Perry, *Chemical Engineer's Handbook*, 4th Edition 3-201.
53. A. Kruis, *Ziet, Phys. Chem.*, 34B, 13 (1936).
54. H.J. Cantow, *Z. Naturforschung*, 7B, 485 (1952).
55. S. Nakagaki and H. Inagaki, "Kōsanran Jikkenhō", Nankōdō, Tokyo (1965).
56. M.J. Richardson, *Proc. Royal. Soc.*, A279, 50 (1964).
57. W.A. Pryor, "Free Radicals", p. 131, McGraw-Hill (1966).
58. D.J. Shield and H.W. Coover, Jr., *J. Poly. Sci.*, 39, 532 (1959).
59. T. Imoto and S.I. Lee, "Juōo Hannō Kōgaku", Nikkan Kogyo Shimbunsha, Tokyo (1970).

Appendix I-1 Viscosity Measurements

The viscometers used were Cannon-Ubbelohde viscometers 50-A620 and 75-L181. These were set in a constant temperature bath operating at $25 \pm 0.1^\circ\text{C}$ as shown in Fig. AI-1-1. Vertical alignment was assisted by the use of a string with a sinker. The supplied viscometer constants and recommended viscosity ranges are listed in Table AI-1-1. The viscosity range corresponds to a flow time of 3 min. to 16 min., this satisfies a pre-requisite for the use of an empirical number-average molecular weight vs. intrinsic viscosity relationship $[\eta] = 6.8 \times 10^{-4} M_n^{0.66}$ obtained with flow times greater than 1.6 min. (10)

The procedures for viscosity measurements are as follows:

- (1) Charge 2-6 ml of sample solution into A and allow 20 min. for the sample to come to the bath temperature.
- (2) Suck the solution above the etch mark E_1 by applying vacuum to B while sealing C by a finger.
- (3) Allow the sample to flow down freely.
- (4) Measure the flow time between the two etch marks E_1 and E_2 by a stop-watch to the order of 1/100 min.
- (5) When the viscosity at several concentrations are required, add a desired amount of solvent from D and repeat the above.

Sample solutions were prepared by weighing the polymer, dissolving into water at 50°C overnight and filtering on a 50μ sintered glass filter.

Viscosities were calculated from the following formula:

Table AI-1-1 Viscometer Constants and Recommended Ranges

Viscometer	Viscometer Constant (centistoke/sec. of flow time)	Recommended Range (centistoke)
50-A620	.003882	0.8 ~ 4.0
75-L181	.00877	1.6 ~ 8.0

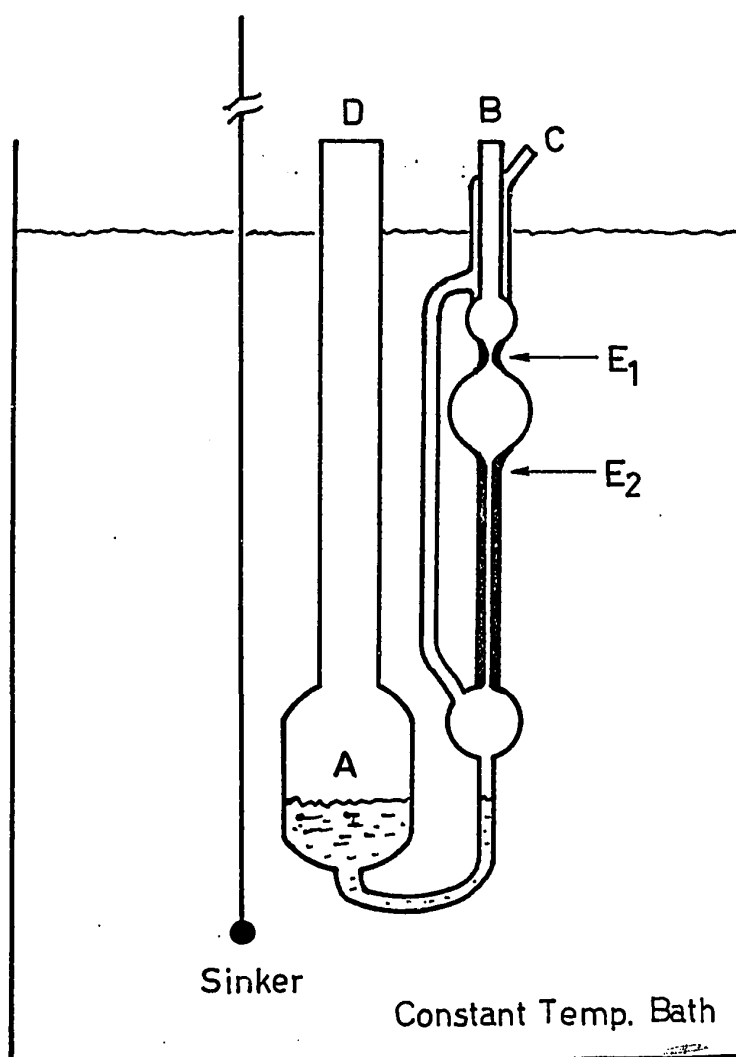


Fig. AI-1-1 Viscometer Set-up

$$\eta(\text{c.p.}) = \text{Viscometer Constant} \times \text{Solution Density} \times \text{Flow time}$$

Specific viscosities were then calculated by,

$$\eta_{\text{sp}} = \frac{\eta_{\text{solution}} - \eta_{\text{solvent}}}{\eta_{\text{solvent}}} = \eta_r - 1$$

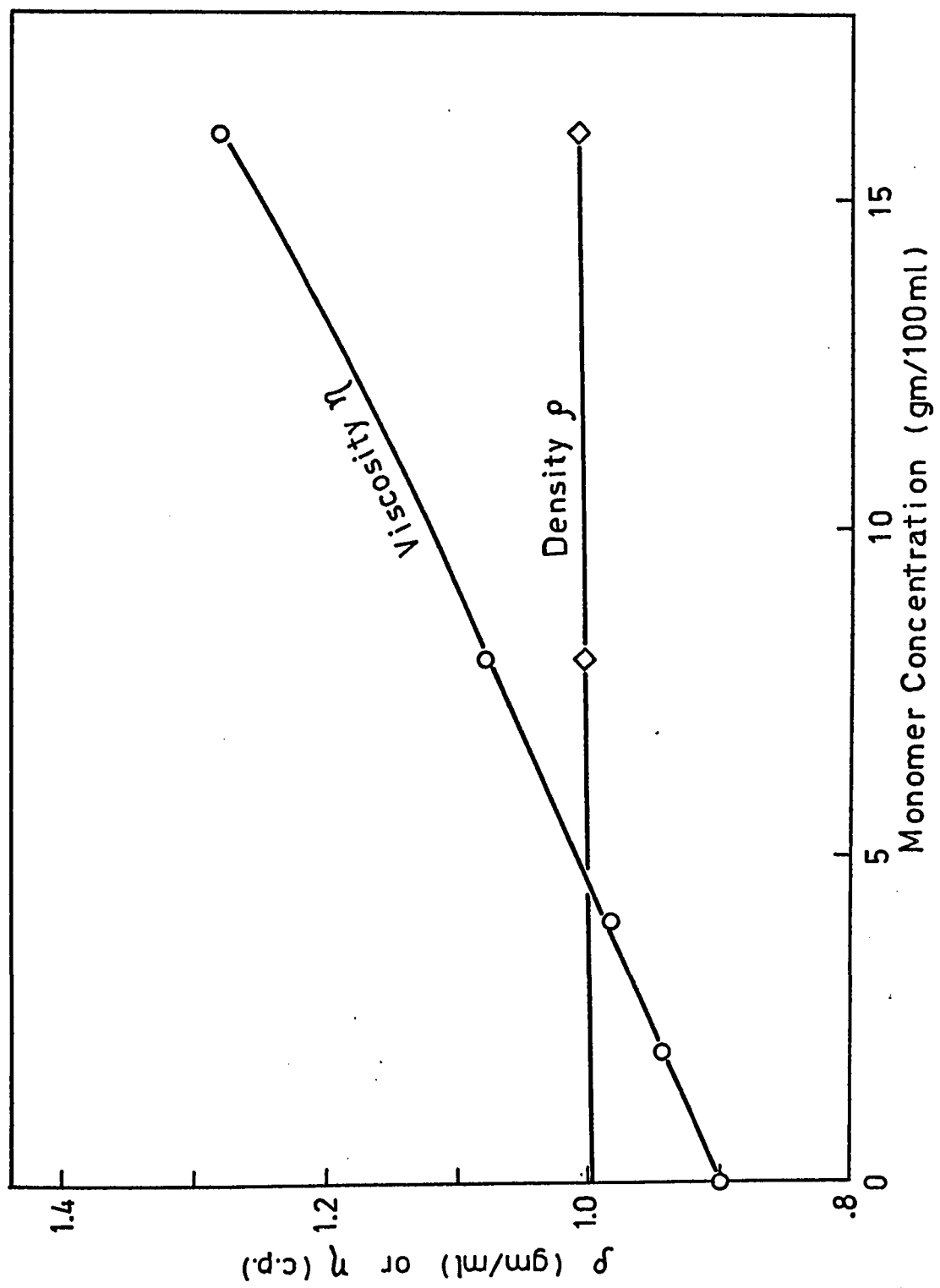
To obtain intrinsic viscosity $[\eta]$, η_{sp}/c where c is the sample concentration in gm/100 ml was plotted against c and extrapolated to $c = 0$, i.e., zero concentration.

A supplied viscometer constant for 50-A620 was checked several times during the viscosity measurements by measuring a flow time of twice-distilled water. An average flow time of 3.86 ± 0.2 min. was obtained. Assigning a literature value on the viscosity of the water (0.8937 c.p. at 25°C ⁽⁵²⁾) the viscometer constant was found to be 0.003859 ± 0.00002 . The difference was less than one percent. Thus the value supplied was used throughout in reporting viscosity. Accordingly $\eta_{\text{solvent}} = 0.899$ c.p. at 25°C was employed to obtain intrinsic viscosity.

Solution density of unity was used since the presence of polyacrylamide in water in the order of 0.1 gm/100 ml has been known to cause no significant change in density.⁽⁴³⁾ The presence of monomer in the amount of 0.5 gm/100 ml or less could increase the viscosity only 0.01 c.p. or less, thus no correction for the presence of monomer was made when the viscosity measurement was made for polymer-monomer mixture in the initial rate runs. Fig. AI-1-2 shows the measured densities and viscosities of monomer solutions.

Viscosity measurements with the two viscometers were made on the

Fig. AI-1-2 Density and Viscosity of Monomer Solution



same sample solutions to see if there was any difference between the two and to find a linear range of η_{sp}/c on c . This was done by taking a sample solution into 75-L181, viscosities were measured at a few successive dilutions. Then the most diluted solution was transferred to 50-A620 and viscosities were again measured at a few dilutions. The results are given in Table AI-1-2. Fig. AI-1-3 shows a plot of η_{sp}/c vs. c . It is now obvious that the viscosities measured by the two viscometers were not identical. However, η_{sp}/c tends to approach each other with decreasing concentration. Intrinsic viscosities were found 12.8 (by 75-L181) and 12.4 (by 50-A620) for sample C5011(D)-7. The corresponding number-average molecular weights are 2.86×10^6 and 3.00×10^6 , differing by $\pm 5\%$. This may be the range of error due to the use of a different viscometer than the one with which the $[\eta]$ vs. \bar{M}_n relationship was obtained.

Reproducibility tests were made on six polymer solutions prepared from two batches (ampoules) of polymer sample, three solutions for each batch. The two batches of polymer samples were obtained under the same reaction conditions. These results are summarized in Table AI-1-3. The plot of η_{sp}/c vs. c is shown in Fig. AI-1-4. Intrinsic viscosities obtained and corresponding \bar{M}_n 's are as follows:

Sample C5011(B)-3		Sample C5011(C)-3	
$[\eta]$	$\bar{M}_n \times 10^{-6}$	$[\eta]$	$\bar{M}_n \times 10^{-6}$
13.7	3.32	13.4	3.21
13.3	3.18	13.2	3.14
13.1	3.11	13.0	3.07
Ave. 3.20		Ave. 3.14	

TABLE AI-1-2 COMPARISON OF VISCOSITIES MEASURED BY
TWO VISCOMETERS 75-L181 AND 50-A620

SAMPLE C5011(A)-5

VISCOMETER	CONC. (GM/100ML)	TIME (MIN.)	η (C.P.)	η_r	η_{sp}	η_{sp}/c (100ML/GM)
75-L181	.1740	9.75	5.13	5.71	4.71	27.05
75-L181	.1160	5.90	3.10	3.45	2.45	21.15
75-L181	.0870	4.51	2.37	2.64	1.64	18.85
75-L181	.0696	3.76	1.98	2.20	1.20	17.25
75-L181	.0580	3.35	1.76	1.96	.96	16.57
50-A620	.0580	7.30	1.70	1.89	.89	15.37
50-A620	.0362	5.84	1.36	1.51	.51	14.15
50-A620	.0264	5.22	1.22	1.35	.35	13.37

SAMPLE C5011(D)-7

VISCOMETER	CONC. (GM/100ML)	TIME (MIN.)	η (C.P.)	η_r	η_{sp}	η_{sp}/c (100ML/GM)
75-L181	.1510	8.53	4.49	4.99	3.99	26.44
75-L181	.1007	5.34	2.81	3.13	2.13	21.12
75-L181	.0755	4.16	2.19	2.43	1.43	19.01
75-L181	.0604	3.55	1.87	2.08	1.08	17.85
50-A620	.0604	7.65	1.78	1.98	.98	16.26
50-A620	.0403	6.20	1.44	1.61	.61	15.06
50-A620	.0242	5.16	1.20	1.34	.34	13.94
50-A620	.0173	4.74	1.10	1.23	.23	13.22

TABLE AI-1-3 SUMMARY OF REPRODUCIBILITY TEST

SAMPLE	CONC. (GM/100ML)	TIME (MIN.)	η (C.P.)	η_r	η_{sp}	η_{sp}/C (100ML/GM)
C5011(B)-3 (SOL.-1)	.0898	10.88	2.53	2.82	1.82	20.25
	.0561	7.70	1.79	1.99	.99	17.73
	.0345	6.04	1.41	1.56	.56	16.36
	.0180	4.90	1.14	1.27	.27	15.01
C5011(B)-3 (SOL.-2)	.0980	11.62	2.71	3.01	2.01	20.52
	.0613	8.08	1.88	2.09	1.09	17.85
	.0377	6.20	1.44	1.61	.61	16.09
	.0196	4.97	1.16	1.29	.29	14.68
C5011(B)-3 (SOL.-3)	.0930	10.98	2.56	2.84	1.84	19.84
	.0465	6.84	1.59	1.77	.77	16.61
	.0358	6.03	1.40	1.56	.56	15.72
	.0232	5.19	1.21	1.34	.34	14.82
C5011(C)-3 (SOL.-1)	.1002	11.98	2.79	3.10	2.10	21.00
	.0626	8.22	1.91	2.13	1.13	18.04
	.0385	6.30	1.47	1.63	.63	16.41
	.0251	5.34	1.24	1.38	.38	15.31
	.0200	5.00	1.16	1.30	.30	14.74
C5011(C)-3 (SOL.-2)	.0774	9.49	2.21	2.46	1.46	18.85
	.0484	6.99	1.63	1.81	.81	16.77
	.0298	5.63	1.31	1.46	.46	15.41
	.0193	4.93	1.15	1.28	.28	14.33
C5011(C)-3 (SOL.-3)	.0822	9.83	2.29	2.55	1.55	18.82
	.0411	6.37	1.48	1.65	.65	15.82
	.0274	5.44	1.27	1.41	.41	14.94
	.0205	5.01	1.17	1.30	.30	14.50

(Viscometer: 50-A620)

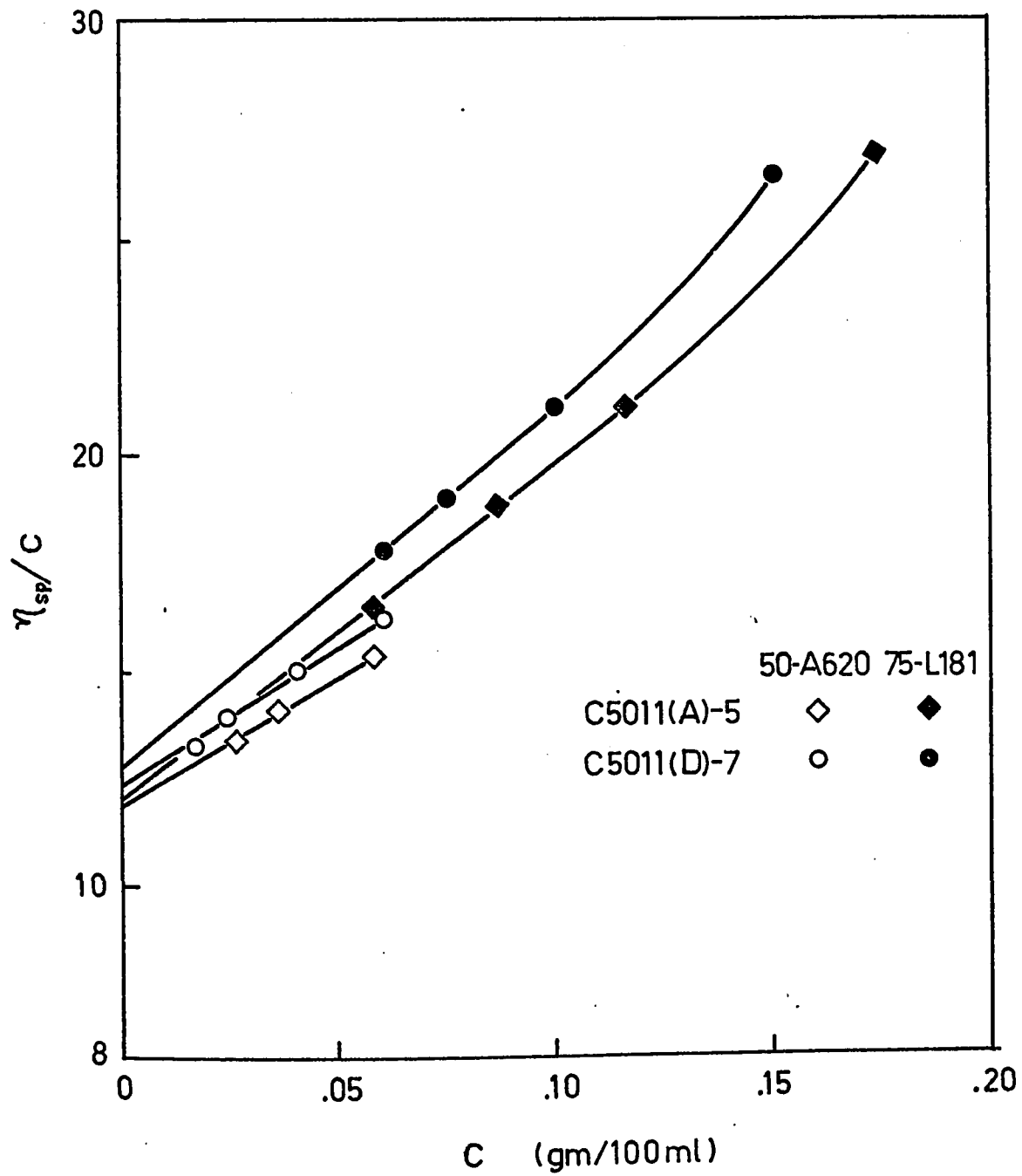


Fig.AI-1-3 Difference in Two Viscometers

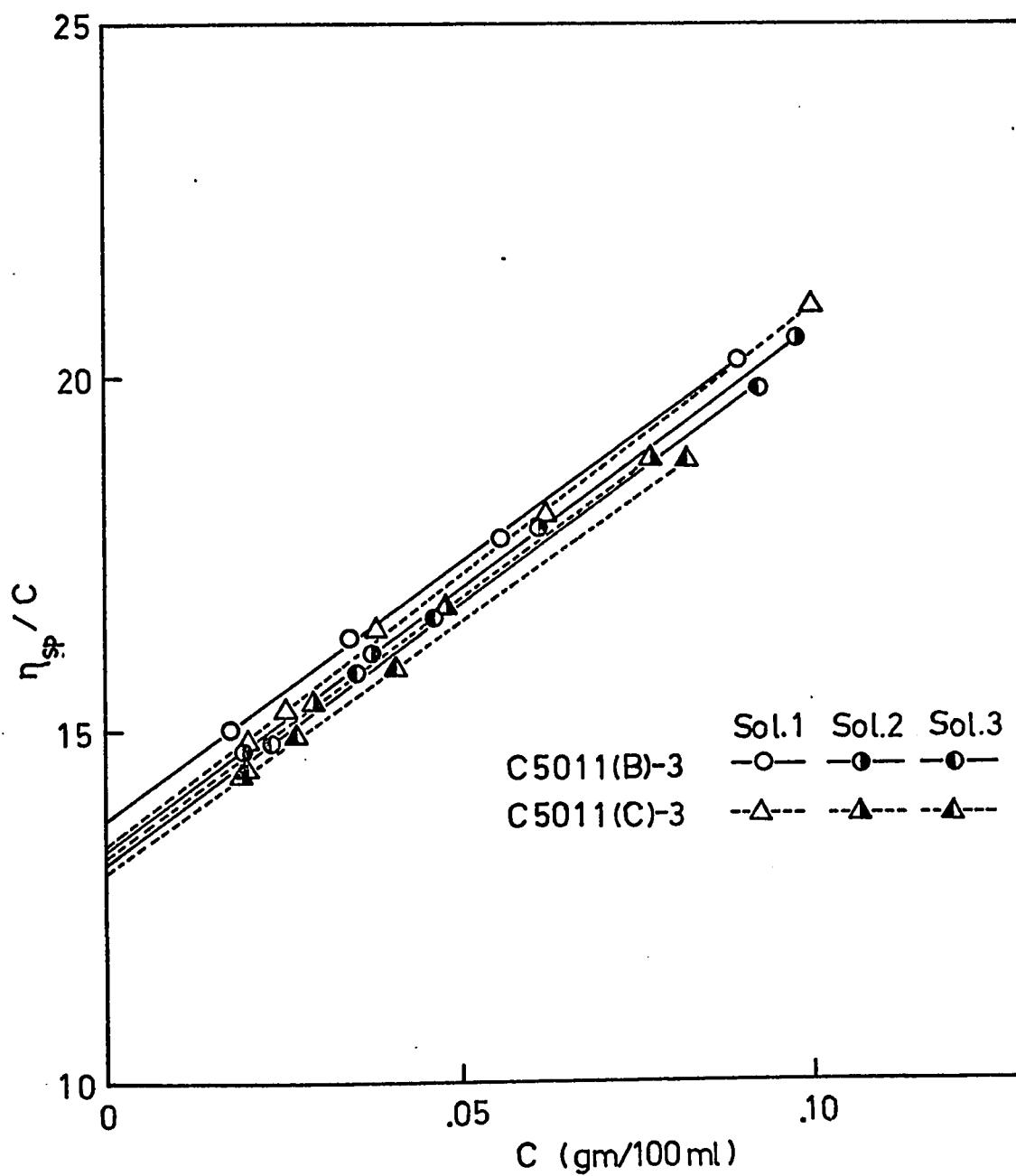


Fig. AI-1-4 Reproducibility Test

It was found that there is no significant difference between the two averages and that the intrinsic viscosity value of a particular polymer sample is reproducible to $\pm 4\%$.

Effect of continuous stirring of a polymer solution by a magnet on polymer degradation was checked by following the viscosity of the solution stirred continuously. The results are given in Table AI-1-4. Decrease in viscosity was surprisingly large. Calculated \bar{M}_n is plotted against the duration of stirring as well as the plot of η_{sp}/c vs. c in Fig. AI-1-5. \bar{M}_n showed a decrease of as much as 15% with one day of stirring. Although the stirring employed in diluting the original reaction mixture to a homogeneous solution may not undergo a similar amount of molecular weight decrease as was seen for the stirring applied for the polymer solution prepared at 50°C , it could well be anticipated that the recovered polymers by precipitation have a smaller molecular weight than the original molecular weight in the reaction mixture. Unfortunately, the separation of polymer from monomer was not satisfactory without first diluting the reaction mixture. Simple addition of methanol to the original reaction mixture taken from an ampoule resulted in a formation of hard outer layer of polymer inside which the reaction mixture remained as a viscous monomer-polymer mixture in water. Now it is apparent that the largest uncertainty in \bar{M}_n values originated from the polymer recovery process. It is greater with higher monomer concentrations at high conversions.

Table AI-1-5 lists all the other viscosity measurements carried out.

TABLE AI-1-4 EFFECT OF STIRRING ON VISCOSITY

SAMPLE C5044-2						
STIRRING (DAY)	CONC. (GM/100ML)	TIME (MIN.)	η (C.P.)	η_r	η_{sp}	η_{sp}/c (100ML/GM)
0	.0502	6.95	1.62	1.80	.80	15.95
	.0314	5.65	1.32	1.46	.46	14.78
	.0193	4.91	1.14	1.27	.27	14.09
1	.0502	6.46	1.50	1.67	.67	13.42
	.0314	5.37	1.25	1.39	.39	12.47
	.0193	4.75	1.11	1.23	.23	11.95
	.0125	4.43	1.03	1.15	.15	11.77
2	.0502	6.18	1.44	1.60	.60	11.98
	.0314	5.22	1.22	1.35	.35	11.23
	.0193	4.66	1.09	1.21	.21	10.74
	.0125	4.38	1.02	1.13	.13	10.74
4	.0502	5.66	1.32	1.47	.47	9.29
	.0314	4.93	1.15	1.28	.28	8.84
	.0193	4.50	1.05	1.17	.17	8.59
	.0125	4.28	1.00	1.11	.11	8.68

(Viscometer: 50-A620)

Fig. AI-1-5 Effect of Stirring on Viscosity

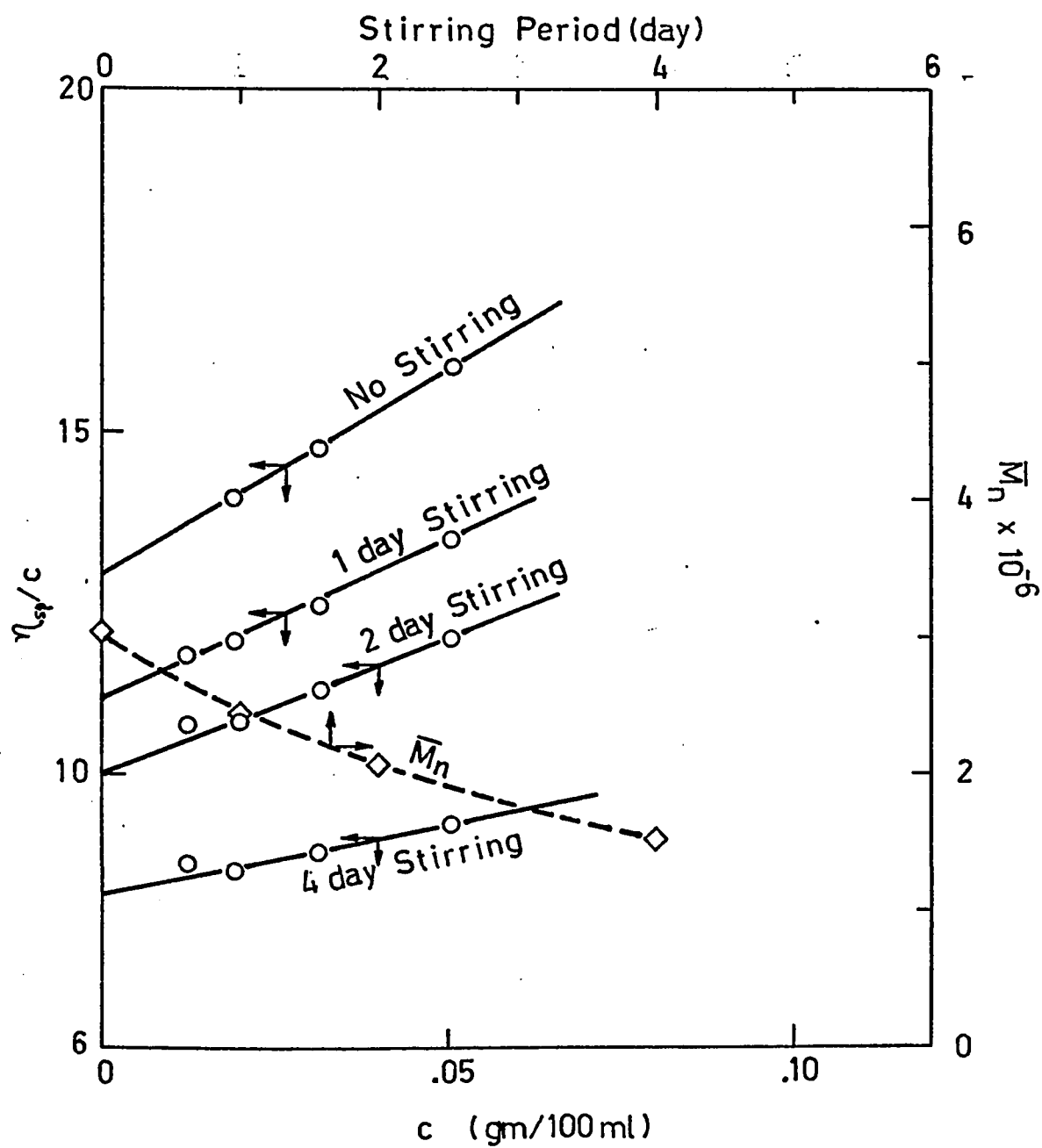


TABLE AI-1-5 SUMMARY OF VISCOSITY MEASUREMENT

SAMPLE	CONC. (GM/100ML)	TIME (MIN.)	η (C.P.)	η_r	η_{sp}	η_{sp}/c (100ML/GM)
I5011	.0360	6.01	1.40	1.56	.56	15.48
	.0225	5.12	1.19	1.33	.33	14.51
	.0138	4.61	1.07	1.19	.19	14.04
	.0090	4.34	1.01	1.12	.12	13.83
I5012	.0424	6.39	1.49	1.66	.66	15.46
	.0265	5.35	1.25	1.39	.39	14.57
	.0163	4.73	1.10	1.23	.23	13.83
	.0106	4.40	1.02	1.14	.14	13.21
I5014	.0450	6.07	1.41	1.57	.57	12.73
	.0281	5.16	1.20	1.34	.34	11.98
	.0173	4.63	1.08	1.20	.20	11.53
	.0112	4.35	1.01	1.13	.13	11.29
I5024	.0472	6.94	1.62	1.80	.80	16.91
	.0295	5.66	1.32	1.47	.47	15.81
	.0182	4.93	1.15	1.28	.28	15.28
	.0118	4.53	1.06	1.17	.17	14.72
I5044	.0550	8.25	1.92	2.14	1.14	20.68
	.0344	6.35	1.48	1.65	.65	18.77
	.0212	5.29	1.23	1.37	.37	17.52
	.0110	4.55	1.06	1.18	.18	16.26
C5011(A)-2	.0688	9.27	2.16	2.40	1.40	20.37
	.0344	6.24	1.45	1.62	.62	17.93
	.0172	4.95	1.15	1.28	.28	16.42
C5011(A)-3	.0722	8.94	2.08	2.32	1.32	18.23
	.0451	6.70	1.56	1.74	.74	16.31
	.0278	5.54	1.29	1.44	.44	15.68
	.0181	4.85	1.13	1.26	.26	14.21
C5011(A)-6	.0850	8.78	2.05	2.27	1.27	15.00
	.0531	6.61	1.54	1.71	.71	13.41
	.0327	5.43	1.26	1.41	.41	12.44
	.0212	4.84	1.13	1.25	.25	11.95

TABLE AI-1-5 (CONTINUED)

SAMPLE	CONC. (GM/100ML)	TIME (MIN.)	η (C.P.)	η_r	η_{sp}	η_{sp}/c (100ML/GM)
C5011(C)-8	.1384	14.68	3.42	3.80	2.80	20.26
	.0865	9.28	2.16	2.40	1.40	16.24
	.0532	6.94	1.62	1.80	.80	14.99
	.0346	5.70	1.33	1.48	.48	13.78
	.0277	5.34	1.24	1.38	.38	13.86
C5011(D)-1	.0556	7.69	1.79	1.99	.99	17.85
	.0348	6.10	1.42	1.58	.58	16.70
	.0214	5.17	1.20	1.34	.34	15.88
	.0139	4.68	1.09	1.21	.21	15.29
C5011(D)-2	.0790	10.21	2.38	2.65	1.65	20.83
	.0395	6.61	1.54	1.71	.71	18.04
	.0198	5.11	1.19	1.32	.32	16.40
C5011(D)-4	.0712	8.56	1.99	2.22	1.22	17.10
	.0356	5.90	1.37	1.53	.53	14.85
	.0178	4.80	1.12	1.24	.24	13.69
C5014(A)-1	.0649	7.42	1.73	1.92	.92	14.21
	.0325	5.45	1.27	1.41	.41	12.70
	.0216	4.89	1.14	1.27	.27	12.34
C5014(A)-2	.1500	14.00	3.26	3.63	2.63	17.51
	.0938	8.95	2.08	2.32	1.32	14.07
	.0682	7.31	1.70	1.89	.89	13.11
	.0469	6.08	1.42	1.58	.58	12.27
	.0300	5.22	1.22	1.35	.35	11.75
C5014(A)-6 (75-L181)	.2478	11.28	5.94	6.60	5.60	22.61
	.1487	5.84	3.07	3.42	2.42	16.26
	.0929	3.85	2.03	2.25	1.25	13.49
	.0676	3.15	1.66	1.84	.84	12.48
	.0465	2.67	1.40	1.56	.56	12.11

TABLE AI-1-5 (CONTINUED)

SAMPLE	CONC. (GM/100ML)	TIME (MIN.)	η (C.P.)	η_r	η_{sp}	η_{sp}/C (100ML/GM)
C5014(A)-6 (IN .15% KBr)	.1778	11.18	2.60	2.90	1.90	10.68
	.1110	7.64	1.79	1.99	0.99	8.89
	.0683	6.04	1.41	1.56	0.56	8.25
	.0445	5.20	1.21	1.35	0.35	7.82
C5014(A)-7	.1288	9.40	2.19	2.44	1.44	11.14
	.0644	6.36	1.48	1.65	.65	10.06
	.0429	5.47	1.27	1.42	.42	9.72
C5021(A)-1 (75-L181)	.9920	6.12	3.22	3.58	2.58	2.60
	.5952	3.92	2.06	2.29	1.29	2.17
	.4251	3.16	1.66	1.85	.85	2.00
C5021(A)-3	.0588	7.98	1.86	2.07	1.07	18.16
	.0367	6.22	1.45	1.61	.61	16.64
	.0226	5.22	1.22	1.35	.35	15.58
	.0147	4.70	1.09	1.22	.22	14.81
C5021(A)-5	.0618	7.94	1.85	2.06	1.06	17.11
	.0309	5.65	1.32	1.46	.46	15.01
	.0206	5.06	1.18	1.31	.31	15.10
	.0154	4.68	1.09	1.21	.21	13.76
C5021(A)-7	.0538	6.95	1.62	1.80	.80	14.88
	.0336	5.65	1.32	1.46	.46	13.79
	.0207	4.90	1.14	1.27	.27	13.03
	.0135	4.52	1.05	1.17	.17	12.72
C5024(A)-2	.0670	7.87	1.83	2.04	1.04	15.51
	.0419	6.14	1.45	1.59	.59	14.11
	.0258	5.20	1.21	1.35	.35	13.48
	.0168	4.70	1.09	1.22	.22	13.00
C5024(A)-3	.0514	7.03	1.64	1.82	.82	15.98
	.0321	5.68	1.32	1.47	.47	14.68
	.0198	4.92	1.15	1.27	.27	13.90
	.0128	4.52	1.05	1.17	.17	13.31

TABLE AI-1-5 (CONTINUED)

SAMPLE	CONC. (GM/100ML)	TIME (MIN.)	η (C.P.)	η_r	η_{sp}	η_{sp}/C (100ML/GM)
C5024(A)-4	.0820	9.48	2.21	2.46	1.46	17.76
	.0513	6.96	1.62	1.80	.80	15.67
	.0315	5.61	1.31	1.45	.45	14.38
	.0205	4.94	1.15	1.28	.28	13.65
C5044-5	.0588	7.72	1.80	2.00	1.00	17.01
	.0367	6.09	1.42	1.58	.58	15.72
	.0226	5.13	1.19	1.33	.33	14.55
	.0147	4.66	1.09	1.21	.21	14.11
C50S(A)-1	.1990	14.62	3.41	3.79	2.79	14.01
	.1244	9.45	2.20	2.45	1.45	11.65
	.0765	6.99	1.63	1.81	.81	10.60
	.0433	5.50	1.28	1.42	.42	9.82
C50S(A)-2	.2620	>16.0				
	.1638	11.84	2.76	3.07	2.07	12.63
	.1191	8.78	2.05	2.27	1.27	10.70
	.0771	6.78	1.58	1.76	.76	9.82
	.0595	6.08	1.42	1.58	.58	9.66
C50S(A)-3	.1968	12.03	2.80	3.12	2.12	10.76
	.1230	8.40	1.96	2.18	1.18	9.56
	.0757	6.51	1.52	1.69	.69	9.07
	.0492	5.53	1.29	1.43	.43	8.80
I4014	.0520	7.41	1.73	1.92	.92	17.69
	.0325	5.95	1.39	1.54	.54	16.66
	.0200	5.10	1.19	1.32	.32	16.07
	.0130	4.62	1.08	1.20	.20	15.15
C4014-3	.0568	7.32	1.70	1.90	.90	15.78
	.0355	5.92	1.38	1.53	.53	15.04
	.0218	5.04	1.17	1.31	.31	14.00
	.0142	4.62	1.08	1.20	.20	13.87

TABLE AI-1-5 (CONTINUED)

SAMPLE	CONC. (GM/100ML)	TIME (MIN.)	η (C.P.)	η_r	η_{sp}	η_{sp}/C (100ML/GM)
C4014-7	.0460	6.43	1.50	1.67	.67	14.48
	.0288	5.35	1.25	1.39	.39	13.43
	.0177	4.75	1.11	1.23	.23	13.04
	.0115	4.42	1.03	1.15	.15	12.62
C4044-2	.0409	6.25	1.46	1.62	.62	15.14
	.0256	5.28	1.23	1.37	.37	14.40
	.0186	4.85	1.13	1.26	.26	13.80
	.0120	4.49	1.05	1.16	.16	13.58
C4044-3	.0656	7.43	1.73	1.93	.93	14.10
	.0410	5.89	1.37	1.53	.53	12.83
	.0252	5.00	1.16	1.30	.30	11.71
	.0164	4.60	1.07	1.19	.19	11.70
C4044-6	.0710	8.15	1.90	2.11	1.11	15.66
	.0444	6.28	1.46	1.63	.63	14.13
	.0273	5.26	1.23	1.36	.36	13.29
	.0178	4.76	1.11	1.23	.23	13.14
C4044-E1	.0634	8.35	1.94	2.16	1.16	18.35
	.0396	6.38	1.49	1.65	.65	16.48
	.0244	5.30	1.23	1.37	.37	15.30
	.0159	4.76	1.11	1.23	.23	14.72
I2511	.0380	6.94	1.62	1.80	.80	21.00
	.0238	5.70	1.33	1.48	.48	20.08
	.0146	4.95	1.15	1.28	.28	19.33
	.0095	4.53	1.06	1.17	.17	18.28
I2512	.0340	6.75	1.57	1.75	.75	22.02
	.0212	5.56	1.30	1.44	.44	20.73
	.0131	4.85	1.13	1.26	.26	19.62
	.0085	4.47	1.04	1.16	.16	18.60
I2514	.0310	6.37	1.48	1.65	.65	20.98
	.0194	5.33	1.24	1.38	.38	19.66
	.0119	4.72	1.10	1.22	.22	18.69
	.0078	4.41	1.03	1.14	.14	18.40

(Viscometer: 50-A620 unless otherwise stated)

Appendix I-2 Light Scattering Measurements

Light scattering measurements were done using a Brice-Phoenix Universal Light Scattering Photometer. A sample polymer solution was prepared in the same manner as for viscometry. This solution was then filtered with a 1.2 μ millipore filter under pressure (~25 lbs/in²). Attempt to filter the solution with a 0.22 μ filter was not successful due to plugging leaving a thick mass of polymer on the filter. Light scattering measurements made for polyacrylamide of molecular weight $\bar{M}_w = 1.1 \times 10^6$ or less involved the use of 0.45 μ millipore filter for filtration. (5)

Refractive index increment of polymer solutions in water was obtained with Brice Phoenix Differential Refractometer. These results are given in Table AI-2-1. A plot of refractive index difference vs. concentration is shown in Fig. AI-2-1. The value dn/dc obtained from the slope of the line was 0.161 (cc/gm). This compares to the reported values of 0.163⁽⁵⁴⁾ and 0.186⁽⁹⁾.

Measurement of scattered light intensity was made by a cylindrical cell of 100 ml (Brice Phoenix Catalog No. C101) with the wave length of 546 m μ . Concentration and angular dependence of the scattered light intensity is summarized in Table AI-2-2 together with the calculated Rayleigh ratio. All the calculation and correction for cell size (Standard: 40 x 40 mm semi-octagonal) and for the beam width (Standard: 1.20 cm) were made according to the reference manual and the text by Nakagaki et.al.⁽⁵⁵⁾ A Zimm plot for the sample C5011(C)-8 is shown in

Table A1 -2-1 Refractive Index Difference Measurements

System	Difference in Scale Reading Δd (546 $m\mu$)	Refractive Index Difference $\Delta n \times 10^6$ (546 $m\mu$)
D.W. - KCl (2.9821 gm/100 ml)	4.284	3,994*
D.W. - KCl (1.0794 gm/100 ml)	1.585	1,469*
D.W. - C5021(A)-7 (0.4558 gm/100 ml)	.824	766
D.W. - C5011(C)-8 (0.2768 gm/100 ml)	.492	457
D.W. - C5011(C)-8 (0.0692 gm/100 ml)	.122	114

*These values⁽⁵³⁾ were used to obtain the instrument calibration constant $K' = \Delta n / \Delta d$. The values of $K' = 932 \times 10^{-6}$ and 927×10^{-6} were obtained from D.W. - KCl systems. Average value of the two, $K' = 930 \times 10^{-6}$ was used to calculate $\Delta n = K' \Delta d$ for polyacrylamide solutions.

Fig. AI-2-2. The extrapolation of Kc/R_{θ} to zero angle and zero concentration yielded $\bar{M}_w = 6.3 \times 10^6$.

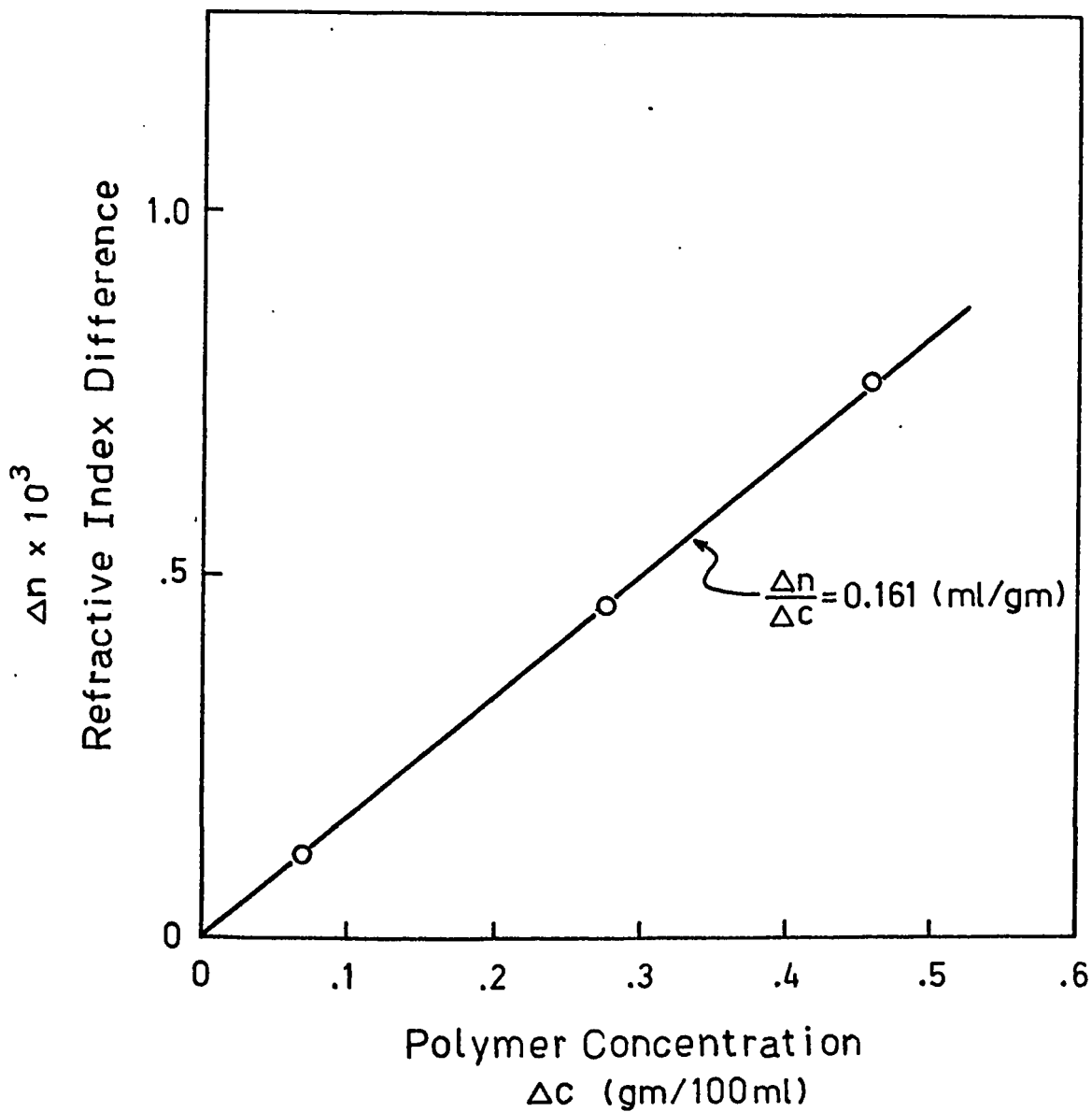


Fig. AI-2-1 Refractive Index Difference vs. Polymer Concentration (546 m μ)

Table A1-2-2 Angular and Concentration Dependence of Scattered
Light Intensity

c	θ	G'_θ	F	G_θ	$(G_\theta/G_w) \times 10^2$	$R_\theta \times 10^4$	$(Kc/R_\theta) \times 10^6$
.2768	0	92	$F_1 F_2 F_3$	6,021			
	45	107	F_1	270	4.48	2.57	2.75
	60	76	"	162	2.69	2.24	2.63
	75	114	none	114	1.89	2.04	2.46
	90	100	"	100	1.66	1.97	2.39
	105	105	"	105	1.74	1.85	2.71
	120	134	"	134	2.23	1.80	3.27
	135	88	F_1	187	3.11	1.67	4.22
.1384	0	112	$F_1 F_2 F_3$	7,330			
	45	75	F_2	295	4.02	2.32	1.52
	60	83	F_1	177	2.41	2.03	1.45
	75	117	none	117	1.60	1.74	1.45
	90	100	"	100	1.36	1.61	1.46
	105	102	"	102	1.39	1.48	1.70
	120	125	"	125	1.71	1.36	2.17
	135	83	F_1	177	2.41	1.27	2.77
.0692	0	70	$F_3 F_4$	10,190			
	45	102	F_2	402	3.95	2.31	.765
	60	106	F_1	226	2.22	1.89	.779
	75	136	none	136	1.34	1.47	.855
	90	100	"	100	.982	1.17	1.01
	105	103	"	103	1.01	1.06	1.18
	120	129	"	129	1.27	.98	1.50
	135	87	F_1	185	1.82	.92	1.78

Table IA-2-2 (continued)

c	θ	G'_θ	F	G_θ	$(G_\theta/G_w) \times 10^2$	$R_\theta \times 10^4$	$(Kc/R_\theta) \times 10^6$
	0	102	$F_3 F_4$	14,839			
	45	114	F_2	449	3.03	1.78	.497
	60	112	F_1	238	1.60	1.37	.535
	75	133	none	133	.896	.984	.638
.0346	90	100	"	100	.674	.800	.736
	105	97	"	97	.654	.680	.923
	120	120	"	120	.808	.609	1.21
	135	87	F_1	185	1.25	.612	1.44

c : Concentration (gm/100 ml)

θ : Angle of measurement ($^\circ$)

G'_θ : Observed scattered light Intensity at θ with F

F : Filter or filter combinations ($F_1 = .470$, $F_2 = .254$, $F_3 = .128$, $F_4 = .0537$)

G_θ : Scattered light intensity without filter

G_w : Equal to G_θ where $\theta = 0$

R_θ : Rayleigh ratio

K : $(2\pi^2/\lambda_o^4 N) \cdot n_o^2 \cdot (\frac{\Delta n}{\Delta c})^2 (1 + \cos^2 \theta)$ where λ_o is the wave-length,
N, Avogadros Number, n_o , refractive index of the solvent,
and $(\Delta n/\Delta c)$, refractive index increment.

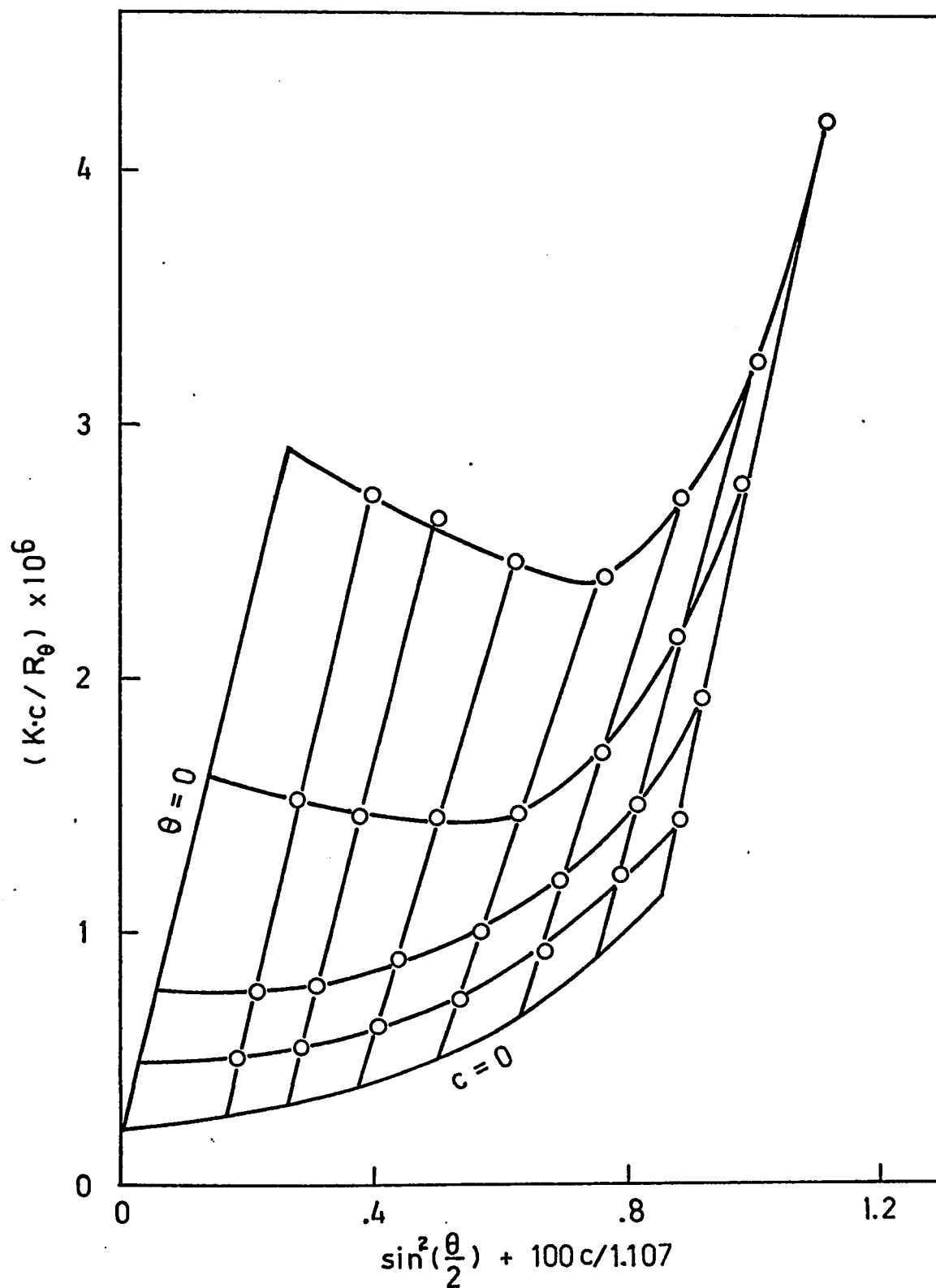


Fig. AI-2-2 Zimm Plot for Sample C5011(C)-3

Appendix I-3 Electron Microscope Measurements of Molecular Weight Distribution

Experimental technique of observing single molecules of polyacrylamide by electron microscopy was first reported by Quayle.⁽⁴⁵⁾ Further development has been made in the Department of Mechanical Engineering, McMaster University by Wade and Kumar in relation to the study on drag reduction in aqueous solutions of polyacrylamide.⁽⁴⁶⁾ Specimen preparation followed their procedure in the present experiment. Polyacrylamide solutions of 40 w ppm in water was slowly added with n-propanol to the ratio 20% water and 80% n-propanol. Polystyrene latex (Dow Chemical) of particle diameter 0.264μ was added to these solutions for a calibration standard. Then the solutions were sprayed onto copper substrate, shadowed with gold-palladium and then protected by carbon.

Micrographs were obtained at a magnification of $\times 20,000$ on a Phillip EM40 electron microscope. Fig. AI-3-1 shows examples of the micrographs obtained. Polystyrene standard appeared as a well formed sphere while smaller polyacrylamide molecules were distorted to some extent. Shadow lengths of well-isolated molecules were measured by particle size analyzer TGZ3 (Carl Zeiss) after magnification of the micrographs into $\sim \times 4$.

The shadow length L_s' and diameter D_s' of the standard polystyrene were also measured for calibration purpose. Table AI-3-1 lists the results for styrene. Since the absolute diameter of the standard polystyrene is 2640 \AA , the sphere-approximated radius r_p' (cm., in the

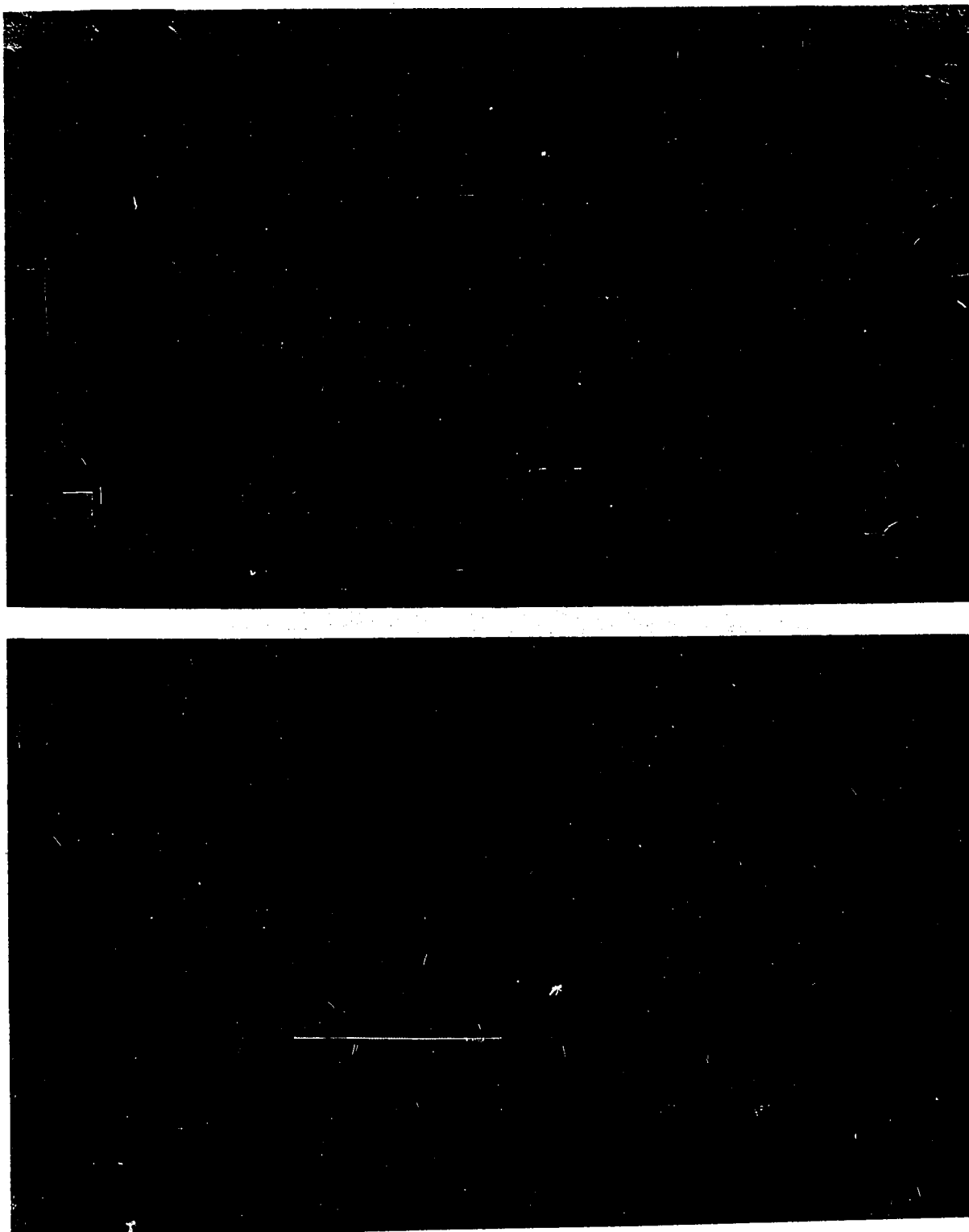


Fig. AI-3-1 Examples of Micrographs (original \sim x 20,000, enlarged to 1.5 times)

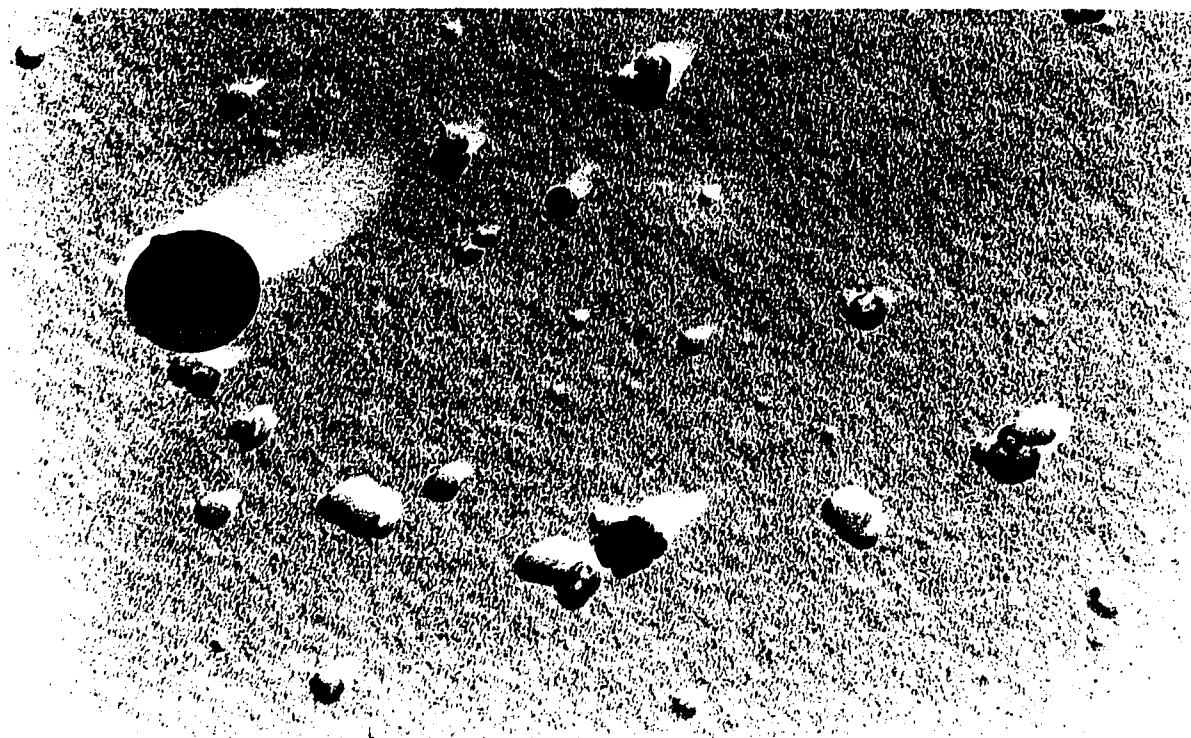
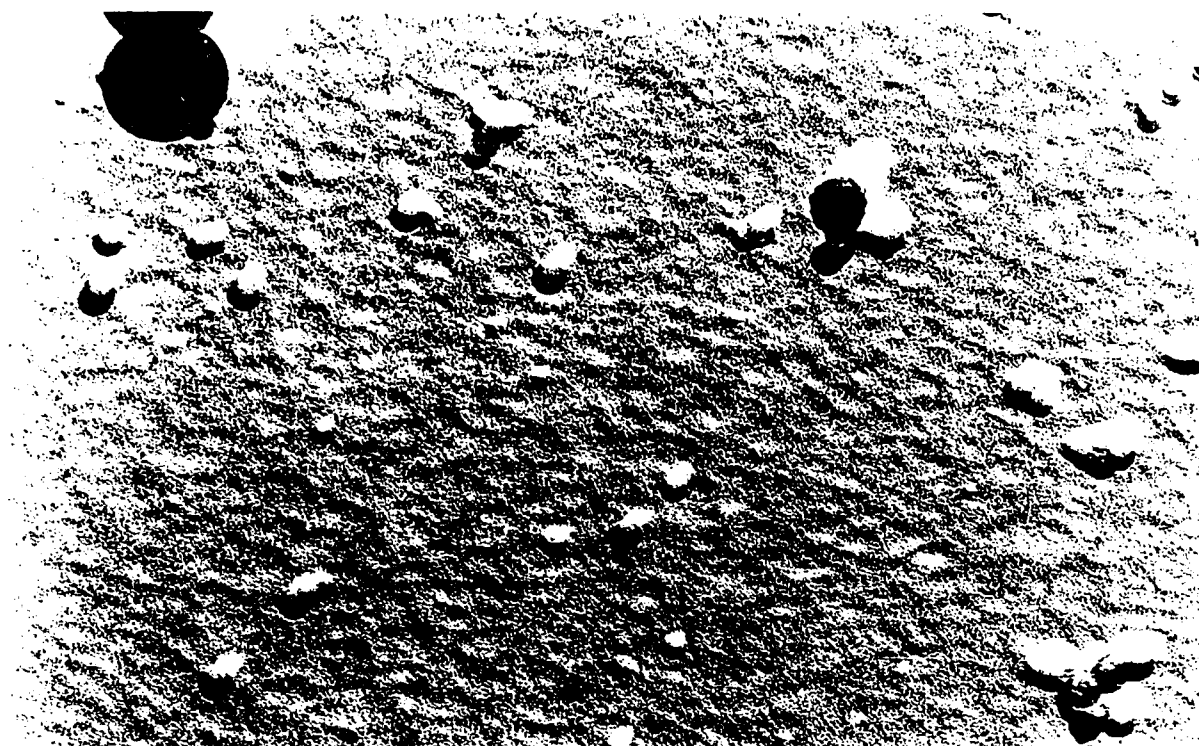


Fig. A1.5.1. Examples of micrographs (original $\times 20,000$ enlarged to 1.5 times)

Table AI-3-1 Shadow Length and Diameter of Standard Polystyrene Particle

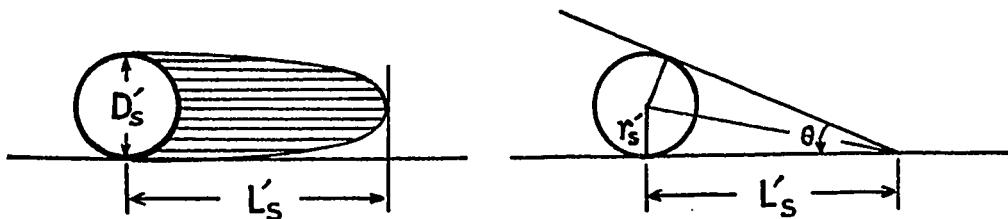
Particle No.	D'_s (cm)	L'_s (cm)
1	3.33	7.06
2	3.41	5.90
3	3.40	5.98
4	3.45	6.24
5	3.46	6.44
6	3.64	6.89
Ave.	3.45	Ave. 6.42

D'_s : Diameter, the average of the one vertical and the other parallel to the direction of shadowing

L'_s : Shadow length

Fig. AI-3-2 Shadow Length and Particle Dimension

Polystyrene Standard



picture) of a polyacrylamide molecule with a shadow length L' has the absolute value r_p given by (See Fig. AI-3-2)

$$r_p = L' \tan\left(\frac{\theta}{2}\right) \left(\frac{2640}{D_{S'}}\right) = L' \left(\frac{D_{S'}}{2L_{S'}}\right) \cdot \frac{2640}{D_{S'}} = 206 L' \text{ (Å)}$$

Richardson⁽⁵⁶⁾ has demonstrated that the shadow length provides an accurate estimate of the height of the particle although there is a distortion of small particles due to the deposition of shadowing materials upon them.

Table AI-3-2 lists the number of polyacrylamide molecules and the shadow length. Fig. AI-3-3 shows the histogram with respect to shadow length.

Molecular weight distribution or molecular weight averages can be obtained from the distribution of number of molecules with respect to molecular radius. Since the previous works report no details on the procedure, it was treated as follows:

A polymer molecule having a radius r_p (cm) has the molecular weight of

$$M(r_p) = \rho \cdot \left(\frac{4}{3} \pi r_p^3\right) \cdot N \quad (\text{gm/gm-mole})$$

where M is the molecular weight, ρ is the density of the molecule (gm/cm^3) and N is Avogadro's Number. The number-based distribution function $f_N(r_p)$ with respect to molecular radius and the number-based distribution $F_N(M)$ with respect to molecular weight are related in the following manner.

Table AI-3-2 Number of Molecule vs. Shadow Length

Counter Scale	Shadow Length L' (cm)	No. of Molecules
1	.120	1
2	.176	6
3	.232	34
4	.288	53
5	.344	64
6	.400	68
7	.456	73
8	.512	67
9	.568	60
10	.624	38
11	.680	17
12	.736	18
13	.792	18
14	.848	10
15	.904	7
16	.960	1
17	1.016	1

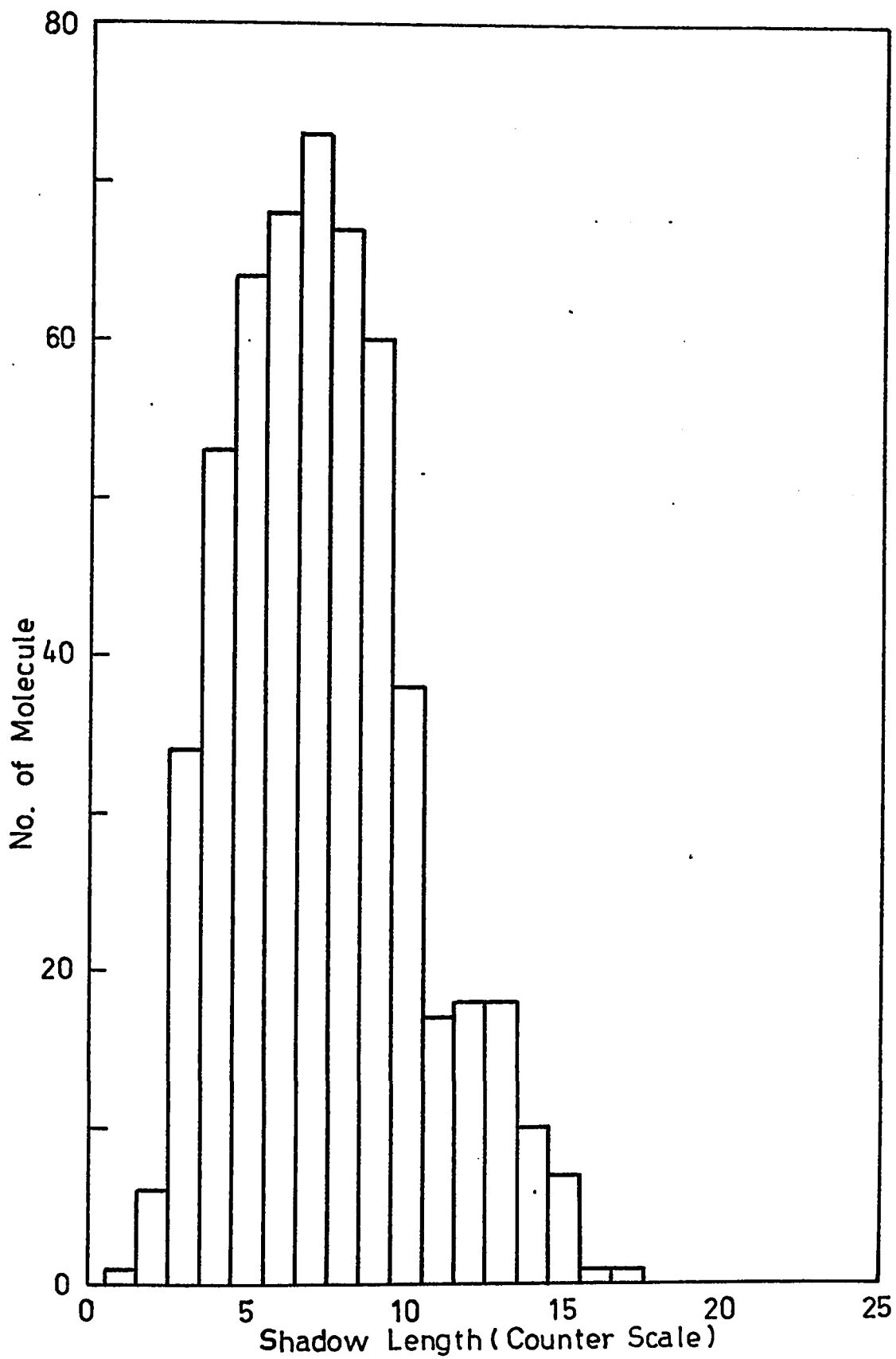


Fig. AI-3-3 Shadow Length Histogram Sample C5011(C)-8

$$f_N(r_p) dr_p = F_N(M) dM$$

$$\text{where } \frac{dM}{dr_p} = \rho (4\pi r_p^2) N = \rho \left(\frac{4}{3}\pi r_p^3\right) N \cdot \left(\frac{3}{r_p}\right) = \frac{3M}{r_p}$$

Therefore

$$F_N(M) = f_N(r_p) / \left(\frac{dM}{dr_p}\right) = \frac{r_p}{3M} f_N(r_p)$$

The number-average molecular weight is then

$$\begin{aligned} \bar{M}_n &= \frac{\int_0^\infty M F_N(M) dM}{\int_0^\infty F_N(M) dM} = \int_0^\infty \left(\frac{r_p}{3}\right) f_N(r_p) \cdot \rho \left(\frac{4}{3}\pi r_p^3\right) N \cdot \left(\frac{3}{r_p}\right) dr_p \\ &= \frac{4}{3}\pi \rho N \int_0^\infty r_p^3 f_N(r_p) dr_p \end{aligned}$$

The weight-based molecular weight distribution may be written as

$$F_W(M) = \frac{M F_N(M)}{\int_0^\infty M F_N(M) dM} = \frac{\left(\frac{r_p}{3}\right) f_N(r_p)}{\bar{M}_n}$$

$$\therefore \bar{M}_w = \frac{\int_0^\infty M F_W(M) dM}{\int_0^\infty F_W(M) dM}$$

$$= \int_0^\infty M \cdot \frac{\left(\frac{r_p}{3}\right) f_N(r_p)}{\bar{M}_n} \cdot \left(\frac{3}{r_p}\right) M dr_p$$

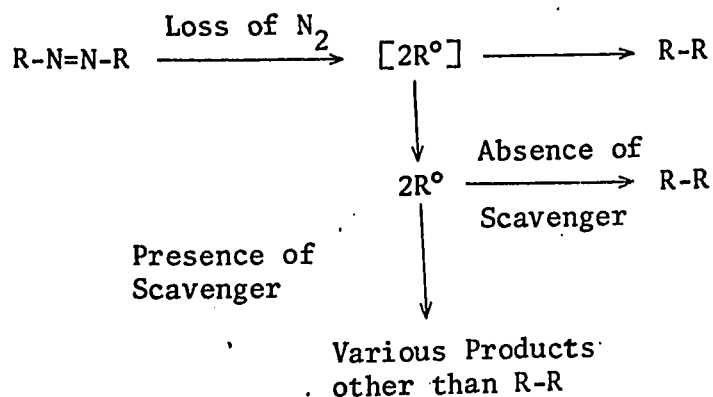
$$= \frac{1}{\bar{M}_n} \int_0^\infty M^2 f_N(r_p) dr_p = \frac{\int_0^\infty \left(\frac{4}{3}\pi \rho N\right)^2 r_p^6 f_N(r_p) dr_p}{\frac{4}{3}\pi \rho N \int_0^\infty r_p^3 f_N(r_p) dr_p} = \left(\frac{4}{3}\pi \rho N\right) \frac{\int_0^\infty r_p^6 f_N(r_p) dr_p}{\int_0^\infty r_p^3 f_N(r_p) dr_p}$$

The bulk density of polymers has been assigned for the density of single molecule for obtaining molecular weight averages. Experiments with polystyrene has shown the validity. However, the previous work on polyacrylamide, though the average molecular weights were calculated from observed shadow lengths, the bulk density of this polymer is not reported. Therefore, for the present data interpretation, the density of single molecule was estimated by using \bar{M}_n measured by viscometry and setting this equal to \bar{M}_n by electron microscopy. Molecular weight distribution thus obtained is shown in Fig. I-4-19.

Appendix I-4 Decomposition Rate of ACV at 80°C

During a study of decomposition of various azo-initiators, the rate of ACV decomposition in water was measured by measuring the rate of nitrogen evolution.⁽³⁰⁾ The decomposition reaction was found to be first order with respect to the initiator concentration. The decomposition rate constant k_d (at 80°C) and activation energy of the reaction were found to be 8.97×10^{-5} (1/sec.) and 34.0 (K cal/mol) respectively. When these data are applied to the temperature where the polymerization was carried out, ($k_d = 1.0 \times 10^{-6}$, 1.18×10^{-8} (1/sec) at 50°C and 25°C respectively) it was found that the previous polymerization study by Cavell and Gilson^(21,43) as well as the present study gave an initiator efficiency far greater than one. Therefore, it was decided to check the reported k_d value at 80°C. Although measurement of k_d within the polymerization temperature range 25-50°C was desirable, the decomposition rate at these temperatures is too slow to follow directly.

The principal reaction paths for decomposition of azobisisobutyronitrile (AIBN) have been shown to involve⁽⁵⁷⁾.



where R and R° denote functional group of $\text{CH}_3-\overset{\text{CN}}{\underset{\text{CH}_3}{\text{C}}}$ and its radical form.

Under the assumption that the substitution of R by $\text{HOOC}-\text{CH}_2-\overset{\text{CN}}{\underset{\text{CH}_3}{\text{C}}}$ (then

R-N=N-R represents ACV) does not alter the main reaction paths, a GPC analysis was carried out for ACV decomposition in water with and without presence of hydroquinone (HQ) known as an efficient radical scavenger. (38)

It was clearly observed that the concentration of ACV decreased with time giving a rise of secondary peak representing some products of decomposition. The examples of these are shown in Part II, Fig. II-4-5. The secondary peak is composed mainly of products other than R-R since this peak showed a faster growth with presence of hydroquinone than without its presence. The molecular weight of R-N=N-R (280) and R-R (252) may be too close to separate. While the products expected from the reaction with hydroquinone may range 140 to 252. Fig. AI-4-1 shows the change of C/C_0 obtained from the decrease of the peak area of ACV. The data did not exhibit the behaviour of the first order decomposition but this may be due to the fact that some of the products may be counted as ACV peak. Faster decrease of C/C_0 with the presence of hydroquinone indicates this possibility. From the slope of the initial decrease of C/C_0 , k_d was evaluated as 7.5×10^{-5} (1/sec) at 80°C, slightly lower than the reported value. (30) Since k_d thus estimated could possibly be lower than the true value because some of the decomposed products might have been counted as the original ACV due to imperfect separation, the reported value appears reasonable.

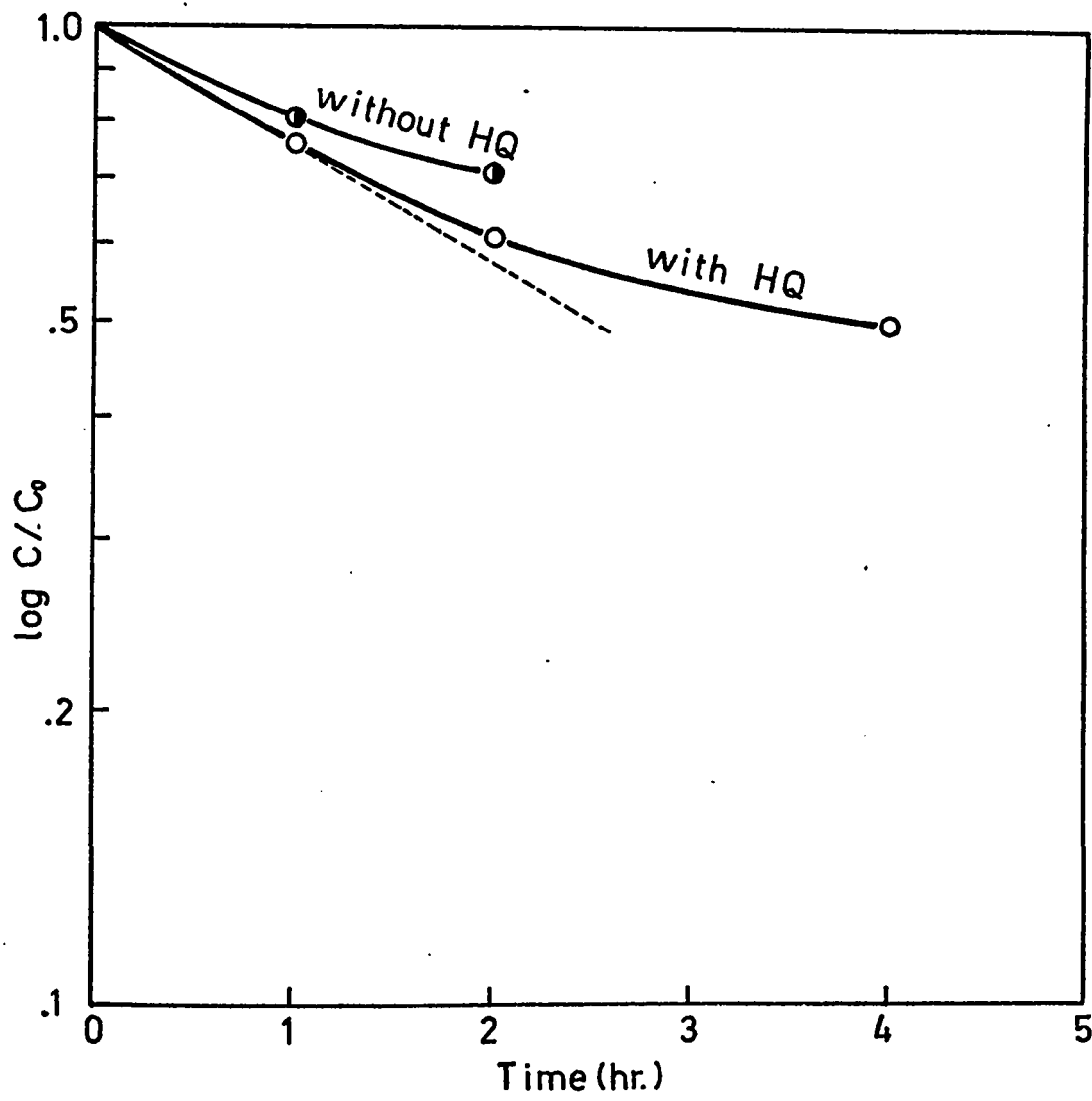


Fig. AI-4-1 Change of C/C_0 with Time

Appendix I-5: Calculation of Molecular Weight Distributions from the Kinetic Model

In order to keep the generality of derivation, the following kinetic scheme is considered here.

Initiation: Thermal or catalyst initiation $\rightarrow R_1^\bullet$

$I \equiv$ rate of formation of R_1^\bullet

Propagation: $R_r^\bullet + M \xrightarrow{k_p} R_{r+1}^\bullet$

$R_p \equiv$ rate of polymerization $= k_p [M][R^\bullet]$

Transfer: (a) to Monomer

$R_r^\bullet + M \xrightarrow{k_{fm}} P_r + M^\bullet$

(b) to solvent, or catalyst, or transfer agent S

$R_r^\bullet + S \xrightarrow{k_{fs}} P_r + S^\bullet$

Reinitiation: $M^\bullet + M \xrightarrow{k_{pm}} R_1^\bullet$

$S^\bullet + M \xrightarrow{k_{ps}} R_1^\bullet$

Termination: $R_r^\bullet + R_s^\bullet \xrightarrow{k_{tc}} P_{r+s}$ (Recombination)

$R_r^\bullet + R_s^\bullet \xrightarrow{k_{td}} P_r + P_s$ (Disproportionation)

Applying the kinetic stationary-state assumption, assuming rate constants independent of chain length and negligible volume change upon reaction, we may write

$$\frac{dR^\bullet}{dt} = I - k_{fm} M R^\bullet - k_{fs} S R^\bullet + k_{pm} M M^\bullet + k_{ps} M S^\bullet - k_{tc} R^{\bullet 2} - k_{td} R^{\bullet 2} = 0 \quad (\text{AI-5-1})$$

$$\frac{dM^*}{dt} = k_{fm} M R^* - k_{pm} M M^* = 0 \quad (\text{AI-5-2})$$

$$\frac{dS^*}{dt} = k_{fs} S R^* - k_{ps} M S^* = 0 \quad (\text{AI-5-3})$$

From equations (AI-5-1) to (AI-5-3) we obtain

$$I = (k_{tc} + k_{td}) R^{*2} = \left(\frac{k_{tc}}{k_p} + \frac{k_{td}}{k_p} \right) \cdot \frac{R_p^2}{M^2} \quad (\text{AI-5-4})$$

For convenience let us define the following two dimensionless groups

$$\alpha \equiv \frac{k_{td} R_p}{k_p^2 M^2} \quad \text{and} \quad \beta \equiv \frac{k_{tc} R_p}{k_p^2 M^2}$$

Therefore $I = (\alpha + \beta) R_p$.

Now, the radical concentration of different chain-length can be written as

$$R_1^* = \frac{(I + k_{fm}[M] + k_{fs}[S])[R^*]}{k_p[M] + k_{fm}[M] + k_{fs}[S] + (k_{tc} + k_{td})[R^*]}$$

$$R_r^* (r \geq 2) = \frac{k_p[M][R_{r-1}^*]}{k_p[M] + k_{fm}[M] + k_{fs}[S] + (k_{tc} + k_{td})[R^*]}$$

Let us define two new parameters, also dimensionless, T and τ where

$$T = \frac{k_{fm}}{k_p} + \frac{k_{fs}[S]}{k_p[M]} \quad \text{and} \quad \tau = T + \alpha$$

Then we can write

$$[R_1^*] = \frac{\left(\frac{R_p}{k_p[M]}\right) \left(T + I/R_p\right)}{1 + T + \alpha + \beta} = \frac{\left(\frac{R_p}{k_p[M]}\right) (\tau + \beta)}{1 + \tau + \beta}$$

$$[R_r^*] = \phi [R_{r-1}^*] = \phi^{r-1} [R_1^*]$$

where $\phi = \frac{1}{1 + \tau + \beta}$

The differential equations for polymer may be written as;

$$\begin{aligned} \frac{dP_r}{dt} &= \{k_{td}[R_r^*][R] + \frac{1}{2}k_{tc} \sum_{j=1}^{r-1} [R_{r-j}^*][R_j^*] + k_{fm}[M][R_r^*] + k_{fs}[S][R_r^*]\} \\ &= R_p \cdot \tau \cdot (\tau + \beta) \phi^r + R_p \cdot \left(\frac{1}{2}\beta\right) \cdot (\tau + \beta)^2 \{(r - 1) \cdot \phi^r\} \end{aligned} \quad (AI-5-5)$$

The instantaneous differential molecular weight may be written as

$$w(r) = \tau \cdot (\tau + \beta) \cdot (r \phi^r) + \frac{1}{2} \beta (\tau + \beta)^2 \cdot \{r^2 \phi^r\}$$

where $w(r)$ is the weight fraction of polymer of chain length r .

Approximating ϕ^r by $\exp\{-(\tau + \beta)r\}$,

$$w(r) = \tau(\tau + \beta)[r \exp\{-(\tau + \beta)r\}] + \frac{1}{2} \beta(\tau + \beta)^2 [r^2 \exp\{-(\tau + \beta)r\}]$$

Application of method of moment leads to

$$\bar{r}_n = \frac{1}{\tau + \beta/2}$$

$$\frac{\bar{r}_w}{\bar{r}_n} = 2 - 2 \frac{\frac{1}{2} \beta \cdot 2}{\tau + \beta}$$

In the present system of acrylamide polymerization, $\beta=0$ ($k_{tc} = 0$) and $k_{fs} = 0$ (transfer only to monomer), therefore,

$$\bar{r}_n = \frac{1}{\tau} = \frac{1}{\frac{k_{td}}{k_p} \frac{R_p}{[M]^2} + \frac{k_{fm}}{k_p}}$$

$$\bar{r}_w = 2\bar{r}_n$$

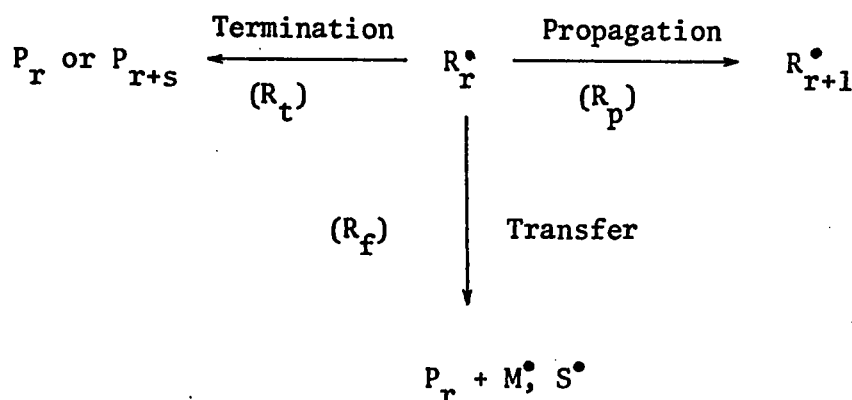
$$w(r) = \frac{r}{\bar{r}_n} \exp\left(-\frac{r}{\bar{r}_n}\right)$$

It should be noted that \bar{r}_n , \bar{r}_w and $w(r)$ thus derived are the values corresponding to polymers being produced at a certain time instant. Therefore in a batch reaction they must be integrated over a reaction time to obtain the number- and weight-average chain length \bar{P}_n and \bar{P}_w or differential molecular weight distribution of the final product polymer. Also, the above treatment related the molecular weight distribution with easily measurable quantity (R_p , M , S) in dimensionless forms. However, the physical meanings of these parameters are not clear because of their interrelationship. There exists another way of defining dimensionless parameters clearly retaining their physical meanings as well as the ease of their assessments. This has been developed by Lee et.al. and its application to variety of polymerization systems has been shown. (59)

Their formulation is described in the following since it is relatively less

known on this continent. A good summary of other methods of calculating molecular weight distribution has been made by Bamford et.al.⁽³¹⁾ and Hui.⁽⁴⁴⁾

Firstly, consider possible reaction paths a growing polymer radical may take. These are either propagation or termination, or transfer to monomer or to some other molecules present in a reaction system as shown below.



The symbols in parentheses represent the velocity of each path. Then the probability that R_r^\bullet grows to R_{r+1}^\bullet can be written as

$$\lambda = \frac{R_p}{R_p + R_t + R_f}$$

Therefore the concentration of the growing radical R_r^\bullet and the concentration of total radical R^\bullet are expressed in the following manner.

$$[R_r^\bullet] = \lambda [R_{r-1}^\bullet] = \dots = \lambda^{r-1} [R_1^\bullet]$$

$$[R^\bullet] = \sum_{r=1}^{\infty} [R_r^\bullet] = \sum_{r=1}^{\infty} \lambda^{r-1} [R_1^\bullet] = \frac{[R_1^\bullet]}{1-\lambda}$$

$$[R_r^\bullet] = \lambda^r \left(\frac{1-\lambda}{\lambda}\right) \cdot [R]$$

Now define ν as follows. It will be soon seen that ν is the average chain-length of all the growing radicals.

$$\nu \equiv \frac{\lambda}{1-\lambda} = \frac{R_p}{R_t + R_f} = \frac{I}{\left(\frac{k_t}{k_p}\right) \cdot \left(\frac{R_p}{M^2}\right) + \left(\frac{k_{fm}}{k_p}\right) + \left(\frac{k_{fs}}{k_p}\right) \frac{[S]}{[M]}}$$

Using this ν instead of λ ,

$$[R_r^\bullet] = \left(\frac{\nu}{1+\nu}\right)^r \cdot \frac{1}{\nu} \cdot [R]$$

Since $\nu \gg 1$, $e^{-\frac{r}{\nu}} \approx 1 - \frac{r}{\nu} \approx \frac{\nu}{1+\nu}$

Therefore,

$$[R_r^\bullet] = \frac{1}{\nu} \exp\left(-\frac{r}{\nu}\right) [R]$$

or

$$\bar{f}_n(r) \equiv \frac{\text{Number of polymer radicals with chain length } r}{\text{Number of total polymer radicals}}$$

$$= \frac{[R_r^\bullet]}{[R]} = \frac{1}{\nu} \exp\left(-\frac{r}{\nu}\right)$$

The $\dot{f}_n(r)$ is the number-based distribution of polymer radicals. Similarly, the weight-based distribution of polymer radicals can be written as follows.

$$\dot{f}_w(r) \equiv \frac{\text{Weight of polymer radicals with chain length } r}{\text{Total weight of polymer radicals}}$$

$$\begin{aligned} \dot{f}_w(r) &= \frac{r [R_r^\bullet]}{\sum_{r=1}^{\infty} r [R_r^\bullet]} = \frac{r \exp(-\frac{r}{v})}{\sum_{r=1}^{\infty} r \exp(-\frac{r}{v})} \\ &= \frac{r}{v} \exp(-\frac{r}{v}) = \frac{r}{v} \dot{f}_n(r) \end{aligned}$$

Further, one more distribution function on polymer radicals is defined for later convenience.

$$\begin{aligned} \dot{f}_z(r) &= \frac{r^2 [R_r^\bullet]}{\sum_{r=1}^{\infty} r^2 [R_r^\bullet]} = \frac{r^2}{2v^3} \exp(-\frac{r}{v}) \\ &= \frac{r}{2v} \dot{f}_w(r) = \frac{r^2}{2v^2} \dot{f}_n(r) \end{aligned}$$

The average chain length of the total polymer radicals can be shown to be equal to v .

$$\frac{\sum_{r=1}^{\infty} r \dot{f}_n(r)}{\sum_{r=1}^{\infty} \dot{f}_n(r)} = \sum_{r=1}^{\infty} \frac{r}{v} \exp(-\frac{r}{v}) = v$$

So far, the distributions of polymer radicals were expressed by a single parameter v . Next, consider the dead polymers being produced in a differential time interval $t \sim t + dt$. From Eq. (AI-5-5), this can be written as follows:

$$\begin{aligned} d[P_r]_{t \sim t+dt} &= \{k_{td}[R_r^\bullet][R^\bullet] + \frac{1}{2} k_{tc} \sum_{j=1}^{r-1} [R_{r-j}^\bullet][R_j^\bullet] + k_{fm}[M][R_r^\bullet] + k_{fs}[S][R_r^\bullet]\} dt \\ &= k_t \left\{ \frac{k_{td}}{k_t} \frac{[R^\bullet]^2}{v} \exp\left(-\frac{r}{v}\right) + \frac{1}{2} \frac{k_{tc}}{k_t} \frac{r[R^\bullet]^2}{v^2} \exp\left(-\frac{r}{v}\right) \right. \\ &\quad \left. + \frac{k_{fm}}{k_t} [M] \frac{[R^\bullet]}{v} \exp\left(-\frac{r}{v}\right) + \frac{k_{fs}}{k_t} [S] \frac{[R^\bullet]}{v} \exp\left(-\frac{r}{v}\right) \right\} dt \end{aligned}$$

where $k_t = k_{tc} + k_{td}$.

Defining the following two ratios a and γ ,

$$a \equiv \frac{k_{tc}}{k_t}, \quad \gamma \equiv \frac{R_f}{R_t} = \frac{\left(\frac{k_{fm}}{k_p}\right) + \left(\frac{k_{fs}}{k_p}\right) \frac{[S]}{[M]}}{\left(\frac{r}{k_p}\right) \cdot \left(\frac{r}{M^2}\right)}$$

$$d[P_r]_{t \sim t+dt} = k_t [R^\bullet]^2 \left\{ (1-a+\gamma) \dot{f}_n(r) + \frac{1}{2} a \dot{f}_w(r) \right\} dt$$

The total dead polymer being produced in $t \sim t+dt$ is a sum of $d[P_r]_{t \sim t+dt}$.

$$d[P]_{t \sim t+dt} = \sum_{r=1}^{\infty} d[P_r] = k_t [R^\bullet]^2 \left(1 - \frac{1}{2} a + \gamma\right) dt \quad (\text{AI-5-6})$$

Now we can find number- and weight-based distribution functions of the instantaneous polymer.

$$f_n(r) \equiv \frac{\text{Number of polymer with chain length } r \text{ produced in } t-t+dt}{\text{Total Number of Polymer produced in } t-t+dt}$$

$$= \frac{d[P_r]_{t-t+dt}}{d[P]_{t-t+dt}} = \frac{\frac{1}{2} a f_w(r) + (1-a+\gamma) f_n(r)}{1 - \frac{1}{2} a + \gamma}$$

$$f_w(r) \equiv \frac{\text{Weight of polymer with chain length } r \text{ produced in } t-t+dt}{\text{Total Number of Polymer produced in } t-t+dt}$$

$$= \frac{r d[P_r]_{t-t+dt}}{\sum_{r=1}^{\infty} r d[P_r]_{t-t+dt}} = \frac{r f_n(r)}{\sum_{r=1}^{\infty} r f_n(r)} = \frac{a f_z(r) + (1-a+\gamma) f_w(r)}{1 + \gamma}$$

Corresponding number- and weight-average chain length of the instantaneous polymer are written as,

$$\bar{r}_n \equiv \frac{\sum_{r=1}^{\infty} r f_n(r)}{\sum_{r=1}^{\infty} f_n(r)} = \frac{1 + \gamma}{1 - \frac{1}{2} a + \gamma} v$$

$$\bar{r}_w \equiv \frac{\sum_{r=1}^{\infty} r f_w(r)}{\sum_{r=1}^{\infty} f_w(r)} = \frac{2 + a + 2\gamma}{1 + \gamma} v$$

Finally, the number- and weight- based distribution of all the polymer produced from time zero to t can be given as the integrations of the above instantaneous polymer equations.

$$F_n(r) = \frac{[P_r]}{[P]} = \frac{1}{[P]} \int_0^{[P]} f_n(r) d[P]$$

$$F_w(r) = \frac{r[P_r]}{\sum_{r=1}^{\infty} r[P_r]} = \frac{1}{x} \int_0^x f_w(r) dx$$

Number- and weight-average chain lengths of all the polymers produced can be written as,

$$\bar{P}_n = \frac{1}{[P]} \int_0^{[P]} \bar{r}_n d[P]$$

$$\bar{P}_w = \frac{1}{x} \int_0^x \bar{r}_w dx$$

Thus the distributions of the final product polymer were written in terms of instantaneous polymer distribution functions which were characterized by the three dimensionless parameters ν = average chain length of polymer radicals, a = the ratio of termination rate by recombination to total termination rate, and γ = the ratio of transfer rates to termination rate. They are related to the previously defined dimensionless groups as follows.

$$\nu = \frac{1}{\tau + \beta} \quad , \quad a = \frac{\beta}{\alpha + \beta} \quad , \quad \gamma = \frac{T}{\alpha + \beta}$$

Although the stationary-state assumption was not explicitly made in the above formulation, it was inherent in the very beginning where the propagation probability is defined. The principal of derivation and application starting from the average chain length of polymer radicals has been called the ν -model. (59)

A computer program was written for acrylamide polymerization based upon the ν -model. Conversion was calculated by numerical integration

(4-th order Runge-Kutta) on dx/dt (Eq.I-4-8) while the dead polymer produced in $0 \sim t$ was calculated by the summation of $d[P]$ (Eq.AI-5-6) by equating $k_t[R]^2$ with I . The step size Δt was always adjusted so that the conversion increase in this time interval was 0.5 to 1%. It was found that this step size for the numerical integrations is sufficient to satisfy an obvious relationship $\bar{P}_n \cdot [P] = [M]_0 \cdot X$ within 1% error.

PART II DEVELOPMENT OF GPC TECHNOLOGY

II-1 INTRODUCTION

Gel permeation chromatography has been gaining wide popularity as a tool to measure molecular weight of various polymers. One great advantage of the instrument is the relatively small analysis time required. Speedy supply of information on product polymers from commercial reactors is an important asset in industry. Also as a research tool in kinetic studies of polymerization, it can provide more extensive information on the distribution of molecular species in comparison to single average molecular weight measurements such as viscometry, osmometry or light scattering. However, its separation characteristics with respect to molecular weight have to be evaluated prior to analysis on known molecular weight samples. This relative nature of the measurements gives two problems for data interpretation. First, a few polymer samples of well characterized molecular weight called polymer standards must be available to construct a calibration curve of retention volume vs. molecular weight and to characterize the chromatogram spreading due to the instrument. Second, the observed chromatograms for unknowns must be corrected for instrumental spreading to obtain true molecular weight distributions.

The first problem has been partly resolved because polymer standards are now commercially available for such polymers as polystyrene, polymethylmethacrylate, polyvinylchloride and polybutadiene. In addition, methods of constructing a universal calibration curve have been developed thus enabling the use of the above mentioned polymer standards in analyzing

other polymers. As for the instrumental spreading, an approximation with a Gaussian distribution has often been made for a single molecular weight species. Later it was pointed out that the Gaussian approximation for the spreading is often inadequate.

The second problem, the instrumental spreading correction, is essentially a problem of solving for $W(y)$, corrected chromatogram, in the following integral equation known as "Tung's axial dispersion equation" with known $F(v)$, the observed GPC chromatogram, and $G(v,y)$, the instrumental spreading function.

$$F(v) = \int_0^{\infty} W(y) G(v,y) dy$$

Several methods have been proposed to obtain $W(y)$ for limited case of $G(v,y)$, mostly as a Gaussian distribution. However, there are no satisfactory general methods available to cope with non-symmetrical as well as non-uniform spreading function.

During the course of the present study, two numerical techniques have been developed and evaluated for the above case as a general problem in GPC data interpretation.

In relation to the kinetic study of acrylamide polymerization, a feasibility of conversion and molecular weight determination by GPC was investigated. Also an attempt was made to follow the decomposition of the initiator employed (ACV) from GPC responses.

II-2 THEORETICAL BACKGROUND AND LITERATURE REVIEW

II-2-1 Separation Mechanism and Calibration Curve

The generally accepted concept of molecular weight analysis by gel permeation chromatography is the separation of molecules according to molecular size in solution^(1,2) with the use of a porous packing material. A simplified representation of the process is shown in Fig. II-2-1. When a mixture of two different molecular weight materials, one larger and the other smaller than the internal pores of the packing material, is injected into the column, the larger molecules since they are too large to diffuse into the pores pass through the column in liquid phase outside the porous particles. The smaller molecules, however, diffuse into the particle pores and thus have a significantly larger distance to flow before they elute from the column. Therefore, the molecules are eluted from the column in order of decreasing molecular size. Porous materials of various pore size have been developed and are commercially available to provide separation over wide range of molecular weight.⁽³⁾ With a combination of various pore sizes, polymeric materials which generally have continuous molecular weight distributions can be separated according to the molecular size of each of the constituent species. It should be mentioned here, however, that a single molecular weight species injected as a pulse or near pulse elutes in a dispersed manner (see Fig. II-2-1). This response to an input of a single molecular weight species is called the spreading due to imperfect

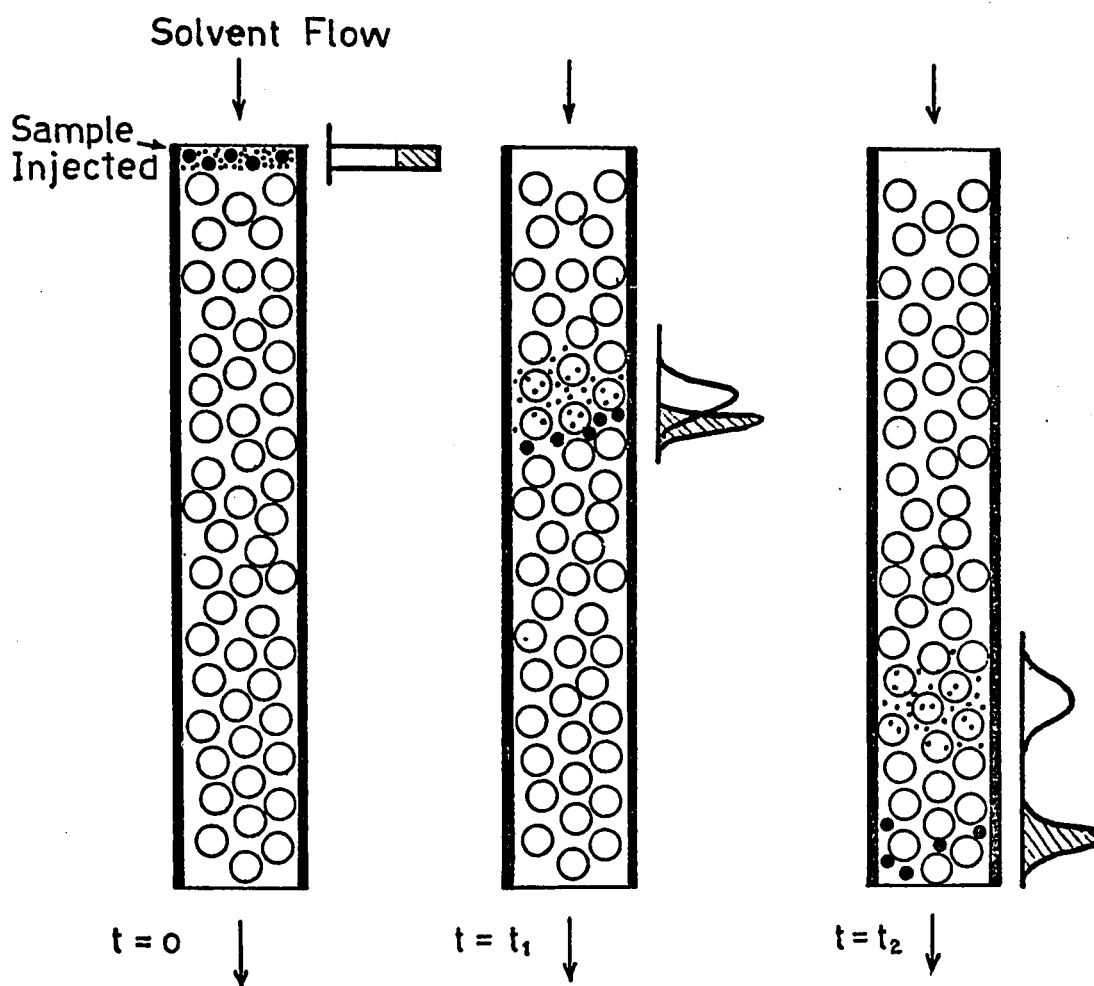


Fig. II-2-1 GPC Separation Process

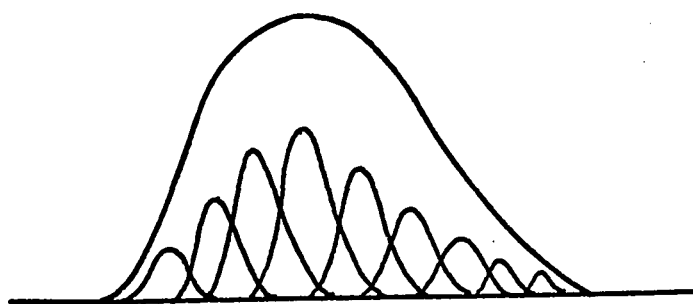


Fig. II-2-2 GPC Chromatogram

resolution, (4,5,6) or spreading due to axial dispersion.⁽⁷⁾ More recently, the "instrumental spreading"⁽⁸⁾ is meant to include extra-column spreading as well as spreading in the column. Thus a general GPC chromatogram obtained for a polymer with a molecular weight distribution is composed of distributions of each molecular weight species as is shown in Fig. II-2-2. Now it is clear that the chromatogram height at a certain retention volume does not represent the abundance of a single species at that position, it also reflects the abundance of neighbouring species.

A calibration curve of molecular weight vs. retention volume can be constructed from a series of injections of mono-dispersed (single molecular weight species) or narrow-distributed polymer samples with known molecular weight or molecular weight averages. These samples are called polymer standards. A usual method is to plot the peak retention volume vs. logarithm of molecular weight or some average of \bar{M}_n and \bar{M}_w in case of narrow-distributed standards. The general behaviour of this plot is shown in Fig. II-2-3. There is an upper and lower limit of resolution which is possible, i.e., molecules above or below certain molecular sizes cannot be separated. In between the two limits, a linear portion of retention volume vs. $\log M$ has often been found. This is the range that molecular weight or its distribution can be analyzed by GPC. A linear calibration curve is particularly useful since it permits an easier interpretation of chromatograms.^(9,10,11) Non-linear calibration curves however can also be used but the analysis is a little more involved.

When mono-dispersed or narrow-distributed polymer samples are not available, the above mentioned procedures cannot be used. Methods of constructing a calibration curve from one or two broad samples have been developed to overcome this problem. It was first attempted by Rodriguez et.al.⁽¹²⁾ and followed by Frank et.al.⁽¹³⁾ Their techniques involve a graphical approximation which makes it difficult to employ. A more precise computer technique has been developed by Balke et.al.⁽¹⁴⁾ This method utilizes two sets of information, for example \bar{M}_n and \bar{M}_w of one broad sample or two \bar{M}_n 's of two broad samples, and searches for an effective linear calibration curve that gives the best fit to these values when applied to the raw chromatograms. When this effective calibration curve was applied to unknown samples, it was shown to yield reasonable agreement in the average molecular weights with those measured by osmometry or by light scattering. This method could be said to be a practical technique since the use of the effective calibration curve does not require correction for instrumental spreading and overcomes the problem of having to identify $G(v,y)$. The characteristics of the instrumental spreading is accounted in the calibration curve itself.

Another approach of constructing a calibration curve is to seek a universal parameter that can treat the different polymers on a common base. Since the separation process of GPC is by molecular size, the hydrodynamic volume of the polymer in a solution was looked into.⁽¹⁵⁾ A number of experimental studies was made using this concept and very often a common curve of $M[\eta]$ vs. retention volume was obtained for various types

of polymers.⁽¹⁵⁻²⁰⁾ The quantity $M[\eta]$ is a measure of hydrodynamic volume of a polymer in a dilute solution when the shape of polymer in the solution is approximated by a sphere of random coiling.⁽²¹⁾ This approach makes it possible to calibrate a column with one polymer and use it for molecular weight determination of all others.

II-2-2 Criteria for Effectiveness of Separation

The effectiveness of separation of a particular column can partly be accounted for by the slope of the calibration curve. Generally the smaller the slope, the better the separation. Since a longer column provides a longer process of separation, it can be immediately said that the longer column enables a better separation. Recycling of a once-eluted sample to the column has been proposed⁽¹¹⁾ to effectively double the column length. This effect is shown in Fig. II-2-3. However, no matter how the slope is small, if the spreading of individual species is too large, the net result would be a poor one. This situation is shown in Fig. II-2-4 for the mixture of two species. Accounting this fact, Bly⁽²²⁾ employed the following expression of resolution, whose form is commonly used in gas chromatography.

$$R_s = \frac{2(v_2 - v_1)}{(w_1 + w_2)(\log \bar{M}_{w_1} - \log \bar{M}_{w_2})} = \frac{2}{w_1 + w_2} \cdot \frac{1}{D_2} \quad (\text{II-2-1})$$

where v_1 and v_2 are retention volume of species 1 and 2 and w_1 and w_2 are the associated peak widths (width of the baseline of the curve between two tangents drawn on the point of inflexion of the curve and extended to the base line) and \bar{M}_{w_1} and \bar{M}_{w_2} are the associated weight-average molecular

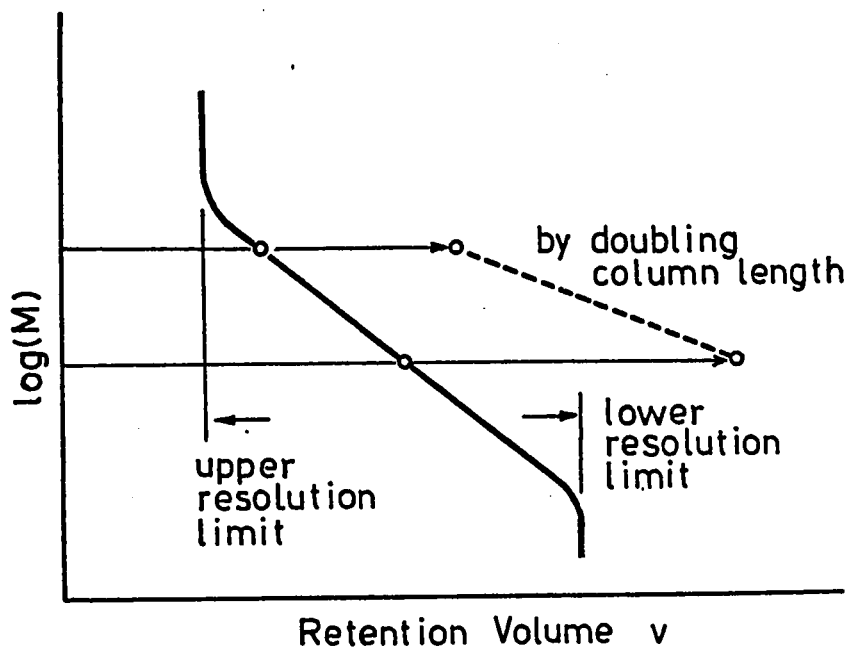


Fig. II-2-3 General Shape of Calibration Curve

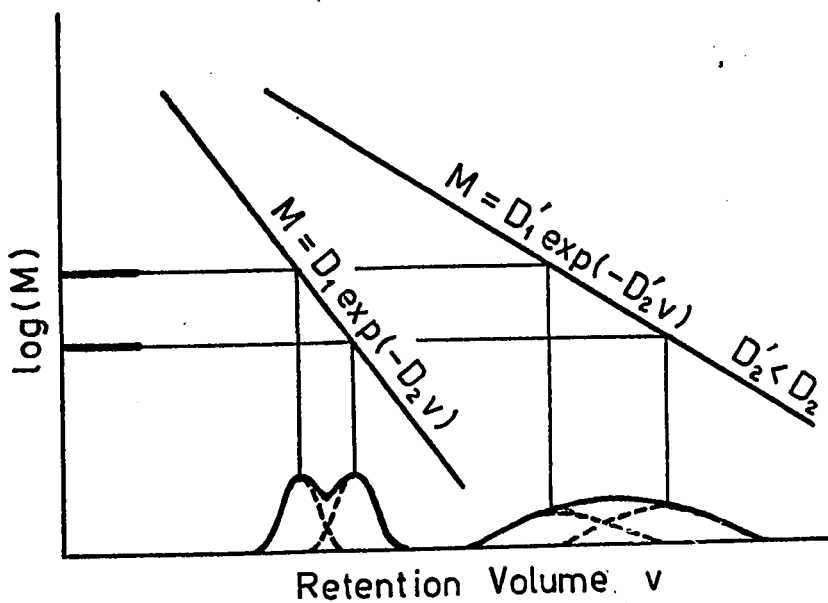


Fig. II-2-4 Effectiveness of Separation

weights. However, the formula depends on the assumption that the two samples have the same molecular weight distribution.

Later, Hamielec⁽¹¹⁾ proposed a more general form obtainable from a single polymer sample. In his series of both theoretical and experimental works with his co-workers, it was shown that if the instrumental spreading is assumed to be Gaussian, the ratio of spreading corrected molecular weight averages to those uncorrected can be written as

$$\frac{\bar{M}_k(t)}{\bar{M}_k(\infty)} = \exp\{ (3-2k) D_2^2/4h \} \quad (\text{II-2-2})$$

where \bar{M}_k corresponds to number-, weight- and z-average molecular weight for $k = 1, 2$ and 3 , (t) refers to the spreading corrected and (∞) uncorrected, h is Gaussian resolution factor (see Section II-2-3, Equation (II-2-4) and (II-2-18) for definition of h and derivation of equation II-2-2). Since it is apparent that, to minimize the correction for imperfect resolution, $D_2^2/4h$ must be as small as possible. With this regard, the following specific resolution factor $R_s(k, M_0)$ was defined as follows.

$$R_s(k, M_0) = \frac{(-1)^{k!} 4h}{(2k-3) D_2^2} \quad (\text{II-2-3})$$

The subscripts k and M_0 are used to emphasize the need to specify the particular molecular weight average and the molecular weight at the peak retention volume. This formula was shown to be consistent with Bly's⁽²²⁾ formula in the limit of mono-dispersed standards.

II-2-3 Instrumental Spreading Function

In expressing the effectiveness of separation, it was shown that the spreading of the individual species is important as well as the slope of a calibration curve. Its importance will be further understood when the necessary correction for the spreading is required. In this section, however, the proposed mathematical formula for expressing the instrumental spreading will be dealt together with an experimental method of determining the parameters involved in this expression. This mathematical formula is called the instrumental spreading function.

The instrumental spreading can be easily evaluated if truly mono-dispersed polymer standards were available. The elution chromatograms represent the true instrumental spreading. However, none of the available standards are truly mono-dispersed. They are polymer samples with narrow molecular weight distribution, having a polydispersity of generally less than 1.1. Their distributions are sufficiently narrow for purposes of constructing a molecular weight calibration curve, however if they are considered mono-dispersed to evaluate the instrumental spreading, a significant error results because of the overlapping of two processes, one due to the instrumental spreading and the other due to the separation according to molecular size of the species in the standard.

Tung⁽⁴⁾ observed that monomeric compounds gave an approximately Gaussian distribution and proposed the following instrumental spreading function.

$$G(v-y) = \sqrt{\frac{h}{\pi}} \exp\{-h(v-y)^2\} \quad (\text{II-2-4})$$

where v and y represent retention volume and mean retention volume and h represents the sharpness of the distribution ($= 1/2\sigma^2$ where σ^2 is the variance) and is called resolution factor. The above form has long been used and found satisfactory for intermediate molecular weights, when applied for correcting chromatograms. In order to evaluate the resolution factor h with narrow-distributed polymer standards, the technique of reverse flow has been developed by Tung, Moore and Knight.⁽⁵⁾ This technique considers the spreading due to molecular size difference to be reversible. If the elution of a standard is allowed to proceed to some part of the column and then the direction of flow is reversed, the chromatogram of the eluent reflects only the effect of spreading due to axial dispersion. Thus by reversing the direction of flow at one half of the retention volume for the pre-measured peak position the resolution factor for the front half of the column can be obtained. The procedure has to be repeated for the rear half of the column. The resolution factors for each portion of the columns were calculated from the obtained chromatograms by the method of moments.

$$h_f(\text{or } h_r) = \mu_0^2 / 2(\mu_2\mu_0 - \mu_1^2) \quad (\text{II-2-5})$$

where μ_0 , μ_1 and μ_2 are the zero, first and second moment of the chromatogram, h_f and h_r are the resolution factors for front and rear halves of the columns. The resolution factor for all of the columns was calculated using the formula

$$h = \frac{2}{(1/h_f) + 1/(h_r)} \quad (\text{II-2-6})$$

Subsequent investigation by Duerksen and Hamielec⁽²³⁾ has indicated that the reverse-flow technique gives reliable resolution factors for relatively low molecular weight samples. However, the presence of impurity peaks caused an interference with the sample chromatograms of high molecular weight standards and thus made the evaluation difficult.

Due to the time-consuming and sometimes difficult procedures of the reverse-flow technique, a method of evaluating h from once-through measurements has been developed. Balke and Hamielec⁽²⁴⁾ made use of Eq.(II-2-2) and derived

$$h = \frac{D_2^2}{2} / \ln\{p(\infty)/p(t)\} \quad (\text{II-2-7})$$

where $p(t)$ and $p(\infty)$ are the polydispersity of the standard and that obtained from the chromatogram without spreading correction. The former is usually supplied, thus the h can be easily obtained from once-through measurements. Tung and Runyon⁽⁸⁾ claimed that the method is not too accurate due to the sensitiveness to the slope of the calibration curve. They suggested that the leading half of the chromatogram be fitted with a Gaussian distribution. The resolution factor thus determined showed a good agreement with that obtained by the reverse flow technique for polystyrene standards of large molecular weight but was significantly smaller for smaller molecular weight standards.

With the development of chromatogram interpretation techniques there arose a question of the validity of the Gaussian approximation for the instrumental spreading. It has been generally observed that the chromatogram skews to higher retention volumes with increasing concentration.^(26,27) Hamielec et.al.^(23,24) showed that the skewing causes significant error in corrected \bar{M}_n and \bar{M}_w if the Gaussian assumption is made. From a theoretical point of view, the response to a pulse input predicted by a plug-flow dispersion model was shown to deviate significantly from symmetry as Peclet Number decreases.⁽²⁸⁾ Viscosity of sample solutions being analyzed may develop a velocity profile and thus Taylor diffusion⁽²⁹⁾ may also account for non-symmetrical responses.

The approaches to account for the non-symmetrical instrumental spreading followed two directions. One is to approximate the spreading with a non-symmetrical spreading function,^(7,10,30) the other is to preserve the Gaussian expression and introduce the over-all correction factor to account for the error associated with the Gaussian assumption.⁽²⁴⁾ With either approach, the representation of the instrumental spreading must be a practical form that permits easy handling for the spreading correction. In earlier work on GPC interpretation, the instrumental spreading function of log-normal distribution or two Gaussian halves by Smith,⁽³⁰⁾ axial distribution equation by Hess and Kratz⁽⁷⁾ were proposed. However, in an extensive evaluation of these methods, it was found that low molecular weight standards were corrected in moderate agreement but the agreement was poor for high molecular weight standards.⁽²³⁾ Recently, Provder and Rosen⁽¹⁰⁾ proposed more general form of the spreading function which can

account for wide variations of the shape of the instrumental spreading. This has been called general statistical shape function and has the following form:

$$G(v,y) = \phi(v-y) + \sum_{n=3}^{\infty} (-1)^n \frac{A_n}{n!} \frac{\phi^n(v-y)}{(\sqrt{2h})^n} \quad (\text{II-2-8a})$$

where $\phi(v) = \sqrt{h/\pi} \exp\{-h(v-y)^2\}$ and $\phi^n(v)$ denotes its n-th order derivative. The coefficients A_n are the function of μ_n , the n-th order moments about the mean retention volume μ_1 of the observed GPC chromatograms. For practical purpose, the series were truncated at the third term and the use of the three parameter expression was suggested,

$$G(v-y) = G_0(v-y) \cdot \left\{ 1 + \frac{\mu_3}{6} (\sqrt{2h})^3 \cdot H_3[\sqrt{2h}(v-y)] + \frac{1}{24} (\mu_4(2h)^2 - 3) H_4[\sqrt{2h}(v-y)] \right\} \quad (\text{II-2-8b})$$

where

$$G_0(v-y) = \sqrt{\frac{h}{\pi}} \exp\{-h(v-y)^2\}$$

$$H_3[x] = x^3 - 3x$$

$$H_4[x] = x^4 - 6x^2 + 3$$

The above form preserves the merit of Gaussian function when applied to a linear calibration curve. The ratio of a true average molecular weight to the uncorrected can be analytically given as follows:

$$\frac{\bar{M}_n(t)}{\bar{M}_n(\infty)} = \exp(D_2^2/4h) \cdot \left\{ 1 + \frac{D_2^3 \mu_3}{6} + \frac{D_2^4}{24} \left(\mu_4 - \frac{3}{4h^2} \right) + \frac{D_2^6 \mu_3^2}{72} \right\} \quad (\text{II-2-9a})$$

$$\frac{\bar{M}_w(t)}{\bar{M}_w(\infty)} = \exp(-D_2^2/4h) / \left\{ 1 - \frac{D_2^3 \mu_3}{6} + \frac{D_2^4}{24} \left(\mu_4 - \frac{3}{4h^2} \right) + \frac{D_2^6 \mu_3^2}{72} \right\} \quad (\text{II-2-9b})$$

$$\frac{\eta(t)}{\eta(\infty)} = \exp(-a^2 D_2^2/4h) / \left\{ 1 - \frac{a^3 D_2^3 \mu_3}{6} + \frac{a^4 D_2^4}{24} \left(\mu_4 - \frac{3}{4h^2} \right) + \frac{a^6 D_2^6 \mu_3^2}{72} \right\} \quad (\text{II-2-9c})$$

where η denote the intrinsic viscosity and a is the exponent in the Mark-Houwink intrinsic viscosity-molecular weight expression. From the observed GPC chromatogram of a polymer standard, the parameters h , μ_3 and μ_4 can be evaluated by solving the above equations simultaneously. Obviously, when the original function is truncated at the second term, either two sets of \bar{M}_n , \bar{M}_w and η make it possible to obtain h and μ_3 .

II-2-4 Instrumental Spreading Correction

In section II-2-1, the observed GPC chromatogram $F(v)$ was shown to be composed of the spreaded forms of each molecular species. Therefore, in order to obtain the distribution with respect to the species, $F(v)$ must be corrected for the spreading which is characterized by the instrumental spreading function $G(v,y)$. When one denotes the distribution with respect to molecular weight species $W(y)$, this can be related to the chromatogram $F(v)$ by the following form:

$$F(v) = \int_0^{\infty} W(y) \cdot G(v, y) dy \quad (\text{II-2-10})$$

This was first mentioned by Tung⁽⁴⁾ and the equation has been called Tung's axial dispersion equation. $W(y)$ is often called the dispersion corrected chromatogram. The spreading correction is essentially a mathematical problem of solving the above integral equation for $W(y)$ with given $F(v)$ and $G(v, y)$.

When the distribution of molecular species $W(v)$ is obtained, it can be converted to molecular-weight scale distribution $F_w(M)$ by the following equation. ($F_w(M)$ and $W(v)$ are normalized.)

$$W(v) dv = -F_w(M) dM$$

$$\therefore F_w(M) = -W(v) \cdot \frac{1}{\left(\frac{dM}{dv}\right)} \quad (\text{II-2-11})$$

where dM/dv is a slope of the calibration curve. Then the average molecular weights can be given as follows by assuming the molecular weight is a continuous variable

$$\bar{M}_w(t) = \frac{\int_0^{\infty} M F_w(M) dM}{\int_0^{\infty} F_w(M) dM} = \int_0^{\infty} M(v) W(v) dv \quad (\text{II-2-12a})$$

$$\bar{M}_n(t) = \frac{\int_0^{\infty} M \frac{1}{M} F_w(M) dM}{\int_0^{\infty} \frac{1}{M} F_w(M) dM} = \frac{1}{\int_0^{\infty} \frac{W(v)}{M(v)} dv} \quad (\text{II-2-12b})$$

In general,

$$\bar{M}_k(t) = \frac{\int_0^{\infty} M^{k-1}(v) W(v) dv}{\int_0^{\infty} M^{k-2}(v) W(v) dv} \quad (\text{II-2-12c})$$

where $k = 1, 2, 3, \dots$ correspond to number-, weight, z- --- average molecular weight. Subscript (t) refers to the instrumental spreading corrected (or true) molecular weight average. A calibration curve of M vs. v is necessary to perform the above integrations. The direct use of $F(v)$ instead of $W(v)$ leads to the following uncorrected molecular weight averages:

$$\bar{M}_k(\infty) = \frac{\int_0^{\infty} M^{k-1}(v) \cdot F(v) dv}{\int_0^{\infty} M^{k-2}(v) \cdot F(v) dv} \quad (\text{II-2-13})$$

The process of obtaining $W(v)$ from $F(v)$ is the instrumental spreading correction. The spreading function $G(v, y)$ may be an identical shape for all the molecular weight species (uniform $G(v, y)$) or it may vary with the species (non-uniform $G(v, y)$). It may be symmetrical in shape or it may be non-symmetrical in shape. A graphical representation of the processes involved is given in Fig. II-2-5.

Under the assumption that $G(v, y)$ is a Gaussian distribution function, or log-normal distribution, or the distribution that the dispersion model in packed bed predicts, several numerical techniques have been suggested. These include the use of the Gaussian quadrature formula,⁽⁴⁾ Hermite polynomial expansion⁽⁴⁾ and Fourier transformation.⁽³¹⁾ Common problems associated with these techniques were the presence of artificial oscillations

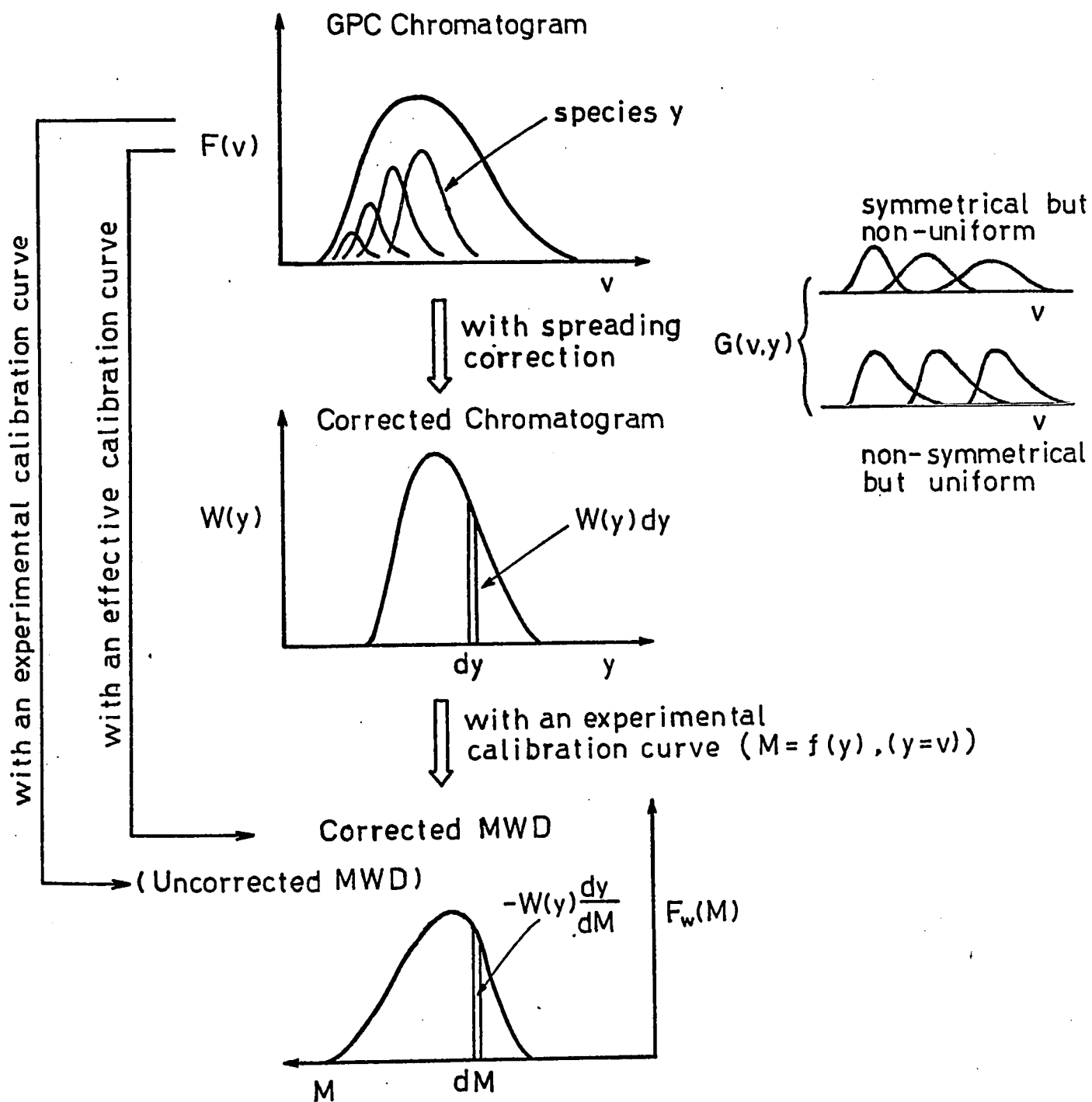


Fig. II-2-5 Processes Involved in Chromatogram Interpretation

in obtained $W(v)$.⁽²³⁾ Since an excellent review is available for these techniques⁽³²⁾ and the extensive evaluation^(23,24) have shown them not always satisfactorily, the recent development in this area will be described in the following.

The most powerful technique developed since 1969 may be the analytical solutions for corrected average molecular weights developed by Hamielec and Ray.⁽⁹⁾ The ratio of corrected average molecular weights to those uncorrected can be written as

$$\frac{\bar{M}_k(t)}{\bar{M}_k(\infty)} = \frac{\int_0^{\infty} W(v) M^{k-1}(v) dv}{\int_0^{\infty} W(v) M^{k-2}(v) dv} \bigg/ \frac{\int_0^{\infty} F(v) M^{k-1}(v) dv}{\int_0^{\infty} F(v) M^{k-2}(v) dv} \quad (\text{II-2-14})$$

By assuming a linear calibration curve of,

$$M(v) = D_1 \exp(-D_2 v) \quad (D_2 > 0) \quad (\text{II-2-15})$$

$$\frac{\bar{M}_n(t)}{\bar{M}_n(\infty)} = \frac{\int_{-\infty}^{\infty} F(v) e^{D_2 v} dv}{\int_{-\infty}^{\infty} W(v) e^{D_2 v} dv} = \frac{\bar{F}(-D_2)}{\bar{W}(-D_2)} \quad (\text{II-2-16a})$$

$$\frac{\bar{M}_w(t)}{\bar{M}_w(\infty)} = \frac{\int_{-\infty}^{\infty} W(v) e^{-D_2 v} dv}{\int_{-\infty}^{\infty} F(v) e^{-D_2 v} dv} = \frac{\bar{W}(D_2)}{\bar{F}(D_2)} \quad (\text{II-2-16b})$$

where \bar{F} and \bar{W} are the bilateral Laplace transforms of F and W , there is no loss in generality in letting $v=0$ to $v=-\infty$. The transforms are claimed to exist since $\lim_{v \rightarrow \infty} \{F(v) e^{D_2 v}\} < \infty$ and $\lim_{v \rightarrow \infty} \{W(v) e^{D_2 v}\} < \infty$

By assuming a Gaussian instrumental spreading, Eq. II-2-4, Tung's axial dispersion equation II-2-5 can be written as,

$$F(v) = \sqrt{\frac{h}{\pi}} \int_{-\infty}^{\infty} W(y) \exp\{-h(v-y)^2\} dy$$

where a uniform Gaussian $G(v,y)$ is assumed. By performing the Laplace transform,

$$\begin{aligned} \bar{F}(s) &= \bar{W}(s) \sqrt{\frac{h}{\pi}} \int_{-\infty}^{\infty} \exp(-hv^2) \exp(-sx) dx \\ &= \bar{W}(s) \sqrt{\frac{h}{\pi}} \exp\left(\frac{s^2}{4h}\right) \int_{-\infty}^{\infty} \exp(-hx^2) dx \\ &= \bar{W}(s) \sqrt{\frac{h}{\pi}} \exp\left(\frac{s^2}{4h}\right) \cdot \sqrt{\frac{\pi}{h}} \\ &= \bar{W}(s) \exp\left(\frac{s^2}{4h}\right) \end{aligned} \tag{II-2-17}$$

Applying this result to equations (II-2-16a) and (II-2-16b) one obtains,

$$\frac{\bar{M}_n(t)}{\bar{M}_n(\infty)} = \exp\left(-\frac{D_2^2}{4h}\right) \tag{II-2-18a}$$

$$\frac{\bar{M}_w(t)}{\bar{M}_w(\infty)} = \exp\left(-\frac{D_2^2}{4h}\right) \tag{II-2-18b}$$

In general,

$$\frac{\bar{M}_k(t)}{\bar{M}_k(\infty)} = \exp\{(3-2k) D_2^2/4h\} \quad (\text{II-2-18c})$$

Thus, once the Gaussian resolution factor h and the slope of linear calibration curve D_2 are given, the corrected average molecular weights can be immediately obtained from uncorrected average-molecular weights. In order to account for the error involved in the Gaussian assumption for skewed chromatograms, the overall correction factor SK was introduced as follows: (24)

$$SK = \frac{\bar{M}_n(t)}{\bar{M}_n(\infty)} + \frac{\bar{M}_w(\infty)}{\bar{M}_w(\infty)} - \left(e^{\frac{D_2^2}{4h}} + e^{-\frac{D_2^2}{4h}} \right) \quad (\text{II-2-19})$$

(= 0 if $G(v,y)$ is truly Gaussian)

The value of h in this case was first evaluated by equation (II-2-2).

This assumes that the effect of skewing can be accounted for by shifting the calibration curve and thus affects the uncorrected (for skewing)

\bar{M}_n and \bar{M}_w in the same manner.

$$\bar{M}_n(t) = \bar{M}_n(\infty) \left(1 + \frac{1}{2} SK \right) e^{D_2^2/4h} \quad (\text{II-2-20a})$$

$$\bar{M}_w(t) = \bar{M}_w(\infty) \left(1 + \frac{1}{2} SK \right) e^{-D_2^2/4h} \quad (\text{II-2-20b})$$

The elimination of SK from the above two equations derives

$$h = \frac{D_2^2}{2} / \ln\{p(\infty)/p(t)\}$$

Note that the value of h thus defined loses its original meaning as it was in Eq. II-2-4 when SK \neq 0, since the instrumental spreading is no longer Gaussian. In other words, the assumption on skewing effect given by equations (II-2-20a) and (II-2-20b) derives the parameter h, which when used in a Gaussian expression may give an approximate shape of the instrumental spreading function. This would be the deficiency of introducing an overall correction factor after assuming a Gaussian spreading for non-Gaussian spreading. This deficiency has been eliminated by the use of general statistical shape function⁽¹⁰⁾ which still permits the analytical expressions for the corrected molecular weight averages. The instrumental spreading function defined in Equation (II-2-8a,b) can express non-Gaussian, non-symmetrical spreading rigorously. The axial dispersion equation for this G(v,y) is written as follows:

$$F(v) = \int_0^{\infty} W(y) \cdot \sqrt{\frac{h}{\pi}} \exp\{-h(v-y)^2\} \left\{ 1 + \frac{\mu_3}{6} (\sqrt{2h})^3 H_3[2h(v-y)] + \right. \\ \left. \left(\frac{\mu_4}{24} (2h)^2 - 3 \right) H_4[\sqrt{2h}(v-y)] \right\} dy$$

Upon the Laplace transformation of the above as was described, the ratio of $\bar{M}_k(t)/\bar{M}_k(\infty)$ were shown to be given by equations (II-2-9a), (II-2-9b) and (II-2-9c). Again the knowledge of h, μ_3 , μ_4 and D_2 immediately

gives the spreading corrected molecular weight averages.

The analytical methods of spreading correction by-pass the construction of $W(y)$ explicitly. Only the infinite number of moments of $W(y)$ can be obtained. Also, the assumptions of a linear calibration curve as well as uniform instrumental spreading are inherent. Numerical solution of Tung's axial dispersion equation will directly lead to $W(y)$, which once obtained, a non-linear calibration curve can easily be employed to convert to $F_w(M)$. Chang and Huang⁽³³⁾ proposed a new search technique for this purpose and claimed that the method does not suffer from the oscillation in obtained $W(y)$, the difficulty encountered in applying most of the previous techniques. They introduced an integral operator $G\{ \}$ to describe Tung's axial dispersion equation.

$$G\{W(y)\} \equiv \int_0^{\infty} G(v,y) W(y) dy \quad (\text{II-2-21})$$

The operator $G\{ \}$ physically represents a GPC operation on the polymer sample. Then equation (II-2-10) can be written,

$$G\{W(y)\} = F(v) \quad (\text{II-2-22})$$

Further defined was the inner product,

$$(W,X) = \int_0^{\infty} W(v) X(v) dv \quad (\text{II-2-23})$$

The equation (II-2-22) was then converted into an equivalent variational problem described by Mikhlin⁽³⁴⁾ by assuming a symmetrical instrumental spreading. It was stated that equation (II-2-22) has a solution if and only if the functional

$$J(W) = (G\{W\}, W) - 2(W, F) \quad (\text{II-2-24})$$

attains its minimum with respect to W . The minimum of $J(W)$ was thus searched by the method of steepest descent in function space. Choosing W_1 as the first approximate solution of equation (II-2-22), the following iteration scheme was derived.

$$W_{i+1} = W_i - \epsilon \cdot X_i \quad (\text{II-2-25a})$$

where

$$X_i = G\{W_i\} - F \quad (\text{II-2-25b})$$

$$\epsilon = \frac{(X_i, X_i)}{(G\{X_i\}, X_i)} \quad (\text{II-2-25c})$$

and i represents the number of iterations.

Starting from F itself as W_1 , they showed successful recovery of W with a few iteration and oscillation free. Only limitation appeared to be the assumption of symmetrical instrumental spreading in this method. The method

was tested and compared with two numerical methods developed during the present study. This will be described in Section II-3.

II-3 DEVELOPMENT AND EVALUATION OF NUMERICAL METHODS FOR INSTRUMENTAL SPREADING CORRECTION

As has been stated in Section II-2-4, the rigorous techniques leading to explicit form of $W(y)$ from the Tung's axial dispersion equation are limited to mostly uniform and symmetrical instrumental spreading. In the present study, new iterative methods have been developed which can be applied to any shape of spreading function and are yet relatively stable (oscillation-free) in obtaining $W(y)$. The performances of the methods were compared with the method of Chang and Huang⁽³³⁾ since it appeared as a most promising one for the numerical solution of the Tung's axial dispersion equation.

II-3-1 Theory

The development of the present two iterative methods will be given in chronological order, first the development of the present Method-1 and then followed by Method-2.

Method-1

In order to simplify the formulation, the operator notation used by Chang and Huang is applied.

$$F(v) = G\{W(y)\}$$

(II-3-1)

where $G\{ \}$ is the integral operator given by equation (II-2-21). Instead of developing a searching scheme for $W(y)$, let us operate with $G\{ \}$ on F and take the difference from F itself.

$$\Delta F_1 = F - G\{F\} \quad (\text{II-3-2})$$

Repeat the above for ΔF_1 .

$$\Delta F_2 = \Delta F_1 - G\{\Delta F_1\} \quad (\text{II-3-3})$$

Figures II-3-1 and II-3-2 illustrate the operations given by Eqs. (II-3-2) and (II-3-3). For the i -th operation we have

$$\Delta F_i = \Delta F_{i-1} - G\{\Delta F_{i-1}\} \quad (\text{II-3-4})$$

Now, sum up Eq. (II-3-4) from $i=1$ to N , denoting F by ΔF_0 for convenience.

$$F = \sum_{i=0}^{N-1} G\{\Delta F_i\} + \Delta F_N \quad (\text{II-3-5})$$

When the instrumental spreading is linear, i.e., by doubling an input the output is doubled, the order of summation and G -operation is interchangeable.

$$\sum_{i=0}^N G\{\Delta F_i\} = G\left\{ \sum_{i=0}^N \Delta F_i \right\} \quad (\text{II-3-6})$$

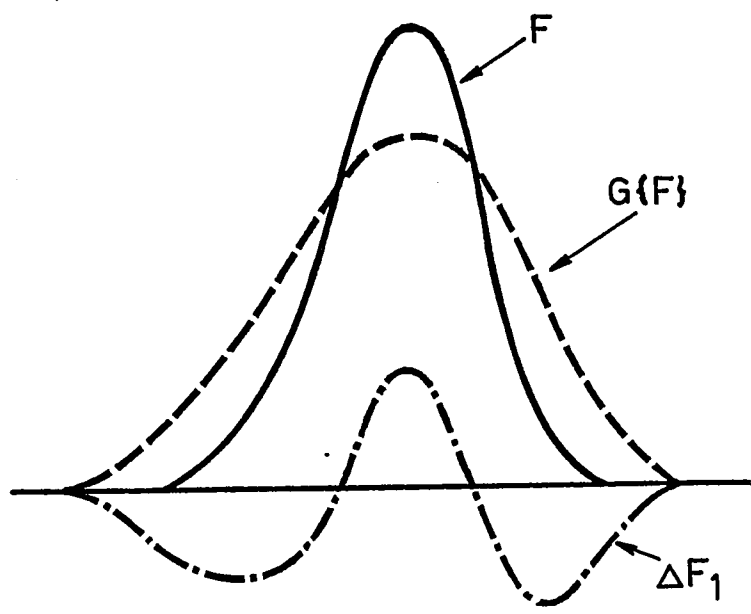


Fig. II-3-1 $\Delta F_1 = F - G\{F\}$

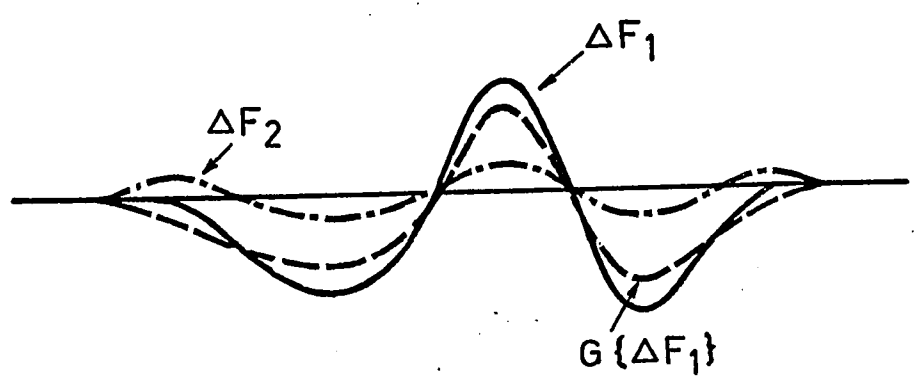


Fig. II-3-2 $\Delta F_2 = \Delta F_1 - G\{\Delta F_1\}$

Therefore it follows that

$$F = G\left\{ \sum_{i=0}^{N-1} \Delta F_i \right\} + \Delta F_N \quad (\text{II-3-7})$$

Now, by defining

$$W_i = \sum_{i=0}^i \Delta F_i \quad (\text{II-3-8})$$

we obtain

$$F = G\{W_{N-1}\} + \Delta F_N \quad (\text{II-3-9})$$

This equation indicates that W_∞ can be the solution for Eq. (II-3-1) if ΔF_N converges uniformly to zero as $N \rightarrow \infty$.

It should be noted that the above operation may result in a $W(y)$ with small negative values when the iteration is stopped at a certain stage. To overcome this difficulty the iterative procedure is changed to use the height ratio of F and F_i rather than their difference. This is now described under Method-2.

Method-2

This method uses the fact that any GPC response F always has a broader distribution than the input distribution W . Hence if a distribution F_i is broader than F , the assumed W_i must be sharpened to give a response closer to F . Using W_i and F_i , we introduce the $(i+1)$ -th guess as follows:

$$W'_{i+1} = \left(\frac{F}{F_i} \right) \cdot W_i \quad (\text{II-3-10})$$

This is equivalent to giving a correction ΔW_i on W_i such that,

$$\Delta W_i = \left(\frac{F - F_i}{F_i} \right) W_i \quad (\text{II-3-11})$$

$$W'_{i+1} = W_i + \Delta W_i \quad (\text{II-3-12})$$

It is necessary to normalize W'_{i+1} .

$$W_{i+1} = N\{W'_{i+1}\} \quad (\text{II-3-13})$$

where $N\{ \}$ is an integration operator normalizing with respect to area. The initial guess W_1 was started from F itself. Fig. II-3-3 illustrates the operation.

The above correction can never yield a negative value in W'_{i+1} , however it is possible that $(F - F_i)$ may not converge to zero in some cases.

II-3-2 Evaluation of Method-1, Method-2 and a Comparison with the Method of Chang and Huang

Experimental GPC chromatograms with a precisely known instrumental spreading function are not available. Since it is essential to use an exact form of $G(v, y)$ to evaluate correction methods, synthesized $F(v)$ were used. The evaluation routine is illustrated in Fig. (II-3-4).

Six different $F(v)$ were synthesized from two kinds of hypothetical $W(y)$, one having three peaks and another having two peaks and a shoulder. This latter one was used by Chang and Huang for their evaluation. The

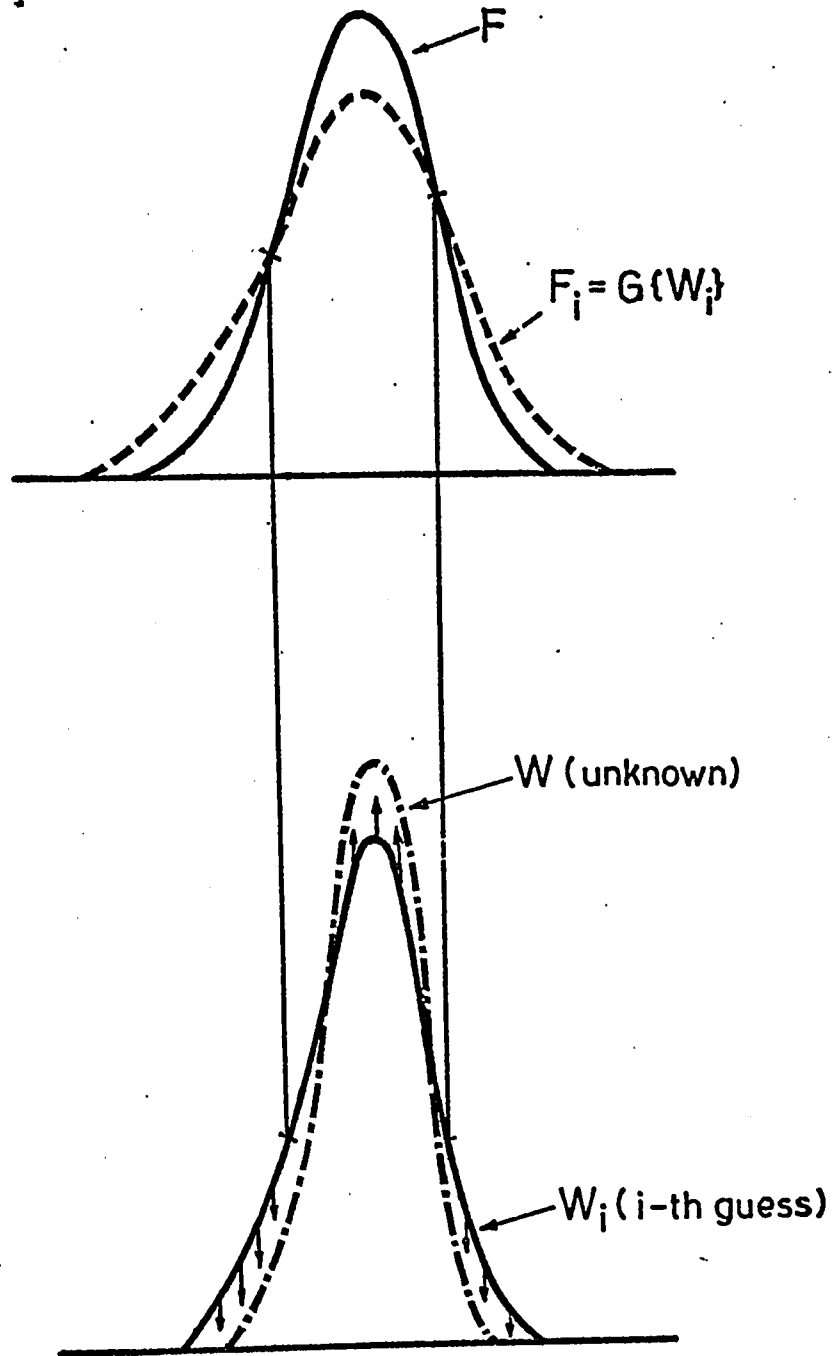


Fig. II-3-3 Direction of Correction by Method-2

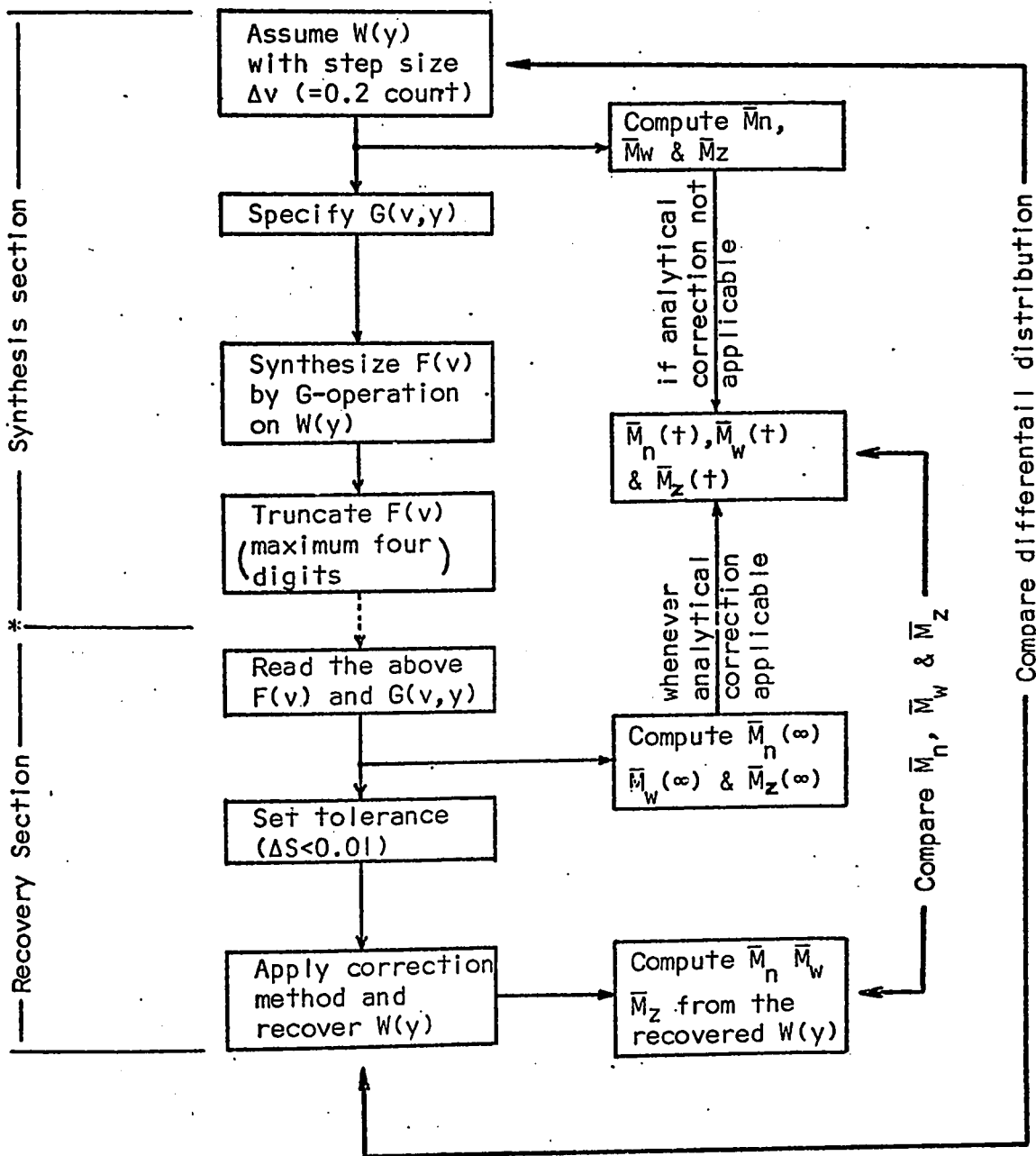


Fig. II-3-4

Evaluation Routine

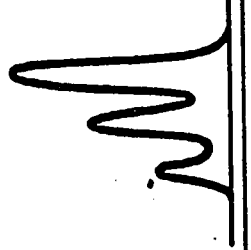

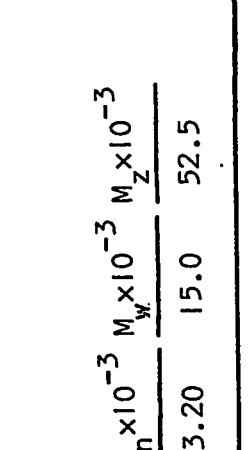
approximate shape of these $W(y)$ and $F(v)$ are shown in the first two rows of Table II-3-1. A Gaussian and a skewed shape was employed as examples of instrumental spreading functions.

Starting from a known set of $F(v)$ and $G(v,y)$, the $W(y)$ were recovered by method-1, method-2 and by the method of Chang and Huang. Table-1 summarizes the comparison of corrected \bar{M}_n , \bar{M}_w and \bar{M}_z by each of the methods.

The heights of the synthesized $F(v)$ were truncated before use. The maximum number of figures used was four. In later evaluations, the last figure in the above was truncated, i.e., $F(v)$ had three significant figures at most. Table II-3-2 lists this latter $F(v)$ for Gaussian spreading with $h = 0.5$. The recoveries from the less accurate $F(v)$ are compared with the first case. The figures in brackets in Table II-3-1 show corrected \bar{M}_n , \bar{M}_w and \bar{M}_z for the less accurate $F(v)$.


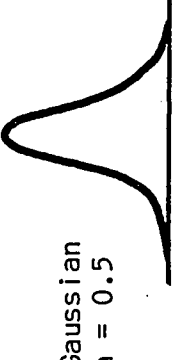
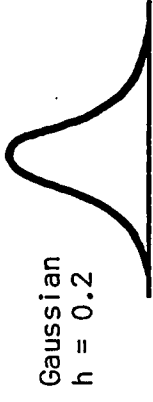
A linear calibration curve, $\log_{10} M = (46.0-v)/4.0$ was used to obtain $\bar{M}_n(t)$, $\bar{M}_w(t)$ and $\bar{M}_z(t)$ analytically from uncorrected values $\bar{M}_n(\infty)$, $\bar{M}_w(\infty)$ and $\bar{M}_z(\infty)$. A step size of 0.2 count was used for all the examples shown in Table II-3-1. This step is sufficient to obtain \bar{M}_z to $\pm 0.5\%$ for the present examples. When the analytical solution is not applicable, \bar{M}_n , \bar{M}_w and \bar{M}_z directly computed from the assumed $W(y)$ are considered true values. The differences between molecular weight averages obtained using the analytical solution and $W(y)$ directly are mainly due to errors in synthesis and truncation of $F(v)$. When the resolution factor, h , is large, these differences are not significant.

Table II-3-1 Comparisons of Average Molecular Weights

Original W(y)	3 peak W(y)			
	Case IA Gaussian h = 0.5	Case IB Gaussian h = 0.2	Case IC Gaussian Variable h (0.5 ~ 1.5)	
Starting Set of G(v,y) and F(v)	Gaussian h = 0.5	Gaussian h = 0.2	Gaussian Variable h (0.5 ~ 1.5)	
Uncorrected Ave. Mol, Wt.	$\frac{\bar{M}_n(\infty)}{10^{-3}} \quad \frac{\bar{M}_w(\infty)}{10^{-3}} \quad \frac{\bar{M}_z(\infty)}{10^{-3}}$ 2.71 17.6 85.2 (2.74) (17.2) (78.4)	$\frac{\bar{M}_n(\infty)}{10^{-3}} \quad \frac{\bar{M}_w(\infty)}{10^{-3}} \quad \frac{\bar{M}_z(\infty)}{10^{-3}}$ 2.12 22.5 169.5 (2.17) (21.6) (140.8)	$\frac{\bar{M}_n(\infty)}{10^{-3}} \quad \frac{\bar{M}_w(\infty)}{10^{-3}} \quad \frac{\bar{M}_z(\infty)}{10^{-3}}$ 2.97 17.1 8.30 (2.98) (16.8) (77.8)	$\frac{M_n \times 10^{-3}}{3.20} \quad \frac{M_w \times 10^{-3}}{15.0} \quad \frac{M_z \times 10^{-3}}{52.5}$
Corrected Ave. Mol. Wt.	$\frac{\bar{M}_n \times 10^{-3}}{10^{-3}} \quad \frac{\bar{M}_w \times 10^{-3}}{10^{-3}} \quad \frac{\bar{M}_z \times 10^{-3}}{10^{-3}}$ 3.19 14.9 54.7 (3.28) (15.0) (31.2)	$\frac{\bar{M}_n \times 10^{-3}}{10^{-3}} \quad \frac{\bar{M}_w \times 10^{-3}}{10^{-3}} \quad \frac{\bar{M}_z \times 10^{-3}}{10^{-3}}$ 3.10 15.0 23,321 (2.75) (16.9) (62,667)	$\frac{\bar{M}_n \times 10^{-3}}{10^{-3}} \quad \frac{\bar{M}_w \times 10^{-3}}{10^{-3}} \quad \frac{\bar{M}_z \times 10^{-3}}{10^{-3}}$ 3.20 14.9 51.4 (3.21) (14.9) (54.1)	
Method-1	$\frac{\bar{M}_n \times 10^{-3}}{10^{-3}} \quad \frac{\bar{M}_w \times 10^{-3}}{10^{-3}} \quad \frac{\bar{M}_z \times 10^{-3}}{10^{-3}}$ 3.18 15.1 53.7 (3.18) (15.0) (52.7)	$\frac{\bar{M}_n \times 10^{-3}}{10^{-3}} \quad \frac{\bar{M}_w \times 10^{-3}}{10^{-3}} \quad \frac{\bar{M}_z \times 10^{-3}}{10^{-3}}$ 3.13 15.5 59.7 (3.15*) (15.8*) (60.2*)	$\frac{\bar{M}_n \times 10^{-3}}{10^{-3}} \quad \frac{\bar{M}_w \times 10^{-3}}{10^{-3}} \quad \frac{\bar{M}_z \times 10^{-3}}{10^{-3}}$ 3.21 15.3 55.3 (3.21) (15.2) (54.0)	
Method-2	$\frac{\bar{M}_n \times 10^{-3}}{10^{-3}} \quad \frac{\bar{M}_w \times 10^{-3}}{10^{-3}} \quad \frac{\bar{M}_z \times 10^{-3}}{10^{-3}}$ 3.08 15.8 96.0 (3.09) 15.5 (95.8)	$\frac{\bar{M}_n \times 10^{-3}}{10^{-3}} \quad \frac{\bar{M}_w \times 10^{-3}}{10^{-3}} \quad \frac{\bar{M}_z \times 10^{-3}}{10^{-3}}$ 3.04 16.2 125.6 (3.03*) (16.4*) (159.1*)	Not applicable	
Method of Chang & Huang Analytical (or true)	$\frac{\bar{M}_n \times 10^{-3}}{10^{-3}} \quad \frac{\bar{M}_w \times 10^{-3}}{10^{-3}} \quad \frac{\bar{M}_z \times 10^{-3}}{10^{-3}}$ 3.20 14.9 51.8 (3.23) (14.6) (47.7)	$\frac{\bar{M}_n \times 10^{-3}}{10^{-3}} \quad \frac{\bar{M}_w \times 10^{-3}}{10^{-3}} \quad \frac{\bar{M}_z \times 10^{-3}}{10^{-3}}$ 3.21 14.9 48.9 (3.28) (14.3) (40.6)	Not applicable	

* did not satisfy $\Delta S < 0.01$

Table II-3-1 continued.....

Original W(y)	3-peak W(y)	Chang and Huang's W(y)	$\frac{M_n \times 10^{-3}}{237}$ $\frac{M_w \times 10^{-3}}{603}$ $\frac{M_z \times 10^{-3}}{2,043}$
Starting Set of G(v,y) and F(v)	<p>Case 1D</p> <p>General shape h = 0.5 $\mu_3 = 1.0$</p> 	<p>Case 2A</p> <p>Gaussian h = 0.5</p> 	<p>Case 2B</p> <p>Gaussian h = 0.2</p> 
Uncorrected Ave. Mol. Wt.	$\frac{\bar{M}_n(\infty)}{10^{-3}} \frac{\bar{M}_w(\infty)}{10^{-3}} \frac{\bar{M}_z(\infty)}{10^{-3}}$ 2.65 17.8 79.2 (2.69)(17.4)(75.1)	$\frac{\bar{M}_n(\infty)}{10^{-3}} \frac{\bar{M}_w(\infty)}{10^{-3}} \frac{\bar{M}_z(\infty)}{10^{-3}}$ 201 710 3,267 (214) (675)(2,486)	$\frac{\bar{M}_n(\infty)}{10^{-3}} \frac{\bar{M}_w(\infty)}{10^{-3}} \frac{\bar{M}_z(\infty)}{10^{-3}}$ 158 896 5,574 (172) (821)(3,594)
Corrected Ave. Mol. Wt. Method-1 Method-2 Method of Chang & Huang Analytical (or true)	$\frac{\bar{M}_n \times 10^{-3}}{3.20}$ $\frac{\bar{M}_w \times 10^{-3}}{15.9}$ $\frac{\bar{M}_z \times 10^{-3}}{27,663}$ (3.17) (15.5) (16,049) 3.16 14.9 55.0 (3.16*) (14.7*) (53.7*) Not applicable	$\frac{\bar{M}_n \times 10^{-3}}{238}$ $\frac{\bar{M}_w \times 10^{-3}}{599}$ $\frac{\bar{M}_z \times 10^{-3}}{622}$ (254) (574) (2,206) 235 613 2,382 (242) (586) (1,864) 213 635 4,291 (221*) (623*) (2,800*)	$\frac{\bar{M}_n \times 10^{-3}}{227}$ $\frac{\bar{M}_w \times 10^{-3}}{595}$ $\frac{\bar{M}_z \times 10^{-3}}{69,269}$ (284) (492) (201,750) 233 614 2,919 (243*) (592*) (2,667*) 220 653 3,165 (228*) (611*) (2,503*)
	$\frac{3.23}{(3.27)}$ $\frac{15.5}{(15.3)}$ $\frac{60.0}{(56.9)}$	$\frac{238}{(252)}$ $\frac{601}{(572)}$ $\frac{1,987}{(1,512)}$	$\frac{239}{(260)}$ $\frac{592}{(543)}$ $\frac{1,608}{(1,037)}$

* did not satisfy $\Delta S < 0.01$

Table II-3-2 Numerical Values of F(v) used in Case IA and Case 2A

<u>Case IA</u>				<u>Case 2A</u>			
V	F(v)	V	F(v)	V	F(v)	V	F(v)
23.0	0	30.0	120	16.0	0	23.0	93
23.2	0	30.2	121	16.2	0	23.2	98
23.4	0	30.4	120	16.4	0	23.4	101
23.6	1	30.6	120	10.6	0	23.6	102
23.8	1	30.8	121	16.8	0	23.8	103
24.0	2	31.0	122	17.0	0	24.0	102
24.2	3	31.2	125	17.2	1	24.2	100
24.4	5	31.4	131	17.4	1	24.4	96
24.6	7	31.6	137	17.6	1	24.6	92
24.8	10	31.8	145	17.8	2	24.8	87
25.0	14	32.0	153	18.0	2	25.0	81
25.2	18	32.2	160	18.2	2	25.2	74
25.4	22	32.4	165	18.4	3	25.4	67
25.6	27	32.6	168	18.6	4	25.6	60
25.8	32	32.8	168	18.8	4	25.8	52
26.0	38	33.0	164	19.0	5	26.0	45
26.2	43	33.2	156	19.2	6	26.2	38
26.4	47	33.4	145	19.4	7	26.4	32
26.6	51	33.6	132	19.6	8	26.6	27
26.8	54	33.8	117	19.8	10	26.8	22
27.0	57	34.0	101	20.0	12	27.0	18
27.2	59	34.2	84	20.2	14	27.2	14
27.4	61	34.4	69	20.4	17	27.4	12
27.6	63	34.6	55	20.6	20	27.6	9
27.8	65	34.8	42	20.8	24	27.8	8
28.0	69	35.0	32	21.0	29	28.0	6
28.2	73	35.2	23	21.2	34	28.2	5
28.6	79	35.4	17	21.4	39	28.4	4
28.6	85	35.6	11	21.6	46	28.6	3

Table II-3-2 continued Numerical Values of F(v) used in Case 1A and Case 2A

<u>Case 1A</u>				<u>Case 2A</u>			
V	F(v)	V	F(v)	V	F(v)	V	F(v)
28.8	92	35.8	8	21.8	53	28.8	3
29.0	99	36.0	5	22.0	60	29.0	2
29.2	106	36.2	3	22.2	67	29.2	2
29.4	112	36.4	2	22.4	75	29.4	1
29.6	116	36.6	1	22.6	82	29.6	1
29.8	119	36.8	0	22.8	88	29.8	1
						30.0	0

Retention volume v in counts and
F(v) not normalized.

The iteration in each of the correction methods was carried out until the following tolerance was satisfied:

$$\Delta S = \int_0^{\infty} | F(v) - F_i(v) | dv < 0.01$$

This corresponds to the area difference between the two chromatograms of less than one percent of the total area under $F(v)$. In the case where repeated iterations failed to decrease ΔS but rather gave an oscillation in ΔS without satisfying the tolerance, the iteration was stopped when the first minimum in ΔS was obtained.

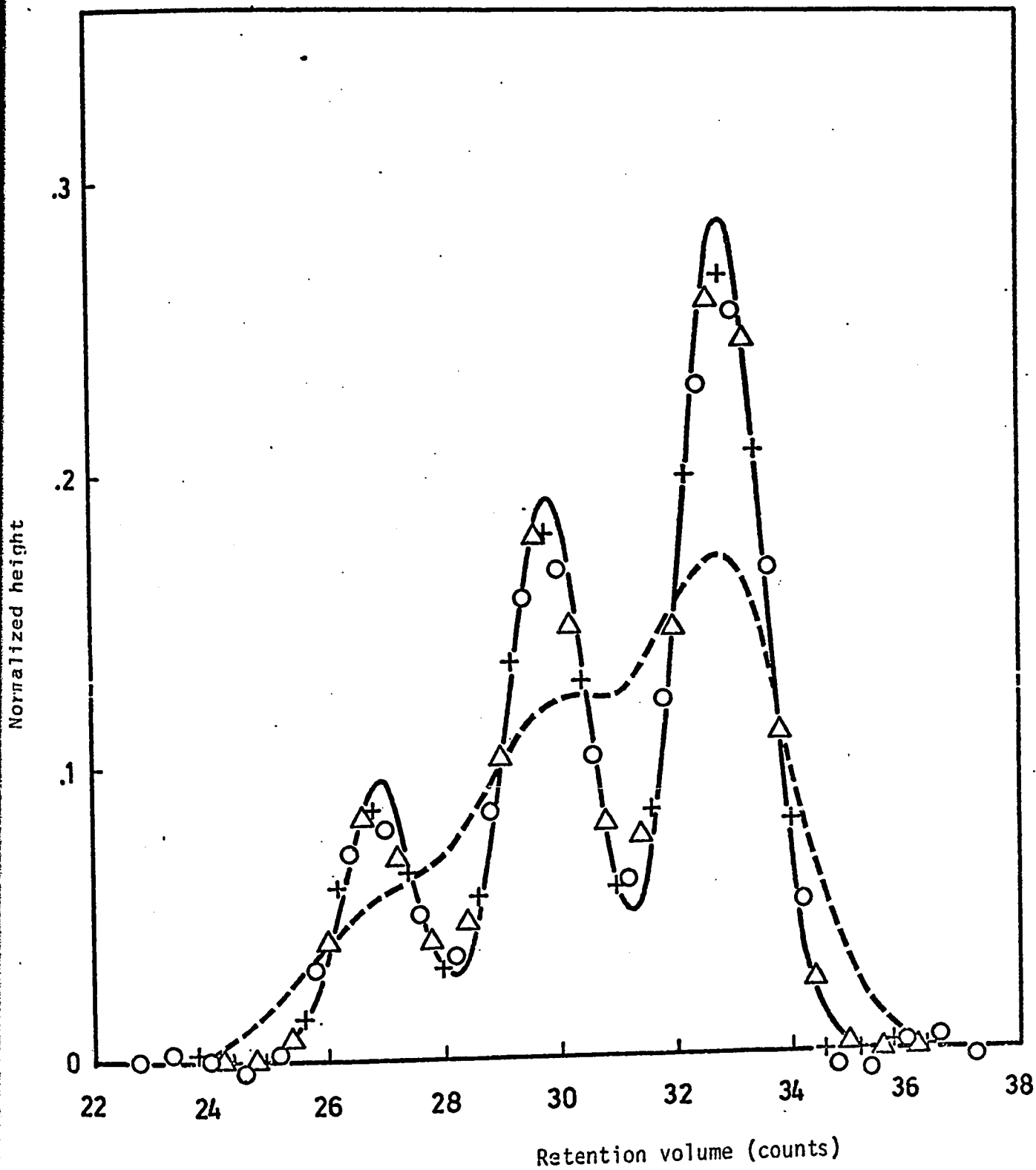
Case 1A and 2A Gaussian spreading function with $h = 0.5$

These are examples of a symmetrical and uniform instrumental spreading function. For a resolution factor of $h = 0.5$, the corrections to \bar{M}_n , \bar{M}_w and \bar{M}_z are about 15%, 20% and 60% respectively.

The recovered $W(y)$ for case 1A by the three methods are compared with the original $W(y)$ in Fig. II-3-5. All the methods gave a good smooth recovery except for somewhat blunt peaks and small fluctuations at both ends of the chromatogram.

Method-1 and method-2 gave corrected \bar{M}_n and \bar{M}_w to within $\pm 2\%$ of their true values and the method of Chang and Huang gave them to within $\pm 5\%$. As for corrected \bar{M}_z , the first two methods gave $\sim 5\%$ larger values than the true one while the latter method gave $\sim 80\%$ error.

Reduction of the accuracy in reading $F(v)$ to a maximum of three



II-3-5 Recovery of $W(y)$ - Case 1A ($h = 0.5$)

— original $W(y)$, ---- $F(v)$, O Method-1, Δ Method-2, + Method of Chang and Huang

figures still resulted in a good recovery of the original $W(y)$ similar to those shown in Fig.II-3-5. The errors in corrected \bar{M}_n and \bar{M}_w also remained about the same as before. However, the error in the corrected \bar{M}_z increased to $\sim 35\%$ for method-1, to $\sim 10\%$ for method-2 and to $\sim 100\%$ for the method of Chang and Huang.

Fig. II-3-6 shows the comparison of the recoveries for case 2A. Neither of the methods could recover a $W(y)$ with two peaks. Increased number of iterations with a smaller tolerance ($\Delta S < 0.0025$) resulted in slightly better recoveries with the second peak recovered as a shoulder in all three methods. The reduction of the step size for the whole evaluation routine from 0.2 to 0.1 count did not give any significant improvement. The values of the corrected \bar{M}_n and \bar{M}_w were still within $\pm 2\%$. The method of Chang and Huang gave these to within $\pm 10\%$. The corrected \bar{M}_z however differed significantly from the true value, the best \bar{M}_z obtained was $\sim 20\%$ in error. This was by method-2. When $F(v)$ was truncated still further by one figure, all three methods gave oscillations in the main portion of the recovered $W(y)$. The method of Chang and Huang gave an oscillation in the value of ΔS from the beginning and could not satisfy the tolerance despite their data smoothing process before the iteration procedure. However, once more the corrected \bar{M}_n and \bar{M}_w of the three methods are reasonable even though the recovered $W(y)$ appears to be significantly different from the true $W(y)$.

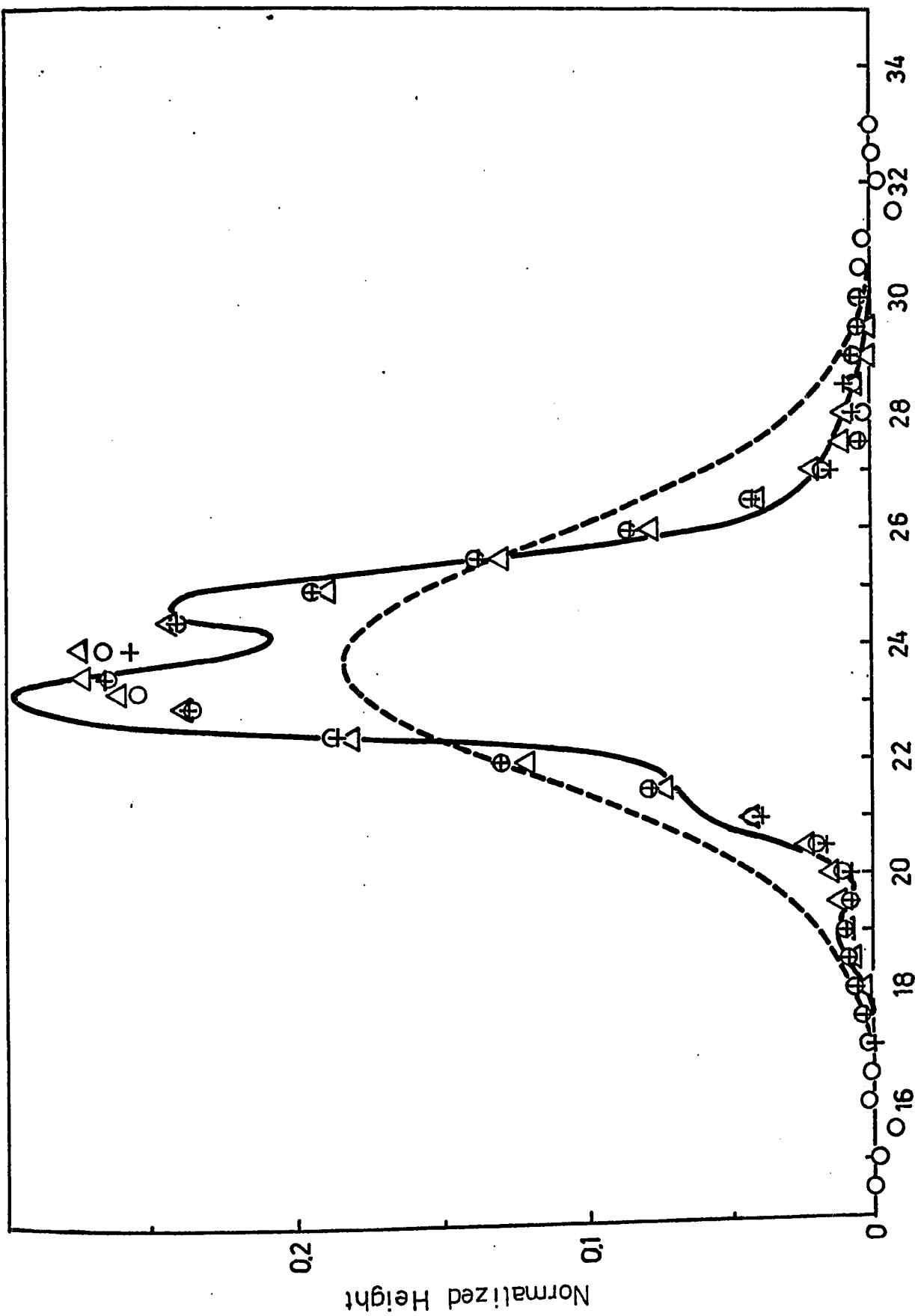


Fig. II-3-6 Recovery of $W(y)$ - Case 2A ($h = 0.5$)

--- $F(y)$, O Method-1 Δ Method-2
 + Method of Chang and Huang

Case 1B and 2B Gaussian spreading function with $h = 0.2$

A set of GPC columns having a Gaussian spreading function with an h value as low as 0.2 may be considered unsatisfactory. However, if the slope of the molecular weight calibration curve is small, this column set may give satisfactory separations. The use of a small resolution factor provides a much more difficult test for any numerical method of recovering $W(y)$.

Recovered $W(y)$ for case 1B is shown in Fig. II-3-7. Although the recoveries were smooth and the peaks were shown to exist, the recovery of $W(y)$ as a whole was rather poor. The method of Chang and Huang gave a slightly better recovery than the other two methods, however this advantage was lost when corrected \bar{M}_n and \bar{M}_w were compared. Method-1 and method-2 gave smaller errors in \bar{M}_n ($\sim 3\%$), \bar{M}_w ($\sim 5\%$). Only Method-2 gave \bar{M}_z within $\sim 20\%$ error. A significant improvement was observed in the recovered $W(y)$ by all three methods when the iteration was continued until a smaller tolerance $\Delta S < 0.0025$ was satisfied. The magnitude of recovered peaks in this case was much closer to the original ones.

The recoveries for case 2B were about the same as for case 2A. No significant difference in the three methods was observed. Two peaks were not detected in the recovered $W(y)$, since with a high resolution ($h = 0.5$), neither method could show their existence. Method-1 and -2 again gave smaller errors in \bar{M}_n ($\sim 3\%$) and \bar{M}_w ($\sim 5\%$) than the method of Chang and Huang. It can be seen that the recovered \bar{M}_z by method-1 is out of the ball park for both cases 1B and 2B. Method-2 gave the smallest errors in \bar{M}_z for

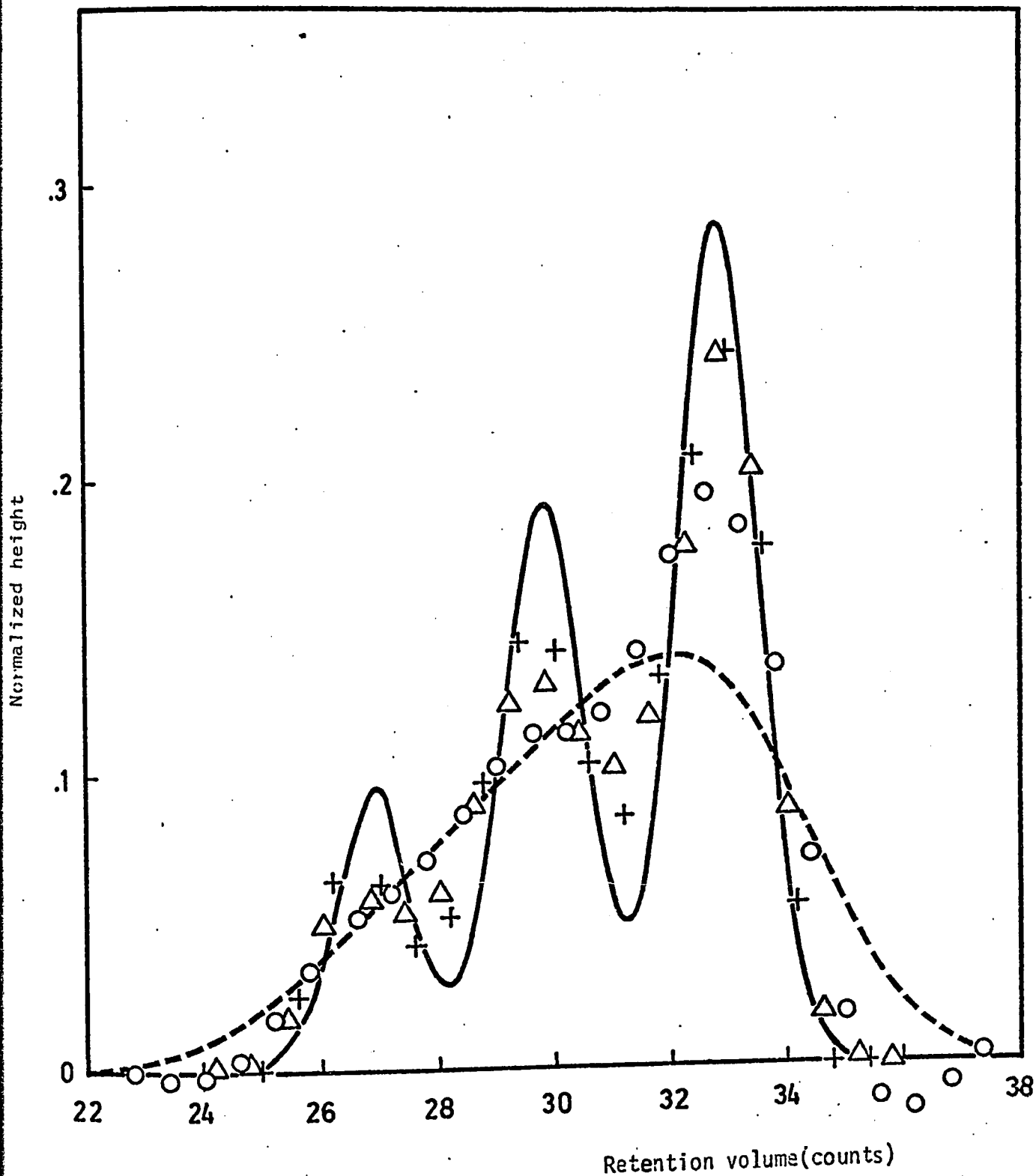


Fig. II-3-7 Recovery of $W(y)$ - Case 1B ($h=0.2$).

— original $W(y)$, --- $F(v)$, ○ Method-1, △ Method-2, + Method of Chang and Huang

for both cases.

Only method-1 could reach $\Delta S < 0.01$ when the accuracy in reading $F(v)$ was reduced one digit. But corrected \bar{M}_n and \bar{M}_w by this method were not any better than those of the other two methods in this instance. Oscillations in the recovered $W(y)$ were found for all three methods.

Case 1C Gaussian spreading function with variable h

This is an example of an instrumental spreading function which is symmetrical but non-uniform. For the case of non-uniform G , neither the analytical solution nor the method of Chang and Huang apply. The change of h with respect to input species was given by the following quadratic equation.

$$h = 4.879 - 0.373 y + 0.008 y^2$$

This give h values from 0.5 to 1.5 in the retention volume range of the given $F(v)$. Uncorrected \bar{M}_n , \bar{M}_w and \bar{M}_z show about 10, 20 and 60% deviation from their true values in this example.

Good recoveries of $W(y)$ by both method-1 and method-2 can be seen in Fig. II-3-8. Corrected \bar{M}_n and \bar{M}_w differ only by $\sim 2\%$ from the true ones and \bar{M}_z by $\sim 5\%$. A reduction of the reading accuracy of $F(v)$ did not affect the recovery of $W(y)$ and the corrected molecular weight averages.

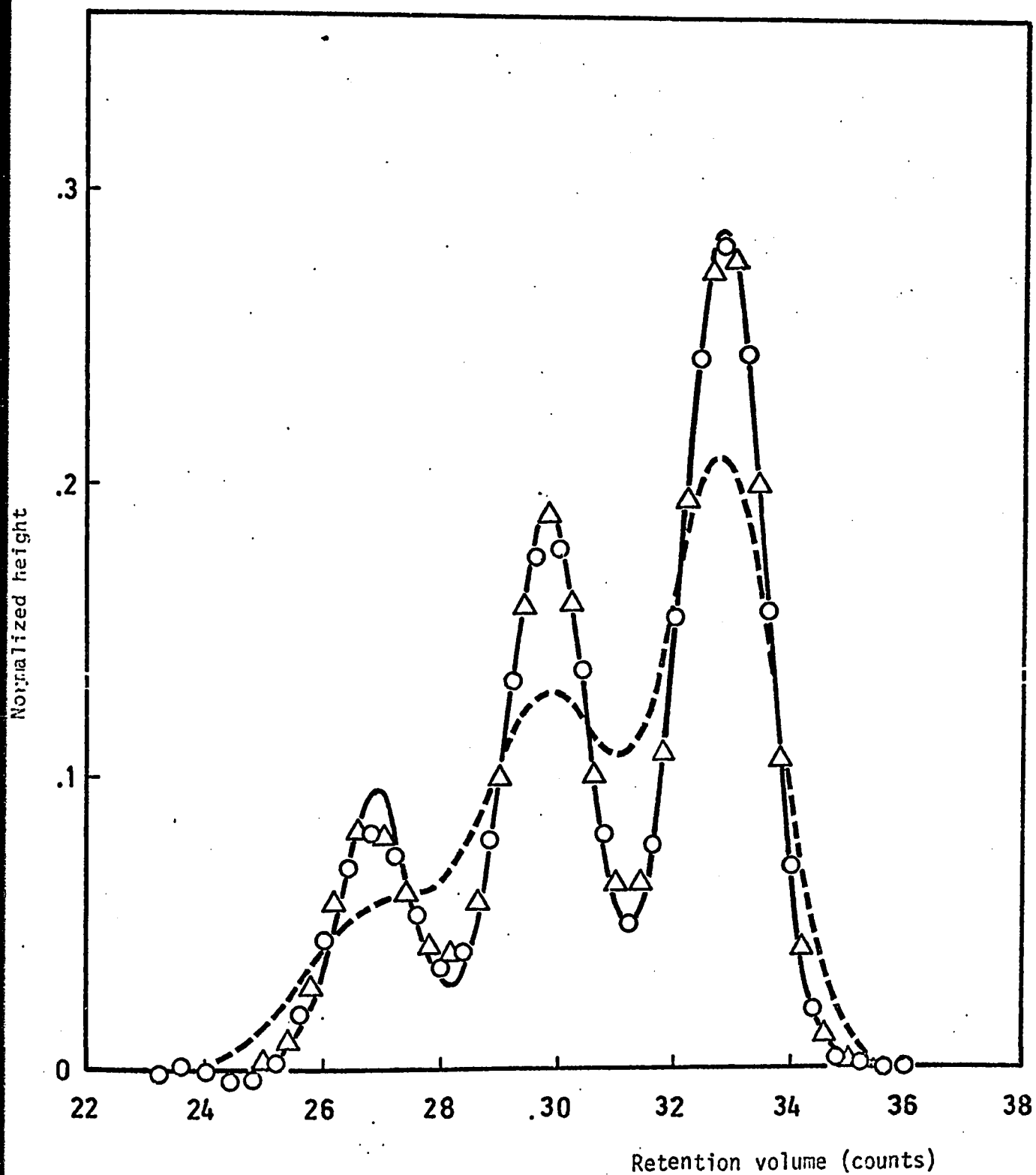


Fig. II-3-8 Recovery of $W(y)$ - Case 1C (variable h)

— original $W(y)$, --- $F(v)$, ○ Method-1, △ Method-2

Case 1D General instrumental spreading function with $h = 0.5$ and $\mu_3 = 1.0$

This gives an example of non-symmetrical, uniform spreading function. Only the two shape parameters h and μ_3 were used with the remaining ones set equal to zero. The combination of $h = 0.5$ and $\mu_3 = 1.0$ gives a spreading function significantly skewed toward higher retention volumes. Because the two parameter expression in the general spreading function is essentially a cubic function, small negative values appear at about 2.5 counts from its peak position. These negative portions were set to zero and the shape was normalized for use in the $F(v)$ synthesis and with the correction methods. Deviation of uncorrected \bar{M}_n , \bar{M}_w and \bar{M}_z from the true values were nearly the same as with case 1A where a Gaussian spreading function with $h = 0.5$ was used.

Fig. II-3-9 compares the recovered $W(y)$ with the original one. The shape recovered seems slightly poorer than for case 1A with recovered peaks sharper than the true ones.

Corrected \bar{M}_n and \bar{M}_w had errors within $\pm 5\%$. Corrected \bar{M}_z by method-1 was again out of the ball park, while method-2 gave a reasonable value (10% error). When the $F(v)$ reading was reduced in accuracy by one figure, both methods gave oscillations in the main portion of the recovered $W(y)$. Again the corrected molecular weight averages seemed equally good as those obtained from a more accurate $F(v)$.

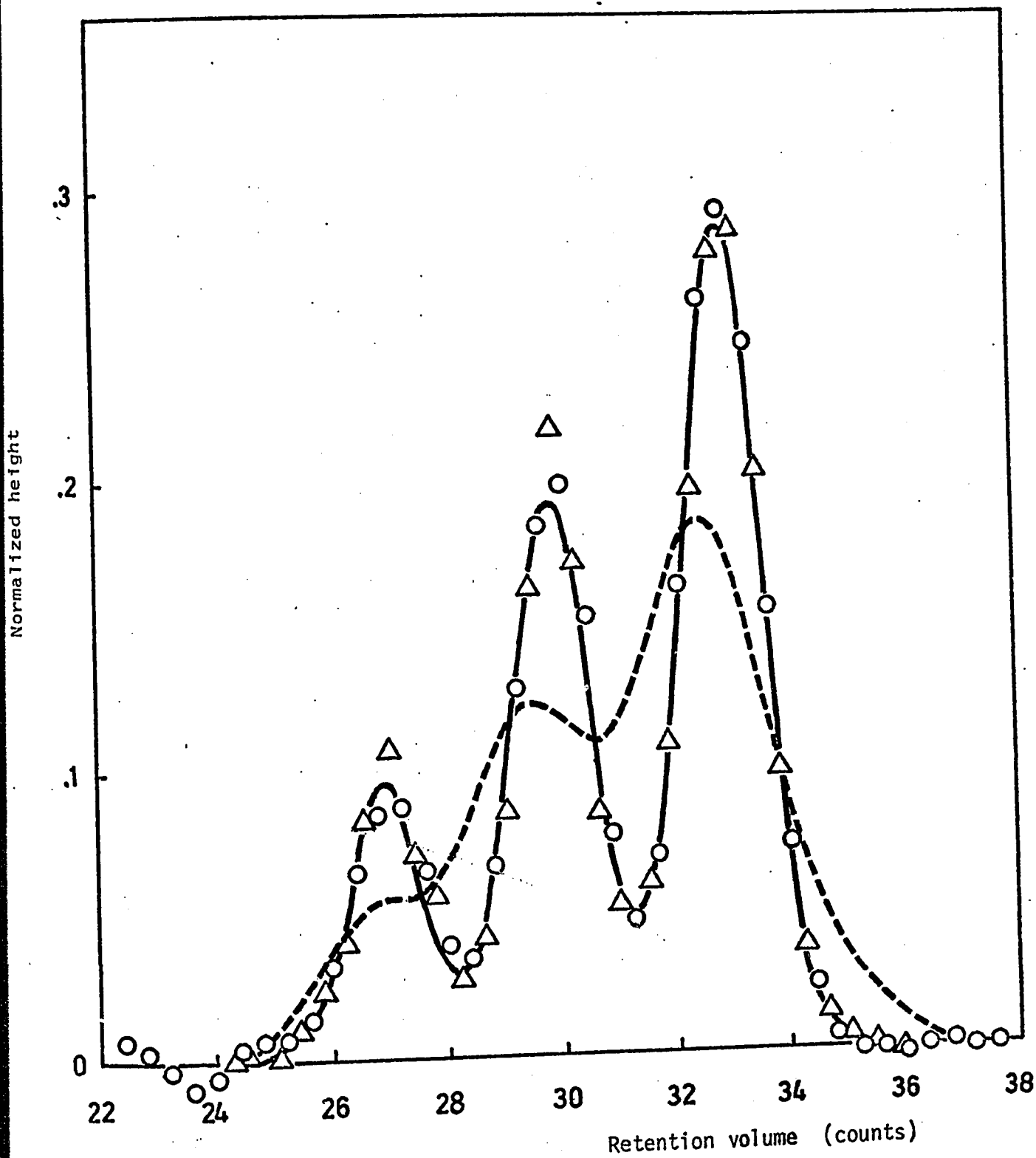


Fig. II-3-9 Recover of $W(y)$ Case 1D ($h = .5, \mu_3 = 1.0$)

— original $W(y)$, --- $F(v)$ O Method-1, Δ Method-2

Computation Time

Computation times required for method-1, method-2 and the method of Chang and Huang are compared in Table II-3-3 for four cases. It was found that the method of Chang and Huang and Method-2 are approximately the same while method-1 required more time due to its G-operation beyond the retention volume range of $F(v)$. Fifty more zero data points on $F(v)$ were added to both ends of the chromatogram in the last case to enable iterative G-operations. In each of the methods, the most time-consuming part is the multitude of G-operations necessary. However the number of iterations to reach the specified tolerance does not directly represent the computation time because of the differences in operation in each of the methods. The present tolerance $\Delta S \leq 0.01$ was found similar to the one recommended by Chang and Huang. This appeared reasonable in recovering $W(y)$ and correcting \bar{M}_n , \bar{M}_w and \bar{M}_z for resolution factor h higher than 0.5, however it may be necessary to reduce it at lower resolution to obtain good recoveries for differential distributions.

The digital computer used for all of the above calculation was the CDC 6400.

Table II-3-3 Comparisons of Computation Time and Number of Iterations (CDC6400 Computer with time in seconds)

	Case 1A	Case 1B	Case 2A	Case 2B
Method-1	14.9 (14)	17.5 (12)	10.5 (5)	15.8 (10)
Method-2	9.6 (17)	21.5 (47)	7.3 (6)	9.3 (10)
Method of Chang & Huang	7.2 (3)	18.0 (17)	7.0 (2)	6.7 (2)

The first value shows the time in seconds and the value in bracket is the number of iteration to reach $\Delta S < 0.01$

II-3-3 Application of Method-1 and Method-2 to Experimental Chromatograms

Corrections on experimentally obtained GPC chromatograms were attempted by Method-1 and Method-2 to evaluate their performances in practical applications. Experimentally obtained chromatograms and instrumental spreading functions are generally subject to errors, hence it is important to know whether these errors cause any significant difficulties in obtaining $W(y)$. Polymer standards analyzed here are narrow distributed polystyrene samples for which the correction have been known to be much more difficult than the broad-distributed samples.

Method-1 and Method-2 were added with the data smoothing routine used by Chang and Huang. Although it was found that the data smoothing did not show any significant improvement in obtaining the corrected chromatograms in the presently obtained chromatograms, it was found useful in eliminating large artificial oscillation in $W(y)$ when the significant digit of $F(v)$ is only two. (An example chromatogram of polyethylene sent from Haifa, Israel.)

Polymer samples used were polystyrene standards of molecular weight range of $6 \times 10^2 - 2 \times 10^6$. GPC used was the standard Waters unit Model 100. The solvent was tetrahydrofuran (THF) and operating temperature was $24 \pm 2^\circ\text{C}$. The sample solutions of 1 ml was injected into a combination of four styragel columns (7×10^6 , 10^4 , 900 and 800 Å). The flow rate was 3.0 ml/min, sample concentration was at three levels, 1.0, 0.25 and 0.0625 wt %. The experiments with different concentrations were aimed to give the concentration effect in SK suggested by Balke and Hamielec. Number- and

weight- average molecular weight of the polystyrene standards are listed in Table II-3-4 together with the calculated polydispersity and $\bar{M}_{rms} = \sqrt{\bar{M}_n(t) \times \bar{M}_w(t)}$. Table II-3-5 summarizes the observed peak retention volumes for these samples. The calibration curve of molecular weight (\bar{M}_{rms} was used) vs. retention volume is shown in Fig. II-3-10. No significant difference in peak retention volumes was observed in the sample concentration levels at 0.0625 wt % and 0.25 wt % for the polymer standards less than 10^5 . However at 1.0 wt % level, they shifted to the higher retention volume. At molecular weight $\sim 10^6$, the shift of the peak retention volume was magnified and it was also seen at .0625 \sim .25 wt % level. A good linearity between $\log M$ vs. v was observed in $6 \times 10^2 < M < 5 \times 10^4$, or $25.2 < v < 33.6$. The three samples, PC11a, PC8A and WA4190039 were almost eluted in this linear range as shown in Fig. II-3-10. Therefore, the use of analytically derived relations between $\bar{M}_k(t)/M_k(\infty)$ and h and SK or h and μ_3 could be justified for these samples. Table II-3-6 summarizes the obtained parameters from $\bar{M}_n(t)/\bar{M}_n(\infty)$ and $\bar{M}_w(t)/\bar{M}_w(\infty)$. It is seen that the resolution factor h decreases with increasing molecular weight in the range of molecular weight $6 \times 10^2 \sim 2 \times 10^4$ in both cases. However, their absolute values were different in the magnitude of ten. Concentration dependence of SK was not observed in the molecular weight range. It is probably counted in the shift of calibration curve.

Effective calibration curve constants D_1 and D_2 obtained were listed in Table II-3-7. These constants D_1 and D_2 differed significantly

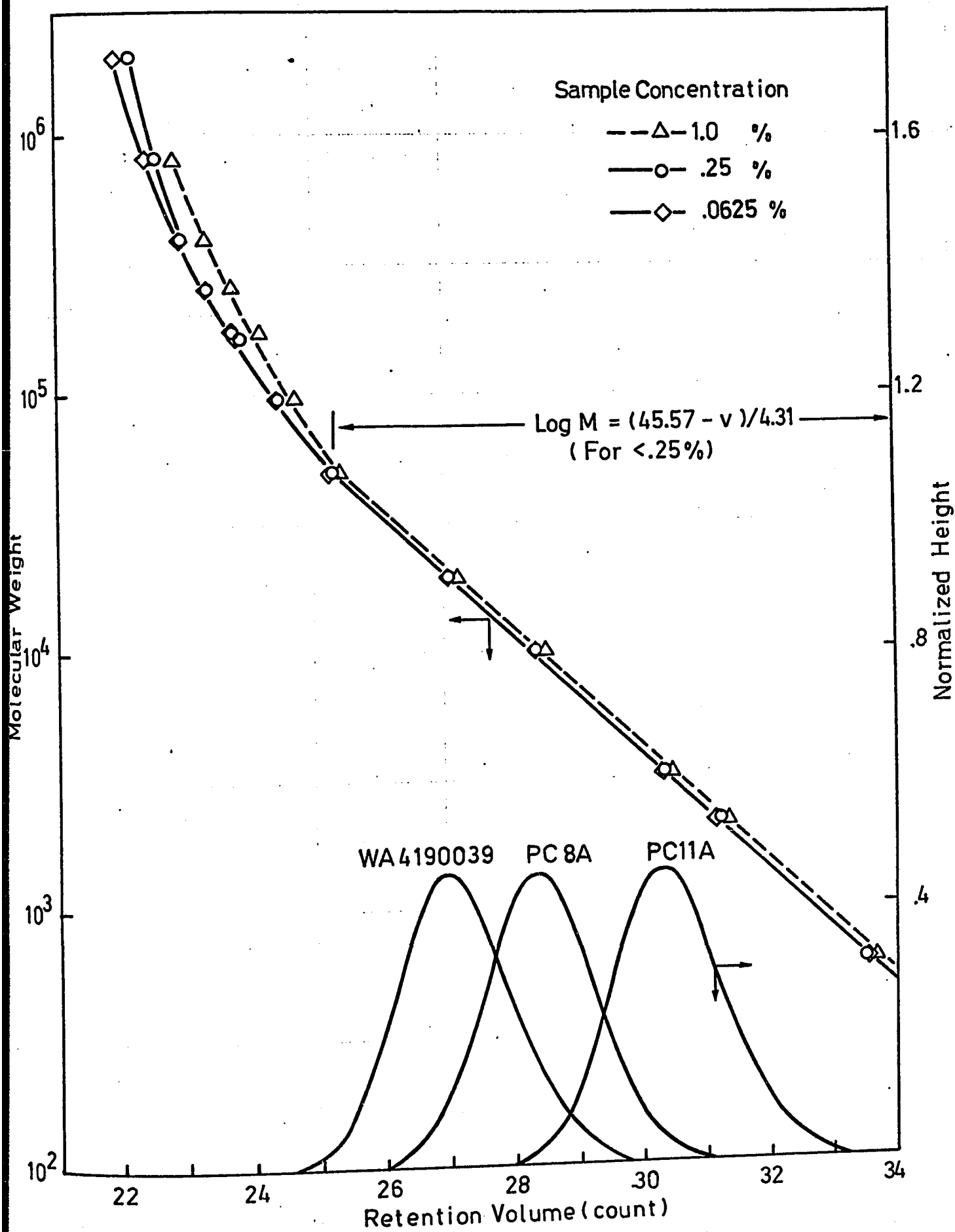


Fig. II-3-10 Molecular Weight Calibration Curve

TABLE II-3-4 REPORTED AVERAGE MOLECULAR WEIGHT OF STANDARDS

SAMPLE	$\bar{M}_n(t)$ $\times 10^{-3}$	$\bar{M}_w(t)$ $\times 10^{-3}$	$p(t)$	\bar{M}_{rms} $\times 10^{-3}$
PC16A	.578	.636	1.10	.606
PC12A	2.07	2.20	1.06	2.14
PC11A	3.18	3.53	1.11	3.36
PC 8A	9.70	10.3	1.06	10.0
WA4190039	19.65	19.85	1.01	19.75
PC 7A	49.0	51.0	1.04	50.0
PC 4A	96.2	98.2	1.02	97.2
WA41984	164.2	173.2	1.06	168.5
S108	247.	267.	1.08	257.
PC 3A	392.	411.	1.05	401.
PC 6A	773.	867.	1.12	819.
WA61970	1780.	2145.	1.21	1987.
NBS705	170.9	179.3	1.05	175.
NBS706	136.5	257.8	1.89	
G-35	190.	570.	3.00	
COOPA	116.	304.	2.62	

TABLE II-3-5 LIST OF PRV, $\bar{M}_n(\infty)$, $\bar{M}_w(\infty)$ AND $p(\infty)$

--- 1.0 WT. PER CENT ---				
SAMPLE	PRV	$\bar{M}_n(\infty)$ $\times 10^{-3}$	$\bar{M}_w(\infty)$ $\times 10^{-3}$	$p(\infty)$
PC16A	33.64	0.544	0.670	1.233
PC12A	31.37	1.580	2.106	1.333
PC11A	30.49	2.662	3.457	1.299
PC 8A	28.50	8.208	10.29	1.254
WA4190039	27.17	17.43	21.47	1.232
PC 7A	25.37	43.13	60.29	1.398
PC 4A	24.69	78.91	121.6	1.541
WA41984	24.18	112.7	205.8	1.827
S108	23.76	142.8	351.2	2.459
PC 3A	23.33	217.9	609.7	2.798
PC 6A	22.87	493.1	1287.	2.610
NBS705	23.96	132.9	284.8	2.143
NBS706	23.66	108.0	452.0	4.185
G-35	23.26	175.8	892.6	5.077

TABLE II-3-5 (CONTINUED)

--- 0.25 WT. PER CENT ---

SAMPLE	PRV	$\bar{M}_n(\infty)$ $\times 10^{-3}$	$\bar{M}_w(\infty)$ $\times 10^{-3}$	$p(\infty)$
PC16A	33.51	0.460	0.628	1.365
PC12A	31.30	1.529	2.038	1.333
PC11A	30.34	2.841	3.550	1.249
PC 8A	28.38	8.500	10.54	1.239
WA4190039	27.02	16.86	21.15	1.255
WA4190039	27.01	17.42	21.62	1.241
PC 7A	25.22	43.53	55.96	1.286
PC 4A	24.43	74.39	108.8	1.462
WA41984	23.89	112.6	188.9	1.678
S108	23.39	154.7	369.2	2.387
PC 3A	22.97	278.4	761.2	2.734
PC 3A	22.99	257.8	707.5	2.745
PC 3A	22.63	440.6	1562.	3.545
WA61970	22.27	657.0	8312.	12.65
NBS705	23.78	118.4	223.7	1.889
NBS706	23.33	113.6	933.2	8.214
G-35	22.90	177.6	1326.	7.469
COOPA	23.37	99.71	602.4	6.041
COOPA	23.32	99.70	641.7	6.436

--- 0.0625 WT. PER CENT ---

SAMPLE	PRV	$\bar{M}_n(\infty)$ $\times 10^{-3}$	$\bar{M}_w(\infty)$ $\times 10^{-3}$	$p(\infty)$
PC16A	33.54	0.367	0.571	1.555
PC12A	31.28	1.491	2.017	1.353
PC11A	30.34	2.800	3.524	1.259
PC 8A	28.39	8.404	10.46	1.245
WA4190039	26.99	17.26	21.40	1.240
WA4190039	27.05	16.90	20.98	1.242
WA4190039	27.02	17.75	21.64	1.219
PC 7A	25.19	44.68	56.07	1.255
P3 4A	24.40	78.85	108.1	1.371
WA41984	23.79	114.7	181.5	1.582
S108	23.34	150.5	311.6	2.070
PC 3A	22.92	257.9	581.2	2.253
PC 3A	22.95	256.0	532.5	2.080
PC 3A	22.96	260.2	515.1	1.980
PC 6A	22.48	499.5	1143.	2.289
WA61970	22.00	725.0	2652.	3.659
NBS705	23.71	120.3	239.1	1.987
NBS706	23.27	128.9	354.8	2.753
G-35	22.85	180.3	810.3	4.494
COOPA	23.30	98.44	444.9	4.519

Table II-3-6 Two Parameters for Instrumental Spreading

<u>Sample</u>	<u>Concentration</u>	⁽²⁴⁾ <u>Balke and Hamielec</u>		⁽¹⁰⁾ <u>Provder and Rosen</u>	
		<u>h</u>	<u>SK</u>	<u>h</u>	<u>μ_3</u>
PC11A	1.00	.908	.210	10.487	.091
	.25	1.207	.110	14.456	.049
	.06 25	1.137	.134	13.496	.059
PC8A	1.00	.858	.175	10.095	.077
	.25	.923	.113	11.107	.050
	.06	.898	.133	10.741	.059
WA4190039	1.0	.720	.042	8.809	.019
	.25	.658	.092	8.001	.041
	.0625	.696	.056	8.511	.025

Table II-3-7 Effective Calibration Curve Constants in $M = D_1 \exp(-D_2 v)$ A) From $\bar{M}_n(t)$ and $\bar{M}_w(t)$ of one Sample (0.25 wt %)

<u>Sample</u>	<u>D_1</u>	<u>D_2</u>
PC11A	2.3242×10^8	3.6581×10^{-1}
PC8A	3.0709×10^7	2.8244×10^{-1}
WA4190039	4.2314×10^5	1.1624×10^{-1}

B) From Two $\bar{M}_n(t)$ of Two Samples (0.25 wt %)

<u>Sample Set</u>	<u>D_1</u>	<u>D_2</u>
PC11A-PC8A	1.4539×10^{10}	5.0000×10^{-1}
PC11A-WA4190039	1.4539×10^{10}	5.0000×10^{-1}
PC8A-WA4190039	1.5912×10^{10}	5.0000×10^{-1}

when searched by fitting $\bar{M}_n(t)$ and $\bar{M}_w(t)$ of one samples. However, when they were searched by fitting the two $\bar{M}_n(t)$ of the two samples, the agreements in different sets of two samples were almost perfect. This reflects the reliability of $\bar{M}_n(t)/\bar{M}_w(t)$ as compared to that of $\bar{M}_n(t)_{\text{sample-1}} / \bar{M}_n(t)_{\text{sample-2}}$ since the searching of D_1 and D_2 was carried out on these ratios. The chromatogram obtained for WA190039 at 0.25 wt % was corrected by Method-1 and Method-2, using a Gaussian instrumental spreading function with the resolution factor h obtained by the method of Balke and Hamielec.⁽²⁴⁾ Although this h does not precisely represent the instrumental spreading due to $SK \neq 0$, the effect of SK was assumed to be the shifting of the experimental calibration curve, hence it was thought that this did not cause a significant error in obtaining the shape of corrected chromatogram $W(y)$. The use of parameter set h and μ_3 in the spreading function⁽¹⁰⁾ was more desirable and rigorous to obtain $W(y)$, however, the obtained set of h and μ_3 gave significantly negative values in leading portion together with the presence of positive double peaks, physically almost impossible situation. Thus their use was abandoned. Fig. II-3-11 compares the obtained $W(y)$ by Method-1, Method-2 and by the effective calibration curve (from two known \bar{M}_n 's of PC11A and WA4190039 and their experimental chromatograms at 0.25 wt%). Since the search for the effective calibration curve by-passed the construction of corrected chromatograms $W(y)$, they were back-calculated for comparison from the molecular weight distributions (obtained by combining uncorrected chromatograms with the effective calibration curve) using the experimentally determined calibration curve. Both Method-1 and Method-2 resulted in

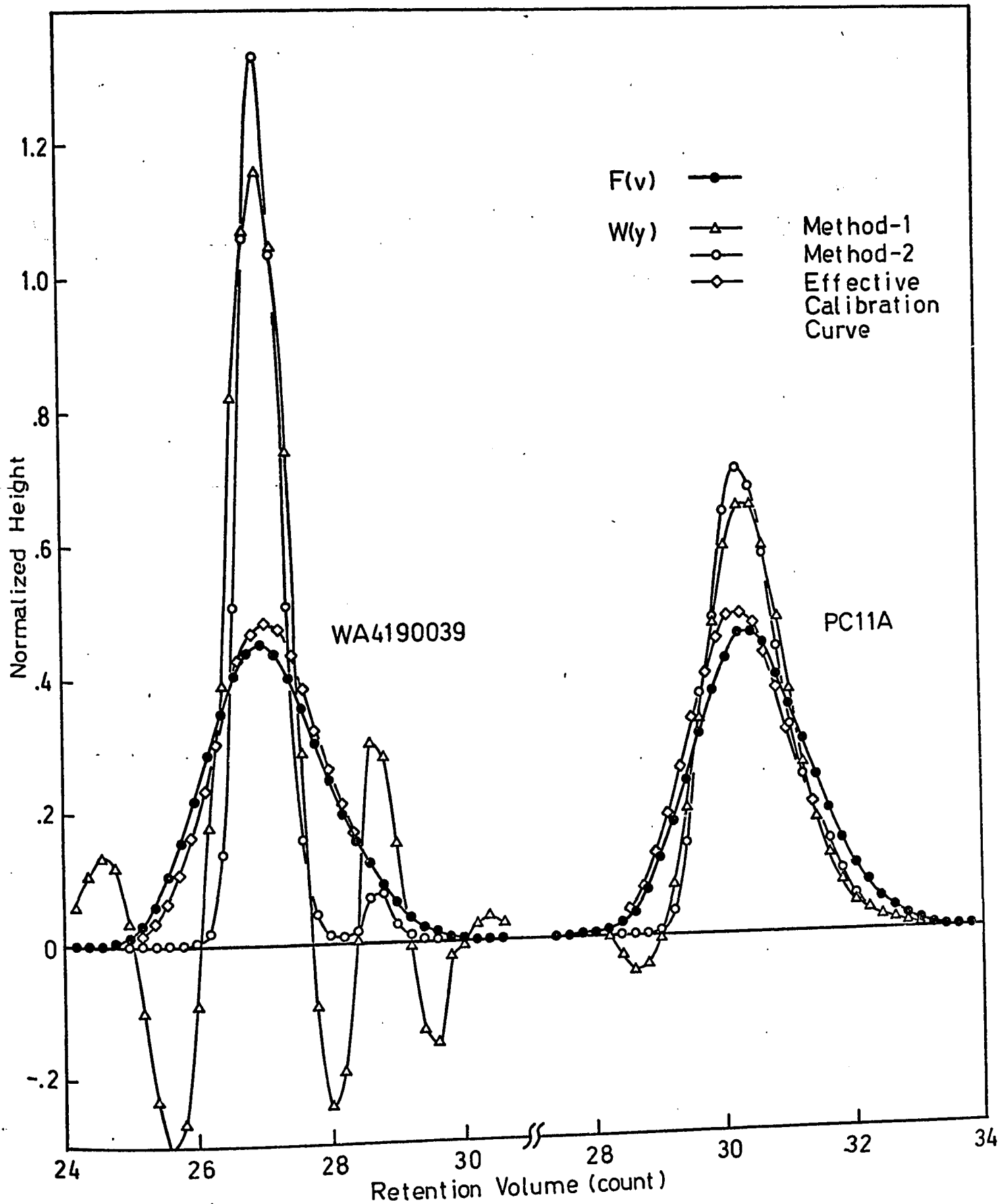


Fig. II-3-11 Comparisons of Corrected Chromatograms

similar corrected chromatograms in the main portion of their peaks. However, the corrections at the both ends of the peaks suffered an unrealistic oscillation. The Method-1 again showed significantly negative heights in these range for the both samples. The Method-2 resulted in a small second peak in the sample WA4190039, indicating either the insufficiency of the Gaussian spreading or the noise in the original chromatogram. While for the sample PC11A, this was not seen, probably due to the larger resolution factor for this sample.

The use of the effective calibration curve did not sharpen the chromatograms as much as the Method-1 or Method-2 did. Its effect appeared small due to closeness of D_1 and D_2 to those of experimental ones. Since the construction of $W(y)$ from $F(v)$ in this case is simply mappings of the chromatograms, no oscillation results unless $F(v)$ itself is oscillating. Number- and weight-average molecular weight obtained from the corrected chromatograms are compared in Table II-3-8. The two average molecular weights by Method-1 and Method-2 were raised by $1 + \frac{1}{2} SK$ as was suggested. The polydispersities of the samples were recovered within 5% by Method-1 and Method-2 while the effective calibration curve gave them within 20%. The larger error in the last method may not be attributed to the method itself. It is possible that the effective calibration curve may not be the linear one. The best set of D_1 and D_2 gave $\bar{M}_n(t)_{PC11A} / \bar{M}_n(t)_{WA4190039} - \bar{M}_n(D_1, D_2)_{PC11A} / \bar{M}_n(D_1, D_2)_{WA4190039} = 7.336 \times 10^{-4}$. This might be further reduced by using a non-linear calibration curve, then the agreement in polydispersity should be improved.

Table II-3-8 Comparison of Average Molecular Weights

Sample PC11A

	\bar{M}_n	\bar{M}_w	\bar{p}
Supplied Value	3.18×10^3	3.53×10^3	1.11
Method-1 (10-th iteration) ($\Delta S = 0.0095$)	3.19×10^3	3.54×10^3	1.11
Method-2 (50-th iteration)* ($\Delta S = 0.0111$)	3.19×10^3	3.57×10^3	1.12
Effective Calibration curve	3.18×10^3	3.86×10^3	1.23

Sample WA4190039

	\bar{M}_n	\bar{M}_w	\bar{p}
Supplied Value	1.965×10^4	1.985×10^4	1.01
Method-1 (50-th iteration)* ($\Delta S = 0.0168$)	1.878×10^4	1.959×10^4	1.04
Method-2 (20-th iteration)** ($\Delta S = 0.0823$)	1.940×10^4	2.049×10^4	1.06
Effective Calibration curve	1.683×10^4	2.052×10^4	1.22

* Converging to smaller ΔS but iteration stopped

** Reached the first smallest ΔS

II-4 EXPERIMENTS RELATED TO KINETIC STUDY OF ACRYLAMIDE POLYMERIZATION

II-4-1 Experimental Set-up of the Instrument

Commercially available GPC column packing materials compatible with water and suited for molecular weight analysis over one million appeared to be only porous glass of large pore size. The largest pore size available were employed for this purpose together with an intermediate one for conversion analysis. These are listed below.

	<u>CPG10-700</u>	<u>CPG10-2000</u>	<u>Bio-Glas2500</u>
Average pore size (Å)	700	2000	2500
Exclusion Limit	4×10^5 a) 1×10^6 b)	$> 1 \times 10^6$ a) 2×10^6 b)	9×10^6 c)
Supplier	WA*	WA*	BR**

- a) Dextran polymer in Water
- b) Polystyrene in THF
- c) Polystyrene in Toluene

* WA Waters Associates, Framingham, Mass.

** BR Bio-Rad Laboratory, Richmond, California

Porous glass of controlled pore size was first developed by Haller⁽³⁵⁾ for chromatographic use and it has been shown to be a superior GPC column packing as compared to styragel in view of stability over wide range of operational conditions, ease of packing and long usable life^(36,37). Extensive study has been made of the structure of the pores and their size distribution.^(38,39,40) However, one detracting feature of the porous

glass is the presence of active sites for adsorption which retard the elution of some molecules, particularly polar materials. This results in a significant tailing of the chromatogram⁽³⁷⁾ or in no elution of the injected sample at all.⁽⁴¹⁾ Nevertheless, pretreatment of the glass has been reported to reduce adsorption in aqueous media.⁽⁴²⁾ In organic solvent, the pretreatment of the porous glass with hexamethyldisilazane resulted in the complete elution of injected polymers.⁽⁴¹⁾

The manufacturer of Bio-Glas recommended that it be silanized before use in order to reduce its adsorptive properties in aqueous media. This was done as follows:

- 1) The Bio-Glas was heated at 160°C for 24 hours in a vacuum oven to remove water.
- 2) After cooling in vacuum, the Bio-Glas was quickly transferred to a 1 l flask containing 5% hexamethyldisilazane (HMDS) in 500 ml n-hexane.
- 3) A condenser was attached and the solution was refluxed for 6 hours.
- 4) The mixture was filtered and rinsed with n-hexane to removed excess HMDS and then dried at atmospheric pressure.

The CPG10-700 and -2000 were packed as received from the manufacturer. However, high molecular weight proteins (available as protein calibration kit from Pharmacia Canada Ltd., Montreal) were injected as is recommended by Waters Associates prior to routine operation.

The packing of the materials into a column (O.D. 3/8", 4 ft., stainless steel) was done as follows. Firstly, the empty column was filled with the porous glass under vibration. Then a vacuum was applied

to the top of the column and distilled water was sucked from the bottom. A column thus packed eluted air bubbles for a few hours of operation time.

The new columns adsorbed a certain amount of acrylamide and polyacrylamide. This was observed by a successive injection of an acrylamide or polyacrylamide solution. The response to each injection gradually increased in peak size and reached nearly a constant peak after several injections.

The GPC employed was Waters ALC model 201. The injection septum was replaced with an injection valve having a 1 ml sample loop. Two pressure dampers were removed. During the study of conversion measurements from peak areas, it was found that the variation of flow rate was not negligible over an operating period of several days. Therefore, a hand-made syphon dump flow counter was attached to the end of sample flow. This is shown in Fig. II-4-1. The volume per count was 3.91 ml.

II-4-2 Conversion Analysis by GPC

Gravimetric determination of conversion is very tedious and time consuming. When the polymer sample size is small it is almost impossible to perform. Therefore it was desired to establish a quick and reliable technique for the determination of conversion.

Since GPC gives a separation of molecules according to their molecular size, it can be applied to evaluate the amount of monomer and polymer present in a mixture. In gas chromatography, it is common practice to make composition analysis from peak areas. The procedure is simple, merely to obtain a relationship between the peak area of

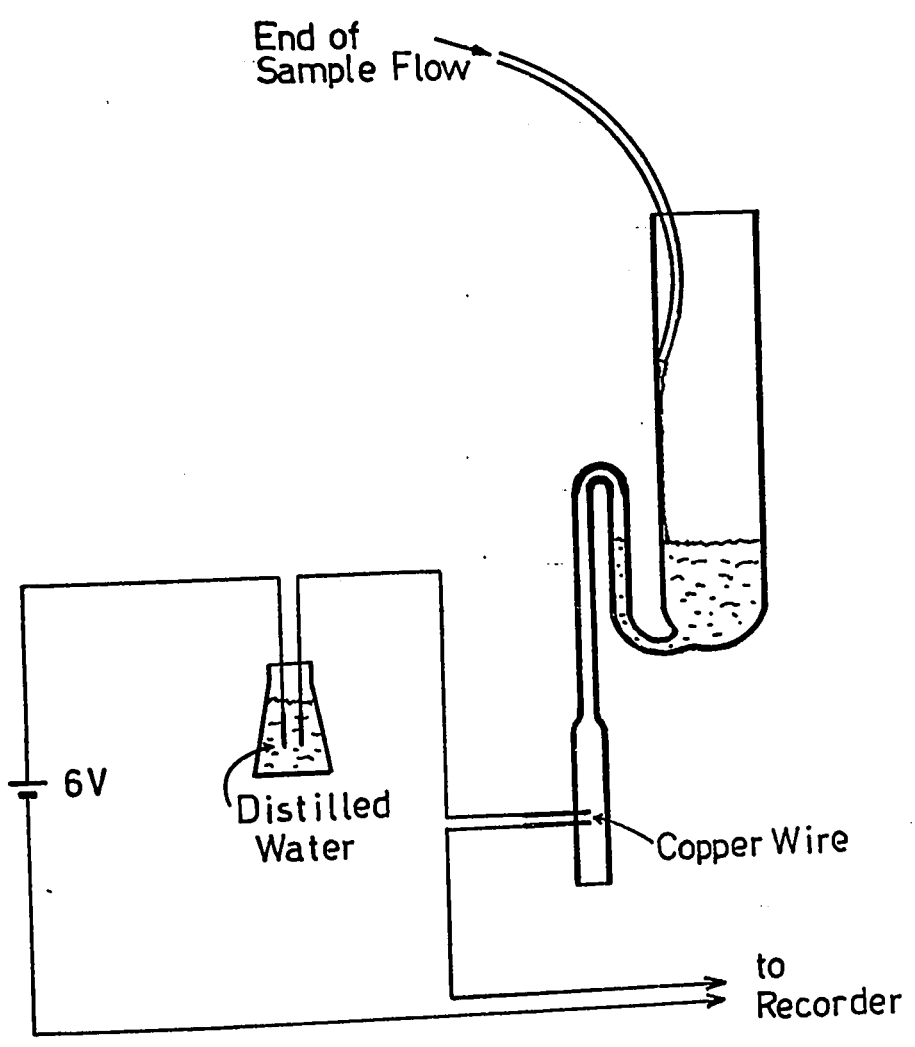


Fig. II-4-1 Syphon Dump Flow Counter

monomer and polymer against the composition of the mixture. The only difficulty results from the interference of impurity peaks which very often overlap the monomer peak. This is true with a GPC operating with THF as carrier solvent, in which case the impurities are water and air injected with the sample. However, with water (doubly distilled) as a carrier solvent it was found that there is no appreciable impurity peaks. Air has a very small solubility in water. Also found was that a single 4-ft. column packed with porous glass (CPG10-700) gave a satisfactory separation of monomer and polymer. Therefore, polymer and monomer were preweighed to make up solutions of known composition, then the solution was injected into the GPC. Resultant peak area of monomer and polymer were measured initially by cutting out and weighing the peaks from recorder trace. Later this was switched to numerical integration (Simpson's rule) of the peak heights using an on-line minicomputer. Table II-4-1 summarizes the polymer-monomer mixtures prepared and their area fractions obtained by GPC. They are plotted in Fig. II-4-2. A typical example of a response curve is shown in Fig. II-4-3 together with the area fraction calculation by the minicomputer. It can be seen that there is an excellent one-to-one correspondence between weight fraction and peak area fraction over the entire conversion range. The standard deviation of the data points from the line of perfect fit was 0.0094 weight fraction. Thus the polymer peak area fraction was equated to conversion in the kinetic runs reported in Part I. The presence of initiator in this case did not interfere with the area measurements since its peak size was negligible as compared to the peak sizes of monomer

Table II-4-1 Polymer-Monomer Mixture Prepared* and Their Peak Area Fraction

<u>Polymer (gm)</u>	<u>Monomer (gm)</u>	<u>Polymer Wt. Fraction</u>	<u>Polymer Area Fraction by GPC</u>
.0085 ²⁾	.0577	.128	.122, .126, .140
.0220 ¹⁾	.0739	.230	.240, .245, .251
.0282 ⁴⁾	.0580	.327	.334
.0335 ²⁾	.0474	.415	.418, .422
.0734 ³⁾	.0384	.657	.662
.0839 ⁴⁾	.0366	.695	.701
.0768 ¹⁾	.0179	.810	.815
.0987 ³⁾	.0055	.956	.946

*Weighed polymer and monomer were dissolved into 70-100 ml doubly distilled water.

- 1) C5014(A)-7
- 2) C5011(A)-5
- 3) C5021(A)-7
- 4) N8207-3 (Supplied from Nalco Chem. Co.)

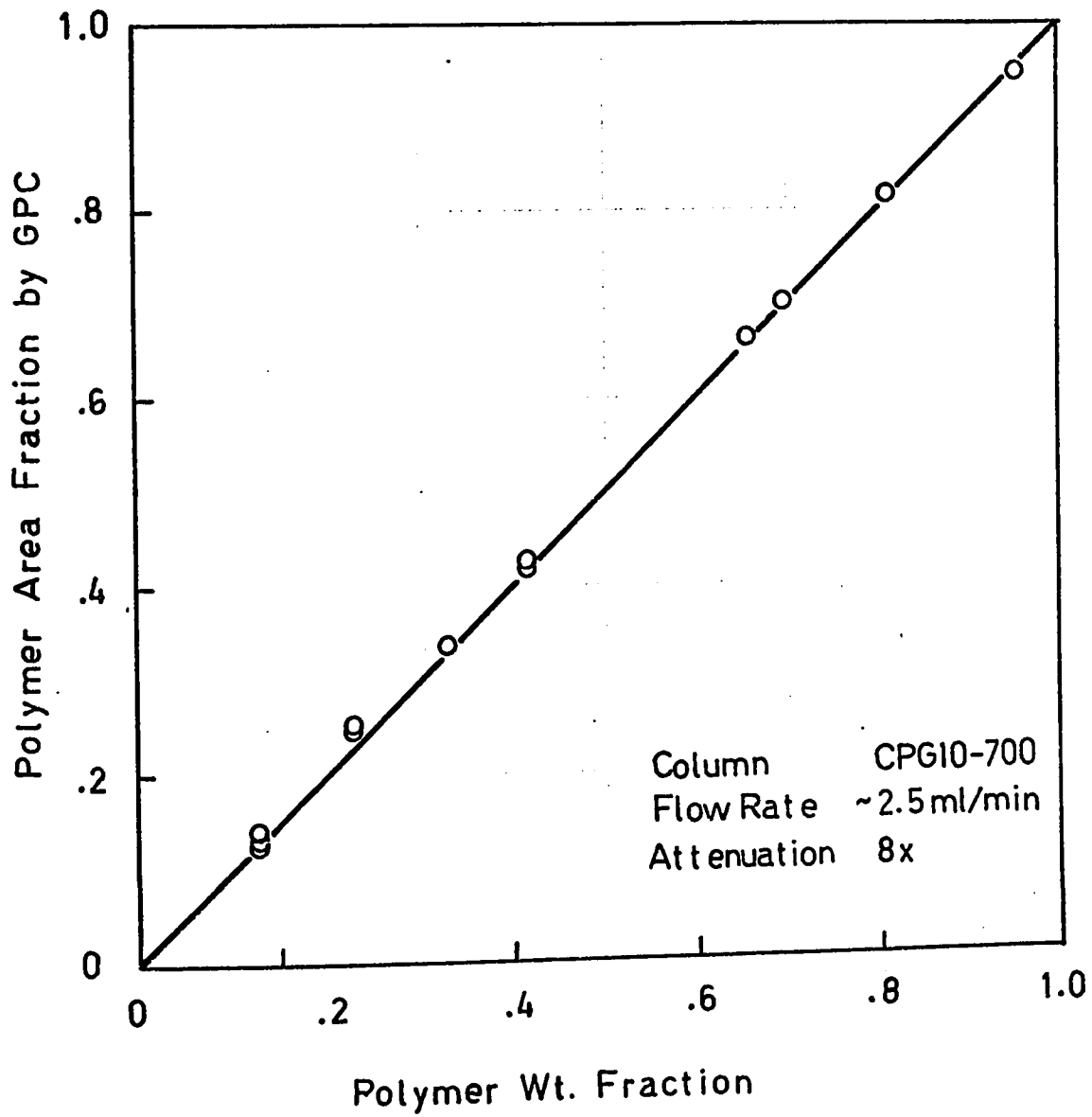


Fig. II-4-2 Comparison of Weight Fraction vs. Peak Area Fraction

and polymer.

Next, it was attempted to convert to an absolute concentration of polymer or monomer solution from the peak size. Table II-4-2 lists the observed peak area vs. concentration in two series of measurements. The measurements given as Series (B) were made about two months later than those of Series (A). These are compared in Fig. II-4-4. It can be seen that both polymer and monomer peak areas are proportional to their concentration, in agreement with previous weight fraction measurements. However, the proportionality constant was not constant over the period of operation, due to the change in the flow rate and the instrument sensitivity. The solid line of the Series (B) measurements was used to evaluate polymer concentration when the viscosities of the products in the initial rate runs were measured. This was done during the Series (B) measurements to avoid a significant change in the proportionality constant.

A similar technique was applied in the study of the decomposition of ACV at 80°C, although in this case the separation of the original ACV from the products was not complete. Therefore, the concentration dependence of ACV peak was first investigated. It was found that the linearity between peak height of ACV vs. its concentration does not exist. By reducing the concentration, higher retention volume portion of the peak gradually disappeared. This is a very strange phenomena indicating some interaction, possibly strong adsorption of the ACV with the column packing. The decomposition followed by GPC is shown in Fig. II-2-5. Considering the fact that the ACV peak shifts to lower elution volume

Table II-4-2 Observed Peak Area vs. Concentration

Series (A) (8x, Chart Speed 2 min/in, 4 ft. CPG10-700)

<u>Sample Solution (gm/100 ml)</u>	<u>GPC Peak Area (in²)</u>
AM 0.0833	5.70, 5.61, 5.64
AM 0.0658	4.10, 4.32, 4.35
PAM ^{a)} 0.0871	5.70, 5.64, 5.64
PAM ^{b)} 0.0620	4.13
PAM ^{a)} 0.0436	2.71, 2.92, 2.80
PAM ^{a)} 0.0218	1.54, 1.33, 1.45

Series (B) (8x, Chart Speed 2 min/in, 4 ft. CPG10-700)

<u>Sample Solution (gm/100 ml)</u>	<u>GPC Peak Area (in²)</u>
AM 0.0450	2.27, 2.41, 2.39
PAM ^{a)} 0.0619	3.37, 3.52, 3.53
PAM ^{b)} 0.0620	3.50, 3.66, 3.77
PAM ^{c)} 0.0209	1.17, 1.16, 1.13, 1.20
PAM ^{a)} 0.0310 + AM0.0225	PAM: 1.64, 1.65, 1.75, 1.67, 1.62
	AM: 1.15, 1.18, 1.21, 1.16, 1.12

a) C5014(A)-6

b) N8207-3 (Supplied from Nalco Chem. Co.)

c) C50S(A)-1

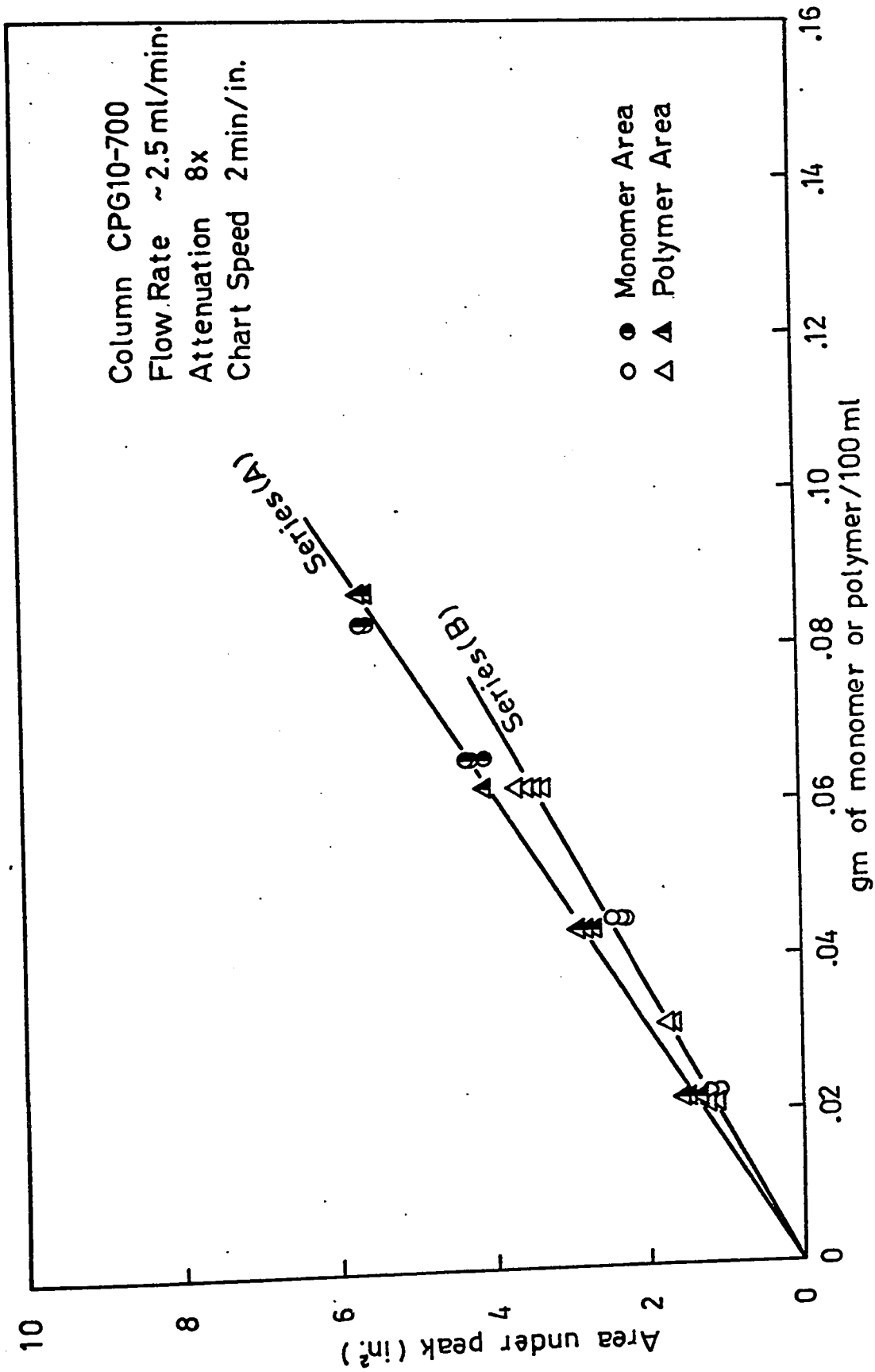


Fig. II-4-4 Concentration Dependence of Area Under Peak

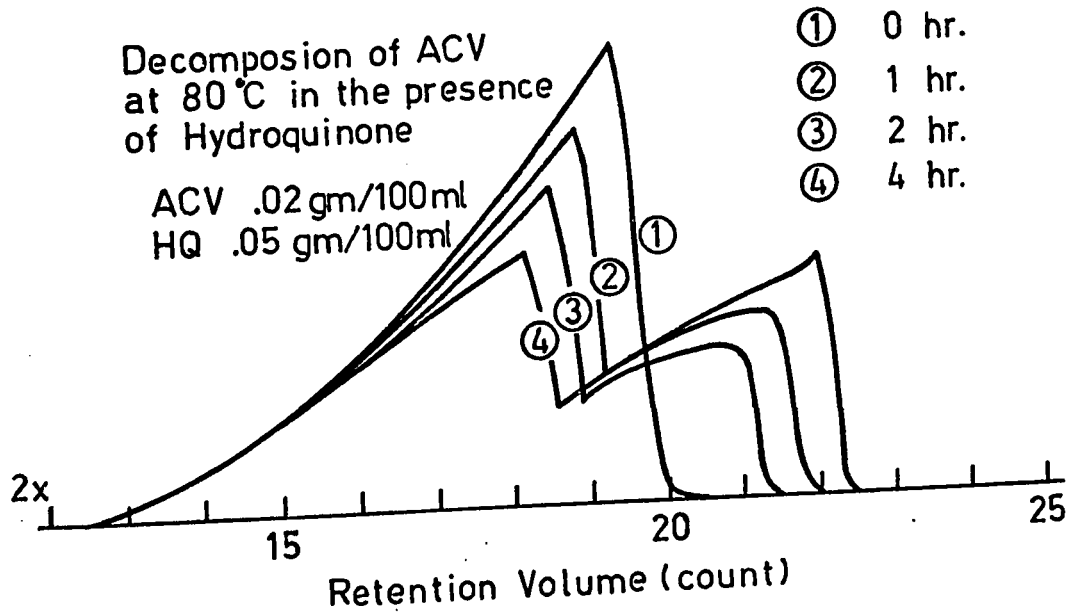
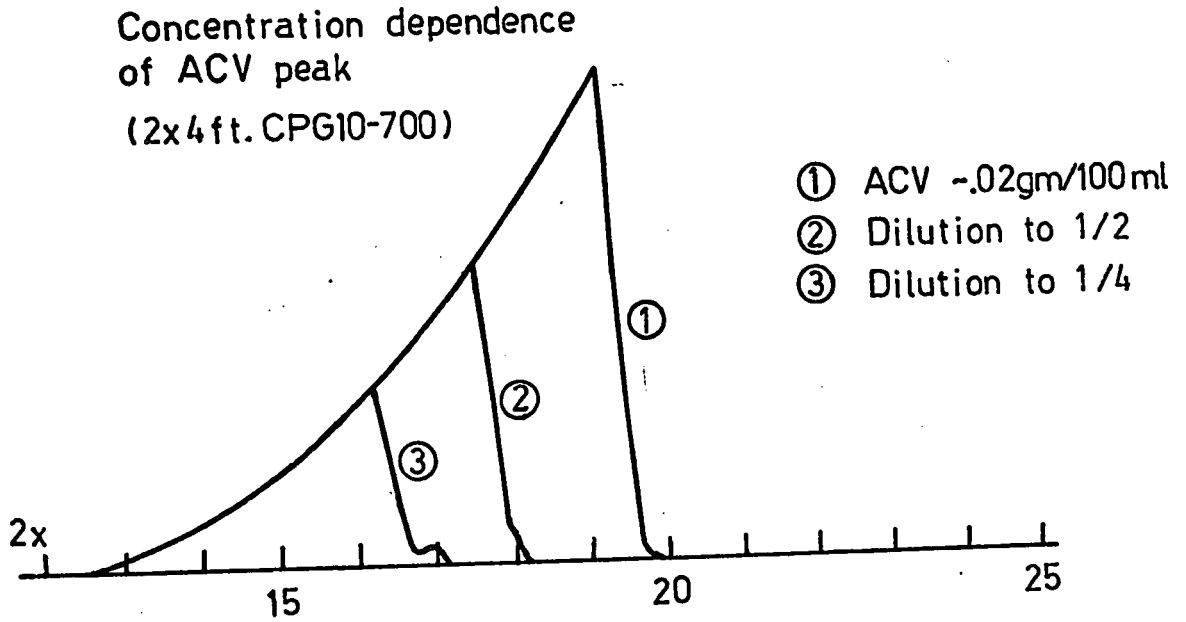


Fig. II-4-5 GPC Response for ACV

with dilution, conversion was determined as $1 - \text{ACV peak area} / \text{Total peak area}$.

II-4-3 Molecular Weight Analysis of Polyacrylamide.

The combination employed was six 4-ft. columns of the following:

2x (Bio-Glas 2500) + 3x (CPG10-2000) + 1x (CPG10-700)

The GPC was operated at room temperature. The solvent contained KB_r in 0.15 wt %. Use of a buffered carrier solvent appeared to be preferable in an aqueous system,^(41,42) however, no definite criteria are known for material to be used for particular polymer. The addition of KB_r reduced the strong concentration effect in the present system. Also the exclusion limit on molecular weight might be extended since the intrinsic viscosity of polyacrylamide showed a decrease from 9.9 in distilled water to 7.2 in .15 wt % KB_r solution (Sample C5014(A)-6). The practical sample concentration range was determined to be 0.05 - 0.10 wt %, above this range the linearity of the responses was found poor. Fig. II-4-6 shows the responses of a polymer sample C5014(A)-6 with successive dilution. Long tailing of the chromatogram was observed indicating possible surface phenomena such as adsorption was taking place. The sensitivity of the instrument was raised to 2x for this concentration range. The chromatogram heights were monitored by Waters analog to digital transformer every 20 sec. Since the received signals were

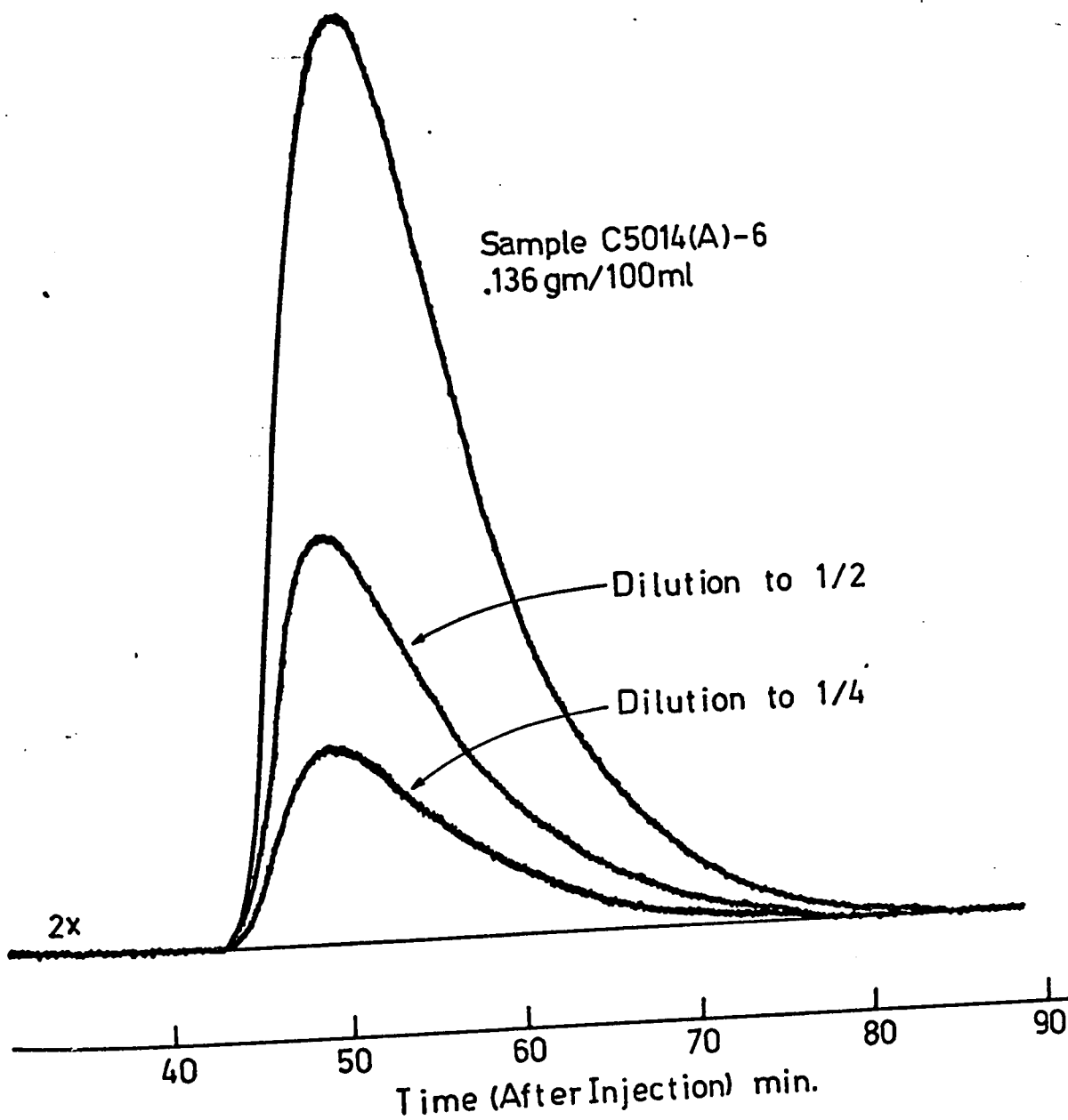


Fig. II-4-6 Linearity Test

found fluctuating even at the stable portion of baseline, they were smoothed by 13-point cubic method⁽⁴⁴⁾ and then interpreted in 0.5 count interval. In Fig. II-4-7, the interpreted chromatograms for different number-average molecular weight samples are shown together with the effective calibration curves obtained from two \bar{M}_n 's. Since there are no narrow distributed polyacrylamide standards available, usual manner of constructing a calibration curve and evaluation of instrumental spreading were not made. In Fig. II-4-7, it can be immediately seen that the leading portions of the chromatograms starts nearly constant retention volume, indicating that the molecular weight range is apparently near the column exclusion limit. This is well interpreted in the sharp rise in the slope of the effective calibration curve. Neither the operation of the columns at elevated temperature (50°C - 80°C), nor the reduction of flow rate to 1.0 ml/min improved this situation. Calculated weight average molecular weights thus significantly differed from predicted. Only reasonable \bar{M}_w was obtained for the lowest molecular weight sample (C50S(A)-2) which gave a molecular weight distribution in fair agreement with that predicted. This is shown in Fig. I-4-17 in Part I. Next, the use of an effective calibration curve in lower molecular weight (higher retention volume) range was attempted to make extensive use of the information from the GPC. If there exist a single calibration curve that can be applied say, to lower 50% of molecular weight range, this could be a useful one to check the predicted molecular weight distribution in this range. The task was done as follows. By using a certain effective calibration curve,

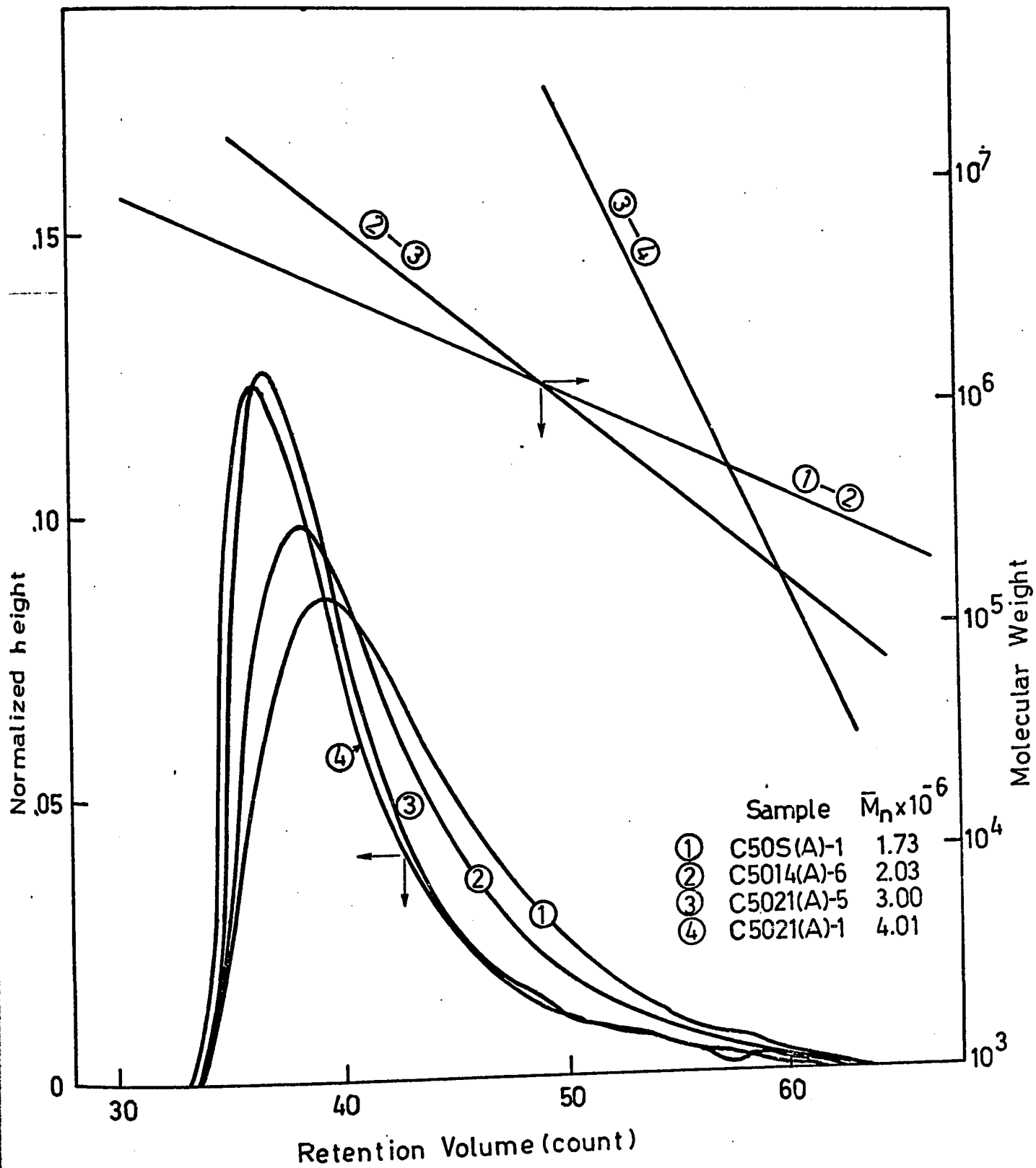


Fig. II-4-7 Chromatograms and Effective Calibration Curves

one can convert the observed $F(v)$ into $F^*(z)$ where $z = \ln M$. Similarly one can convert the predicted molecular weight distribution $f_w(M)$ into a distribution $f_w^*(z)$. If the effective calibration curve is a valid one in lower molecular weight range, say $M \leq M_{30}$, where M_{30} represents the molecular weight at which lower molecular weight species reaches to 30% of the total wt. of the species, $F^*(z) = f_w^*(z)$ at $z \leq z_{30}$. Equating $F^*(z_{30})$ by $f_w^*(z_{30})$ (or any value less than z_{30}), the slope of the calibration curve D_2 can be calculated. It will be shown that no actual transformations of the $F(v)$ and $f_w(M)$ into z -scale are needed. Fig. II-4-8 gives the picture of the transformation.

The 70% area point v_{70} in $F(v)$ can be defined as follows:

$$\int_{v_0}^{v_{70}} F(v) dv = 0.7$$

Corresponding z_{70} to this v_{70} is

$$z_{70} = \ln D_1 - D_2 v_{70}$$

This z_{70} gives the 30% fraction point in $F^*(z)$ since

$$\int_{z_f}^{z_{70}} F^*(z) dz = \int_{v_{70}}^{v_f} F(v) dv = 1 - \int_{v_0}^{v_{70}} F(v) dv = 0.3$$

Similarly, corresponding z_{30} to M_{30} is

$$z_{30} = \ln M_{30}$$

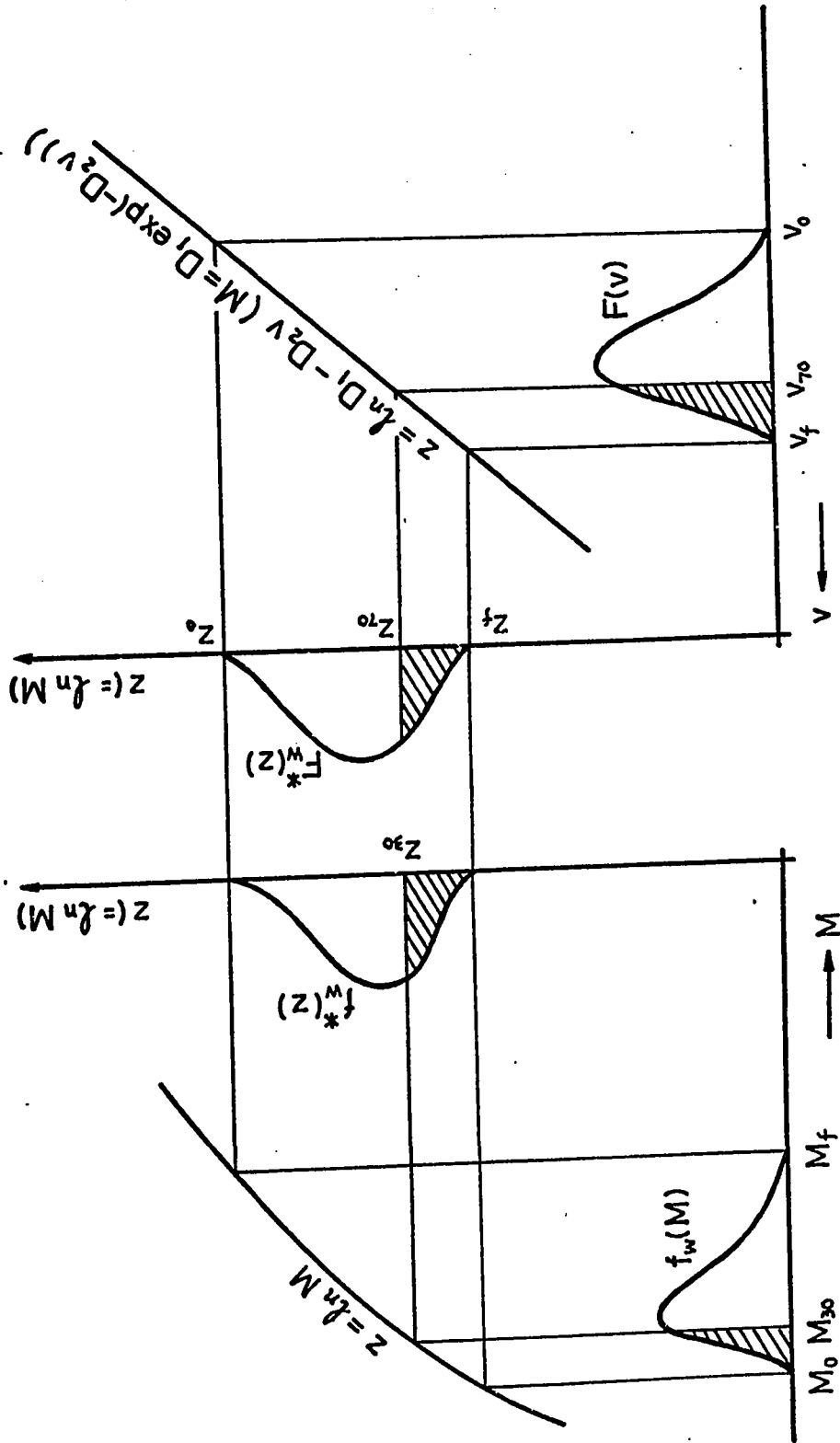


Fig. II-4-8 Finding an Effective Calibration Curve in Low Molecular Weight End

Firstly, z_{30} must be equal to z_{70} , therefore

$$\ln M_{30} = \ln D_1 - D_2 v_{70}$$

$$\therefore D_1 = M_{30} \cdot e^{D_2 v_{70}}$$

Secondly, $F^*(z_{70})$ must be equal to $f_w^*(z_{30})$,

$$F^*(z_{70}) = -F(v_{70}) \frac{dv}{dz} = \frac{F(v_{70})}{D_2}$$

$$= f_w^*(z_{30}) = f_w(M_{30}) \frac{dM}{dz} = M_{30} f_w(M_{30})$$

$$\therefore D_2 = F(v_{70}) / M_{30} \cdot f_w(M_{30})$$

The values v_{70} , M_{30} , $F(v_{70})$, $f_w(M_{30})$ can easily be calculated. Results of D_1 and D_2 obtained for sample C5014(A)-6 were as follows:

<u>Matching Point (%)</u>	<u>$D_1 \times 10^{-8}$</u>	<u>D_2</u>
5	3.31	.115
10	2.91	.112
15	2.62	.110
20	3.60	.117
25	4.38	.121
30	5.74	.127
35	7.53	.133
40	10.43	.141

Fig. II-4-9 shows the calibration curves with the above constants together with the molecular weight ranges they cover. It is apparent that no single calibration curve holds up to lower 40% of the total molecular weight species, D_1 and D_2 can be said nearly constant below 20% level. The obtained calibration curves in this range showed fair agreement with that obtained from \bar{M}_n 's of samples C50S(A)-1 and C5014(A)-6. The 20% limit corresponds to $M \sim 2 \times 10^6$. Since the range was too small to compare the other chromatograms with those predicted, no further attempt was made.

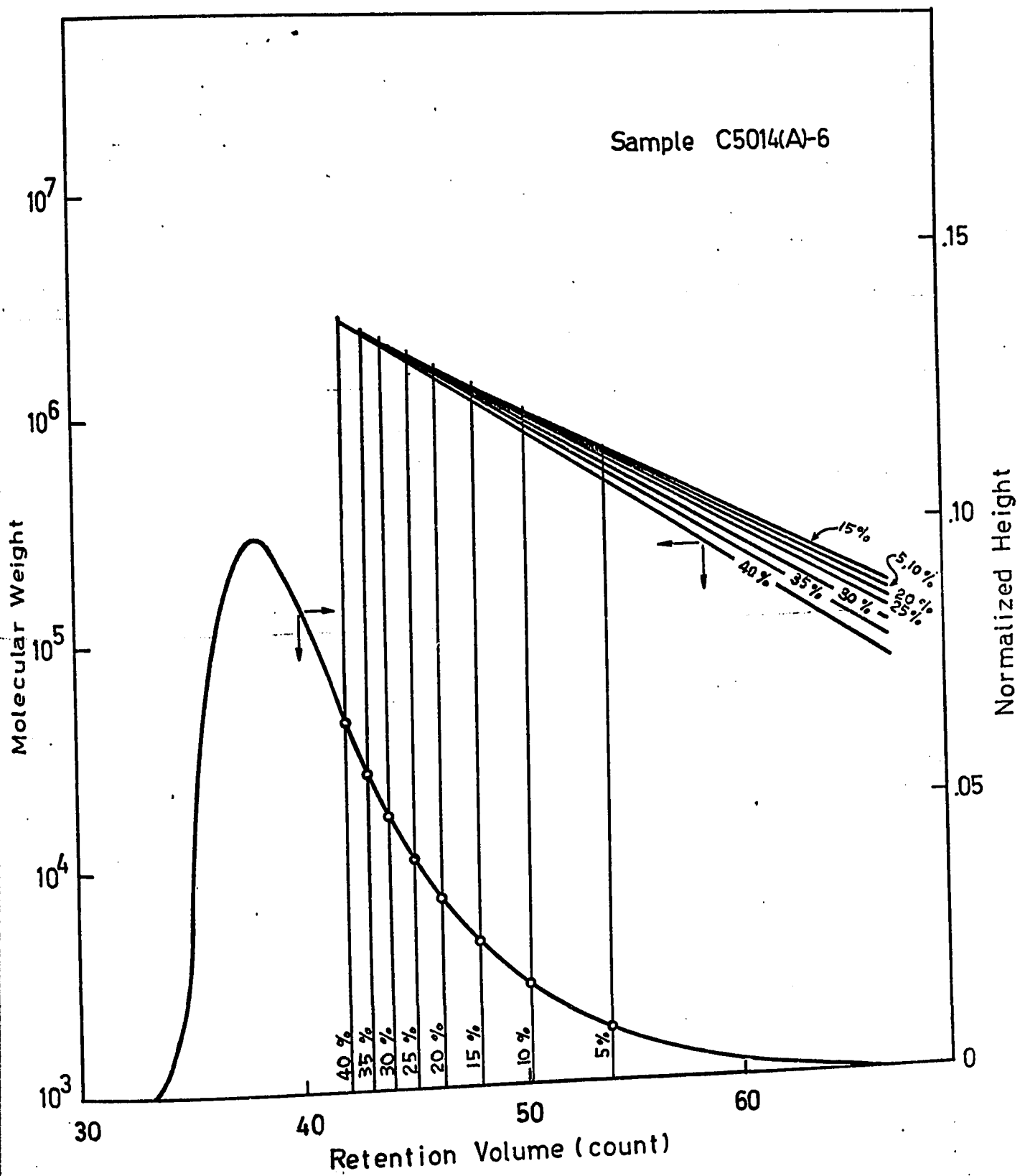


Fig. II-4-9 Effective Calibration Curves in Lower Molecular Weight Ranges

II-5 DISCUSSION

The instrumental spreading function proposed by Provder and Rosen⁽¹⁰⁾ is the most general form among others so far proposed. However, it is necessary to truncate the series for practical use. When a two parameter expression is used (truncation after first two terms), the instrumental spreading function $G(v,y)$ results in negative values at some retention volume range due to a cubic expression of $H_3[x]$ in equation (II-2-8b). If the negative appears in the retention volume range of a chromatogram, which is not a rare occasion, this is physically almost an impossible situation. The apparent contradiction of negative molecular weight average shown by Hamielec⁽¹¹⁾ may be due to this negative values in $G(v,y)$. By using the three parameter expression (truncation after third term) this problem may be eliminated. However, this requires a knowledge of three characteristics \bar{M}_n , \bar{M}_w and η (or \bar{M}_z) on one sample, together with the constants in Mark-Houwink intrinsic viscosity vs. molecular weight. The last constants often differ from one source to the other. Even if they are all available, the values of h , μ_3 and μ_4 are very sensitive to the known quantities, which usually involve at least a few percent error.

The basic problem associated with the determination of the instrumental spreading is the fact that the precise characterization of the input form is difficult, at the most only three information on distributed input. In the field of control theory, a transfer function of some process has been characterized by investigating the response signal to a

well characterized input signal. From this view, the precise characterization of GPC instrumental spreading would be almost impossible until truly mono-dispersed polymer standards become available. With narrow-distributed polymer standards as they are today, the author feels that the recycle technique may give a better understanding of the nature of spreading. When once eluted sample is recycled to the column, the resulting chromatogram is the response to the input characterized by the chromatogram firstly obtained. Of course, any undesirable distortion of the chromatogram by the recycling operation itself has to be investigated as well.

With regard to the methods of the spreading correction, it appears that the realization of the above mentioned uncertainty in the spreading function was lacking in the previous evaluation of these methods. Some of the proposed methods might have worked perfectly if there were no errors involved in the employed instrumental spreading function. Unfortunately, the current evaluation was limited to the method of Chang and Huang⁽³³⁾ and presently developed two methods from this view point.

It was shown that the present methods of instrumental spreading correction work as well as the method developed by Chang and Huang if the spreading function is precise. The advantage of Method-1 and -2 is their applicability to a wide variety of spreading functions.

Method-1 resulted in negative heights of appreciable size when the resolution factor h was as small as 0.2. This negative recovery appears inherent to the method when the iteration is stopped at certain stage. However, it is practically impossible to iterate infinite number of time in the retention volume range $-\infty < v < +\infty$. In this

respect, Method-2 is more useful since it guarantees the positive height, though it sometimes did not converge ΔS to zero. When applied to the experimental chromatograms, both Method-1 and Method-2 gave the corrected number- and weight-average molecular weight within the error of only 5%. However, the corrected chromatograms were not always realistic ones. Particularly with Method-1, the large oscillation in both positive and negative heights is an impossible situation. With Method-2, a small second peak was observed for the sample WA4190039. This might indicate the errors in approximating a non-Gaussian instrumental spreading by a Gaussian spreading function, or it might have resulted from the inaccuracy of reading these small heights in the tailing part of the chromatogram.

Use of an effective calibration curve, on the other hand, was shown to by-pass these troublesome corrections for the spreading. It was also shown that a single effective calibration curve is obtainable in certain retention volume range. Large differences in the constant D_1 and D_2 obtained from \bar{M}_n and \bar{M}_w of one narrow distributed sample, however indicated the requirements of accurate ratio of \bar{M}_w/\bar{M}_n . With this respect, it would be better to employ the two samples of molecular weight difference in the magnitude of about two or more. If one is to use only one sample, it is better to be a broad distributed one to obtain more reliable effective calibration curve.

Although the Tung's axial dispersion equation theoretically describes the required interpretation in the obtained elution chromatograms, the

author feels that the use of this equation to correct for the instrumental spreading is too cumbersome to perform and the results are not always meaningful when done with an uncertain instrumental spreading function. Since most users of GPC are interested in two or three average molecular weights not in the spreading corrected chromatogram, obtaining the spreading corrected chromatograms is not always a necessary step to be involved. From this view, the use of an effective calibration curve that accounts the spreading may be the easiest and most practical approach at present.

As for the application of GPC for the kinetic study of acrylamide polymerization is concerned, the conversion analysis was shown to be quite successful. This way of measuring conversion is advantageous since it requires a far smaller sample size as compared to gravimetry. Hence it is possible to use a very small ampoules that provide a better temperature control. Also the time required for one sample analysis was significantly reduced. If both the conversion analysis and molecular weight analysis from a single injection were possible, the use of the GPC would be the fastest analytical tool in the kinetic study. However, the latter one was not too successful due to the resolution limit of the available column together with a long tailing of the chromatograms.

II-6 CONCLUSION

Two numerical methods of solving Tung's axial dispersion equation were developed and evaluated. Simultaneous evaluation of the method of Chang and Huang⁽³³⁾ was made. At the time of this study, their method appeared to be the most promising one available in the literature. For all six different GPC responses investigated (synthesized), none of the methods adequately recovered all of the corrected distribution. However, the present method-1 and method-2 appear to work as well as the method of Chang and Huang, where their method is applicable. The present two methods have wider applicability than the method of Chang and Huang. Since method-2 ensures positive $W(y)$ and require relatively shorter computation times than method-1, method-2 is recommended for obtaining corrected chromatograms. However, the uniform convergence of ΔS to zero by method-1 is a very desirable feature.

In application of method-1 and method-2 to experimental chromatograms, it was pointed out that the establishment of correct instrumental spreading function is very difficult. Without the precise instrumental spreading function, no correction methods can yield reliable corrected chromatograms. The use of an effective calibration curve is attractive with this respect since it does not require the instrumental spreading function. It was experimentally shown that a single effective calibration curve is obtainable in specified retention volume range. Further

investigation on the validity of the effective calibration curve is desirable from this view.

In relation to kinetic study of acrylamide polymerization, it was found that GPC enables a quick and reliable determination of monomer conversion. Analysis of molecular weight by GPC however was not too successful. This was due to the limit of column resolution.

II-7 NOMENCLATURE

a	a constant (exponent) in Mark-Houwink intrinsic viscosity- molecular weight relation
ACV	4, 4 azobis-4- cyanovaleric acid
AIBN	azobis-isobutyronitrile
AM	acrylamide
A_n	coefficients in general shape function
D_1, D_2	constants in retention volume vs. molecular weight calibration curve
D_1', D_2'	weight calibration curve
$f_w(M)$	weight-based molecular weight distribution predicted from a kinetic model (with respect to molecular weight)
$f_w^*(z)$	$f_w(M)$ mapped onto $z (= \ln M)$ domain
$F(v)$	GPC elution chromatogram
\bar{F}	bilateral Laplace transform of $F(v)$
F_i	GPC elution chromatogram corresponding to W_i
$F_w(M)$	weight-based molecular weight distribution (with respect to molecular weight)
$F^*(z)$	$F(v)$ mapped onto $z (= \ln M)$ domain
$G(v,y)$	instrumental spreading function
$G_o(v-y)$	Gaussian instrumental spreading function
$G\{ \}$	integral operator, see Eq. II-2-21
GPC	gel permeation chromatography
h, h_f, h_r	Gaussian resolution factors for total, front half and rear half of GPC column
HMDS	hexamethyldisilazane
HQ	hydroquinone

H_3, H_4	3-rd and 4-th order Hermite polynomials
J	objective function
k	integer constant, (1, 2, 3, ---)
M	molecular weight
M_F, M_0, M_{30}	specified values of M
$\bar{M}_k(t), \bar{M}_k(\infty)$	k-th spreading corrected (or true) and uncorrected molecular weight averages
$\bar{M}_n, \bar{M}_w, \bar{M}_z$	number-, weight- and z-average molecular weights
$\bar{M}_n(t), \bar{M}_n(\infty)$	spreading corrected (or true) and uncorrected number-average molecular weights
$\bar{M}_n(D_1, D_2)$	number-average molecular weight calculated using D_1 and D_2
\bar{M}_{rms}	root mean square of \bar{M}_n and \bar{M}_w
$\bar{M}_w(t), \bar{M}_w(\infty)$	spreading corrected (or true) and uncorrected weight-average molecular weights
$\bar{M}_z(t), \bar{M}_z(\infty)$	spreading corrected (or true) and uncorrected z-average molecular weights
$N\{ \}$	normalizing (with respect to area) operator
p	polydispersity (= \bar{M}_w/\bar{M}_n)
$p(t), p(\infty)$	spreading corrected (or true) and uncorrected polydispersities
PAM	polyacrylamide
PRV	peak retention volume
R_s	effectiveness of column resolution
s	birateral Laplace transform variable
SK	skewing factor
ΔS	difference of area under two curves

t	flow time
THF	tetrahydrofuran
v	retention volume
v_f, v_o, v_{70}	specified values of v, (see Fig. II-4-8)
w_1, w_2	peak widths of chromatogram 1 and 2
W	spreading corrected chromatogram
\bar{W}	bilateral Laplace transform of W
W_i	i-th guess for W
W_i'	unnormalized W_i
ΔW_i	i-th amount of correction on W_i
x	a variable
X_i	see Eq. II-2-25b
y	mean retention volume, used to designate molecular species
z	a variable ($\approx \ln M$)
z_f, z_o, z_{30}, z_{70}	specified values of z

Greek Symbols

ϵ	see Eq. II-2-25a
$\eta(t), \eta(\infty)$	spreading corrected (or true) and uncorrected intrinsic viscosities
$\mu_0, \mu_1, \mu_2, \mu_3, \mu_n$	zero, first, second, third and n-th moments of chromatogram
σ	variance

II-8 REFERENCES

1. K.H. Altgelt, *Advances in Chromatography*, 7, 3 (1968).
2. M.J.R. Cantow, "Polymer Fractionation," p. 123, Academic Press, New York (1967).
3. D.J. Harmon, *Separation Sci.*, 5, 403 (1970).
4. L.H. Tung, *J. Appl. Poly. Sci.*, 10, 375 (1966).
5. L.H. Tung, J.C. Moore, and G.W. Knight, *J. Appl. Poly. Sci.*, 10 1261 (1966).
6. L.H. Tung, *J. Appl. Poly. Sci.*, 10, 1271 (1966).
7. M. Hess and R.F. Kratz, *J. Poly. Sci. A-2*, 4, 731 (1966)
8. L.H. Tung and J.R. Runyon, *J. Appl. Poly. Sci.*, 13, 2397 (1969).
9. A.E. Hamielec and W.H. Ray, *J. Appl. Poly. Sci.* 13, 1319 (1969).
10. T. Provder and E.M. Rosen, *Separation Sci.*, 5, 437.
11. A.E. Hamielec, *J. Appl. Poly. Sci.*, 14, 1519 (1970).
12. F. Rodriguez, R. Kurakowski and O.K. Clark, *Ind. Eng. Chem. Prod. Res. Development*, 5, 121 (1966).
13. F.C. Frank, I.M. Ward and T. Williams, *Preprints, Fifth International Seminar on Gel Permeation Chromatography*, London (1968).
14. S.T. Balke, A.E. Hamielec and B.P. LeClair, *Ind. Eng. Chem. Prod. Res. Development*, 8, 54 (1969).
15. Z. Grubisic, P. Rempp and H. Benoit, *J. Poly. Sci. B*, 5, 753 (1967).
16. H. Benoit, Z. Grubisic, P. Rempp, D. Decker and J.G. Zilliox, *Preprints, Third International Seminar on Gel Permeation Chromatography*, Geneva (1966).
17. E. Drott, *Preprints, Fourth International Seminar on Gel Permeation Chromatography*, Miami Beach (1967).
18. K.A. Boni, F.A. Sliemers and P.B. Stickney, *Preprints, Fourth International Seminar on Gel Permeation Chromatography*, Miami Beach (1967).
19. L. Wild and R. Guliana, *J. Poly. Sci., A-2*, 5, 1087 (1967).

20. M.J.R. Cantow, R.S. Porter and J.F. Johnson, J. Poly. Sci., A-1, 5, 987 (1967).
21. M. Imoto, Y. Saito and K. Fujishiro, "Kobunshi Kagaku", Makishoten, Tokyo (1962).
22. D.D. Bly, J. Poly. Sci., C, No.21, 13 (1968).
23. J.H. Duerksen and A.E. Hamielec, J. Poly. Sci. Part C, No. 21, 83 (1968).
24. S.T. Balke and A.E. Hamielec, J. Appl. Poly. Sci., 13, 1381 (1969).
25. J.E. Hazell, L.A. Prince and H.E. Stapelfeldt, J. Poly. Sci., Part C, No. 21, 43 (1968).
26. F.W. Billmeyer and R.N. Kelley, J. Chromatography, 34 322 (1968).
27. K.J. Bombaugh, W.A. Dark and R.N. King, J. Poly. Sci., Part C, No. 21, 131 (1968).
28. O. Levenspiel, "Chemical Reaction Engineering", John Wiley and Sons, Inc. New York (1962).
29. G.I. Taylor, Proc. Royal Society, A225, 473 (1954).
30. W.N. Smith, J. Appl. Poly. Sci. 11 639 (1967).
31. P.E. Pierce and J.E. Armonas, J. Poly. Sci., Part C, No. 21, 23 (1968).
32. A.E. Hamielec, GPC Lecture Note; Washington Univ., St. Louis, Apr. 1969.
33. K.S. Chang & R.Y.M. Huang, J. Appl. Poly. Sci., 13, 1459 (1969).
34. S.G. Mikhlin, "The Problem of Minimum of a Quadratic Function", Holden-Day, Inc. (1965).
35. W. Haller, Nature, 206, 693 (1965).
36. M.J.R. Cantow and J.F. Johnson, J. Appl. Poly. Sci. 11, 1851 (1967).
37. J.H. Ross and M.E. Casto, J. Poly. Sci., Part C, No. 21, 143 (1968).
38. A.R. Cooper, J.H. Cain, E.M. Barrall II and J.F. Johnson, Separation Sci., 5, 787 (1970).

39. M.J.R. Cantow and J.F. Johnson, J. Poly. Sci., Part A-1, 5, 2835 (1967).
40. E.M. Barrall and J.H. Cain, J. Poly. Sci., Part C, No. 21, 253 (1968).
41. A.R. Cooper and J.F. Johnson, J. Appl. Poly. Sci., 13, 1487 (1969).
42. C.H. Lochmuller and L.B. Rogers, Analytical Chemistry, 41 173 (1969).
43. S. Ohashi, N. Yoza and Y. Ueno, J. Chromatography 24, 300 (1966).
44. P.G. Guest, Numerical Method of Curve Fitting, Cambridge University Press (1961).